Multi-Mode-Driven Molecular Shuttles: Photochemically and Chemically Reactive Benzoxazole-Containing Rotaxanes

By

Weiquan Sun

Degree of Doctor of Philosophy

School of Chemistry

University of Edinburgh

June 2008

Table of Contents

Abstract

The exquisite solutions nature has found to control molecular motion have served as a major source of inspiration for scientists to conceptualise, design and build entirely synthetic molecular machines. Interlocked molecular species, like rotaxanes and catenanes, are ideal structures to create artificial nanomachines, especially now that non-covalent templation strategies allow for the efficient synthesis of rotaxanes and catenanes. Depending on the nature of the molecular components, mechanical motions in these systems can be promoted by chemical, electrochemical and photochemical energy inputs. This thesis focuses on the synthesis of some multi-mode-driven molecular shuttles, which are photochemically and chemically reactive benzoxazole-containing rotaxanes.

Chapter One gives a brief outline of the template directed synthesis of interlocked architectures and some remarkable progress of molecular machines based on mechanically interlocked systems in the last few years.

Chapter Two describes an accessible and efficient synthesis of rotaxanes using benzoxazole-containing template. In this new station one of the amide groups of the fumaramide template is substituted by a benzoxazole moiety, which features a basic nitrogen atom as a hydrogen-bonding acceptor. Two reversible light-driven molecular shuttles have been generated when introduced into the thread of a non-photoactive second station and both exhibit remarkable positional integrity of the macrocycle on the thread before and after the photo stimulus.

Chapter Three describes the synthesis of a hydrogen-bonded benzimidazole-motif-templated rotaxane.

Chapter Four describes how a chemically driven molecular machine has been designed, based on a switchable rotaxane with two different recognition sites. Switching can occur using either the adjustment of pH or addition of zinc ions. This

molecular shuttle can switch the macrocycle between two distinct translational forms with high positional integrity and relatively fast dynamics.

Chapter Five describes the first synthesis and characterisation of a rotaxane containing an octanuclear heterometallic $\{Cr_7Ni\}$ wheel. As $\{Cr_7Ni\}$ is an antiferromagnetically coupled wheel with a nondiamagnetic ground state ($S = 1/2$), this methodology will make it possible to examine such fascinating magnetic properties within interlocked structures for the first time.

Attended Lectures and Meetings

1. Organic Research Seminars, School of Chemistry, University of Edinburgh, 2003-2007.
2. 32nd Scottish Regional Perkin Meeting in Edinburgh, December 2003.
3. UK Macrocycles and Supramolecular Chemistry Meeting in Sheffield, January 2004.
4. 2nd University of Glasgow/Organon Symposium on Synthetic Chemistry in Glasgow, September 2004.
5. 34th Scottish Regional Perkin Meeting in Glasgow, December 2005 and was awarded the runner-up prize for poster presentation (Poster title: A Reversible Light-Driven Molecular Shuttle Based On a Benzoxazole-Containing Rotaxane).
6. 4th University of Glasgow/WestChem-Organon Symposium on Synthetic Chemistry in Glasgow, August 2006.
7. EaStCHEM/IDECAT MINI SYMPOSIUM Homogeneous Catalysis in St Andrews, May 2007.
8. The Young(-ish) Giants of Chemistry Conference- A Meeting to Celebrate the 65th Birthday of Sir J Fraser Stoddart in Edinburgh, June 2007.

Acknowledgments

Firstly I would like to thank my supervisor, **Prof. David A. Leigh**, for giving me the wonderful opportunity to pursue a PhD degree in his group, in the beautiful city of Edinburgh. It has been a great experience to work in a contemporary chemistry lab with state-of-the-art facilities.

Secondly thanks to my collaborators. Thanks to **Dr. Emilio M. Pérez** for his direct supervision over the first year of my PhD study. Thanks to **Dr. Chin-Fa Lee** for developing the photochemistry reaction conditions in the project of light-driven benzoxazole-containing molecular shuttles and many useful discussions. Thanks to **Prof. Alexandra M. Z. Slawin** of the University of St. Andrews for solving the X-ray crystal structures. Thanks to **Prof. Wybren Jan Buma** and **Dr. Koos Kuijt** of the University of Amsterdam for the laser photoisomerisation experiments described in chapter two. Thanks to **Prof. Richard E. P. Winpenny** and **Dr. Grigore A. Timco** of the University of Manchester for the synthesis and X-ray crystal structure solution of the heterometallic-wheel-containing [2]rotaxane.

I would like to express most grateful thanks to **Dr. Bryan Koivisto** and **Dr. Euan Kay**, for their help proof reading the final draft of this thesis. Thanks to all the other members of the Leigh group and the staff of the School of Chemistry, including stores, NMR, MASS, glassware, mechanical, electricity, computer and administrative staff, for their kind help over the four years of my study in Edinburgh.

Special thanks to my local friends here in Edinburgh, **Alex**, **Catherine** and **Kenneth**, for inviting me to have delicious meals and pleasant conversation with them every month and looking after my wife during her visit to Scotland.

And finally great love and thanks to my family in China, especially to my beloved wife, **Sicong Jin**, without their support and encouragement it would have been impossible for me to complete this thesis.

List of Abbreviations

Å: Angstrom

δ: chemical shift

ATP: adenosine triphosphate

Boc: *tert*-butyloxycarbonyl

BPP34C10: bis-*p*-phenylene-34-crown-10

Calcd.: calculated

CBPQT: cyclobis(paraquat-*p*-phenylene) tetracationic

CD: cyclodextrin

CT: charge-transfer

DABCO: 1,4-diazabicyclo[2.2.2]octane

DB24C8: dibenzo-24-crown-8

DMAB: 4,4'-bis(dimethylamino)benzophenone

4-DMAP: 4-dimethylaminopyridine

DMF: *N*,*N*-dimethylformamide

DMSO: dimethylsulphoxide

DNA: deoxyribonucleic acid

DNP: 1,5-dioxynaphthalene

dpbiiq: 8,8'-diphenyl-3,3'-biisoquinoline

dpp: 2,9-diphenyl-1,10-phenanthroline

EDCI: 1-(3-dimethylaminopropyl)-3-ethyl-carbodiimide

EDTA: ethylenediamine tetraacetic acid

en: ethylenediamine

equiv: equivalents

FAB: Fast Atom Bombardment

HPLC: High Performance Liquid Chromatography

HRMS: High Resolution Mass Spectrometry

nm: nanometer

NMR: Nuclear Magnetic Resonance

ppm: part per million

PSS: photostationary states

RCM: ring-closing metathesis

rt: room temperature

SAM: self-assembled monolayer

TFA: trifluoroacetic acid

TLC: Thin Layer Chromatography

TMS: tetramethylsilane

TTF: tetrathiafulvalene

Introduction

1.1 Mechanically Interlocked Architectures

Molecular machines are ubiquitous in nature. Nature has designed a series of useful, yet complex machines called motor proteins. Three classical examples include F_0F_1-ATP synthase[1] (F_0F_1-ATPase, Figure 1.1), a rotary motor which produces ATP through its rotary motion, myosins[2] which can move along actin filaments, acting as linear motors (Figure 1.2), or the kinesins[3] (Figure 1.3), essential motor proteins able to 'walk' on the microtubules and to transport important molecular components of the cell over large distances. Increased understanding of these dynamic biological systems whose controlled motions correspond to important biological functions has led to spectacular recent growth in the field of synthetic molecular machinery.[4] As with motor proteins, synthetic machines attempt to control or induce large amplitude motions to perform useful tasks. In principle, molecular machines can be designed starting from several kinds of molecular and supramolecular systems, including DNA-based systems;[5] however, many of the systems constructed so far are based on two families of mechanically interlocked structures, namely catenanes and rotaxanes.[6]

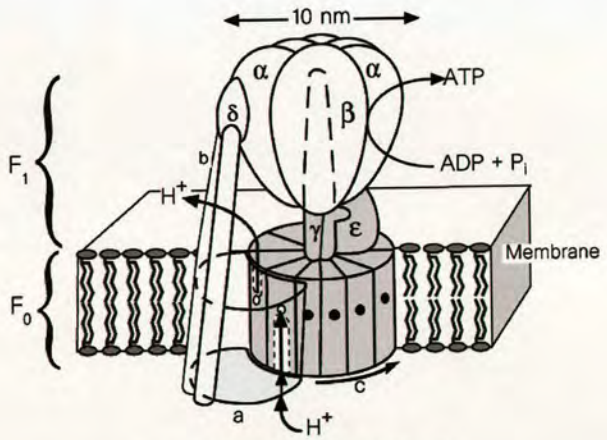

F_0F_1-ATP synthase (F_0F_1-ATPase)

Figure 1.1 Schematic representation of the structure of F_0F_1-ATP synthase (F_0F_1-ATPase):[1f] The ***c*** subunit consists of 9-12 twin α-helices arranged in a central membrane-spanning array; the ***a*** subunit consists of 5-7 membrane-spanning α-helices; the proton channels lie at the interface between the ***a*** and ***c*** subunits (dashed lines indicate the putative inlet and outlet channels); the ***a*** subunit is connected to F_1 by the ***b*** and δ subunits. Proton flow through the channels develops torque between the ***a*** and ***c*** subunits. This torque is transmitted to F_1 via the γ shaft and the ε subunit, where it is used to release ATP sequentially from the three catalytic sites in F_1.

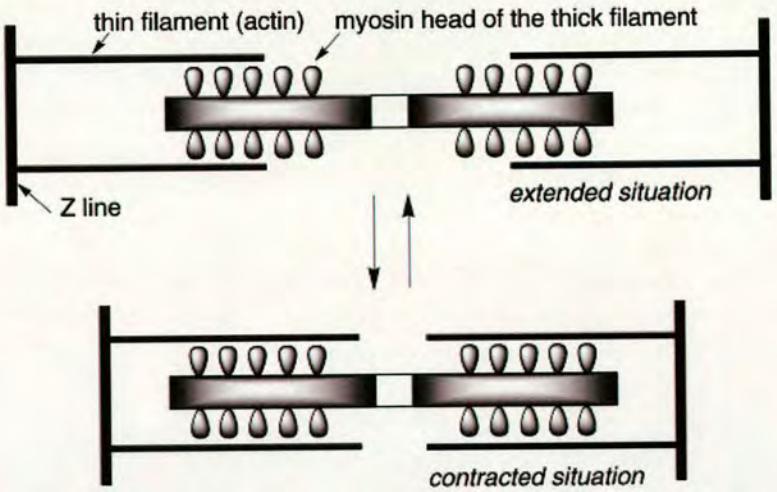

Figure 1.2 Schematic representation of the myosin-actin complex in skeletal muscles.[2e]

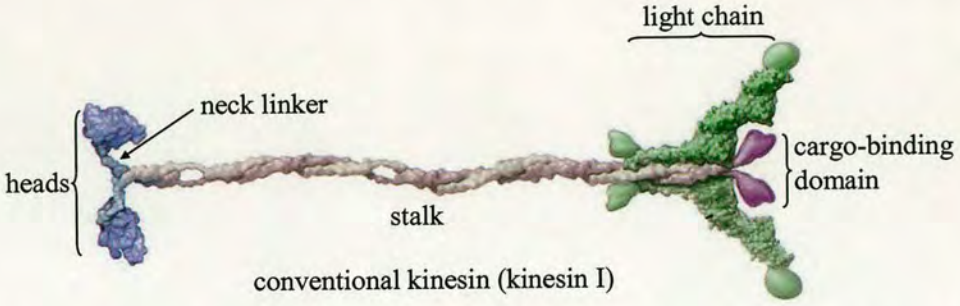

Figure 1.3 Schematic structure of conventional kinesin (kinesin I):[3d] Twin heads (blue) connected *via* short, flexible necks to a long coiled coil stalk (grey) ending in a fan tail (green). The tail binds the cargo, the heads alternately bind to and detach from the microtubule moving in a head-over-head fashion.

Catenanes and rotaxanes are composed of two or more distinct components that are interlocked. These interlocked, or mechanically bound, systems have proved to be an intriguing synthetic challenge to chemists. By definition a mechanical bond prevents distinct components from separating without cleavage of one or more covalent bonds. The catenane (Figure 1.4) derived its name from the Latin, *catena*, meaning chain and it was the first example of a synthetic interlocked molecule.[7] It consists of two or more interlocked macrocyclic rings in which one ring can often move around the other. Closely related to the structure of the catenane is that of the rotaxane; the name again deriving from the Latin *rota* and *axis*, meaning wheel and axle, respectively. The rotaxane (Figure 1.4) consists of macrocyclic rings trapped onto a thread by two bulky stoppers. As with catenanes, there are no covalent bonds

between the macrocycle and the thread, therefore the ring can move around and along the thread portion *via* pirouetting and shuttling motions. In the absence of stoppers, the complex is known as a pseudorotaxane.[8] It is important to note however, that the formation of a pseudorotaxane is a reversible process and as such, the components are not mechanically interlocked.

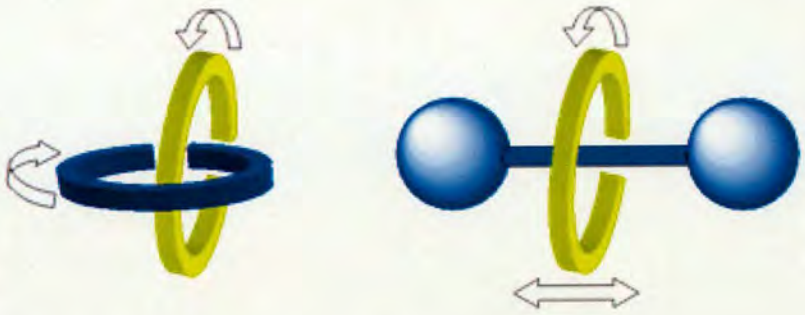

Figure 1.4 Schematic representation of a [2]catenane (left) and a [2]rotaxane (right) and some of the intercomponent motions that can be obtained with catenanes and rotaxanes (shuttling and ring rotation).

1.2 Statistical Threading Approach to Interlocked Structures

Early attempts at the synthesis of interlocked molecules were performed by statistical threading methods. Early catenane and rotaxane synthesis relied on 'chance' for the interlocking of components, inevitably resulting in low yields of the desired products.

The first successful catenane synthesis reported by Wasserman[7] was designed to prove the existence of linked products in macrocyclisation reactions (Scheme 1.1). The reaction of diethyl tetratriacontanedioate **1.1** with sodium yielded the cyclic acyloin **1.2**, Clemmensen reduction of **1.2** with deuterated hydrochloric acid produced the cyclic hydrocarbon **1.3**, the transformation of **1.1** to **1.2** was then carried out with a 1:1 mixture of **1.3** and xylene as solvent and afforded interlocked catenane **1.4**, which could be oxidised with alkaline hydrogen peroxide to give the diacid **1.5**.

Scheme 1.1 First Synthesis of a [2]Catenane by Wasserman[7]

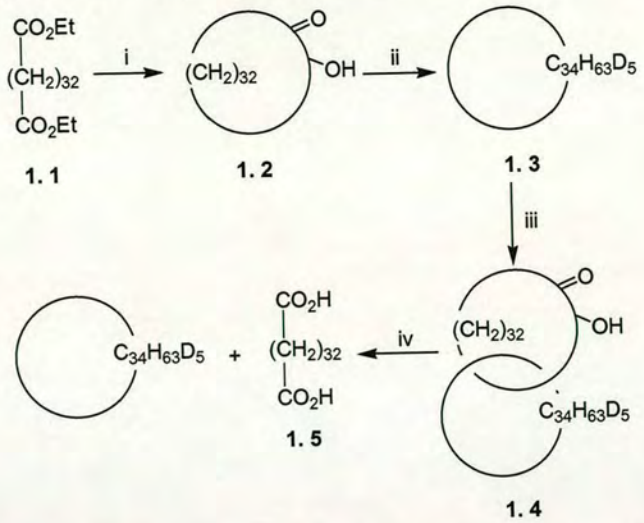

Reagents and conditions: (i) Na, xylene; (ii) Zn, DCl; (iii) bis-ester **1.1**, Na, 1:1 mixture of **1.3** and xylene as solvent; (iv) H_2O_2/OH^-.

Using a similar strategy, the first rotaxane synthesis was reported in 1967 by Harrison and Harrison,[9] using a macrocycle attached to a solid support (Scheme 1.2). The treatment of resin-bound macrocycle **1.6** with a solution of decane-1,10-diol and triphenylmethyl chloride in a mixture of pyridine, DMF and toluene gave traces of the threaded complex, the total yield of this complex was then improved by 70 repetitions of the process, and the reaction products were hydrolysed from the resin, by refluxing with sodium bicarbonate in methanol, yielding only 6% of [2]rotaxane **1.7**.

Scheme 1.2 First Synthesis of a [2]Rotaxane by Harrison and Harrison[9]

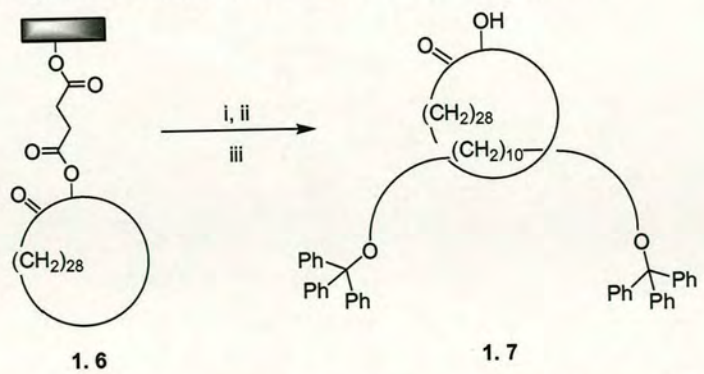

Reagents and conditions: (i) decane-1,10-diol, triphenylmethyl chloride, pyridine, DMF, toluene; (ii) 70 repetitions of process i; (iii) Na_2CO_3, CH_3OH.

1.3 Template Directed Synthesis of Interlocked Architectures

Although the statistical threading approach was subsequently improved, interlocked architectures had remained a chemical curiosity until the early 1980's.[10] The advent of non-covalent templates heralded a new era for interlocked architectures, utilising non-covalent interactions to form stable interlocked complexes (or complexes preorganised for interlocking). Covalent modification of these organised complexes resulted in the synthesis of interlocked molecules in high yields. The application of templation strategies enabled chemists for the first time to contemplate the efficient synthesis of rotaxanes and catenanes.

There are five general strategies for synthesising interlocked molecular architectures (Figure 1.5). These include the 'threading-and-capping' ('threading-followed-by-stoppering'),[11] 'threading-followed-by-swelling',[12] 'threading-followed-by-shrinking',[13] 'clipping'[14] and 'slippage'[15] approaches. Threading-and-capping involves the binding of the unstoppered thread to the macrocycle to form an inclusion complex, or pseudorotaxane; the threading process is in equilibrium with the unthreading process. Capping with bulky stopper groups affords rotaxane; capping with a 'U-shape' leads to catenane formation. It is also possible to swell the non-stoppered end of the pseudorotaxane-like complex to generate a rotaxane (threading-followed-by-swelling). Threading-followed-by-shrinking involves threading a rod-like unit through a macrocycle and then shrinking the free space within the macrocycle through its coordination to a transition metal. The shrinking process involves metal ion coordination by the macrocycle only and the thread does not coordinate to the metal ion, so the ring is not interlocked by the thread in the absence of the metal ion. The clipping approach involves the ring closing after a molecular cross-over point is established. Depending on the nature of the molecular cross-over both rotaxanes and catenanes can be assembled this way. The clipping around a dumbbell shaped thread and another preformed macrocycle generates a rotaxane and a catenane, respectively. Slippage involves the use of a carefully designed, pre-stoppered thread and preformed macrocycle. At elevated temperatures (or pressure), the macrocycle has sufficient energy to slip over the bulky stopper group and an equilibrium between the free components and the inclusion complex is established.

Upon lowering the temperatures (or pressure) the macrocycle is trapped on the thread providing the rotaxane.

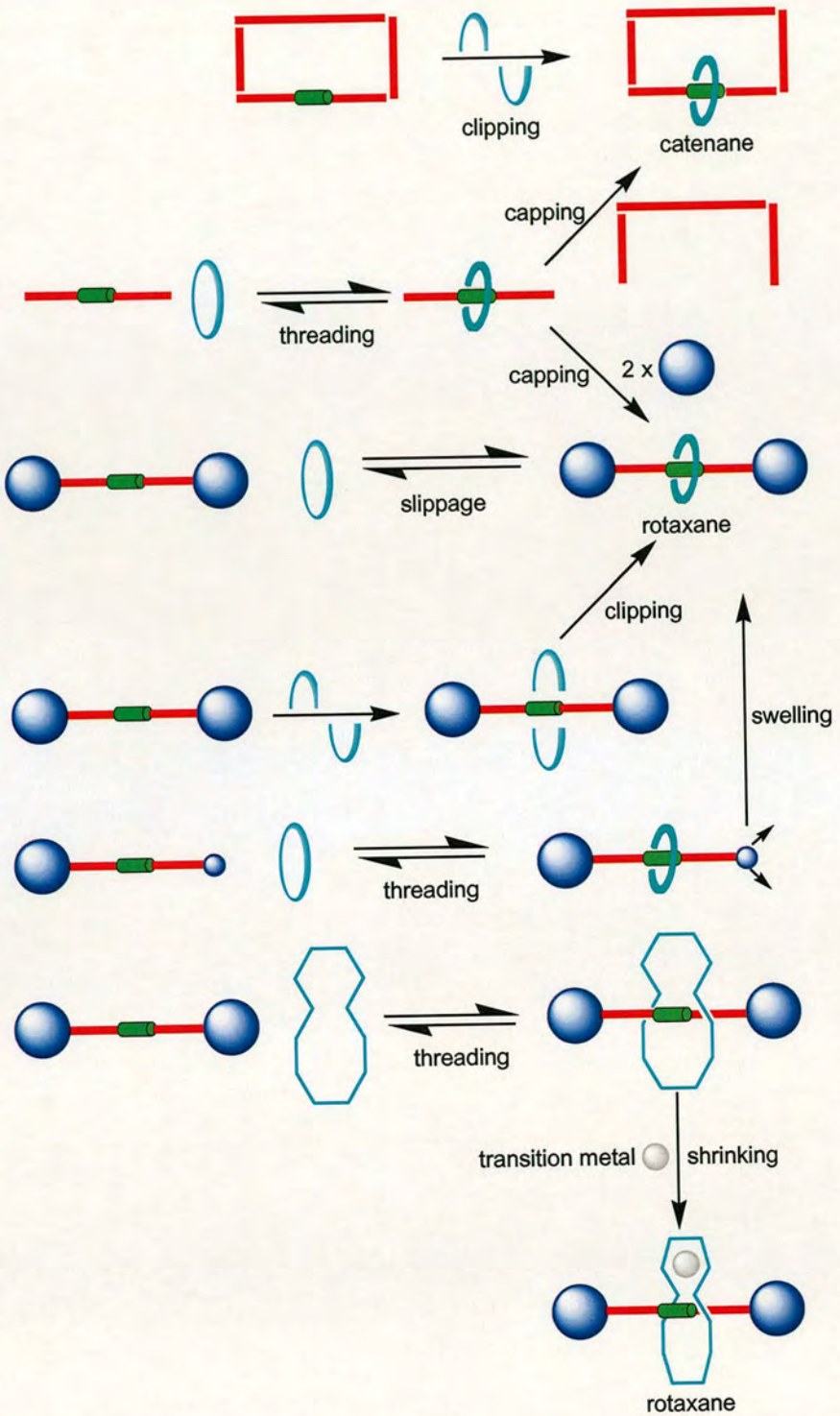

Figure 1.5 Possible synthetic strategies towards interlocked molecular architectures.

1.3.1 Catenanes and Rotaxanes through Transition Metal Coordination

The starting point for the revolution in catenane and rotaxane synthesis occurred during the last part of the 20th century when Sauvage and co-workers observed that metal-ligand coordination can improve yield. They used metal-ligand geometries to fix molecular fragments in three-dimensional space such that they were predisposed to form mechanically interlocked architectures upon macrocyclisation or stoppering reactions. In order to obtain the desired catenate **1.11** they attempted both a threading and a clipping approach (Scheme 1.3).[10] Macrocycle **1.9** endowed with a bidentate phenanthroline ligand was treated with $Cu(CH_3CN)_4BF_4$ and a diphenolic phenanthroline ligand **1.8** to give complex **1.10**. Catenate **1.11** was obtained in a 42% yield by reaction of complex **1.10** with pentaethyleneglycol diiodide (Scheme 1.3, Route A). In the clipping approach complex **1.12**, in which two bidentate phenanthroline ligands are held in a mutually orthogonal manner, was reacted directly with pentaethyleneglycol diiodide in a two ring closing reaction to give catenate **1.11** in a 27% yield (Scheme 1.3, Route B). Demetalation of catenate **1.11** by treatment with $N(CH_3)_4^+ \bullet CN^-$ in acetonitrile-water (1:4) affords catenand quantitatively at room temperature.[10b]

Scheme 1.3 Sauvage's Original Cu(I) Directed [2]Catenate Synthesis[10]

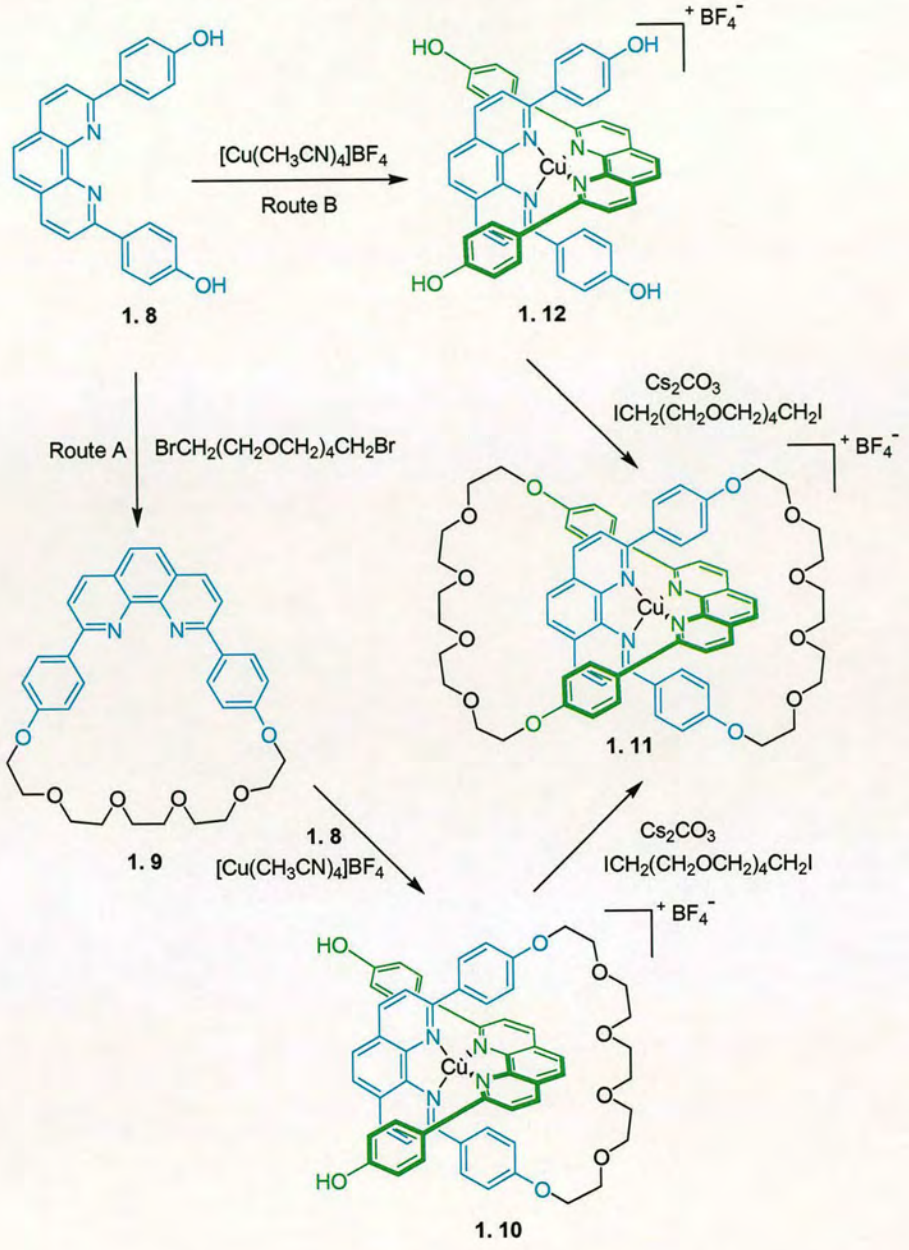

Besides this four-coordinate (tetrahedral)[16] copper(I) template, five- (trigonal bipyramidal and square pyramidal),[17] six- (octahedral)[18] and four-coordinate (square-planar)[19] metal templates were subsequently developed as efficient synthetic methods to rotaxanes and catenanes (Figure 1.6).

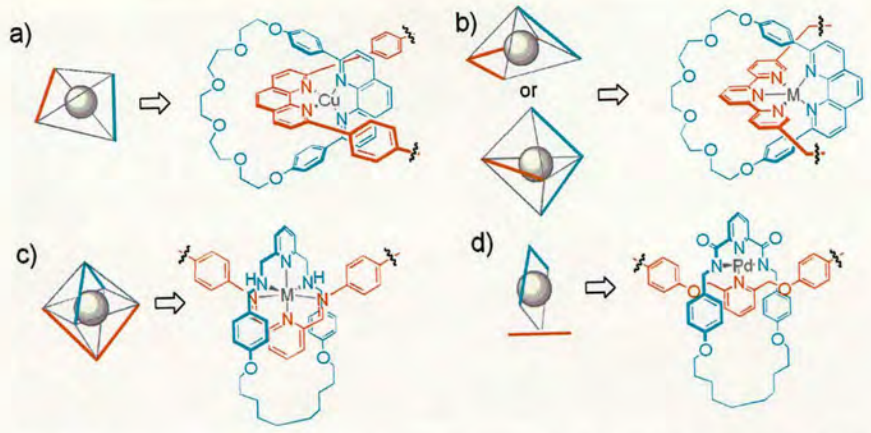

Figure 1.6 Exploiting transition-metal-ligand geometries in the synthesis of mechanically interlocked architectures:[19] a) tetrahedral, b) square pyramidal and trigonal bipyramidal, c) octahedral and d) square-planar coordination motifs.

1.3.2 Catenanes and Rotaxanes through Charge-Transfer (CT) Interactions

The charge-transfer (CT) interactions or electron donor-acceptor interactions between π-systems are an important class of non-covalent interactions and have been exploited in the design and synthesis of self-organising systems.[20] In particular, the CT interactions between electron-deficient 4,4'-bipyridinium derivatives and electron-rich aromatics have been extensively used to build mechanically interlocked molecules such as rotaxanes and catenanes, which later led to an elegant series of molecular machines and switches.[21]

Stoddart and co-workers utilised these electron donor-acceptor interactions as a template to synthesise a catenane incorporating two different macrocycles (Scheme 1.4).[22] By reacting the 'U-shape' precursor bis(pyridinium) salt **1.13** with a stoichiometric amount of *p*-xylylenedibromide **1.14** in the presence of excess of bisparaphenylene-34-crown-10 macrocycle **1.16** (BPP34C10) in acetonitrile at room temperature, the [2]catenane **1.18** was obtained in a 70% yield. The high yield of this one-step template-directed synthesis is remarkable, considering that there is no initial association between **1.13** and **1.16**. After a single reaction of **1.13** with **1.14**, the paraquat dication unit is sufficiently electron-deficient for a favorable interaction to occur with the electron-rich crown ether **1.16**, and the inclusion complex **1.17** is formed. This precursor then undergoes intramolecular ring closure to give the [2]catenane **1.18**. X-ray crystallographic analysis has confirmed the elegantly ordered

structural arrangement with the tetracationic cyclobis(paraquat-*p*-phenylene) intimately interlocked with the bisparaphenylene-34-crown-10. The dominant non-covalent bonding interactions are associated with the mutual sandwiching of a hydroquinol unit between parallel-aligned bipyridinium moieties and of a bipyridinium moiety between parallel-aligned hydroquinol units.

Scheme 1.4 Stoddart's Original Paraquat-Crown Ether [2]Catenane Synthesis[22]

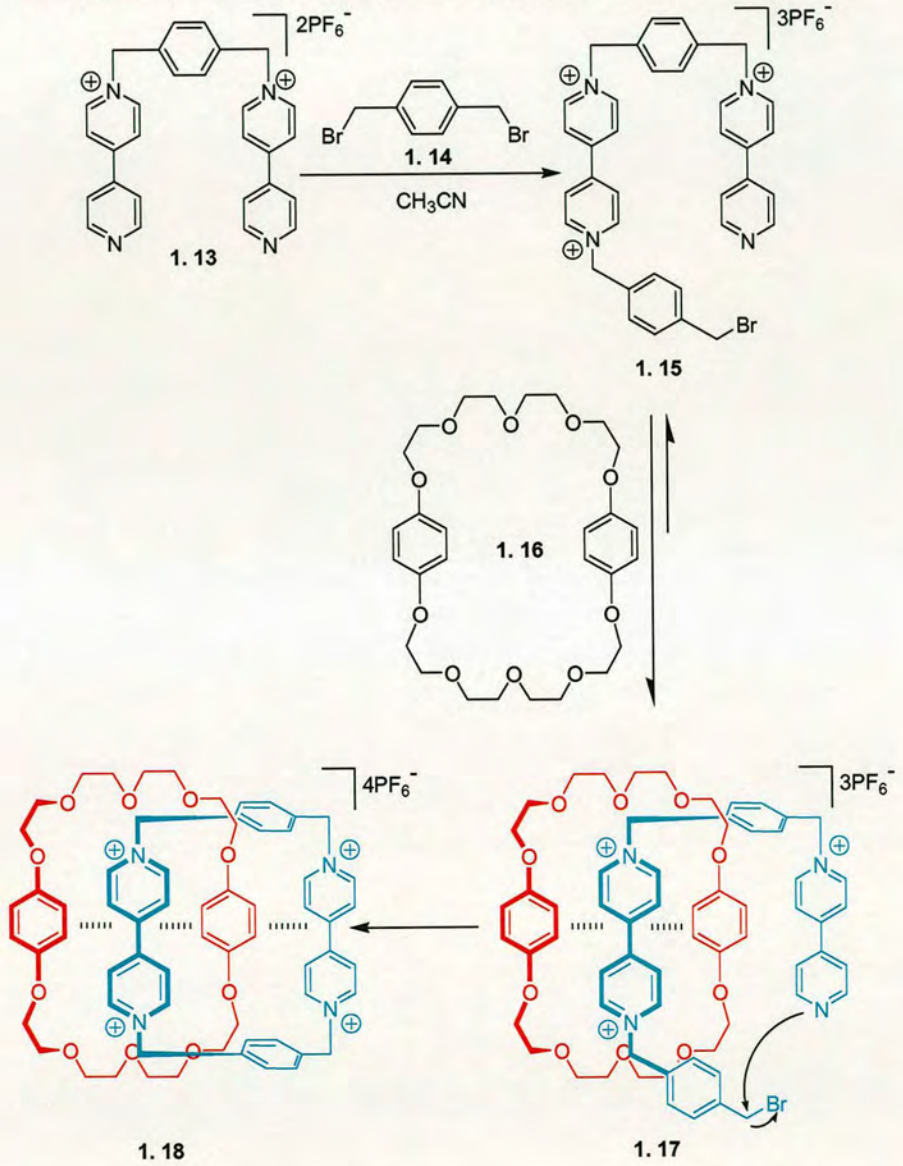

Using a similar strategy, a [2]rotaxane **1.20** was synthesised without the use of a covalent template (Scheme 1.5);[23] this is the first example of two-identical-station

molecular shuttle. Reaction of equimolar amounts of **1.13** with **1.14** at room temperature for 7 days in the presence of an excess of the polyether thread **1.19** and $AgPF_6$ gave **1.20** in a 32% yield. The ^1H NMR spectrum of **1.20** exhibited a single process of shuttling of the macrocycle between the two hydroquinol stations on the polyether thread. Electron-rich tetrathiafulvalene (TTF) derivatives have also been incorporated into more elaborate molecular systems acting as sensors and molecular switches by virtue of their ability to form CT complexes with a variety of π-electron acceptors.[24]

Scheme 1.5 Stoddart's Original Paraquat-Poly Ether [2]Rotaxane Synthesis and Its Shuttling Process[23]

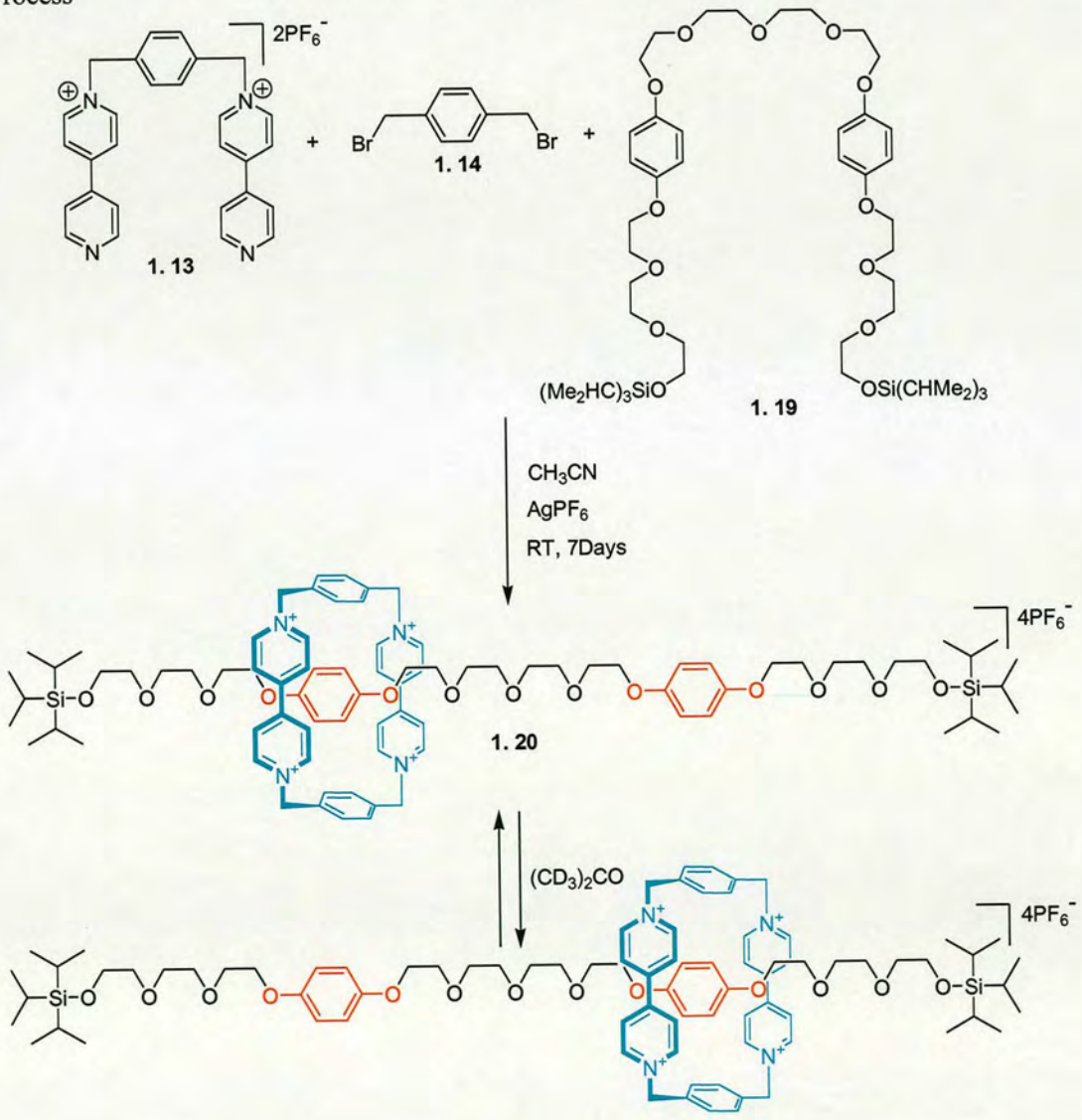

1.3.3 Catenanes and Rotaxanes through Hydrophobic Interactions

Cyclodextrins (CDs) are 1→4 α linked cyclic oligomers of anhydroglucopyranose.[25] Those CDs consisting of six, seven, or eight glucose entities are called α-, β-, or γ-CDs, respectively (Figure 1.7).[26] CDs assume a shape with the primary hydroxyl groups at the narrow side and the secondary hydroxyl groups at the wide side. CDs have been widely used as the ring molecules for rotaxane synthesis,[26, 27, 28] because they are readily available in both high purities and large quantities, and furthermore, CDs can be functionalised by a wide variety of synthetic methods.[25] The general approach currently available for the synthesis of CD rotaxanes is the threading-followed-by-stoppering strategy; the major driving forces for the formation of CD inclusion compounds are hydrophobic and van der Waals interactions between the inner surface of the CD ring and the hydrophobic sites on the guest.[28]

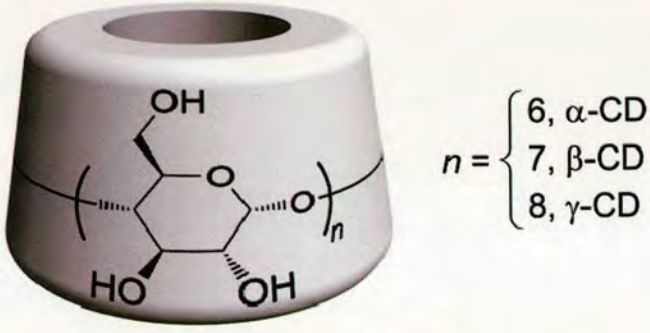

Figure 1.7 Schematic drawing of cyclodextrins (CDs).[28]

Coupling reactions of terminal amino groups are quite useful for the synthesis of CD rotaxanes. In 1981, Ogino reported the first synthesis of a α-CD rotaxane **1.22** in a 19% yield by coupling bulky bis(ethylenediamine)cobalt(III) complex **1.21** to 1,12-diaminododecane threaded through α-CD in DMSO solution (Scheme 1.6).[29]

Scheme 1.6 First Synthesis of a Cyclodextrin-Based [2]Rotaxane by Ogino[29]

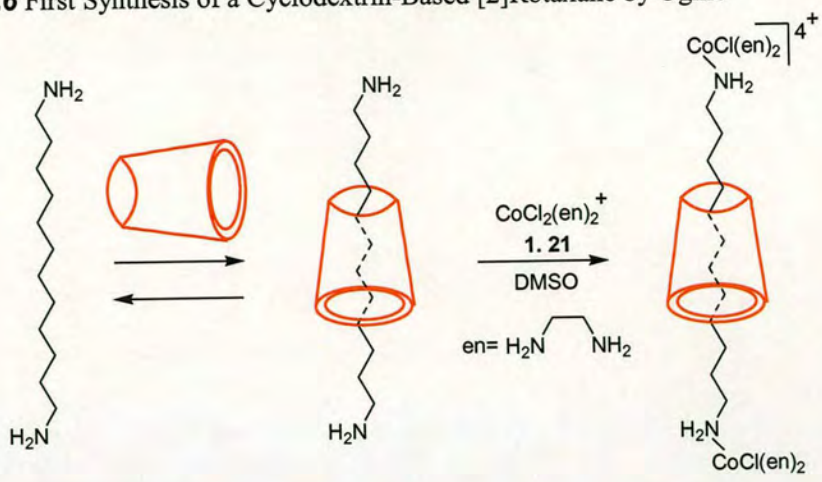

1. 22

Transition metal catalysed C-C bond formation is also useful for rotaxane formation. For example, the α-CD rotaxane with isophthalic acid stoppers **1.25** was synthesised in an excellent yield of 73% by reacting bulky water soluble aryl iodide **1.23** with diboronic acid **1.24** in the presence of α-CD, in an aqueous solution containing palladium(II) acetate (Scheme 1.7).[30] The solid state structure of **1.25** (as the tetracarboxylic acid) was investigated; it represents the first crystal structure determination of any CD-based rotaxane.

Scheme 1.7 Synthesis of a Cyclodextrin-Based [2]Rotaxane by Suzuki Coupling[30]

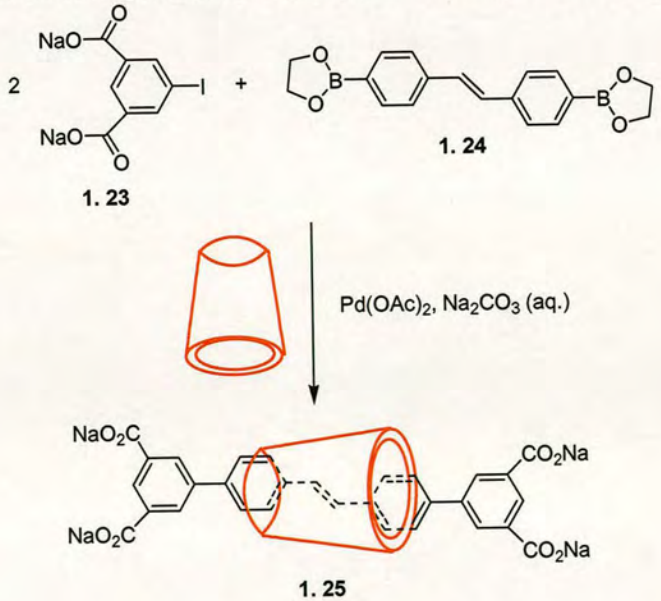

1. 25

1.3.4 Catenanes and Rotaxanes through Hydrogen-Bonding

Reversible molecular interactions in biochemical systems such as folding of macromolecules, binding of substrates to enzymes, and the cellular interactions are mediated by three different kinds of forces:[31] hydrogen bonds, electrostatic bonds and van der Waals forces. These three fundamental non-covalent interactions differ in their geometrical requirements, strength and specificity, and in the influence that water exerts on the interaction or bonding. Of particular importance in non-covalent interactions is the hydrogen bond.[32] Classically, the donor atom in a hydrogen bond is an oxygen atom or a nitrogen atom that has a covalently attached hydrogen atom and the acceptor atom can be either oxygen or nitrogen (X-H•••Y). The bond energies associated with these bonds range from 3 to 7 kcal/mol, thus hydrogen bonding is much weaker than covalent bonds (50-100 kcal/mol). An important feature of the hydrogen bond is that it is highly directional. The strongest hydrogen bond is one in which the donor and acceptor atoms are co-linear and if the acceptor atom is at an angle to the donor atom, the bond is much weaker. In recent times, non-covalent synthesis based on hydrogen bonded interactions has been developed for the construction of a variety of interlocked molecular structures.

1.3.4.1 Amide-Based Catenanes and Rotaxanes

Amide-based unsubstituted (**1.26**, Scheme 1.8)[33] and methoxy-substituted (**1.27**, Scheme 1.9)[34] catenanes were published independently in 1992 by Hunter and Vögtle, respectively. It is reasonable to assume that the perpendicular preorganisation of the catenane building blocks is based on three templating effects: (a) steric complementarity, (b) hydrogen bonding between carbonyl oxygen atoms and amide protons, and (c) π-π interactions between the benzene rings of host and guest subunits.

Scheme 1.8 First Synthesis of a Unsubstituted Amide-Based [2]Catenane by Hunter[33]

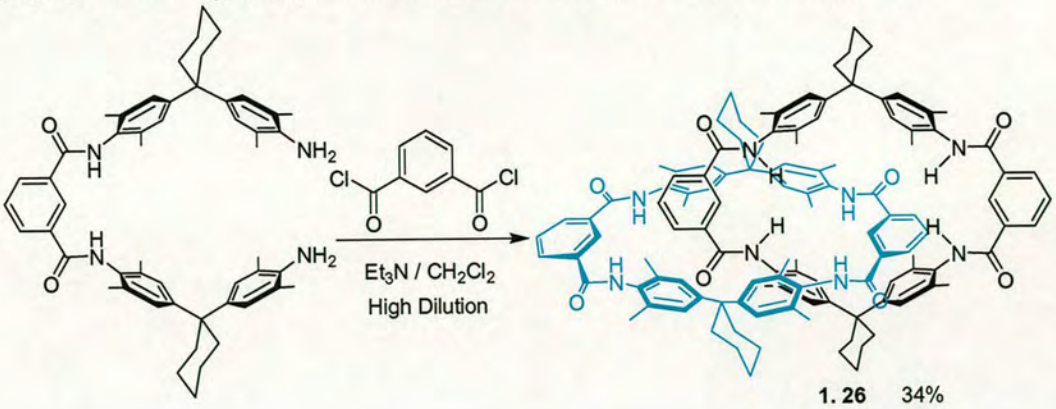

1. 26 34%

Scheme 1.9 First Synthesis of a Methoxy-Substituted Amide-Based [2]Catenane by Vögtle[34]

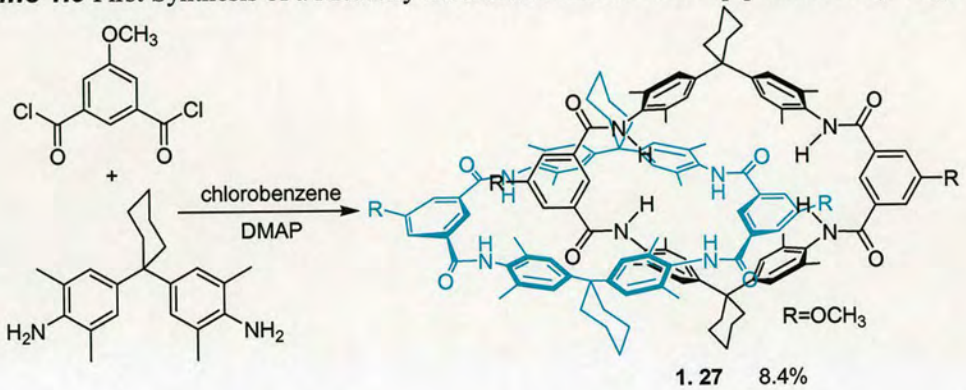

1. 27 8.4%

In 1995, Leigh and co-workers reported the serendipitous formation of a new amide-based [2]catenane **1.28** prepared in one step from two commercially available starting materials in a 20% yield (Scheme 1.10).[35] The [2]catenane **1.28** is the first amide-based catenane for which the structure has been determined by X-ray crystallography (Figure 1.8). The solid-state ensemble is dominated by inter- and intramolecular hydrogen bonding interactions together with π-stacks composed of four aromatic rings.

Scheme 1.10 One-Step, Eight-Molecular Condensation to Give the [2]Catenane[35]

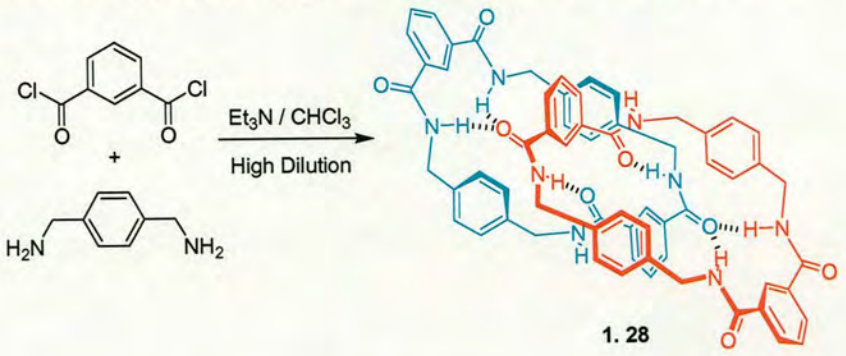

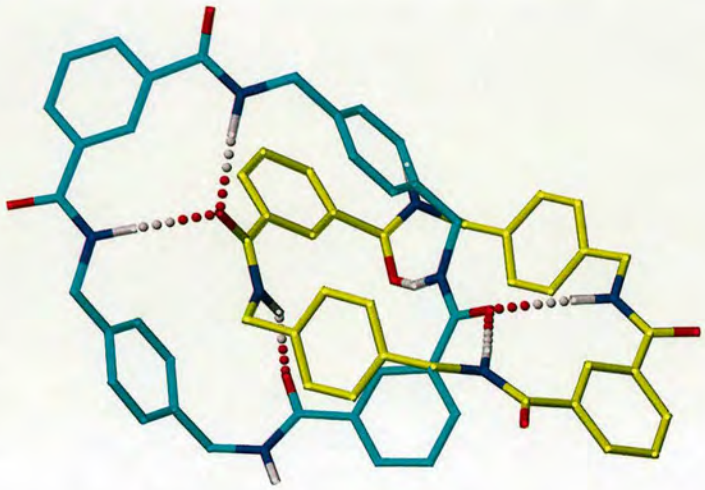

Figure 1.8 First X-ray crystal structure of amide-based [2]catenane **1.28**.[35]

Whereas other approaches need phenanthroline units acting as Cu(I) template (see 1.3.1) or 4,4'-bipyridinium tetracationic units leading to salt structures (see 1.3.2), the amide-based system is electrically neutral and does not need special complexing building blocks. Leigh and co-workers utilised the rigid fumaryl-based threads **1.29-1.31** to template the formation of benzylic amide macrocycles about them to give rotaxanes **1.32-1.34** by five component clipping reactions (Scheme 1.11).[36] With good hydrogen bond acceptors (amides) a 'world record' yield of 97% for a [2]rotaxane **1.32** is obtained, its crystal structure (Figure 1.9) shows that the positioning of the amide groups in the fumaramide thread **1.29** allows them to form four bifurcated intercomponent hydrogen bonds without requiring any distortion in the conjugation of the isophthalamide systems (the amides are close to planar with

the aromatic rings) while the macrocycle adopts a favorable chair conformation. In fact, in the absence of a suitable template, the precursor to macrocycle formation **1.35**, preferentially adopts a linear conformation as a consequence of the preference for the aromatic 1,3-diamide unit to adopt a *syn-anti* conformation, which holds the two reactive ends of **1.35** far apart in a spatial arrangement unsuitable for macrocyclic ring closure. But cooperative multipoint hydrogen bonding between the precursor and a thread can promote a conformational changes (now *syn-syn*) which brings the amine and acid chloride in close proximity leading to rapid cyclisation of **1.35** (Scheme 1.11).

Scheme 1.11 Rotaxane Formation *via* Preorganised, Rigid Fumaryl-Based Hydrogen Bond Templates[36]

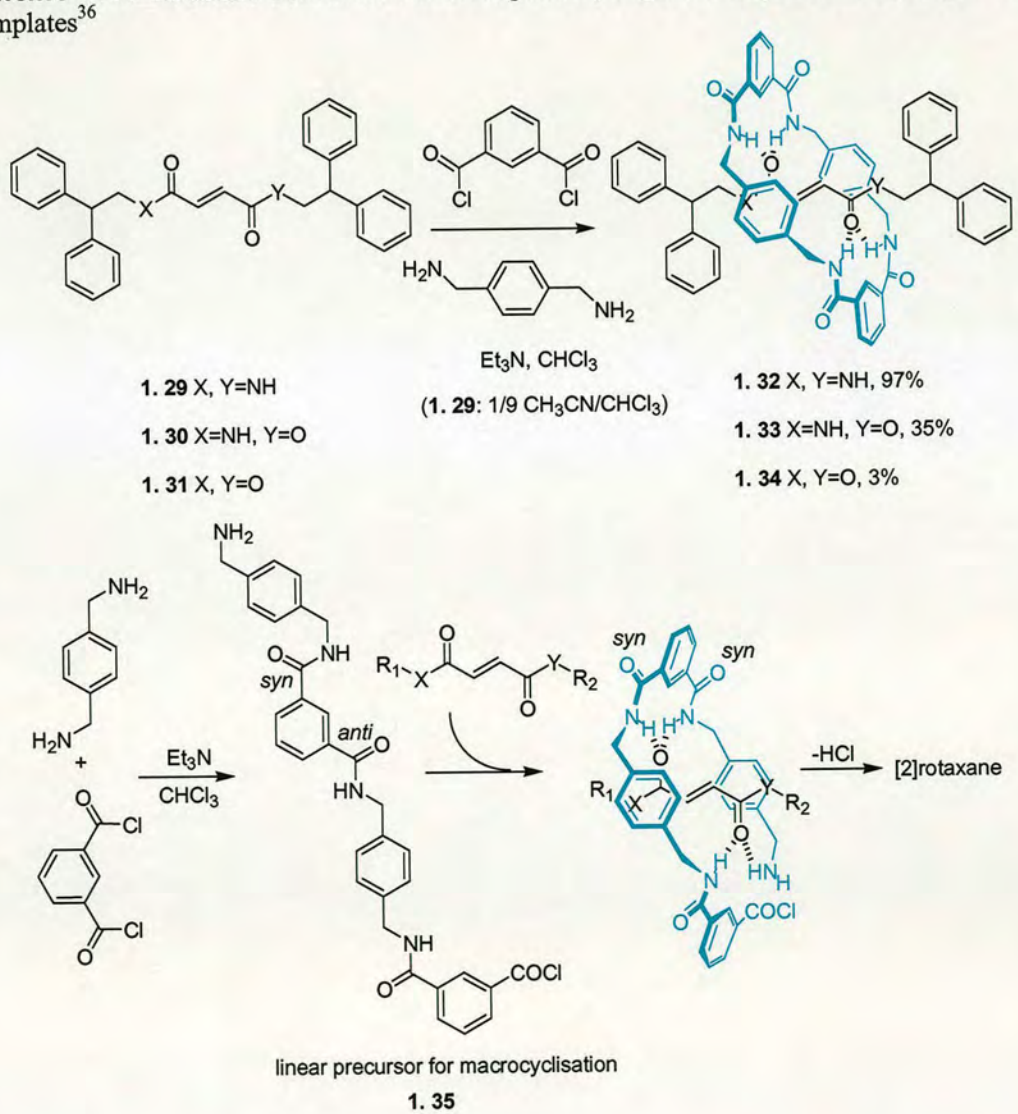

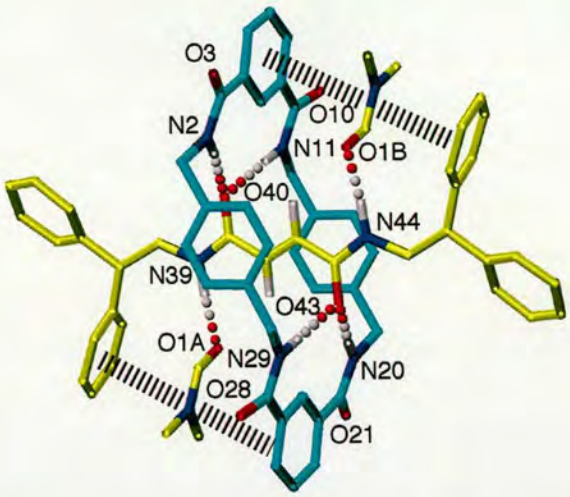

Figure 1.9 X-ray crystal structure of fumaramide-based [2]rotaxane **1.32**.[36] Intramolecular hydrogen bond distances (Å): O40–HN2/O43–HN20 1.98, O40–HN11/O43–HN29 2.06.

1.3.4.2 Anion-Templated Assembly of Interlocked Structures

Inspired by the ubiquitous roles negatively charged species play in chemical, biological and environmental processes, interest in the recognition of anions has grown over the past few decades; anion-templated assembly is now an established and important area of supramolecular chemistry.[37] Beer and co-workers have developed a general anion templation strategy for the construction of a variety of interpenetrated and interlocked molecular structures based on anion recognition and ion-pairing. For example, by virtue of the chloride anion template, a pyridinium chloride thread **1.36** (shown in red, Scheme 1.12) and a neutral acyclic molecule incorporating an isophthalamide anion binding cleft **1.37** (shown in dark blue) associate strongly in non-competitive solvents and undergo ring-closing metathesis (RCM) to give [2]rotaxane **1.38** in a 47% yield (Scheme 1.12).[38] Its single crystal X-ray structure determination confirms the presence of four NH•••Cl^- hydrogen bonds and secondary stabilising π-π stacking interactions and N^+CH_3•••O hydrogen bonding. Interestingly, after exchange of the templating chloride anion for the PF_6 anion using $AgPF_6$, the resulting rotaxane exhibits a high selectivity for chloride; although the pyridinium PF_6 thread alone binds anions with a selectivity trend $AcO^- >> H_2PO_4^- > Cl^-$. These differences in anion selectivity can be ascribed to the creation of a unique hydrogen bond donating pocket formed by the diamide clefts of the cation and

macrocycle in the [2]rotaxane superstructure, which is of complementary topology for the chloride anion.[38]

Scheme 1.12 An Anion-Templated [2]Rotaxane Formation Proceeds *via* RCM Reaction[38]

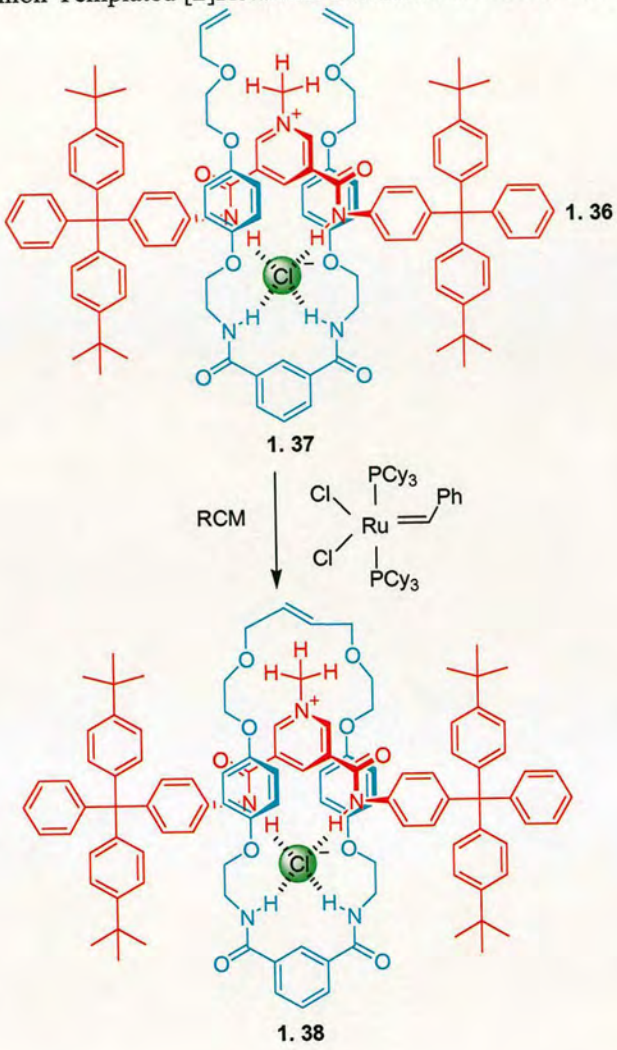

The first example of the use of anion templation to synthesise catenanes was also demonstrated with the development of this methodology.[39] Mixing components **1.39** (shown in red, Scheme 1.13) and **1.40** (shown in dark blue) in DCM followed by addition of Grubbs' catalyst to afford the [2]catenane **1.41** in a 45% yield in addition to a small amount (<5%) of the [3]catenane **1.42** (Scheme 1.13). The crystal structure of **1.41** confirms the interlocked nature of the two macrocyclic rings and the location of the chloride anion within the amide cavity. As was demonstrated in [2]rotaxane **1.38**, after template removal, the [2]catenane **1.41** exhibits chloride anion selective

binding behaviour, which is postulated to be the result of the creation of a unique, topologically constrained catenane binding pocket formed by the two amide clefts of **1.41**.[39]

Scheme 1.13 First Synthesis of Anion-Templated [2]Catenane and [3]Catenane[39]

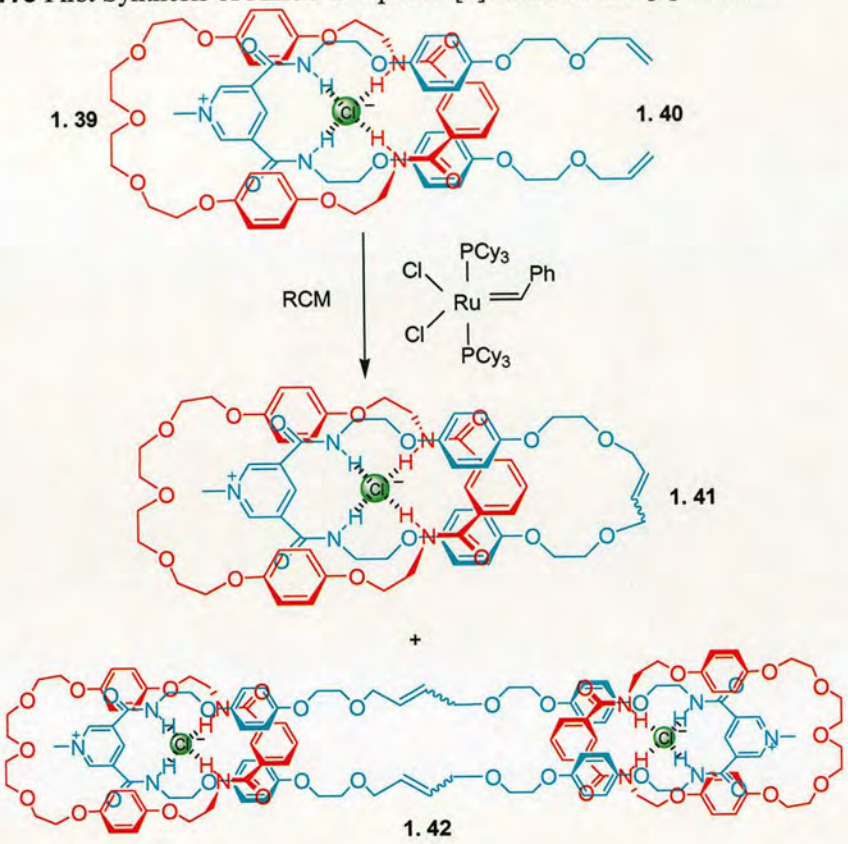

1.3.4.3 Binding of Secondary Dialkylammonium Ions with Crown Ethers

One of the simplest recognition motifs that is used to produce pseudorotaxanes, complexes that are often the precursors of catenanes and rotaxanes, is the binding of secondary dialkylammonium ions with suitably large macrocycles, for example, dibenzo-24-crown-8 (DB24C8) or bis-*p*-phenylene-34-crown-10 (BPP34C10).[40] Rotaxanes based on secondary alkylammonium threads and crown ether rings have been developed by the threading-followed-by-stoppering, clipping and slippage approaches. A representative example was reported by Stoddart and co-workers in 1996 (Scheme 1.14).[41] They used dibenzyl ammonium ion **1.43** and dibenzo-24-crown-8 **1.44** to form a 1:1 complex **1.45** in methylene chloride, which is stabilised

by a result of [N^+-H•••O] and [C-H•••O] hydrogen bonding, and capping the thread component by addition of excess di-*tert*-butyl acetylenedicarboxylate **1.46** and refluxing for several days gave the [2]rotaxane **1.47** in a 31% yield.

Scheme 1.14 Dialkylammonium Ion-Crown Ether-Binding-Directed Synthesis of a [2]Rotaxane[41]

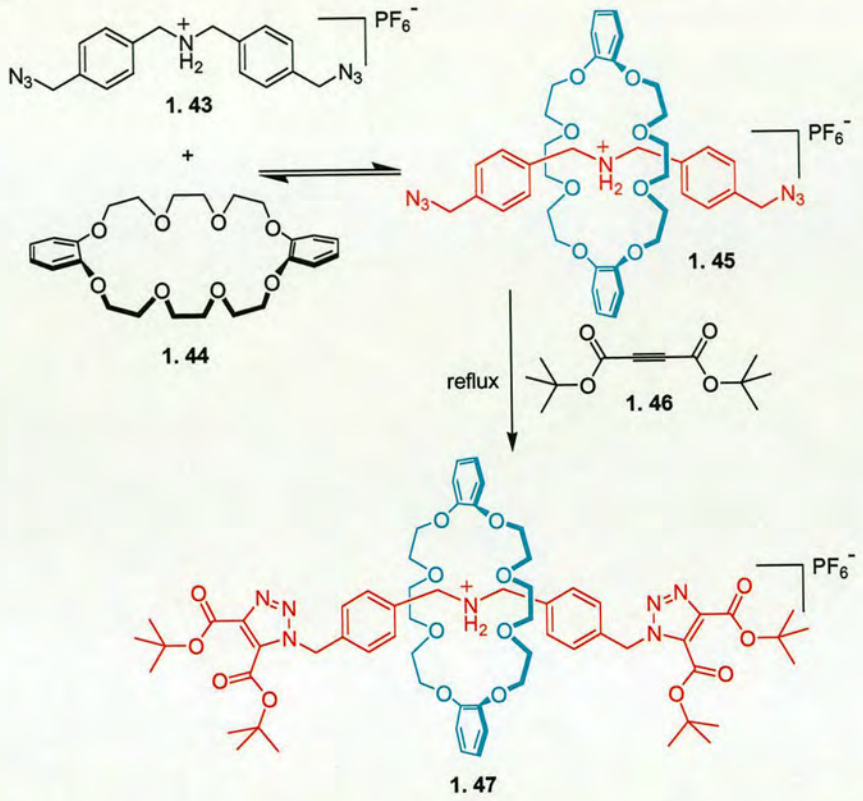

1.4 Molecular Machines Based on Mechanically Interlocked Systems

1.4.1 Concept of Molecular-Level Machines

A machine is defined as an assembly of parts that transmit and modify forces, motion, and energy in a predetermined manner. When the word 'parts' is replaced by 'molecules', a machine turns into a molecular or supramolecular machine. Therefore, a molecular machine is defined as an assembly of a distinct number of molecular components designed to perform machine-like movements in response to an appropriate external stimulus.[27] In addition, a molecular machine has characteristic features imparted on it by the subunits used.

The problem of the construction of molecular-scale mechanical machines was posed for the first time by Richard P. Feynman, Nobel Laureate in Physics, in a famous address entitled 'There is plenty of room at the bottom' to the Meeting of the American Society of Physics in 1959:[42] "*The principles of physics, as far as I can see, do not speak against the possibility of maneuvering things atom by atom. It is not an attempt to violate any laws; it is something, in principle, that can be done; but in practice, it has not been done because we are too big.... An internal combustion engine of molecular size is impossible. Other chemical reactions, liberating energy when cold, can be used instead.... Lubrication might not be necessary; bearings could run dry; they would not run hot because heat escapes from such a small device very rapidly....* ". He described building with atomic precision, and even sketched out a pathway involving a series of increasingly smaller machines. He explained: "*If we go down far enough, all of our devices can be mass produced so that they are absolutely perfect copies of one another.... I can't see exactly what would happen, but I can hardly doubt that when we have some control of the arrangement of things on a small scale we will get an enormously greater range of possible properties that substances can have, and of different things that we can do*". Although he did not use the term, it is clear that Feynman was pointing toward what is today termed as molecular manufacturing, a goal of using systems of molecular machines to build with precision at the atomic level subsequently explored by Drexler as molecular engineering;[43] an approach for the development of general capabilities for molecular manipulation. Thinking in terms of molecular machines leads to a fundamental change of understanding. Rather than thinking physical matter as a given, with an uncontrollable structure needing to be carved into smaller pieces of approximately the correct composition and shape, matter can be perceived as something to be manipulated far more precisely, building products from the 'bottom-up'. The 'top-down' method of constructing miniaturised devices is reaching a fundamental limit for sizes below 50 nanometres,[44] yet molecules are convenient nanometre-scale building blocks to be used to construct ultra-miniaturised devices and machines.[44a] If this could be actualised, it potentially would not only affect every physical object from computers to the human body, but could also open the way to new technologies in the fields of medicine, environment, energy and materials.[45]

Like macroscopic machines, molecular-level machines are characterised[44, 45] by (a) the kind of energy input supplied to make them work, (b) the kind of movement performed by their components, (c) the way in which their operation can be controlled and monitored, (d) the possibility to repeat the operation at will, (e) the time scale needed to complete a cycle of operation, and (f) the function performed. However, there are two main distinctions between motion at the molecular level and in the macroscopic world.[44a] One fundamental difference is that the random thermal fluctuations (Brownian motions) experienced by molecules dominate mechanical behaviour in the molecular world but can be neglected for big objects. Another difference in the macroscopic world, motion is inertia-dominated, but as objects become less massive and smaller in dimension, inertial terms decrease in importance and viscous forces begin to dominate.

1.4.2 Interlocked Architectures as Molecular-Level Machines

As shown in 1.1, the mechanical bond in catenane and rotaxane structures severely restricts the relative degrees of freedom of the components in several directions, while often permitting extraordinarily large amplitude motion in an allowed vector. Just like the restrictions of movement imposed on biological motors by a track, catenanes and rotaxanes can play a central role in the development of synthetic molecular machines.

The molecular machines can be photochemically-, electrochemically- and chemically-driven using an external stimulus (S).[46] The simplest machine (Figure 1.10, Type III) that can be constructed is a pseudorotaxane in which the threading and dethreading is induced by an external input; this is reminiscent of the movement of a piston in a cylinder. In a bistable rotaxane (Figure 1.10, Type I), the machine-like behaviour can be obtained when an outer stimulus causes a shift of a ring between two different stations along a wire, thereby obtaining a prototype of a molecular shuttle. In a catenane (Figure 1.10, Type II), one of the two rings can be forced to rotate around the other one with clockwise or anti-clockwise motion. Control of the motions of the components in those systems results in a change in properties which produce a signal that allows the operation of the machine to be monitored.

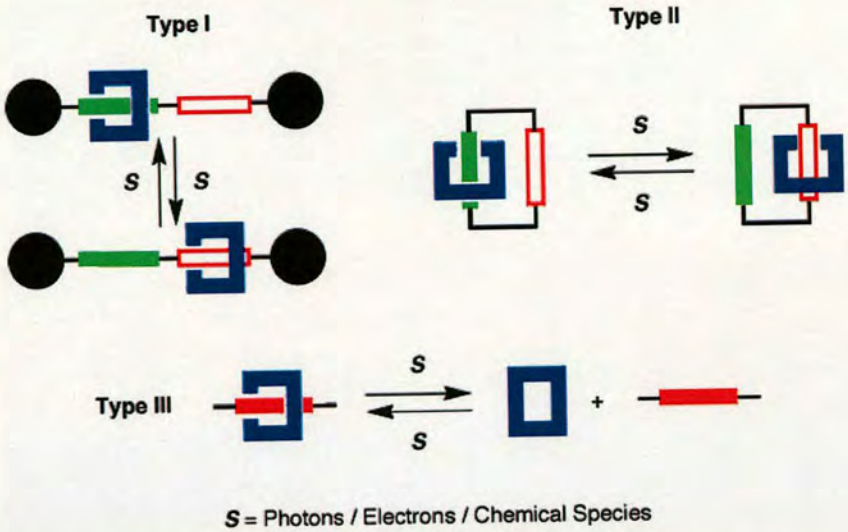

Figure 1.10 Schematic representations of molecular machines based on rotaxane (Type I), catenane (Type II) and pseudorotaxane (Type III) structures.

1.4.2.1 Rotaxane-Based Linear Molecular Motors

Rotaxane-based systems that are capable of translational shuttling have dominated the field of artificial molecular machines. As shown in Scheme 1.5, Stoddart and co-workers reported the first molecular shuttle **1.20** in 1991.[23] In this case, the tetracationic macrocycle exhibits a degenerate shuttling process between the two identical hydroquinol stations along the polyether thread with ca. 13 kcal/mol free energy barriers. Energy barriers are affected by both binding strength and distance between the stations (Figure 1.11).

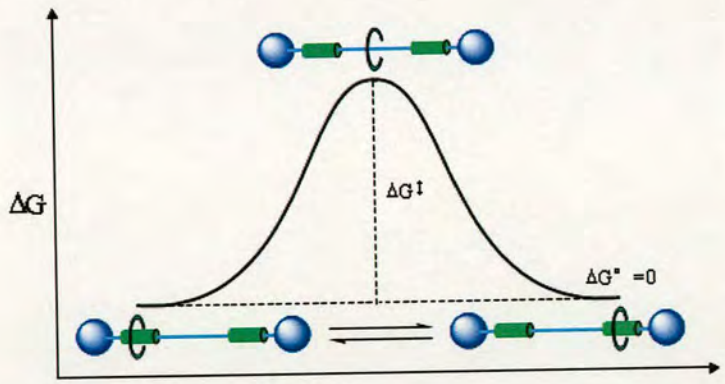

Figure 1.11 A cartoon representing the degenerate shuttling movement between two identical stations in a molecular shuttle and the idealised free energy profile ($\Delta G^{\ddagger}$ contains the energy required to break the non-covalent interactions holding the ring to the station and a distance-dependent diffusional component).

However, the molecular shuttle could be desymmetrised by inserting non-identical stations along the thread and if suitably large differences in macrocycle binding affinity between two stations exists, the macrocycle resides overwhelmingly in one positional isomer or the so-called 'co-conformation'[47] (a Boltzmann distribution at 298 K requires a $\Delta\Delta G$ between translational co-conformers of ~2 kcal/mol for 95% occupancy of one station).[48] An external trigger can be used to chemically modify the system and alter the non-covalent intercomponent interactions such that the second macrocycle binding site becomes energetically more favoured. This results in translation of the ring along the linear thread to the second station through biased Brownian motion. The system ideally should be reversible by using a second stimulus to restore the original order of station binding affinities (Figure 1.12).[48] The change of the net location of the macrocycle can be used to perform a mechanical task.[49]

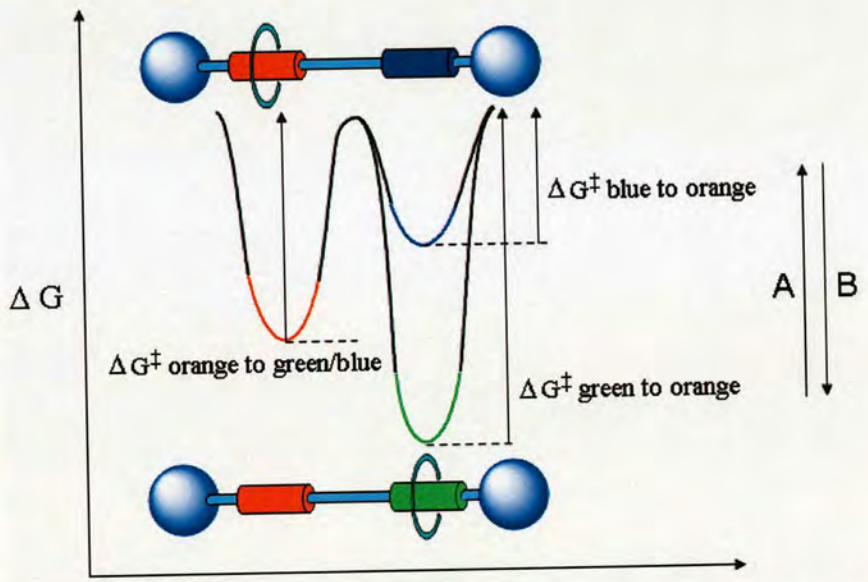

Figure 1.12 Translational submolecular motion in a stimuli-responsive molecular shuttle:[48] Stimulus A induces a green to blue transformation, and stimulus B induces a blue to green transformation. Biased Brownian motion arises from a difference in the activation energies for movement in different directions.

Stimuli-responsive molecular shuttles have been reviewed extensively,[46] it would be impossible to show all the recent advances made in this field, instead, some

original and sophisticated examples will be provided to highlight according to the different external stimuli.

1.4.2.1.1 Acid-Base-Controllable Motion

The first bistable stimuli-responsive molecular shuttle was designed in 1994 (Scheme 1.15).[50] In rotaxane **1.48**$^{4+}$ the tetracationic macrocycle occupies the benzidine site more favourably in a ratio of 84:16 at 229 K due to its better π-electron donor ability. Protonation of the benzidine site with CF_3COOD destabilises its interaction with the macrocycle because of the electrostatic repulsion and now the macrocycle moves to sit preferentially over the biphenol site in **1.48**$^{6+}$. Deprotonation restores the system to its initial state. It is important to note that this system can be switched by electrochemical means as well.[50]

Scheme 1.15 First Synthesis of a Bistable Stimuli-Responsive Molecular Shuttle[50]

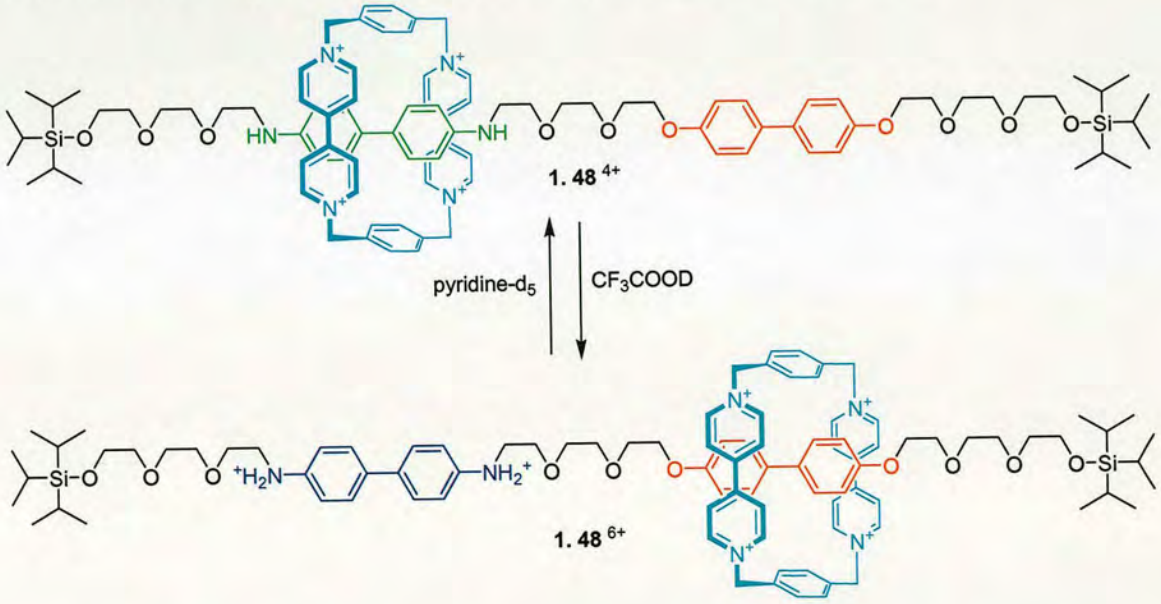

A system denoted as a 'molecular elevator' composed of three rotaxane units interlocked mechanically to a platform was reported recently (Scheme 1.16).[51] The trifurcated guest **1.50** and the tritopic host **1.49** in a $CHCl_3/CH_3CN$ solution form a 1:1 adduct that was converted to the molecular elevator **1.51** in the reaction with 3,5-di-*tert*-butylbenzyl bromide and followed by counterion exchange. At low pH, the dialkylammonium ion ($CH_2NH_2^+CH_2$) site binds the benzo-24-crown-8 macrocycle

preferentially (upper level), at high pH, deprotonation of the ammonium center occurs with loss of [N^+-H•••O] hydrogen bonding and the macrocycle will move to the bipyridinium dication site (lower level) which is stabilised mainly by electron donor-acceptor interactions, this process is completely reversible. As a result, the platform where three macrocycles connected can move between two levels by adding acid or base. Since this initial work a second generation molecular elevator has been synthesised.[52]

Scheme 1.16 First Synthesis of a 'Molecular Elevator'[51]

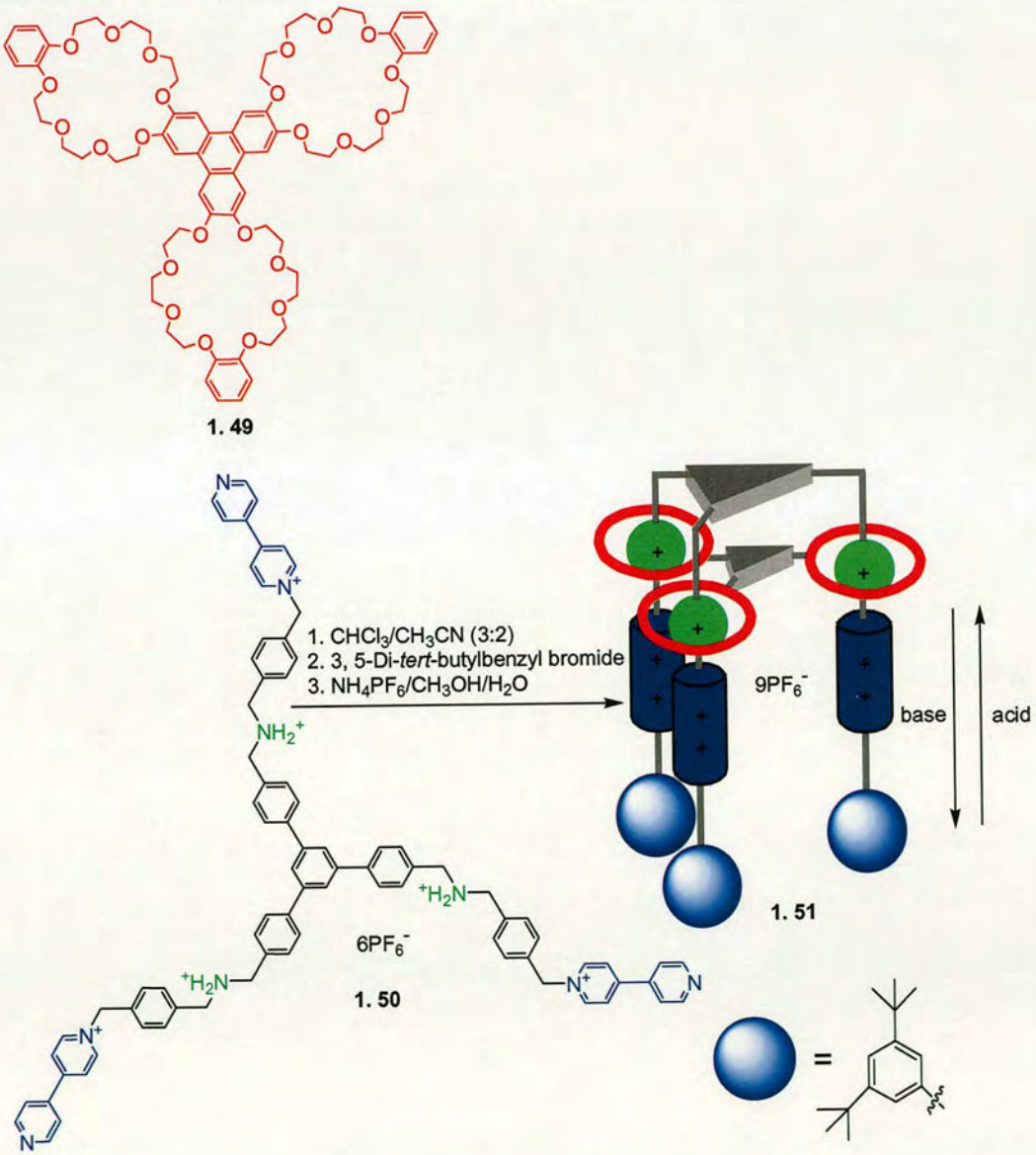

Keaveney and Leigh demonstrated that the rotaxane **1.52**•H, which was formed by neutral hydrogen-bond templation methods previously described (see 1.3.4.1), could be induced to undergo shuttling of the macrocycle by deprotonation of the phenolate unit (Scheme 1.17).[53] This pH dependent process occurs due to the higher macrocycle binding ability of the phenoxide anion compared to the neutral succinamide station.

Scheme 1.17 pH-Switchable Phenoxide Anion-Induced Molecular Shuttle[53]

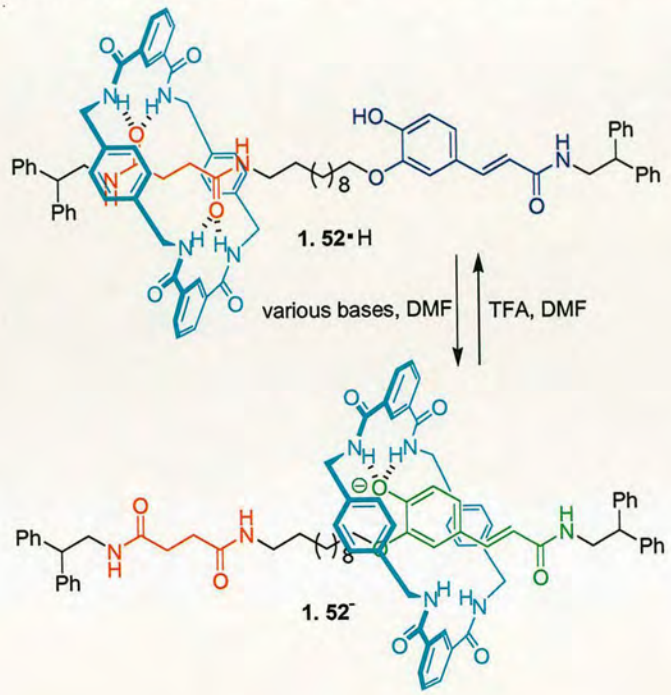

1.4.2.1.2 Solvent-Controllable Motion

A simple solvent change can be used to drive a molecular shuttle without changing the covalent structure of the molecule (Scheme 1.18).[54] In $CDCl_3$ the macrocycle resides principally over the peptide residue of the rotaxane **1.53** or **1.54** because of strong intercomponent hydrogen bonding; as a result the anthracene fluorescence is virtually completely quenched by nitrophenyl or pyridinium moiety respectively on the ring through distance-dependent electron transfer. In $[D_6]$DMSO, which solvates the peptide and macrocycle hydrogen bonding sites more strongly than they bind to each other, the macrocycle is located on the alkyl chain with fluorescence clearly

visible to the naked eye. Remarkably, this system not only works in solution but also in polymer films which are more relevant to materials applications.[54]

Scheme 1.18 Translational Isomerism Exhibited by Solvent-Switchable Molecular Shuttles[54]

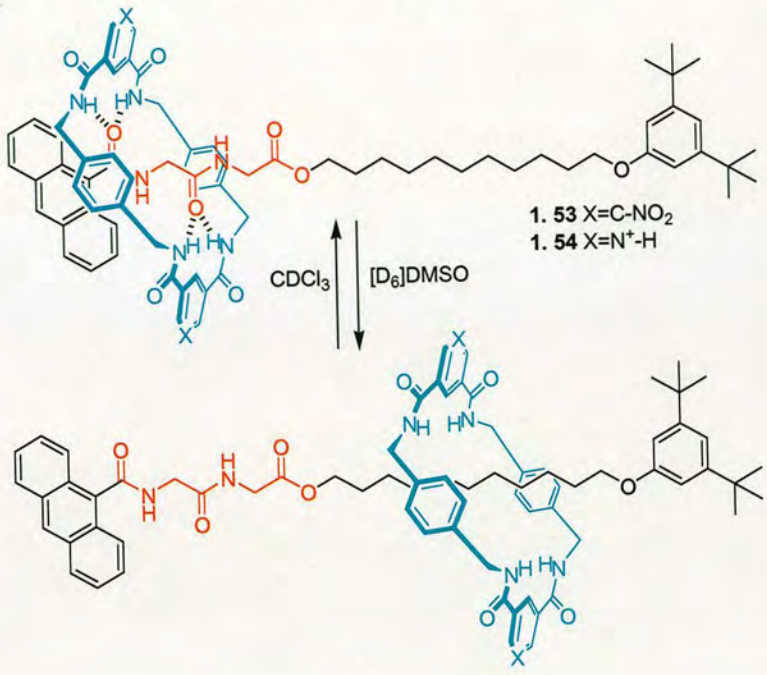

1.4.2.1.3 Temperature-Controllable Motion

Free energy of a macrocycle binding to station is given by ($\Delta G_{binding} = \Delta H_{binding} - T\Delta S_{binding}$). Most stimuli-responsive molecular shuttles are switched by modification of the enthalpy of macrocycle binding to one or both sites (through a chemical change in the molecule); however, if the entropy terms are sufficiently different then the relative binding affinity of the macrocycle for the two stations can be reversed by increasing or lowering the temperature.[55] An example of such phenomenon is presented in Scheme 1.19.[55] The *dodec-Z*-**1.55** co-conformer is enthalpically more favourable than *succ-Z*-**1.55**, because the macrocycle forms four strong hydrogen bonds to amide carbonyls in *dodec-Z*-**1.55** whereas only two strong hydrogen bonds with an amide carbonyl and two significantly weaker bonds to another ester carbonyl exist in *succ-Z*-**1.55**. At low temperature the energy gain from forming the two extra amide-amide hydrogen bonds overcomes the entropic cost required for the thread to bridge the macrocycle binding sites and the *dodec-Z*-**1.55** co-conformation is

preferred. However, raising the temperature increases the contribution of the TΔS to the $\Delta G_{binding}$ until at high temperature the relative binding affinity of the ring for the two sites is reversed and now the shuttle adopts the entropically more favorable *succ-Z*-**1.55** co-conformation.

Scheme 1.19 Entropy-Driven Molecular Shuttle[55]

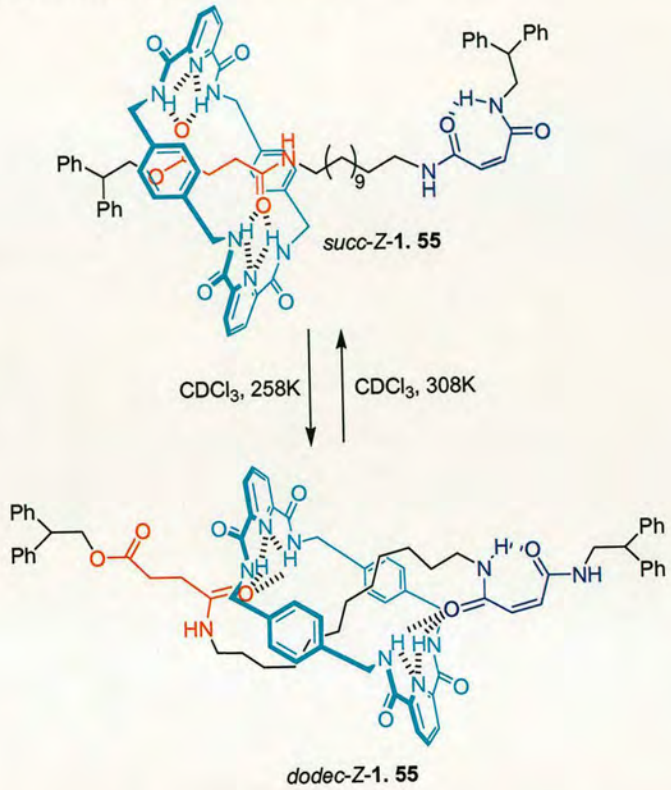

1.4.2.1.4 Redox-Controllable Motion

If an artificial molecular machine has to work by inputs of chemical energy, it will need addition of fresh reactants at any step of its working cycle, with the concomitant formation of waste products. By contrast, electrochemical energy inputs can power molecular machines through heterogeneous electron transfer processes without formation of any waste products. An approach to an electrochemically driven molecular shuttle is realised in the copper-containing rotaxane in Scheme 1.20 due to the remarkable difference between the geometric requirements of copper(I) and copper(II).[56] A coordination number of four (usually with a roughly tetrahedral arrangement of the ligands, see 1.3.1) corresponds to stable copper(I) system.

Copper(II) requires higher coordination numbers of five or six. Thus, switching alternatively from copper(I) to copper(II) induces changes in the molecule so as to afford a coordination situation favourable to the corresponding copper oxidation state. Using copper(I) **1.56**$^{+}$ is formed due to the selective formation of very stable tetrahedral copper(I) complex between two phenanthroline moieties. Upon oxidation to copper(II), the rotaxane stabilises itself by switching the metal-complexed ring from the phenanthroline to the terpyridine site to afford a favourable five coordination.

Scheme 1.20 An Electrochemically Driven Copper-Containing Molecular Shuttle[56]

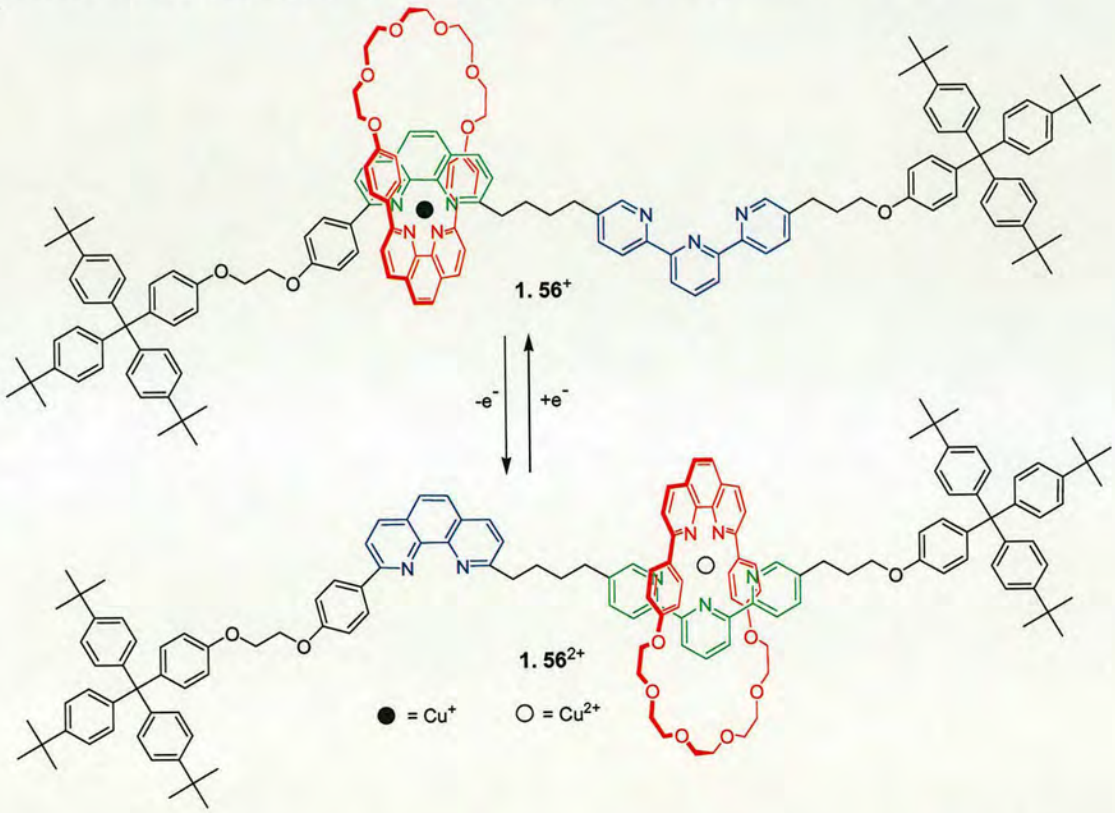

Unfortunately, although the system was set in motion quantitatively by a redox signal, the back-and-forth motion of the ring and its complexed copper center was slow (minutes). As shown in Scheme 1.20, the mobile macrocycle contains a highly shielding and hindered 2,9-diphenyl-1,10-phenanthroline (dpp) moiety as the complexing unit; this makes any ligand substitution within the coordination sphere of the metal center very difficult. Therefore a new ring was designed and synthesised by

the same group, in which a sterically non-hindered but endotopic ligand was incorporated. The new ring, which contains a 8,8'-diphenyl-3,3'-biisoquinoline (dpbiiq) unit, and its corresponding rotaxane **1.57**$^{+}$ are illustrated in Figure 1.13.[57] It was hoped that shuttles containing such a macrocycle would be set in motion faster than its dpp-containing analogue. By utilising the stereoelectronic preferences of copper (I) and copper (II) ions, the dpbiiq-based system is set in motion very readily, with the translation process occurring on the milliseconds to seconds timescale. That is, four orders of magnitude faster than for its dpp-based homologue.[57]

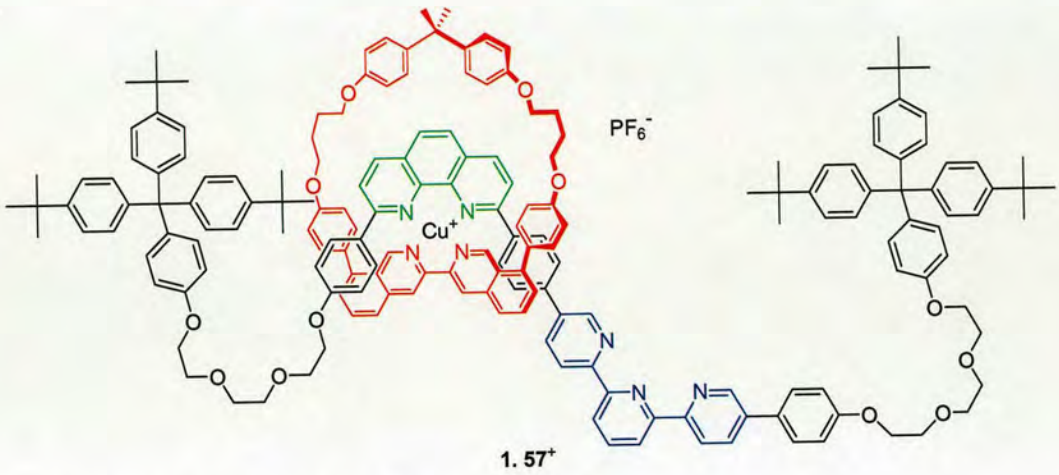

Figure 1.13 Chemical structure of rotaxane **1.57**$^{+}$.[57]

Another advantage of using the electrochemical technique is that electrodes represent one of the best ways to interface molecular-level systems with the macroscopic world. A SAM (self-assembled monolayer) of bistable [2]rotaxanes on gold electrodes was designed to explore nanoelectromechanical switching (Figure 1.14).[58] In the ground state, the cyclobis(paraquat-*p*-phenylene) (CBPQT) tetracationic ring (shown in blue) is located on the tetrathiafulvalene (TTF) unit (green), when a +800 mV voltage is applied, the TTF unit becomes doubly oxidised and charge repulsion drives the ring to the 1,5-dioxynaphthalene (DNP) unit (red). When the voltage is removed, the TTF^{2+} dication loses its positive charges, yet the ring remains weakly bound to the DNP, forming a metastable state. The ring returns to the TTF ground state by either a thermally activated process or, by applying a negative voltage of at least -600 mV.

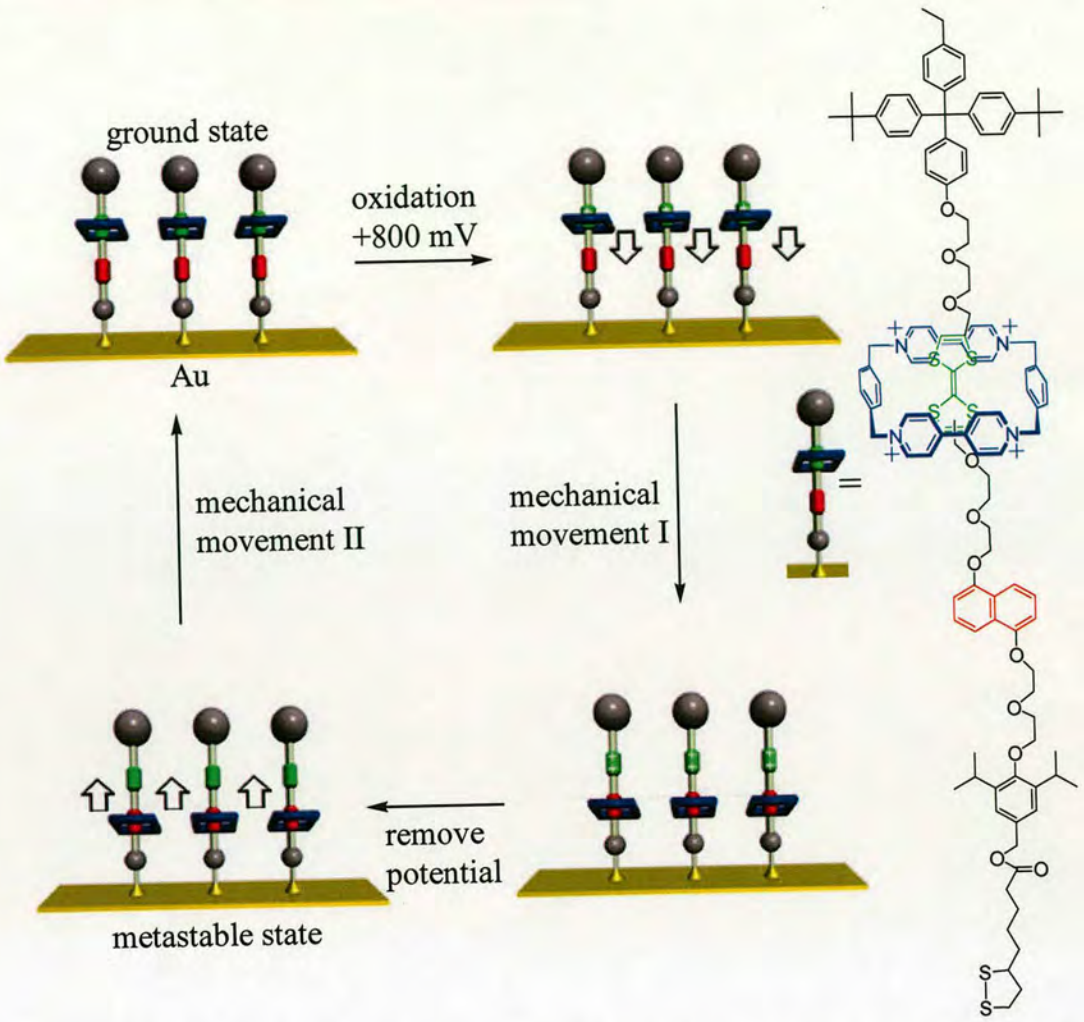

Figure 1.14 The proposed nanoelectromechanical mechanism for the operation of bistable [2]rotaxanes self-assembled onto a gold substrate under voltage control.[58]

1.4.2.1.5 Light-Controllable Motion

Compared to chemical energy inputs, photochemical energy inputs offer other advantages: (a) no waste generated; (b) light can be switched on/off easily and rapidly; (c) lasers provide the opportunity of working in very small space and very short time domains; (d) photons, besides supplying the energy needed to make a machine work, can also be useful to read the state of the system and thus to control and monitor the operation of the machine.[44b]

Light energy can directly cause photochemical reactions involving large nuclear movements. An example is the photoinduced isomerisation of a lower-energy *trans* double bond to the higher-energy *cis* form in a molecule containing –C=C– or –

N=N– double bonds. Such photoisomerisation reactions have indeed been used to design molecular machines driven by light energy inputs.[59]

A series of bistable [2]rotaxanes based on the photochemical and/or thermal interconversion of fumaramide and maleamide groups were reported by Leigh and co-workers recently.[48, 55, 60] Scheme 1.21 shows an example of this kind of molecular shuttle.[60a] In *E*-**1.58** the macrocycle has a higher binding affinity to the fumaramide portion of the thread and the asymmetric center is not close enough to any aromatic rings to influence their absorption spectrum. Upon photoisomerisation of the olefin station (*E*-**1.58**→*Z*-**1.58**), the macrocycle moves to the glycyl-L-leucine unit, locking the molecule in a co-conformation where aromatic rings are held in a well-expressed chiral environment. In fact, of the two rotaxanes and two threads, only rotaxane *Z*-**1.58** gives a CD response, which is both strong and (for the L-enantiomer) negative.

Scheme 1.21 Chiroptical Switching in a Bistable Molecular Shuttle[60a]

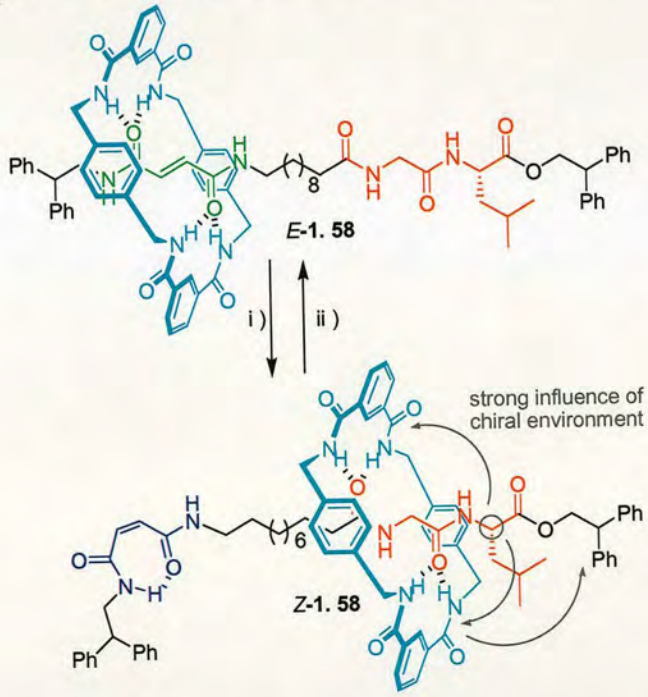

Reagents and conditions: (i) either 254 nm, CH_2Cl_2, 20 min, 56% or 254 nm, CH_3CN, 20 min, 49%, or 350 nm, benzophenone, CH_2Cl_2, 20 min, 70%; (ii) either 312 nm, CH_2Cl_2 or CH_3CN, 20 min, 62% or 400-670 nm, cat. Br_2, CH_2Cl_2, 2 min, >95%, or 130 °C, $C_2H_2Cl_4$, 6 days, 95%.

Translation of the macrocycle between two stations in a molecular shuttle can take place after photoexcitation with a laser pulse (Scheme 1.22).[61] [2]Rotaxane **1.59** is

composed of a hydrogen-bond-donating benzylic amide macrocycle, the thread component is equipped with a strong hydrogen-bond-accepting unit-succinamide (shown in green, *succ*) and a poor hydrogen-bond-accepting 3,6-di-*tert*-butyl-1,8-naphthalimide unit (red, *ni*). Before the 355 nm laser pulse, the translational co-conformer *succ*-**1.59** is predominant ($K_n < 0.01$); however, after photoreduction of the *ni* station to $ni^{-\bullet}$ radical anion (blue) in the presence of an electron donor (D) 1,4-diazabicyclo[2.2.2]octane (DABCO) makes it a stronger hydrogen-bond-acceptor than the *succ* unit and back-electron transfer occurs slowly (spin forbidden). Thus the equilibrium between *succ*-**1.59**$^{-\bullet}$ and *ni*-**1.59**$^{-\bullet}$ changes ($K_{red} > 1500$) and the macrocycle moves to the $ni^{-\bullet}$ radical anion along the C-12 alkyl spacer. Charge recombination between the $ni^{-\bullet}$ radical anion and the $D^{+\bullet}$ radical cation generates the neutral state and the macrocycle shuttles back to its original site. This reversible photo-induced movement of components in **1.59** generates a mechanical power of ~ 10^{-15} W per molecule. The shuttling of macrocycle between the two sites can be driven electrochemically as well.[62]

Scheme 1.22 A Photo-Responsive, Hydrogen-Bond-Assembled Molecular Shuttle[61]

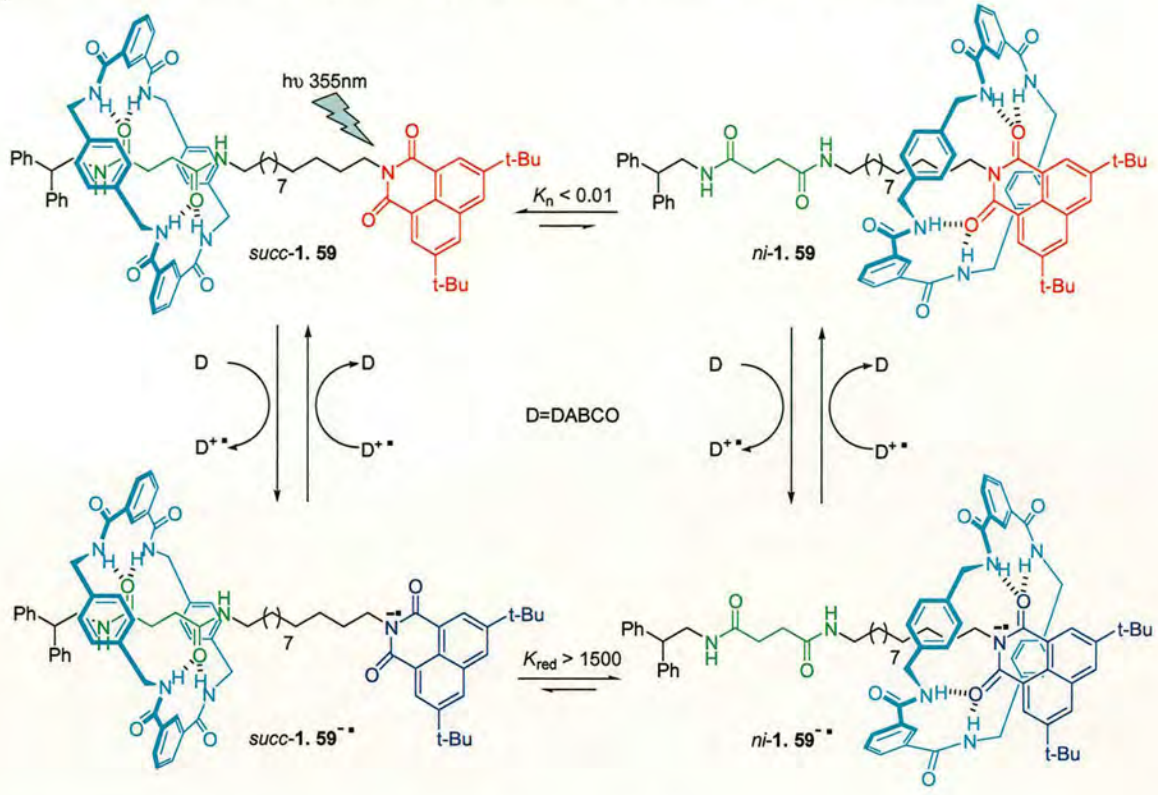

1.4.2.2 Catenane-Based Rotary Molecular Motors

To build synthetic molecular rotary motors, it is apparent that three criteria must be satisfied: (i) repetitive 360° rotation, (ii) consumption of energy and (iii) control over directionality.

Leigh and co-workers have designed a [3]catenane *E,E*-**1.60** comprising a large ring bearing four different stations and two small rings (Figure 1.15).[63] It represents the first example of 360° rotary unidirectional biased Brownian motion in a synthetic molecular system. In *E,E*-**1.60**, the four hydrogen bond accepting stations on the large macrocycle possess gradually decreasing binding affinity to the two small interlocked hydrogen bond donating benzylic amide macrocycles (shown in light blue and purple). The four stations include: a secondary amide fumaramide (A, green) > a tertiary amide fumaramide (B, red) > a succinic amide ester (C, orange) > a single amide group (D, dark green). Station A is located next to a benzophenone unit and this allows selective photosensitised isomerisation of station A at 350 nm, whereas the other fumaramide station B can be isomerised separately at 254 nm. Station C is

not photoactive and its macrocycle binding affinity is intermediate between the two fumaramide stations and their maleamide counterparts (A' and B', not shown in Figure 1.15).

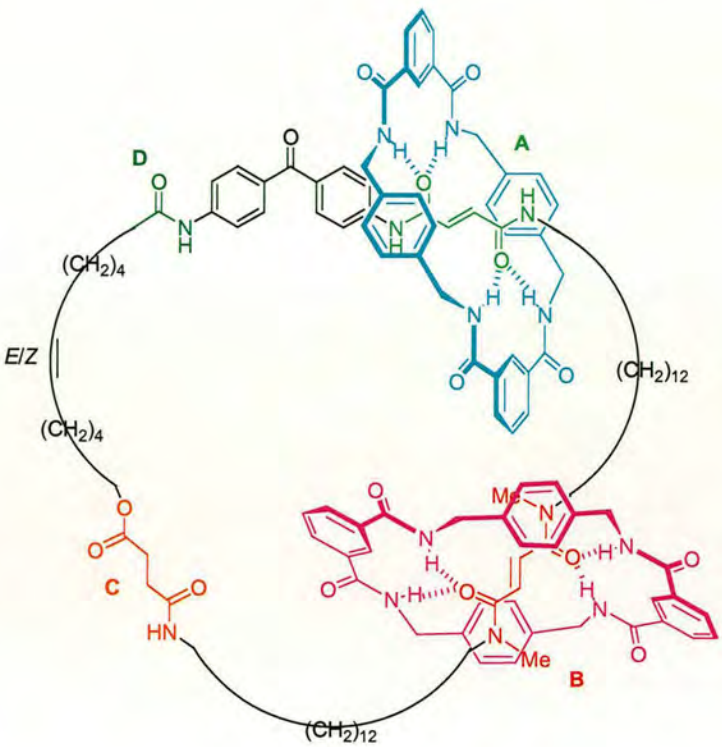

E, E-**1. 60**

Figure 1.15 Chemical structure of the four-station [3]catenane *E,E*-**1.60**.[63a]

Irradiation of *E,E*-**1.60** at 350 nm causes counter-clockwise (as drawn) rotation of the light blue macrocycle to the succinic amide ester station (C, orange) to give *Z,E*-**1.60**. Isomerisation of the remaining fumaramide group at 254 nm causes the other (purple) macrocycle to relocate to the single amide station (D, dark green) to afford *Z,Z*-**1.60** and, again, this occurs counter-clockwise because the clockwise route is blocked by the other (light blue) macrocycle. This 'follow-the-leader' process, each macrocycle in turn moving and then blocking a direction of passage for the other macrocycle, is repeated throughout the sequence of transformation shown in Figure 1.16. After three diastereomer interconversions *E,E*-**1.60** is again formed but 360° rotation of each of the small rings has not yet occurred, they have only swapped

places. Complete unidirectional rotation of both small rings occurs only after the synthetic sequence (i)-(iii) has been completed twice.

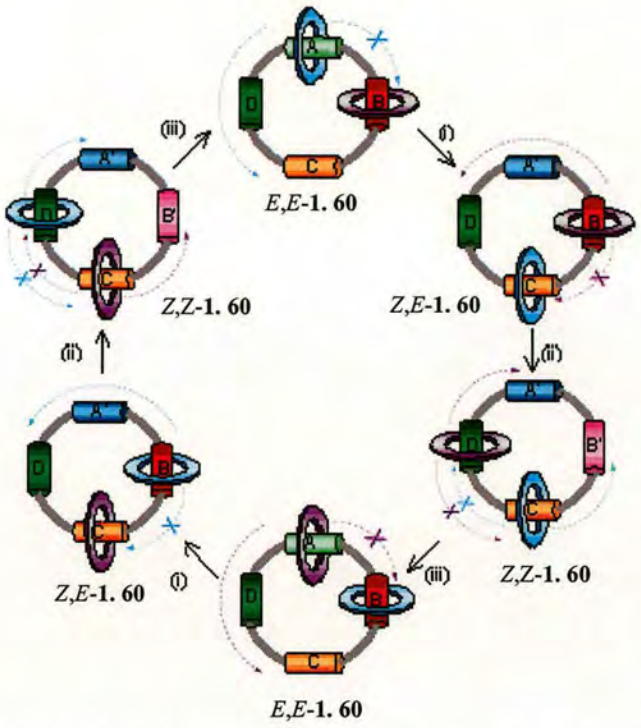

Figure 1.16 Stimuli-induced unidirectional rotation in a four-station [3]catenane **1.60**:[63a] (i) 350 nm, CH_2Cl_2, 5 min, 67%; (ii) 254 nm, CH_2Cl_2, 20 min, 50%; (iii) heat, 100°C, $C_2H_2Cl_4$, 24 h, ~100%; catalytic ethylenediamine, 50°C, 48 h, 65%; or catalytic Br_2, 400-670 nm, CH_2Cl_2, -78°C, 10 min, ~100%.

The second generation synthetic rotary molecular motor is a simplified [2]catenane that can selectively rotate in either direction; it was reported by the same group in 2004 (Scheme 1.23).[64] Net changes in the position or potential energy of the smaller ring were sequentially achieved by: (i) photoisomerisation to maleamide (→*mal-Z*-**1.61**); (ii) de-silylation/re-silylation (→*succ-Z*-**1.61**); (iii) re-isomerisation to fumaramide (→*succ-E*-**1.61**); and finally, (iv) de-tritylation/re-tritylation to regenerate *fum-E*-**1.61**, the whole reaction sequence producing a net clockwise circumrotation of the small ring about the larger one. Exchanging the order of steps (ii) and (iv) – that is, employing steps (v) and (vi) instead – produced an equivalent counter-clockwise rotation of the small ring.

Scheme 1.23 A Reversible [2]Catenane Rotary Molecular Motor[64]

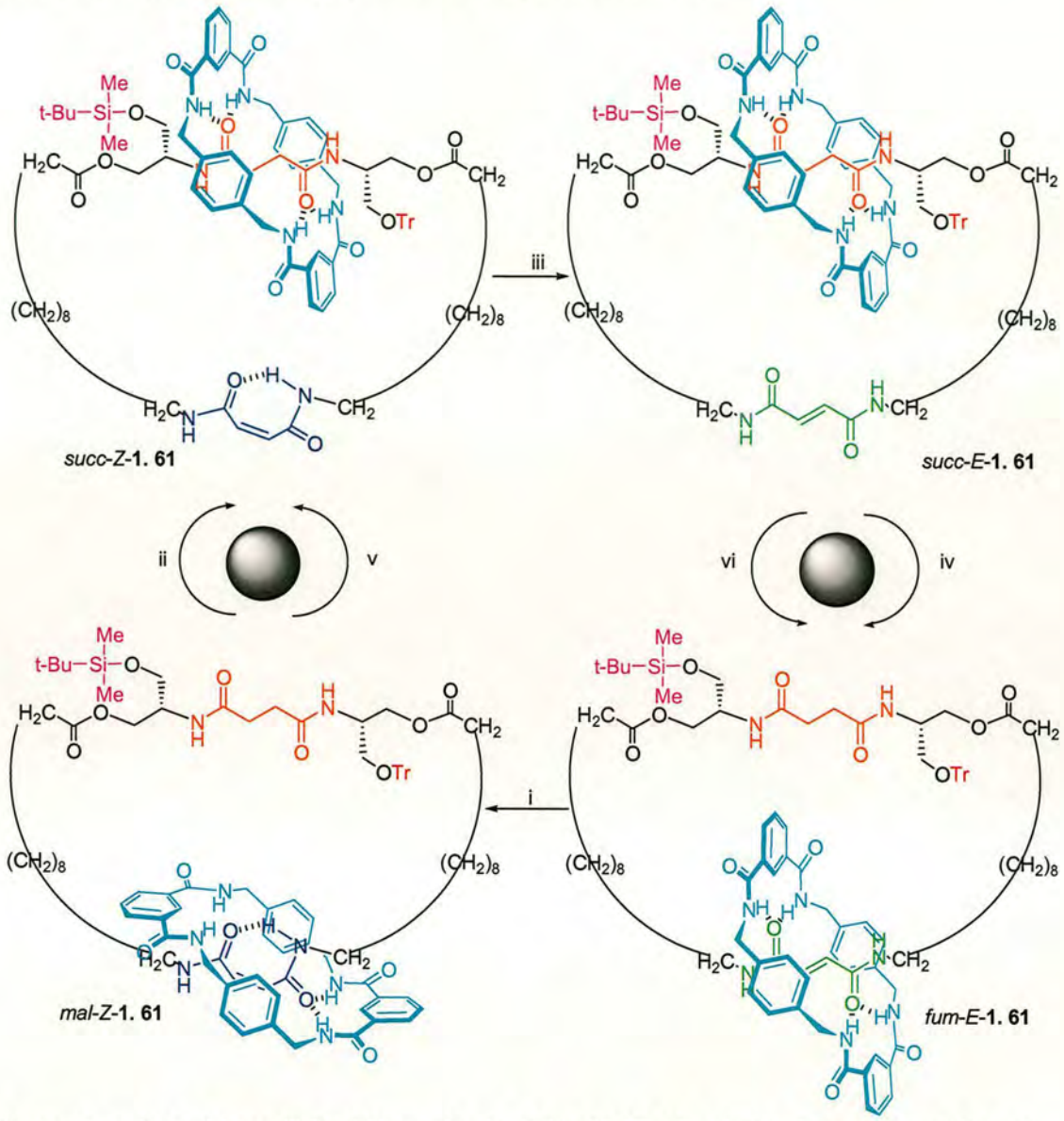

Reagents and conditions: (i) hν 254 nm, 5 min, 50%; (ii) TBAF, 20 min then cool to -78°C and add 2,4,6-collidine, TBDMSOTf, 1 h, overall 61%; (iii) piperidine, 1 h, ~100%; (iv) $Me_2S{\bullet}BCl_3$, -10°C 10 min and then TrCl, Bu_4NClO_4, 2,4,6-collidine, 16 h, overall 74%; (v) $Me_2S{\bullet}BCl_3$, -10°C, 15 min then cool to -78°C and add 2,4,6-collidine, TrOTf, 5 h, overall 63%; (vi) TBAF, 20 min then cool to -10°C and add 2,4,6-collidine, TBDMSOTf, 40 min, overall 76%.

1.5 Property Changes in Interlocked Architectures

Interlocked architectures have resulted in some surprising changes in the physical properties of molecules. Smith and co-workers demonstrated the encapsulation of a squaraine dye into a [2]rotaxane structure **1.62** or **1.63** (Figure 1.17), using a hydrogen bond mediated encirclement methodology.[65] In this system, the assembly of

the wheel component is directed by the squaraine oxygen units, which can be thought of as anionic so as to allow aromaticity at the cyclobutadienyl core of the thread. The resulting dye system has a stability which is greatly increased compared to the naked thread, due to the inhibition of aggregation processes. The same group has also discovered more recently that squaraine-rotaxane dyes can be readily converted into extremely bright and highly stable near-infrared region (650-900 nm) fluorescent probes for in *vitro* and in *vivo* optical imaging of live and fixed cells.[66]

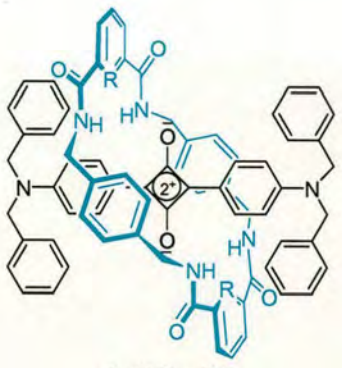

1. 62 R = CH
1. 63 R = N

Figure 1.17 Smith's rotaxinated squaraine dye.[65a]

In 'molecular muscle' $\mathbf{1.64}^{2+}/\mathbf{1.65}^{4+}$ designed by Sauvage and co-workers, shuttling motion results in extension and contraction of the molecular structure (Scheme 1.24).[67] To achieve this motion, a dimeric rotaxane-like molecule was synthesised in which each monomer unit consists of a macrocyclic structure, displaying a bidentate phenanthroline ligand, connected to a thread-like portion which itself contains a phenanthroline ligand and a tridentate terpyridine site. Copper(I) is used to template formation of the dimer in a tetrahedral geometry resulting in the threaded dimeric extended structure $\mathbf{1.64}^{2+}$. Unfortunately, in this case electrochemical oxidation to the copper(II) species did not trigger motion, due to kinetic reasons. Instead, demetallation using KCN to give the free ligand system, followed by treatment with $Zn(NO_3)_2$ yielded the contracted form $\mathbf{1.65}^{4+}$, as evidenced by ^{1}H NMR. During this process, the length of the molecule changes from approximately 83 Å to 65 Å, a reduction of 24%. The molecule can then be returned to its original length simply by treatment with excess $[Cu(CH_3CN)_4]\cdot PF_6$.

Scheme 1.24 Synthetic 'Molecular Muscle':[67] Reversible Chemically Induced Motions between Extended $\mathbf{1.64}^{2+}$ and Contracted $\mathbf{1.65}^{4+}$

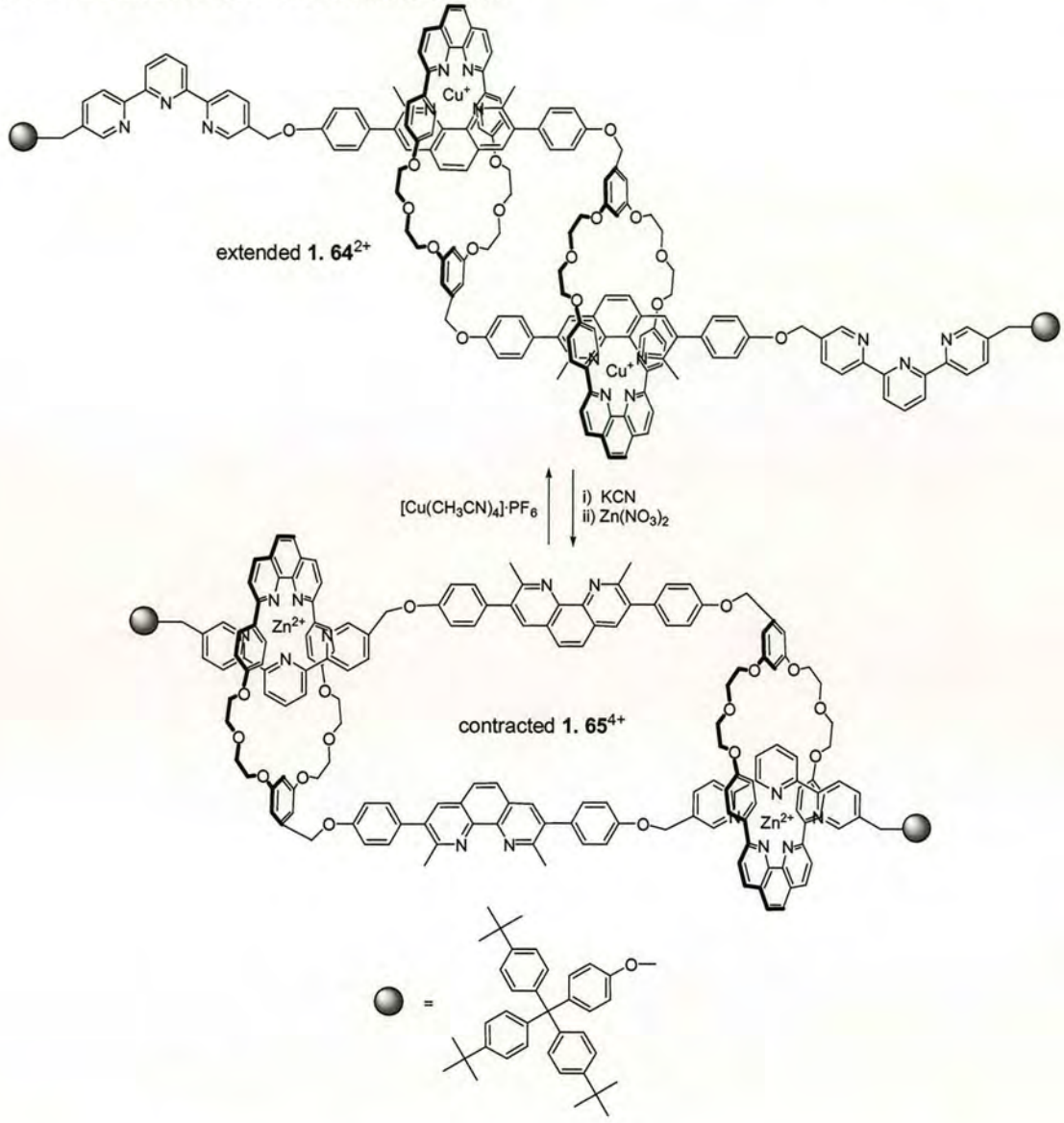

1.6 Conclusions and Outlook

The exquisite solutions nature has found to control molecular motion have served as a major source of inspiration for scientists to conceptualise, design and build entirely synthetic molecular machines, using a bottom-up approach. Interlocked molecular species, like suitably designed rotaxanes and catenanes, are ideal structures to create artificial nanomachines. Depending on the nature of the molecular components, mechanical motions in these systems can be promoted by chemical, electrochemical and photochemical energy inputs. In the last few years remarkable

progress has been made in this field, some of which has been reviewed here. However, the whole field is still very much in its infancy and the presently accessible molecular machines and motors are extremely primitive compared to the beautiful and exceedingly complex molecular machines of nature. Optimistically these useful devices based on artificial nanomachines will have some practical applications in the near future, including the ambitious dream of molecular robots able to perform various functions like: transport molecules through a membrane, sort different molecules, or carry cargo to a designated point. In conclusion, there is still a long way to go, but let us keep in mind what the ancient Chinese philosopher Confucius said: *A journey of a thousand miles begins with a single step.*

1.7 References and Notes

(1) (a)Knowles, A. F.; Penefsky, H. S. *J. Biol. Chem.* **1972**, *247*, 6624-6630. (b) Boyer, P. D.; Cross, R. L.; Momsen, W. *Proc. Natl. Acad. Sci. U.S.A.* **1973**, *70*, 2837-2839. (c) Noji, H.; Yasuda, R.; Yoshida, M.; Kinosita, K. Jr *Nature* **1997**, *386*, 299-302. (d) Walker, J. E. *Angew. Chem., Int. Ed.* **1998**, *37*, 2308-2319. (e) Jones, P. C.; Fillingame R. H. *J. Biol. Chem.* **1998**, *273*, 29701-29705. (f)Elston, T.; Wang, H.; Oster, G. *Nature* **1998**, *391*, 510-513. (g) Dimroth, P.; Wang, H.; Grabe, M.; Oster, G. *Proc. Natl. Acad. Sci. U.S.A.* **1999**, *96*, 4924-4929. (h) Sambongi, Y.; Iko, Y.; Tanabe, M.; Omote, H.; Iwamoto-Kihara A.; Ueda, I.; Yanagida, T.; Wada, Y.; Futai, M. *Science* **1999**, *286*, 1722-1724. (i) Rastogi, V. K.; Girvin, M. E. *Nature* **1999**, *402*, 263-268. (j) Stock, D.; Leslie, A. G. W.; Walker, J. E. *Science* **1999**, *286*, 1700-1705. (k) Seelert, H.; Poetsch, A.; Dencher, N. A.; Engel, A.; Stahlberg, H.; Muller, D. J. *Nature* **2000**, *405*, 418-419.

(2) (a) Howard, J. *Nature* **1994**, *368*, 98-99. (b) Finer, J. T.; Simmons, R. M.; Spudich, J. A. *Nature* **1994**, *368*, 113-119. (c) Spudich, J. A. *Nature* **1994**, *372*, 515-518. (d) Vale, R. D.; Milligan, R. A. *Science* **2000**, *288*, 88-95. (e) Jimenez-Molero, M. C.; Dietrich-Buchecker, C.; Sauvage, J.-P. *Chem. Eur. J.* **2002**, *8*, 1456-1466.

(3) (a) Vale, R. D.; Funatsu, T.; Pierce, D. W.; Romberg, L.; Harada, Y.; Yanagida, T. *Nature* **1996**, *380*, 451-453. (b) Schnitzer, M. J.; Block, S. M. *Nature* **1997**, *388*, 386-390. (c) Asbury, C. L.; Fehr, A. N.; Block, S. M. *Science* **2003**, *302*,

2130-2134. (d) Vale, R. D. *Cell* **2003**, *112*, 467-480. (e) Yildiz, A.; Tomishige, M.; Vale, R. D.; Selvin, P. R. *Science* **2004**, *303*, 676-678.

(4) Champin, B.; Mobian, P.; Sauvage, J.-P. *Chem. Soc. Rev.* **2007**, *36*, 358-366.

(5) (a) Mao, C.; Sun, W.; Shen, Z.; Seeman, N. C. *Nature* **1999**, *397*, 144-146. (b) Yurke, B.; Turberfield, A. J.; Mills, A. P. Jr; Simmel, F. C.; Neumann, J. L. *Nature* **2000**, *406*, 605-608. (c) Yan, H.; Zhang, X.; Shen, Z.; Seeman, N. C. *Nature* **2002**, *415*, 62-65. (d) Kelly, T. R. *Angew. Chem., Int. Ed.* **2005**, *44*, 4124-4127.

(6) (a) Frisch, H. L.; Wasserman, E. *J. Am. Chem. Soc.* **1961**, *83*, 3789-3795. (b) Schill, G. *Catenanes, Rotaxanes and Knots*, Academic Press, New York, **1971**. (c) Dietrich-Buchecker, C. O.; Sauvage, J.-P. *Chem. Rev.* **1987**, *87*, 795-810. (d) Amabilino, D. B.; Stoddart, J. F. *Chem. Rev.* **1995**, *95*, 2725-2828. (e) Breault, G. A.; Hunter, C. A.; Mayers, P. C. *Tetrahedron* **1999**, *55*, 5265-5293. (f) *Molecular Catenanes, Rotaxanes and Knots* (Eds: Sauvage, J.-P.; Dietrich-Buchecker, C. O.), Wiley-VCH, Weinheim, **1999**. (g) Siegel, J. S. *Science* **2004**, *304*, 1256-1258.

(7) Wasserman, E. *J. Am. Chem. Soc.* **1960**, *82*, 4433-4434.

(8) A pseudorotaxane (Ashton, P. R.; Philp, D.; Spencer, N.; Stoddart, J. F. *J. Chem. Soc., Chem. Commun.* **1991**, 1677-1679) is an interwoven inclusion complex in which a molecular thread is encircled by one or more beads (macrorings) so that the thread's extremities are directed away from the bead's center. At least one of the thread's extremities does not possess a bulky stopper group. Hence, the constituents of the assemblage, like any complex, are at liberty to dissociate into separate molecular species. In contrast with rotaxanes, there is no attendant mechanical bond to maintain the system's integrity.

(9) Harrison, I. T.; Harrison, S. *J. Am. Chem. Soc.* **1967**, *89*, 5723-5724.

(10) (a) Dietrich-Buchecker, C. O.; Sauvage, J.-P.; Kintzinger, J. P. *Tetrahedron Lett.* **1983**, *24*, 5095-5098. (b) Dietrich-Buchecker, C. O.; Sauvage, J.-P.; Kern, J.-M. *J. Am. Chem. Soc.* **1984**, *106*, 3043-3045.

(11) (a) Cao, J.; Fyfe, M. C. T.; Stoddart, J. F.; Cousins, G. R. L.; Glink, P. T. *J. Org. Chem.* **2000**, *65*, 1937-1946. (b) Cantrill, S. J.; Fulton, D. A.; Heiss, A. M.; Pease, A. R.; Stoddart, J. F.; White, A. J. P.; Williams, D. J. *Chem. Eur. J.* **2000**, *6*,

2274-2287. (c) Arico, F.; Badjic, J. D.; Cantrill, S. J.; Flood, A. H.; Leung, K. C.-F.; Liu, Y.; Stoddart, J. F. *Top. Curr. Chem.* **2005**, *249*, 203-259. (d) Dichtel, W. R.; Miljanic, O. S.; Spruell, J. M.; Heath, J. R.; Stoddart, J. F. *J. Am. Chem. Soc.* **2006**, *128*, 10388-10390. (e) Miljanic, O. S.; Dichtel, W. R.; Mortezaei, S.; Stoddart, J. F. *Org. Lett.* **2006**, *8*, 4835-4838. (f) Aprahamian, I.; Dichtel, W. R.; Ikeda, T.; Heath, J. R.; Stoddart, J. F. *Org. Lett.* **2007**, *9*, 1287-1290.

(12) Chiu, C.-W.; Lai, C.-C.; Chiu, S.-H. *J. Am. Chem. Soc.* **2007**, *129*, 3500-3501.

(13) Yoon, I.; Narita, M.; Shimizu, T.; Asakawa, M. *J. Am. Chem. Soc.* **2004**, *126*, 16740-16741.

(14) (a) Jeppesen, J. O.; Perkins, J.; Becher, J.; Stoddart, J. F. *Org. Lett.* **2000**, *2*, 3547-3550. (b) Glink, P. T.; Oliva, A. I.; Stoddart, J. F.; White, A. J. P.; Williams, D. J. *Angew. Chem., Int. Ed.* **2001**, *40*, 1870-1875. (c) Asakawa, M.; Brancato, G.; Fanti, M.; Leigh, D. A.; Shimizu, T.; Slawin, A. M. Z.; Wong, J. K. Y.; Zerbetto, F.; Zhang, S. *J. Am. Chem. Soc.* **2002**, *124*, 2939-2950. (d) Wisner, J. A.; Beer, P. D.; Drew, M. G. B.; Sambrook, M. R. *J. Am. Chem. Soc.* **2002**, *124*, 12469-12476.

(15) (a) Ashton, P. R.; Belohradsky, M.; Philp, D.; Stoddart, J. F. *J. Chem. Soc., Chem. Commun.* **1993**, 1269-1274. (b) Ashton, P. R.; Belohradsky, M.; Philp, D.; Spencer, N.; Stoddart, J. F. *J. Chem. Soc., Chem. Commun.* **1993**, 1274-1277. (c) Raymo, F. M.; Stoddart, J. F. *Pure Appl. Chem.* **1997**, *69*, 1987-1997. (d) Handel, M.; Plevoets, M.; Gestermann, S.; Vogtle, F. *Angew. Chem., Int. Ed. Engl.* **1997**, *36*, 1199-1201. (e) Ashton, P. R.; Baxter, I.; Fyfe, M. C. T.; Raymo, F. M.; Spencer, N.; Stoddart, J. F.; White, A. J. P.; Williams, D. J. *J. Am. Chem. Soc.* **1998**, *120*, 2297-2307.

(16) Collin, J.-P.; Dietrich-Buchecker, C.; Gavina, P.; Jimenez-Molero, M. C.; Sauvage, J.-P. *Acc. Chem. Res.* **2001**, *34*, 477-487.

(17) (a) Armaroli, N.; Balzani, V.; Collin, J.-P.; Gavina, P.; Sauvage, J.-P.; Ventura, B. *J. Am. Chem. Soc.* **1999**, *121*, 4397-4408. (b) Raehm, L.; Kern, J.-M.; Sauvage, J.-P. *Chem. Eur. J.* **1999**, 5, 3310-3317.

(18) (a) Pomeranc, D.; Jouvenot, D.; Chambron, J.-C.; Collin, J.-P.; Heitz, V.; Sauvage, J.-P. *Chem. Eur. J.* **2003**, *9*, 4247-4254. (b) Hogg, L.; Leigh, D. A.;

Lusby, P. J.; Morelli, A.; Parsons, S.; Wong, J. K. Y. *Angew. Chem., Int. Ed.* **2004**, *43*, 1218-1221.

(19) Fuller, A.-M.; Leigh, D. A.; Lusby, P. J.; Oswald, I. D. H.; Parsons, S.; Walker, D. B. *Angew. Chem., Int. Ed.* **2004**, *43*, 3914-3918.

(20) Ko, Y. H.; Kim, E.; Hwang, I.; Kim, K. *Chem. Commun.* **2007**, 1305-1315.

(21) Flood, A. H.; Ramirez, R. J. A.; Deng, W.-Q.; Muller, R. P.; Goddard III, W. A.; Stoddart, J. F. *Aust. J. Chem.* **2004**, *57*, 301-322 and references therein.

(22) Ashton, P. R.; Goodnow, T. T.; Kaifer, A. E.; Reddington, M. V.; Slawin, A. M. Z.; Spencer, N.; Stoddart, J. F.; Vicent, C.; Williams, D. J. *Angew. Chem., Int. Ed. Engl.* **1989**, *28*, 1396-1399.

(23) Anelli, P. L.; Spencer, N.; Stoddart, J. F. *J. Am. Chem. Soc.* **1991**, *113*, 5131-5133.

(24) (a) Nielsen, M. B.; Lomholt, C.; Becher, J. *Chem. Soc. Rev.* **2000**, *29*, 153-164 and references therein. (b) Jeppesen, J. O.; Perkins, J.; Becher, J.; Stoddart, J. F. *Angew. Chem., Int. Ed.* **2001**, *40*, 1216-1221. (c) Segura, J. L.; Martin, N. *Angew. Chem., Int. Ed.* **2001**, *40*, 1372-1409 and references therein. (d) Nygaard, S.; Leung, K. C.-F.; Aprahamian, I.; Ikeda, T.; Saha, S.; Laursen, B. W.; Kim, S.-Y.; Hansen, S. W.; Stein, P. C.; Flood, A. H.; Stoddart, J. F.; Jeppesen, J. O. *J. Am. Chem. Soc.* **2007**, *129*, 960-970. (e) Saha, S.; Leung, K. C.-F.; Nguyen, T. D.; Stoddart, J. F.; Zink, J. I. *Adv. Funct. Mater.* **2007**, *17*, 685-693. (f) Nygaard, S.; Laursen, B. W.; Hansen, T. S.; Bond, A. D.; Flood, A. H.; Jeppesen, J. O. *Angew. Chem., Int. Ed.* **2007**, *46*, 6093-6097.

(25) Wenz, G. *Angew. Chem., Int. Ed. Engl.* **1994**, *33*, 803-822.

(26) Nepogodiev, S. A.; Stoddart, J. F. *Chem. Rev.* **1998**, *98*, 1959-1976.

(27) Harada, A. *Acc. Chem. Res.* **2001**, *34*, 456-464.

(28) Wenz, G.; Han, B.-H.; Muller, A. *Chem. Rev.* **2006**, *106*, 782-817.

(29) Ogino, H. *J. Am. Chem. Soc.* **1981**, *103*, 1303-1304.

(30) Stanier, C. A.; O'Connell, M. J.; Clegg, W.; Anderson, H. L. *Chem. Commun.* **2001**, 493-494.

(31) (a) Hellingwerf, K. J.; Hendriks, J.; Gensch, T. *J. Phys. Chem. A* **2003**, *107*, 1082-1094. (b) Mavroidis, C.; Dubey, A.; Yarmush, M. L. *Annu. Rev. Biomed. Eng.* **2004**, *6*, 363-395.

(32) (a) Cantrill, S. J.; Preece, J. A.; Stoddart, J. F.; Wang Z.-H.; White, A. J. P.; Williams, D. J. *Tetrahedron* **2000**, *56*, 6675-6681. (b) Prins, L. J.; Reinhoudt, D. N.; Timmerman, P. *Angew. Chem., Int. Ed.* **2001**, *40*, 2382-2426. (c) Cooke, G.; Rotello, V. M. *Chem. Soc. Rev.* **2002**, *31*, 275-286. (d) Sanchez, L.; Martin, N.; Guldi, D. M. *Angew. Chem., Int. Ed.* **2005**, *44*, 5374-5382.

(33) (a) Hunter, C. A. *J. Am. Chem. Soc.* **1992**, *114*, 5303-5311. (b) Hunter, C. A.; Purvis, D. H. *Angew. Chem., Int. Ed. Engl.* **1992**, *31*, 792-795.

(34) Vögtle, F.; Meier, S.; Hoss, R. *Angew. Chem., Int. Ed. Engl.* **1992**, *31*, 1619-1622.

(35) Johnston, A. G.; Leigh, D. A.; Pritchard, R. J.; Deegan, M. D. *Angew. Chem., Int. Ed. Engl.* **1995**, *34*, 1209-1212.

(36) Gatti, F. G.; Leigh, D. A.; Nepogodiev, S. A.; Slawin, A. M. Z.; Teat, S. J.; Wong, J. K. Y. *J. Am. Chem. Soc.* **2001**, *123*, 5983-5989.

(37) (a) Vilar, R. *Angew. Chem., Int. Ed.* **2003**, *42*, 1460-1477. (b) Beer, P. D.; Sambrook, M. R.; Curiel, D. *Chem. Commun.* **2006**, 2105-2117. (c) Lankshear, M. D.; Beer, P. D. *Coordin. Chem. Rev.* **2006**, *250*, 3142-3160. (d) Sambrook, M. R.; Beer, P. D.; Lankshear, M. D.; Ludlow, R. F.; Wisner, J. A. *Org. Biomol. Chem.* **2006**, *4*, 1529-1538. (e) Vickers, M. S.; Beer, P. D. *Chem. Soc. Rev.* **2007**, *36*, 211-225. (f) Lankshear, M. D.; Beer, P. D. *Acc. Chem. Res.* **2007**, *40*, 657-668.

(38) Wisner, J. A.; Beer, P. D.; Drew, M. G. B.; Sambrook, M. R. *J. Am. Chem. Soc.* **2002**, *124*, 12469-12476.

(39) Sambrook, M. R.; Beer, P. D.; Wisner, J. A.; Paul, R. L.; Cowley, A. R. *J. Am. Chem. Soc.* **2004**, *126*, 15364-15365.

(40) Glink, P. T.; Schiavo, C.; Stoddart, J. F.; Williams, D. J. *Chem. Commun.* **1996**, 1483-1490.

(41) Ashton, P. R.; Glink, P. T.; Stoddart, J. F.; Tasker, P. A.; White, A. J. P.; Williams, D. J. *Chem. Eur. J.* **1996**, *2*, 729-736.

(42) Feynman R. P. http://www.zyvex.com/nanotech/feynman.html (date of access: 19 June, 2008)

(43) Drexler, K. E. *Proc. Natl. Acad. Sci. U.S.A.* **1981**, *78*, 5275-5278.

(44) (a) Balzani, V.; Credi, A.; Silvi, S.; Venturi, M. *Chem. Soc. Rev.* **2006**, *35*, 1135-1149. (b) Balzani, V.; Credi, A.; Venturi, M. *Pure Appl. Chem.* **2003**, *75*, 541-547.

(45) Credi, A. *J. Phys.: Condens. Mat.* **2006**, *18*, S1779-S1795.

(46) For recent reviews, see 4, 16, 20, 21, 24a, 27, 44, 45 and (a) Balzani, V.; Gomez-Lopez, M.; Stoddart, J. F. *Acc. Chem. Res.* **1998**, *31*, 405-414. (b) Sauvage, J.-P. *Acc. Chem. Res.* **1998**, *31*, 611-619. (c) Balzani, V.; Credi, A.; Raymo, F. M.; Stoddart, J. F. *Angew. Chem., Int. Ed.* **2000**, *39*, 3348-3391. (d) Ballardini, R.; Balzani, V.; Credi, A.; Gandolfi, M. T.; Venturi, M. *Acc. Chem. Res.* **2001**, *34*, 445-455. (e) Schalley, C. A.; Beizai, K.; Vogtle, F. *Acc. Chem. Res.* **2001**, *34*, 465-476. (f) Kinbara, K.; Aida, T. *Chem. Rev.* **2005**, *105*, 1377-1400. (g) Collin, J.-P.; Heitz, V.; Bonnet, S.; Sauvage, J.-P. *Inorg. Chem. Commun.* **2005**, *8*, 1063-1074. (h) Bonnet, S.; Collin, J.-P.; Koizumi, M.; Mobian, P.; Sauvage, J.-P. *Adv. Mater.* **2006**, *18*, 1239-1250. (i) Browne, W. R.; Feringa, B. L. *Nature Nanotechnology* **2006**, *1*, 25-35. (j) Tian, H.; Wang Q.-C. *Chem. Soc. Rev.* **2006**, *35*, 361-374. (k) Kay, E. R.; Leigh, D. A.; Zerbetto, F. *Angew. Chem., Int. Ed.* **2007**, *46*, 72-191. (l) Saha, S.; Stoddart, J. F. *Chem. Soc. Rev.* **2007**, *36*, 77-92. (m) Loeb, S. J. *Chem. Soc. Rev.* **2007**, *36*, 226-235.

(47) 'Co-conformation' refers to the relative positions of the mechanically interlocked components with respect to each other, see: Fyfe, M. C. T.; Glink, P. T.; Menzer, S.; Stoddart, J. F.; White, A. J. P.; Williams, D. J. *Angew. Chem., Int. Ed. Engl.* **1997**, *36*, 2068-2070. With few exceptions, the co-conformational changes observed in catenanes and rotaxanes are associated with very much larger amplitude motions than result from conformational changes, at least within relatively small molecules. Indeed, it is the co-conformational motions that can be induced in interlocked molecules that help to make catenanes and rotaxanes such attractive molecules with which to design and construct molecular machinery.

(48) Altieri, A.; Bottari, G.; Dehez, F.; Leigh, D. A.; Wong, J. K. Y.; Zerbetto, F. *Angew. Chem., Int. Ed.* **2003**, *42*, 2296-2300.

(49) Chatterjee, M. N.; Kay, E. R.; Leigh, D. A. *J. Am. Chem. Soc.* **2006**, *128*, 4058-4073.

(50) Bissell, R. A.; Cordova, E.; Kaifer, A. E.; Stoddart, J. F. *Nature* **1994**, *369*, 133-137.

(51) Badjic, J. D.; Balzani, V.; Credi, A.; Silvi, S.; Stoddart, J. F. *Science* **2004**, *303*, 1845-1849.

(52) Badjic, J. D.; Ronconi, C. M.; Stoddart, J. F.; Balzani, V.; Silvi, S.; Credi, A. *J. Am. Chem. Soc.* **2006**, *128*, 1489-1499.

(53) Keaveney, C. M.; Leigh, D. A. *Angew. Chem., Int. Ed.* **2004**, *43*, 1222-1224.

(54) Leigh, D. A.; Morales, M. A. F.; Perez, E. M.; Wong, J. K. Y.; Saiz, C. G.; Slawin, A. M. Z.; Carmichael, A. J.; Haddleton, D. M.; Brouwer, A. M.; Buma, W. J.; Wurpel, G. W. H.; Leon, S.; Zerbetto, F. *Angew. Chem., Int. Ed.* **2005**, *44*, 3062-3067.

(55) Bottari, G.; Dehez, F.; Leigh, D. A.; Nash, P. J.; Perez, E. M.; Wong, J. K. Y.; Zerbetto, F. *Angew. Chem., Int. Ed.* **2003**, *42*, 5886-5889.

(56) Armaroli, N.; Balzani, V.; Collin J.-P.; Gavina, P.; Sauvage, J.-P.; Ventura, B. *J. Am. Chem. Soc.* **1999**, *121*, 4397-4408.

(57) Durola, F.; Sauvage, J.-P. *Angew. Chem., Int. Ed.* **2007**, *46*, 3537-3540.

(58) Tseng H.-R.; Wu, D.; Fang, N. X.; Zhang, X.; Stoddart, J. F. *ChemPhysChem* **2004**, *5*, 111-116.

(59) For representative examples, see (a) Koumura, N.; Zijlstra, R. W. J.; van Delden, R. A.; Harada, N.; Feringa, B. L. *Nature* **1999**, *401*, 152-155. (b) Wang, Q.-C.; Qu, D.-H.; Ren, J.; Chen, K.; Tian, H. *Angew. Chem., Int. Ed.* **2004**, *43*, 2661-2665. (c) Qu, D.-H.; Wang, Q.-C.; Tian, H. *Angew. Chem., Int. Ed.* **2005**, *44*, 5296-5299.

(60) (a) Bottari, G.; Leigh, D. A.; Perez, E. M. *J. Am. Chem. Soc.* **2003**, *125*, 13360-13361. (b) Perez, E. M.; Dryden, D. T. F.; Leigh, D. A.; Teobaldi, G.; Zerbetto, F. *J. Am. Chem. Soc.* **2004**, *126*, 12210-12211. (c) Berna, J.; Leigh, D. A.; Lubomska, M.; Mendoza, S. M.; Perez, E. M.; Rudolf, P.; Teobaldi, G.; Zerbetto, F. *Nature Mater.* **2005**, *4*, 704-710.

(61) Brouwer, A. M.; Frochot, C.; Gatti, F. G.; Leigh, D. A.; Mottier, L.; Paolucci, F.; Roffia, S.; Wurpel, G. W. H. *Science* **2001**, *291*, 2124-2128.

(62) Altieri, A.; Gatti, F. G.; Kay, E. R.; Leigh, D. A.; Martel, D.; Paolucci, F.; Slawin, A. M. Z.; Wong, J. K. Y. *J. Am. Chem. Soc.* **2003**, *125*, 8644-8654.

(63) (a) Leigh, D. A.; Wong, J. K. Y.; Dehez, F.; Zerbetto, F. *Nature* **2003**, *424*, 174-179. (b) Mandl, C. P.; Konig, B. *Angew. Chem., Int. Ed.* **2004**, *43*, 1622-1624.

(64) Hernandez, J. V.; Kay, E. R.; Leigh, D. A. *Science* **2004**, *306*, 1532-1537.

(65) (a) Arunkumar, E.; Forbes, C. C.; Noll, B. C.; Smith, B. D. *J. Am. Chem. Soc.* **2005**, *127*, 3288-3289. (b) Arunkumar, E.; Fu, N.; Smith, B. D. *Chem. Eur. J.* **2006**, *12*, 4684-4690.

(66) Johnson, J. R.; Fu, N.; Arunkumar, E.; Leevy, W. M.; Gammon, S. T.; Piwnica-Worms, D.; Smith, B. D. *Angew. Chem., Int. Ed.* **2007**, *46*, 5528-5531.

(67) See 2e and (a) Jimenez, M. C.; Dietrich-Buchecker, C.; Sauvage, J.-P.; Cian, A. D. *Angew. Chem., Int. Ed.* **2000**, *39*, 1295-1298. (b) Jimenez, M. C.; Dietrich-Buchecker, C.; Sauvage, J.-P. *Angew. Chem., Int. Ed.* **2000**, *39*, 3284-3287.

Light-Driven Reversible Translational Motion in Hydrogen-Bonded Benzoxazole-Containing Molecular Shuttles

For Submission as a Full Paper to *J. Am. Chem. Soc.*

Acknowledgements

The following people are gratefully acknowledged for their contribution to this chapter: Dr. C.-F. Lee for the photochemistry experiments using the multilamp photo-reactor; Dr. E. M. Pérez for many useful discussions; Prof. A. M. Z. Slawin of the University of St. Andrews solved the X-ray crystal structure of rotaxane *E*-**4**; Prof. W. J. Buma and Dr. K. Kuijt of the University of Amsterdam for the laser photoisomerisation experiments.

2.1 Summary

Recently, methods for controlling the position of a benzylic amide macrocycle in [2]rotaxanes with excellent positional integrity have been developed through the photoisomerisation of a fumaramide to a maleamide group. Although these systems represent some of the most effective bistable light-switchable shuttles developed to date, the photoisomerisation yields are typically only 50% in the photostationary states (PSS). With the aim of improving the yields of the photoisomerisation step, while maintaining the excellent positional integrity of these shuttles, *E*-3-(benzoxazol-2-yl)-*N*-methylacrylamide was investigated as a novel type of photo-responsive station. In this new station one of the amide groups of the fumaramide template is substituted by a benzoxazole moiety, which features a basic nitrogen atom as a hydrogen-bonding acceptor. It is expected that this will extend the conjugation, directly affecting the light-absorption properties of the system. A satisfactory yield of 43% for the rotaxane-forming reaction (*E*-**5**→*E*-**4**) validates the new station as a template, and the crystal structure confirms the predicted hydrogen-bonding network; the benzoxazole nitrogen atom behaves as H-bond acceptor. Direct irradiation of *E*-**4** at 350 nm (CH_2Cl_2, 298 K) for 120 s resulted in 70% of *Z*-**4** in the PSS, a significant increase in the photoisomerisation yield when compared to the

fumaramide template (50%). The introduction into the thread of a non-photoactive second station with intermediate macrocycle-binding affinity between *E*- and *Z*-3-(benzoxazol-2-yl)-*N*-methylacrylamide unit, namely succinic amide ester and adipamide stations, resulted in two photo-responsive molecular shuttles *E*-**6** and *E*-**8**. Shuttling of the macrocycle upon $E \rightarrow Z$ photoisomerisation is unambiguously demonstrated by ^{1}H NMR (400 MHz, $CDCl_3$, 298 K). For shuttle *E*-**6**, photochemistry by laser irradiation is performed in order to maximize the *Z*/*E* ratio in the PSS. When irradiated at 365 nm with 3 nm spectral bandwidth, 93% *Z*-**6** was achieved in the PSS, making it one of the highest yielding bistable light-switchable molecular shuttles discovered.

2.2 Introduction

Since their proposal by Stoddart and co-workers in 1991,[1] stimuli-responsive molecular shuttles based on rotaxanes have been widely studied as a type of molecular machines in which the relative positions of the interlocked components can be controlled in response to an external input. Generally, stimuli-responsive molecular shuttles possess two (or possibly more) recognition sites ('stations') and operate through the same basic principle (Figure 2.1). One of the stations on a linear thread should be able to switch between a state in which it shows 'high' affinity (green) for the macrocycle and another one with 'low' affinity (blue). A second non-switchable station (orange) is also required to exhibit a binding affinity somewhere between the high and low affinity states of the switchable one. The macrocycle populates the stations following a Boltzmann distribution according to the difference in binding affinities. Therefore, when the switchable station is in its high affinity state (i), the macrocycle spends most of its time over the green station because its binding affinity is higher than that of the intermediate, non-switchable, orange station. When the switchable station is subject to stimulus 1 it is transformed into its low affinity state. In this new state (ii), the macrocycle will move along the thread to its newly preferred non-reactive station through biased Brownian motion. The system ideally should be reversible by application of a second stimulus 2.

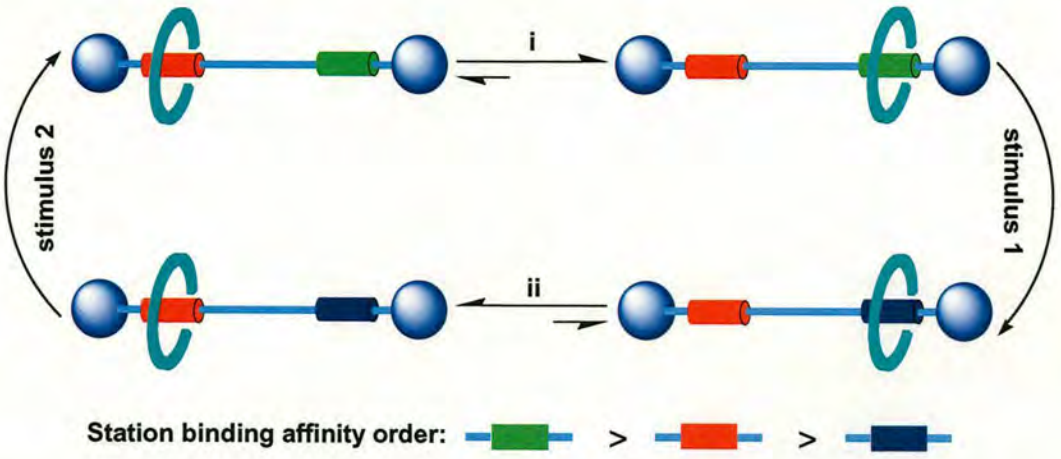

Figure 2.1 Macrocycle translation in a stimuli-responsive molecular shuttle. Stimulus 1 induces a transformation from green to blue and stimulus 2 induces a transformation from blue to green.

Although many different external stimuli such as light,[2] chemical,[3] electrochemical,[4] pH,[5] heat[6] and binding events[7] etc have been used to trigger the position changes of the macrocycle on the thread in such rotaxanes, photochemical reactions are particularly attractive because, firstly, no waste products are formed during the process;[8] secondly, with the advent of modern lasers it is now possible to simultaneously control both the spatial and temporal characteristics of light at a level that approaches nanometre lengths and femtosecond time scales.[9]

Previously, some photo- and thermally responsive shuttles have been described in which the macrocycle moves over 1.5 nm between two discrete stations with good positional integrity (Scheme 2.1).[2j] The basis for these shuttles lies in the photochemical and thermal isomerisation of fumaramide and maleamide groups. While the fumaramide station is a close-to-perfect fit for the benzylic amide macrocycle, its *Z* isomer (maleamide) can only interact very weakly with it.[10] By incorporating into the thread a non-photoactive second station with an intermediate macrocycle-binding affinity, such as succinamide, adipamide and succinic amide ester groups, it is possible to generate photoinduced, thermally reversible translation of the rotaxane components.

Scheme 2.1 Previously Described Photo- and Thermally Responsive Shuttles[2j]

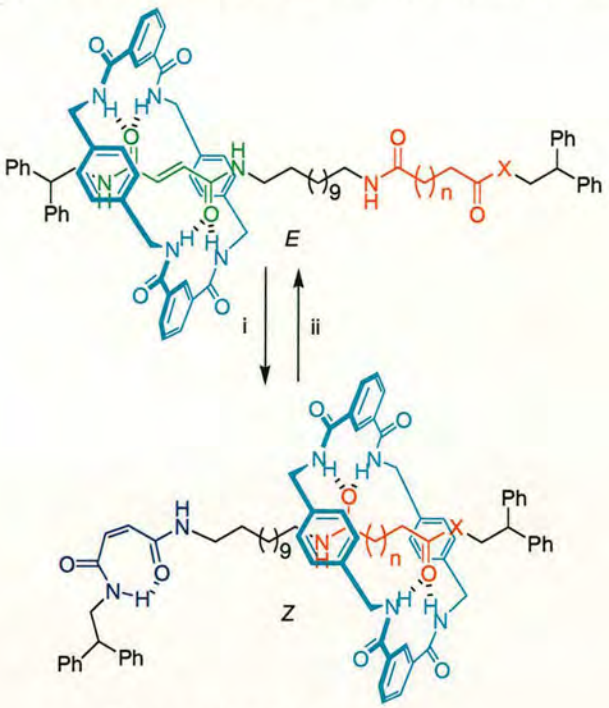

E-**1**, n=1, X=O; *Z*-**1**, n=1, X=O
E-**2**, n=1, X=NH; *Z*-**2**, n=1, X=NH
E-**3**, n=3, X=NH; *Z*-**3**, n=3, X=NH

Reagents and conditions: (i) hν at 254 nm for 30 min, CH_2Cl_2, *Z*-**1**, 54%; *Z*-**2**, 48%; *Z*-**3**, 39%; (ii) $C_2H_2Cl_4$ at 120 °C for 7 days, *E*-**1**, 80%; *E*-**2**, 80%; or 1 day, *E*-**3**, 95%.

Although these systems represent some of the most effective bistable light-switchable shuttles developed to date, the photoisomerisation yields are typically 50% in the PSS. With the aim of improving the yields of the photoisomerisation step, while maintaining the excellent positional integrity of these shuttles, *E*-3-(benzoxazol-2-yl)-*N*-methylacrylamide (*E*-**5**, Scheme 2.2) was investigated as a novel type of photo-responsive station. In this new station, one of the amide groups of the fumaramide template is still kept, because it is an excellent hydrogen bond acceptor and can form bifurcated intercomponent hydrogen bonds with the benzylic amide macrocycle.[10a] The other amide group is substituted by a benzoxazole moiety, which features a basic nitrogen atom as another hydrogen-bonding acceptor and is expected to extend the conjugation; this will directly affect the light-absorption properties of the system and ideally increase the photoisomerisation yields.[11]

2.3 Results and Discussion

Herein, the synthesis of a model [2]rotaxane *E*-**4** (Scheme 2.2) is reported and its application for the assembly of two reversible light-triggered molecular shuttles. For shuttle *E*-**6**, the *E*→*Z* photoisomerisation yield is 93%, upon laser excitation, making it one of the highest yielding bistable light-switchable shuttles discovered.

2.3.1 Synthesis and Photoisomerisation of Model Rotaxanes

A model single-binding-site rotaxane *E*-**4** was prepared in 43% yield from thread *E*-**5** (Scheme 2.2). This rotaxane contains a benzoxazole moiety and a secondary amide both carefully designed to hydrogen bond to the benzylic amide macrocycle. Rotaxane *E*-**4** was fully characterised by ^{1}H and ^{13}C NMR spectroscopy and HRMS. Comparison of the ^{1}H NMR spectra of the rotaxane *E*-**4** and its thread *E*-**5** (Figure 2.2a and b)[12] shows the significant shielding effect of the macrocycle on the olefin protons (H_d and H_e) as they are shifted upfield 1.0 and 1.2 ppm, respectively; this confirms the interlocked structure with the macrocycle over the olefinic bond.

Under the same reaction conditions, the *Z*-olefin thread *Z*-**5** did not give detectable quantities of the corresponding rotaxane *Z*-**4**, however, it can be prepared through photochemical isomerisation. Photoisomerisation experiments were performed in CH_2Cl_2 at room temperature for rotaxane *E*-**4** by using a multilamp photo-reactor (Full experimental procedures can be found in the Experimental Section). Upon irradiation at 350 nm, *E*→*Z* isomerisation produces a new isomer *Z*-**4**, which was monitored by ^{1}H NMR and TLC inspection. The ratio *E*/*Z* was determined by ^{1}H NMR and 30/70 was reached in the PSS after 120 sec (Figure 2.3). Pure *Z*-**4** was isolated by preparative TLC and characterised by ^{1}H and ^{13}C NMR spectroscopy and HRMS as well. In *Z*-**4**, olefin protons $H_{d'}$ and $H_{e'}$ are upfield shifted (0.8 and 1.4 ppm, respectively) with respect to their positions in the thread *Z*-**5** (Figure 2.2c and d).[12] H_a and H_b also significantly shifted upfield (0.6 and 0.9 ppm, respectively), indicating in the *Z* conformation the macrocycle resides closer to $-CH_2CHPh_2$ thread stopper. After irradiating *Z*-**4** for 120 sec at 312 nm, 73/27 *E*/*Z* ratio in the PSS was achieved (Figure 2.3). Compared with previously described fumaramide-derived [2]rotaxanes, the photo-conversion yield of this new station is remarkably better, even with shorter irradiation times and at longer wavelengths (lower energy).[10b]

Scheme 2.2 Synthesis of Model Rotaxanes *E*-**4** and *Z*-**4** [a]

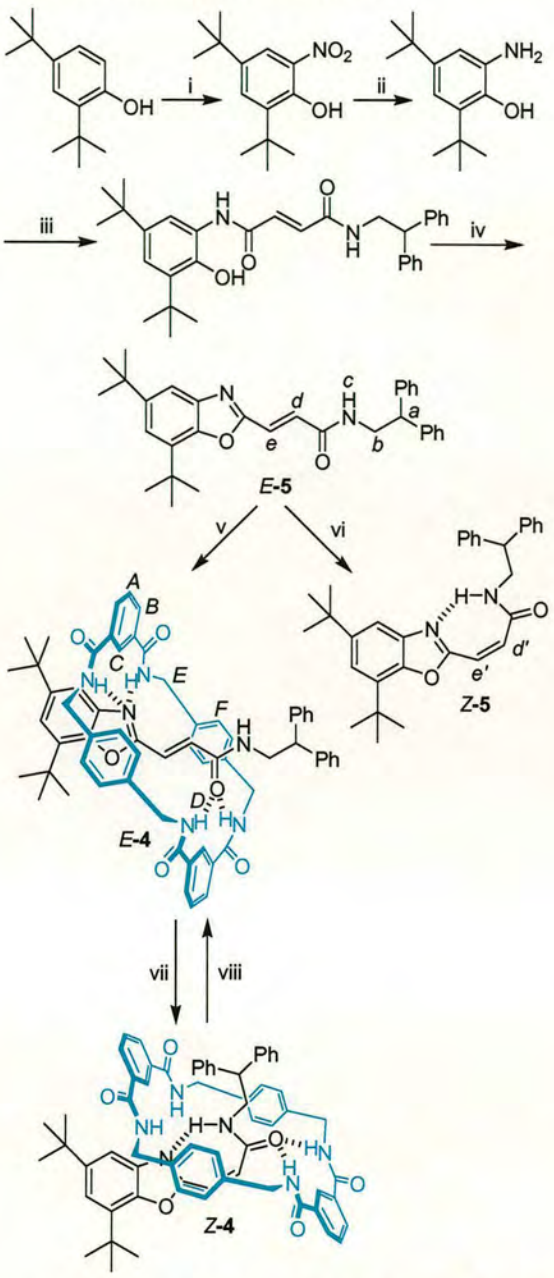

[a] Reagents and conditions: (i) HNO_3, CH_3COOH, 5-10 °C, 55%; (ii) $NH_2NH_2 \cdot H_2O$, Pd-C, EtOH, reflux, N_2, 80%; (iii) *N*-(2,2-diphenylethyl)-fumaramide acid, 4-dimethylaminopyridine (DMAP), 1-(3-dimethylaminopropyl)-3-ethyl-carbodiimide hydrochloride (EDCI·HCl), CH_2Cl_2/DMF, 0 °C to rt, N_2, 90%; (iv) toluene-4-sulfonic acid monohydrate, toluene, reflux, 79%; (v) *p*-xylylenediamine, isophthaloyl dichloride, Et_3N, $CHCl_3$, N_2, rt, 43%; (vi) hν at 350 nm for 20 min, CH_2Cl_2, 78%; (vii) hν at 350 nm for 120 sec, CH_2Cl_2, 70%; (viii) hν at 312 nm for 120 sec, CH_2Cl_2, 73%.

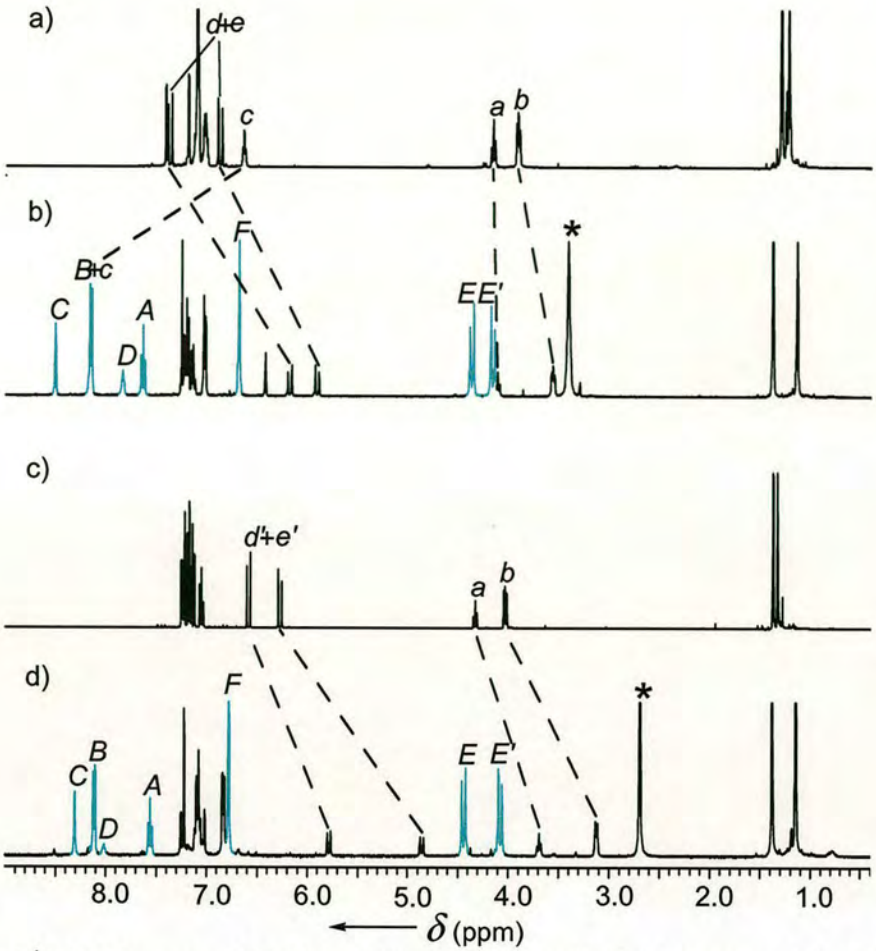

Figure 2.2 ^{1}H NMR spectra (400 MHz, 298 K) of a) thread *E*-**5**, b) rotaxane *E*-**4**, c) thread *Z*-**5** and d) rotaxane *Z*-**4** in $CDCl_3/CD_3OD$, 99:1. The letters correspond to the assignments shown in Scheme 2.2. The peaks highlighted with stars correspond to residual water.

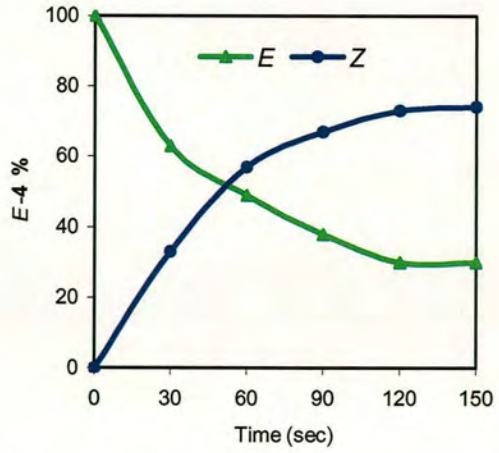

Figure 2.3 Photoisomerisation ratios of rotaxanes *E*-**4** (λ = 350 nm) and *Z*-**4** (λ = 312 nm).

Single crystals of *E*-**4** suitable for investigation by X-ray crystallography were grown directly from slow evaporation of a saturated solution of *E*-**4** in DMF. The crystal structure (Figure 2.4) again unambiguously confirms the interlocked nature of the rotaxane in the solid state and shows four unsymmetrical intercomponent hydrogen bonds; two between benzoxazole-*N* atom and macrocycle amides and the other two NH•••O=C interactions between the thread and the macrocycle.

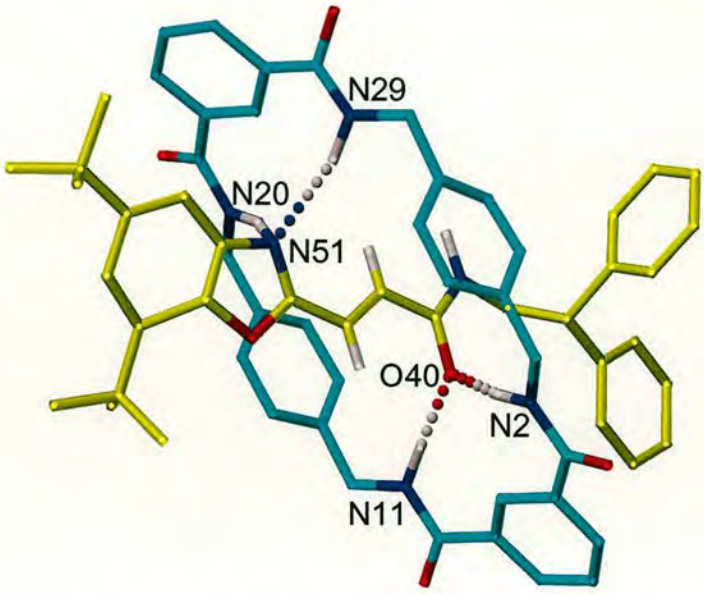

Figure 2.4 X-ray crystal structure of rotaxane *E*-**4** (for clarity carbon atoms of the macrocycle are shown in blue and the carbon atoms of the thread in yellow; oxygen atoms are depicted in red, nitrogen atoms in dark blue, and selected hydrogen atoms for the amide and olefin protons in white). Intramolecular hydrogen bond distances (Å) are the following: N20H-N51 2.774, N29H-N51 2.224, N2H-O40 2.107, N11H-O40 1.901.

2.3.2 Design and Synthesis of Molecular Shuttles

The transition state of the rotaxane-forming reaction is similar in structure to the final rotaxane,[13] therefore it seems likely that the macrocycle-binding affinity of a given station should be related to its ability to template the formation of the rotaxane and could be predicted from rotaxane yield.[14] Compared with their rotaxane formation yields (Figure 2.5), it seems reasonable that the adipamide or succinic amide ester station should possess intermediate hydrogen-bonding strength between *E*- and *Z*-3-(benzoxazol-2-yl)-*N*-methylacrylamide stations and could be utilised as a

second binding site to assemble the molecular shuttle by incorporating it into the thread.

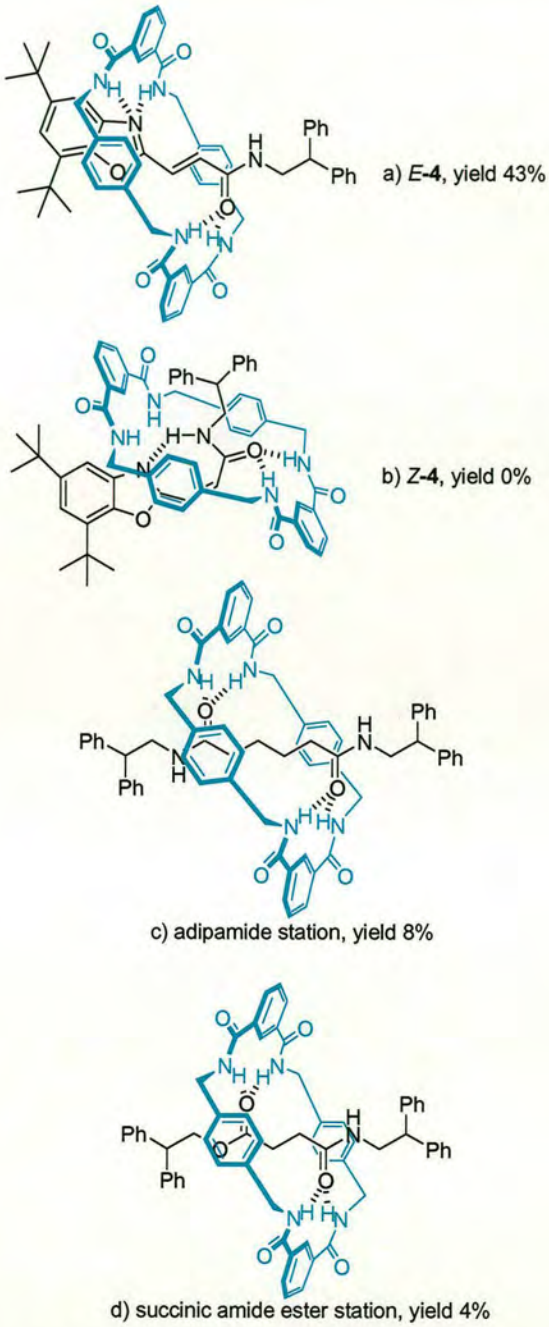

Figure 2.5 Model single-binding-site [2]rotaxanes formation yields from corresponding threads.

Therefore two different molecular shuttles *E*-**6** (Scheme 2.3) and *E*-**8** (Scheme 2.4) were prepared. Each rotaxane contains an *E*-3-(benzoxazol-2-yl)-*N*-methylacrylamide unit (shown in green) plus a non-photoactive second station (orange), namely

succinic amide ester (*E*-**6**) and adipamide (*E*-**8**) units respectively, separated by a C_{12} alkyl spacer.

Scheme 2.3 Synthesis of Molecular Shuttle *E*-**6** [a]

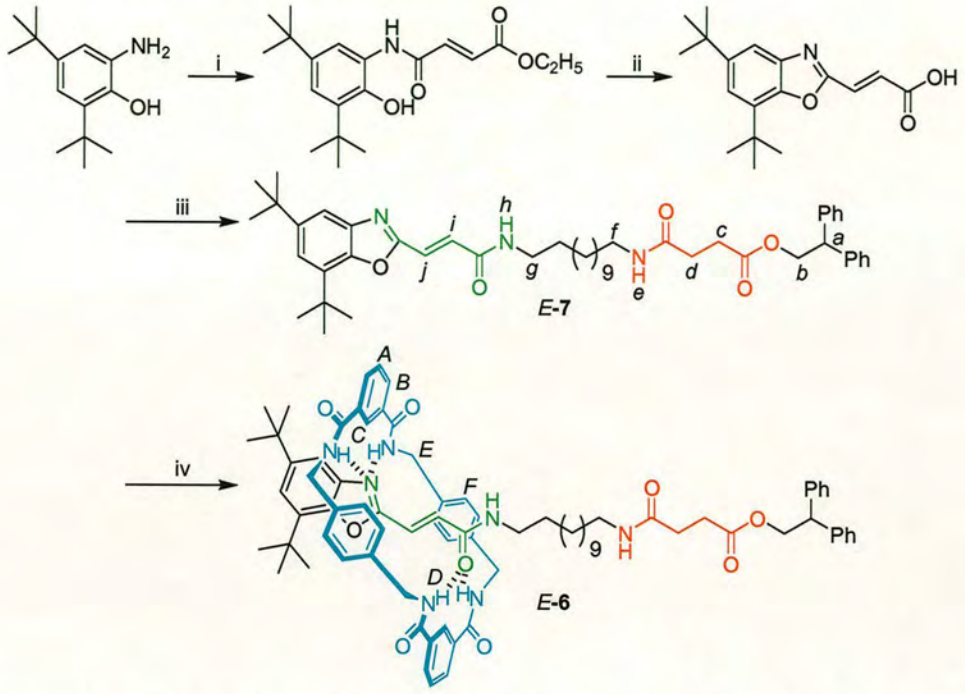

[a] Reagents and conditions: (i) fumaric acid monoethyl ester, 4-DMAP, EDCI·HCl, CH_2Cl_2, 0 °C to rt, N_2, 43%; (ii) toluene-4-sulfonic acid monohydrate, toluene, 90 °C, then 1M NaOH, THF, rt and 1M HCl, rt, 100%; (iii) *N*-(12-*tert*-butoxycarbonylaminododecyl)-succinamic acid 2,2-diphenylethyl ester (deprotected firstly with TFA, $CHCl_3$, rt, 100%), 4-DMAP, EDCI·HCl, CH_2Cl_2, 0 °C to rt, N_2, 96%; (iv) *p*-xylylenediamine, isophthaloyl dichloride, Et_3N, $CHCl_3$, N_2, rt, 51%.

Scheme 2.4 Synthesis of Molecular Shuttle *E*-**8** [a]

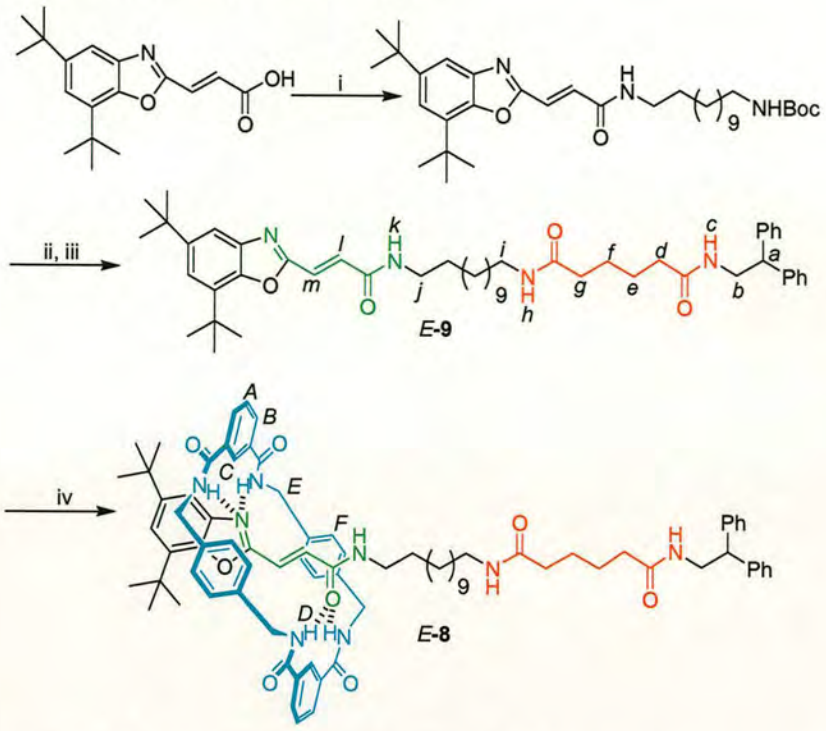

[a] Reagents and conditions: (i) 12-aminododecylcarbamic acid *tert*-butyl ester, 4-DMAP, EDCI·HCl, CH_2Cl_2, 0 °C to rt, N_2, 100%; (ii) TFA, $CHCl_3$, rt, 100%; (iii) 5-(2,2-diphenylethylcarbamoyl)-pentanoic acid, 4-DMAP, EDCI·HCl, CH_2Cl_2, 0 °C to rt, N_2, 86%; (iv) *p*-xylylenediamine, isophthaloyl dichloride, Et_3N, $CHCl_3$, N_2, rt, 43%.

The xylylene rings of the macrocycle shield encapsulated regions of the thread; therefore the positions of the macrocycle in $CDCl_3$ could be determined by comparing the chemical shifts of the protons in the rotaxane with those of the corresponding thread. The spectra of *E*-**6**/*E*-**7** and *E*-**8**/*E*-**9** in $CDCl_3$ (400 MHz, 298 K) are shown in Figure 2.6 and 2.7. For rotaxane *E*-**6** (Figure 2.6a and b), the H_i and H_j protons of the benzoxazole site are shielded, compared to the thread *E*-**7**, by δ = 0.8 and 0.6 ppm, respectively. The H_c and H_d protons of the succinic amide ester group only shift 0.2 and 0.2 ppm, respectively; this indicates that the macrocycle resides principally over the benzoxazole residue of the rotaxane.

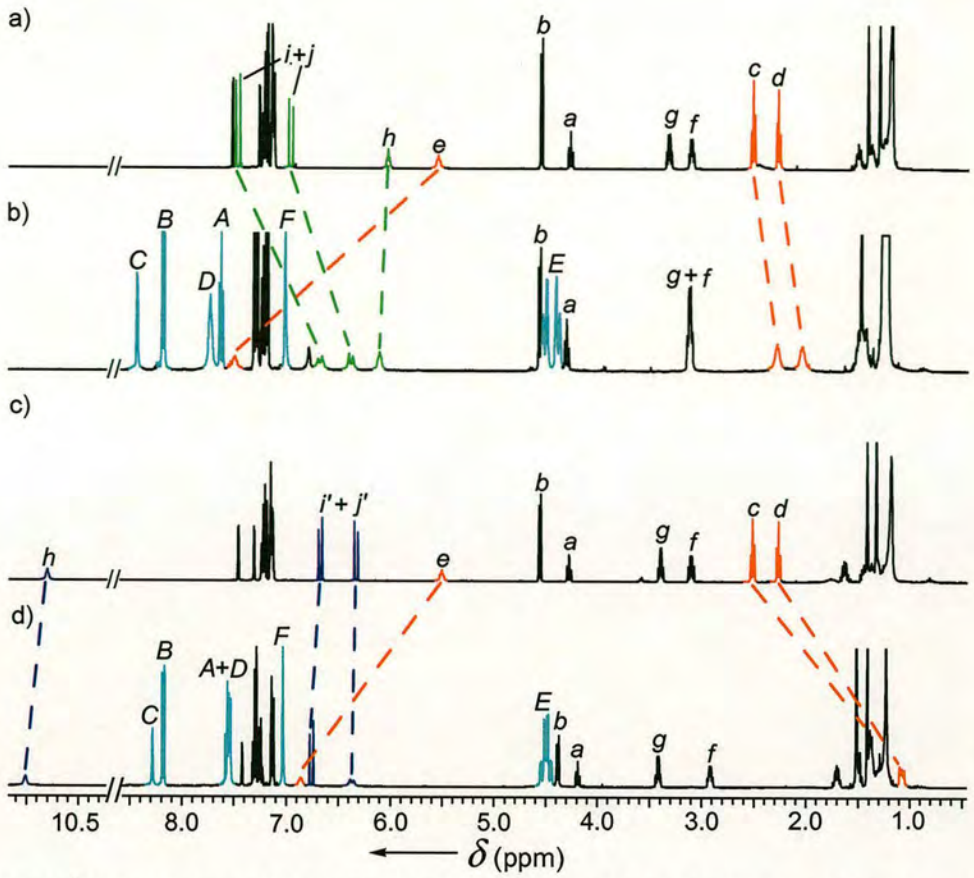

Figure 2.6 ^{1}H NMR spectra (400 MHz, 298 K) of a) thread *E*-**7**, b) rotaxane *E*-**6**, c) thread *Z*-**7** and d) rotaxane *Z*-**6** in $CDCl_3$. The letters correspond to the assignments shown in Scheme 2.3.

For rotaxane *E*-**8** (Figure 2.7a and b), a similar series of shifts occur in the ^{1}H NMR spectra. *E*-**8** shows better discrimination of the macrocycle toward the different stations.[14] In *E*-**8** the H_l and H_m protons are shifted 1.0 and 0.7 ppm upfield with respect to their positions in the thread *E*-**9**; whereas the chemical shifts of the protons of the adipamide group are similar in both compounds.

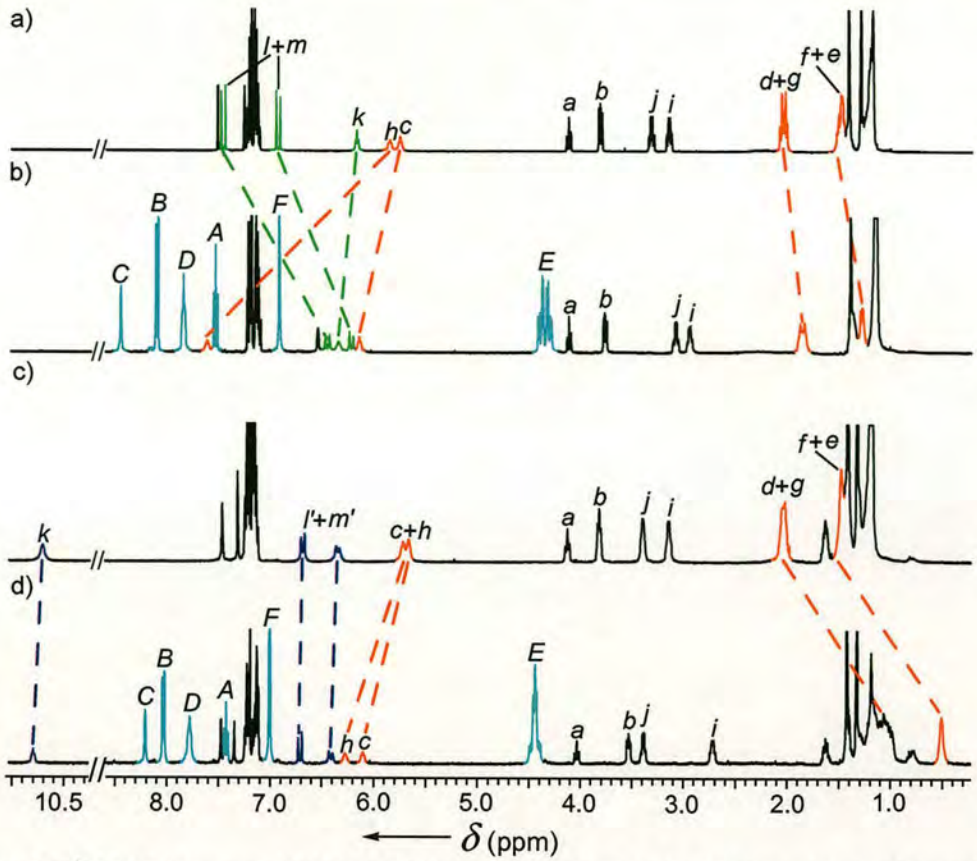

Figure 2.7 ^{1}H NMR spectra (400 MHz, 298 K) of a) thread *E*-**9**, b) rotaxane *E*-**8**, c) thread *Z*-**9** and d) rotaxane *Z*-**8** in $CDCl_3$. The letters correspond to the assignments shown in Scheme 2.4.

2.3.3 Photoisomerisation-Driven Shuttling Behaviour

Both rotaxanes *E*-**6**/*E*-**8** and threads *E*-**7**/*E*-**9** smoothly undergo photoisomerisation to the corresponding *Z* isomers (*Z*-**7**/*Z*-**9** are the *Z*-olefin isomers of threads *E*-**7**/*E*-**9**, their chemical structures are formally provided in the Experimental Section). The rotaxanes were dissolved in CH_2Cl_2 and the solutions were directly irradiated at 350 nm for *E*-**6** and 312 nm for *E*-**8** respectively (Scheme 2.5). The progress was monitored by TLC inspection and ^{1}H NMR. For both samples the PSS was reached in 2 min; *E*-**6**/*Z*-**6** in a 29:71 ratio and *E*-**8**/*Z*-**8** in a 50:50 ratio. As the photoisomerisation process produces few byproducts, *Z* isomers *Z*-**6**/*Z*-**8** and *Z*-**7**/*Z*-**9** were easily isolated from corresponding photoreaction mixtures by flash chromatography (silica gel) or preparative TLC (silica gel). Compared with *E*-shuttle *E*-**6** or *E*-**8**, the occupancy of the macrocycle is completely reversed in *Z*-**6** (Figure 2.6c and d) or *Z*-**8** (Figure 2.7c and d). For *Z*-**6** in $CDCl_3$, the olefin protons ($H_{i'}$ and $H_{j'}$) resonate at almost identical chemical shifts in the rotaxane and thread *Z*-**7**.

However the succinic amide ester methylene groups (H_c and H_d) are each shielded by 1.1 ppm in the rotaxane, indicating that the ring has moved to the succinic amide ester site. The situation is similar for *Z*-**8**, as the macrocycle resides principally over the adipamide station in the rotaxane. The photochemistry is completely reversible; *Z* rotaxane *Z*-**6** (λ = 254 nm) or *Z*-**8** (λ = 350 nm) can be converted to the corresponding *E* isomers. For both samples the PSS was reached in 8 min; *E*-**6**/*Z*-**6** in a 47:53 ratio and *E*-**8**/*Z*-**8** in a 64:36 ratio (Scheme 2.5).

Scheme 2.5 Photo-Driven Shuttling Behaviour of Rotaxanes *E*/*Z*-**6** and *E*/*Z*-**8** [a]

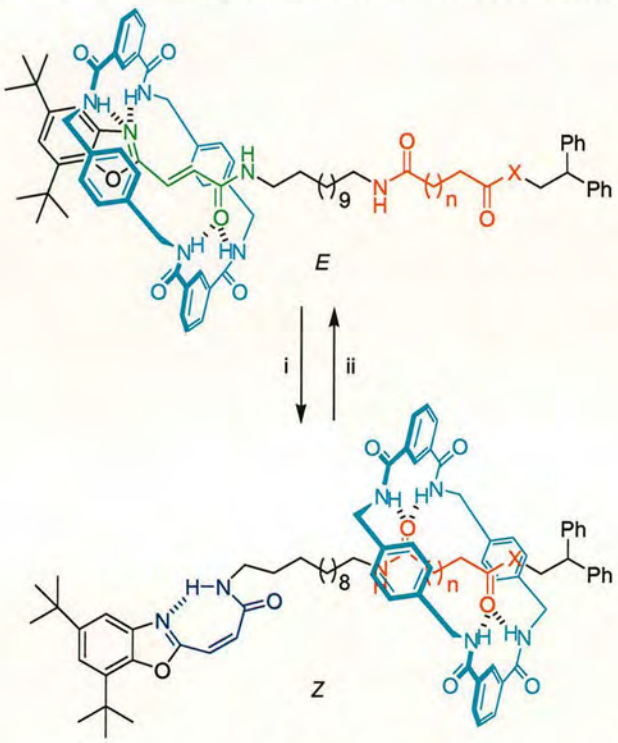

E-**6**, n=1, X=O; *Z*-**6**, n=1, X=O
E-**8**, n=3, X=NH; *Z*-**8**, n=3, X=NH

[a] Reagents and conditions: (i) λ = 350 nm for 2 min, CH_2Cl_2, *Z*-**6**, 71%; λ = 312 nm for 2 min, CH_2Cl_2, *Z*-**8**, 50%; (ii) λ = 254 nm for 8 min, CH_2Cl_2, *E*-**6**, 47%; λ = 350 nm for 8 min, CH_2Cl_2, *E*-**8**, 64%.

2.3.4 PSS Investigation of Shuttles *E*/*Z*-6 upon Laser Irradiation

The photoisomerisation yield with shuttle *E*-**6** is significantly better than the fumaramide shuttles *E*-**1-3**. However, it should be possible to maximize the *Z*/*E* and *E*/*Z* ratio in the PSS for shuttles *E*/*Z*-**6** when using laser light as the stimulus. Three types of experiments were considered: (i) direct one-photon excitation at wavelengths

with maximum difference in the absorption spectrum of both isomers, (ii) sensitised (one-photon) excitation using an appropriate triplet sensitiser, (iii) direct two-photon excitation at different absorption wavelengths. For method (i), the wavelength should be chosen that has the largest absorbance difference while maintaining reasonable molar absorbance, in order to obtain not-too-long conversion times. It is assumed that quantum yields for both conversion directions are the same, although this is not necessarily true. For method (ii), the ideal triplet sensitiser can be excited above ~370 nm where the rotaxanes do not absorb. Its triplet state should have higher energy than the triplet state of the rotaxane isomers.

The absorption spectra of shuttles *E*-**6** (1.7×10^{-5} M)/*Z*-**6** (1.8×10^{-5} M) were recorded in CH_3CN and the ratio of the spectra are shown in Figure 2.8. The *E*/*Z* ratio is close to unity between 215 and 290 nm. At 193 nm (output of ArF excimer laser) the *E*/*Z* ratio is 0.58:1 suggesting irradiation of the *Z* isomer at 193 nm may produce 63% of the *E* isomer. At 365 nm the ratio exceeds 15:1 suggesting that approximately 94% *Z* isomer may be obtained. Thus, it was concluded that the *E*→*Z* isomerisation could be performed quite selectively. As one-photon, direct excitation was not selective enough for *Z*→*E* conversion, two-photon absorption and triplet sensitisation were considered for selective conversion of the *Z* isomer.

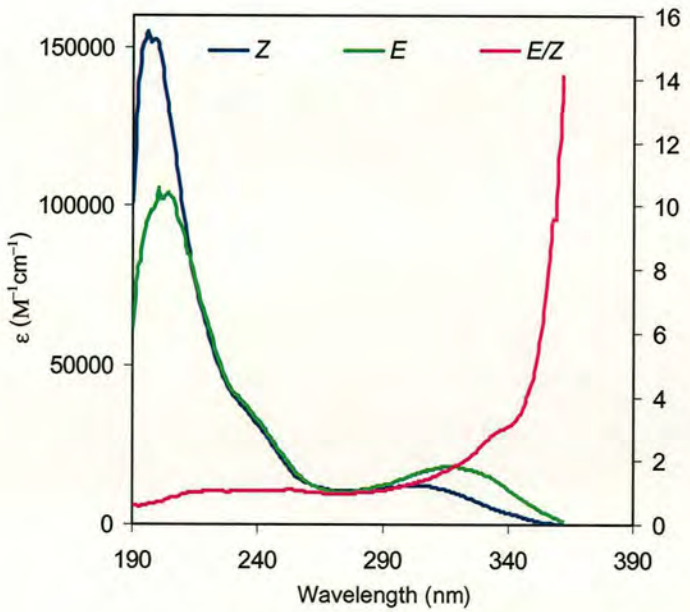

Figure 2.8 Absorption spectra of shuttles *E*-**6** (1.7×10^{-5} M)/*Z*-**6** (1.8×10^{-5} M) in CH_3CN and the ratio of the spectra.

2.3.4.1 One-Photon Irradiation Experiments

At 365 nm the absorption difference between *E* and *Z* isomer exceeds 15, while the intensity of the *E* absorption band may still be high enough to achieve conversion in a reasonable time. As a compromise between speed of conversion and selectivity, the excitation slit width of the SPEX fluorescence spectrometer was set to 3 nm. The conversion was monitored during the irradiation experiment and determined by HPLC (see Experimental Section). About 90% of the *Z* isomer was produced after 5 h irradiation. The conversion was not complete after 5 h and 93% of the *Z* isomer was formed in the PSS after 7 h (Figure 2.9; see also Experimental Section Figure A1 on page 88 and 89). Possibly, these yields can be improved using a slightly longer irradiation wavelength and/or a smaller spectral bandwidth (*e.g.*, 2 nm), but at the expense of even longer irradiation times.

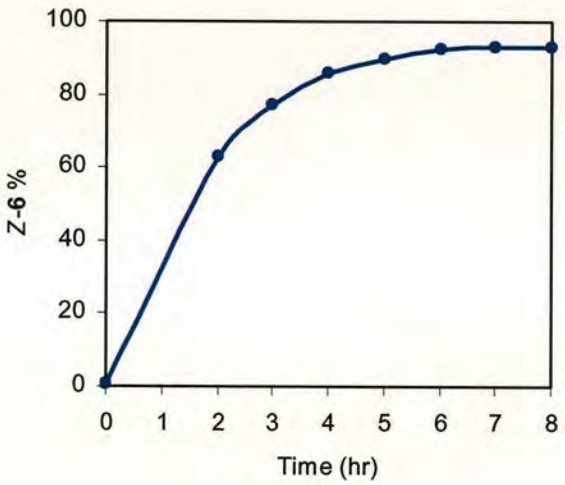

Figure 2.9 One-photon-excited conversion of ***E*-6** into ***Z*-6** at 365 nm with 3 nm spectral bandwidth.

Irradiation of the *Z* isomer during 2.5 h at 254 nm produced 52% of the *E* isomer, which is close to the expectation based on the absorption spectra (assuming equal efficiencies for both isomerisation reactions). One-photon excitation at 193 nm (ArF laser, 30 Hz) for the *Z*→*E* conversion was also performed and ratio up to 59:41 of *E*/*Z* was obtained, but photodecomposition of the *Z* rotaxane also occurred (~12% in 90 min, see Experimental Section Figure A3 on page 90).

2.3.4.2 Two-Photon Irradiation Experiments

The absorption cross sections for two-photon absorption may be quite different from the one-photon molar absorbance. Therefore, two-photon excitation was considered to be an interesting option to enhance the selectivity of $Z \rightarrow E$ conversion. Three wavelengths were used, *i.e.*, 644, 600 and 550 nm. These experiments were performed using CH_3CN as the solvent. The first experiments were performed at 644 nm, using a repetitive rate of 10 Hz and pulse energy of 6.5 mJ (IR energy set to 400 mJ). It was observed that the solvent discoloured upon excitation. In the chromatograms (diode array) several peaks appeared due to photodecomposition of the solvent or impurities in the solvent. The *Z* isomer (present at 8.5×10^{-6} M) showed slow conversion (initially 1.4% *E*; afterwards about 9%); unfortunately the rotaxane also showed significant photodecomposition, *i.e.*, ~30% (see Experimental Section Figure A2 on page 90).

At the other wavelengths (600 and 550 nm) the conversion appeared to be even slower. Possibly, the two-photon absorption cross section is smaller than at 644 nm. Moreover, the average power at the wavelength of interest had to be kept below 65 mW (6.5 mJ/pulse). At higher power the cuvet was severely damaged at both sides from the focal point. As the energy per photon is higher at these wavelengths, the number of photons is lower with constant power and, thus, the probability of two-photon processes is lower. It was also observed that the photodecomposition of CH_3CN was much less than at 644 nm. At 600 nm, the photodecomposition of the rotaxane was comparable to that at 644 nm, while it was less at 550 nm. Therefore, it appears that a two-photon (or multi-photon) process is involved in the photodecomposition of both solvent and rotaxane. 2,2,2-Trifluoroethanol and 2-propanol were also tested; these solvents showed less photodecomposition, especially 2-propanol. However, the rotaxane solubility in 2-propanol is much less and the rotaxane HPLC peaks appeared to be split when it was dissolved in 2-propanol.

2.3.4.3 Triplet-Sensitised Excitation Experiments

Triplet-sensitised excitation experiments for *Z*-**6** were performed with the xenon lamp of a SPEX Fluorolog 3 fluorescence spectrometer at 380 nm using an excitation slit width of 4 nm and 4,4'-bis(dimethylamino)benzophenone (DMAB) as the

sensitiser. The overall results are better than direct irradiation and 65% of the *E*-**6** was obtained after 14 h with only about 5% photodecomposition (Figure 2.10).

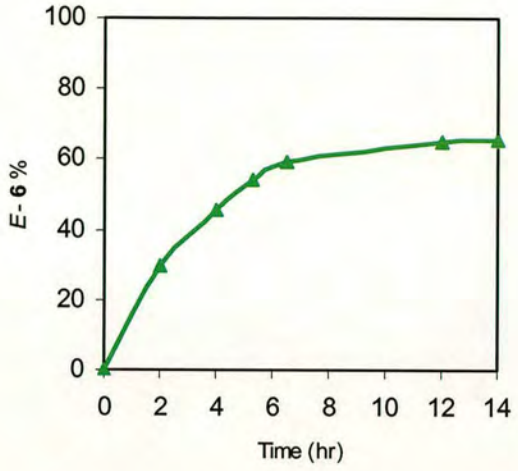

Figure 2.10 Triplet-sensitised conversion of *Z*-**6** into *E*-**6** at 380 nm with 4 nm spectral bandwidth.

2.3.5 Thermally-Driven Shuttling Behaviour of *Z*-6

The conversion from *Z*-**6** to *E*-**6** thermally was also investigated. Relative to conventional thermal heating, microwave heating has shorter reaction times, increase in yields and suppression of side product formation.[15] Here a microwave-assisted thermal isomerisation was developed for shuttle *Z*-**6**. After 5 h (150 °C, $C_2D_2Cl_4$), 94% *E*-**6** was achieved without evidence of any decomposition, determined by ^1H NMR (Figure 2.11).

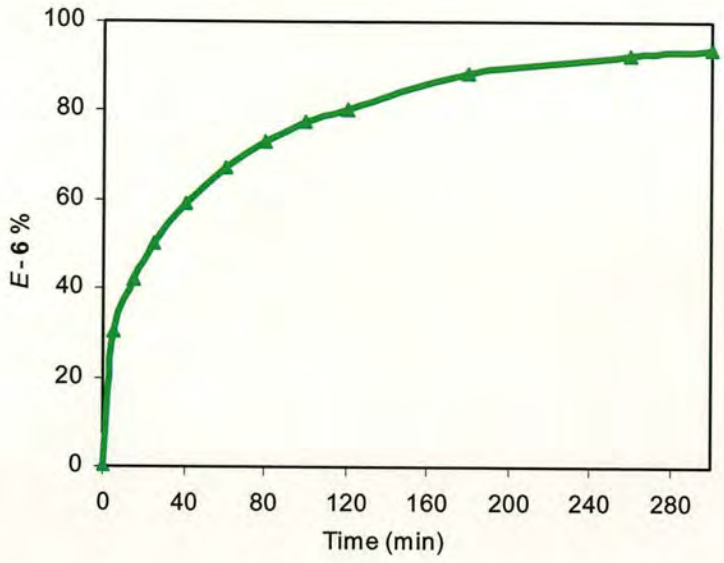

Figure 2.11 Thermally-driven conversion of *Z*-**6** into *E*-**6** at 150 °C upon microwave heating.

2.4 Conclusions

The use of the intercomponent interactions between the benzoxazole-containing motif in the thread and the benzylic amide macrocycle provides an accessible and efficient method for the synthesis of model [2]rotaxane *E*-**4**. Irradiation of *E*-**4** produces the corresponding *Z* isomer *Z*-**4**, in which the maximum number of intercomponent hydrogen bonds changes from four to two, considerably reducing the binding strength between the thread and the macrocycle. Lying in the macrocycle discrimination between the 'matched' (*E*) and 'mismatched' (*Z*) binding sites, two reversible light-driven molecular shuttles *E*-**6** and *E*-**8** were generated by incorporating a second non-photoactive station into the thread, here succinic amide ester and adipamide groups respectively. Furthermore they both exhibit remarkable positional integrity of the macrocycle on the thread before and after the photo stimulus. The 93% yield of *Z*-**6** from *E*→*Z* photoisomerisation by laser irradiation in the PSS provides one of the most efficient photo conversions described to date. The present study would afford the opportunity to design and develop nanoscale switching devices based on external trigger driven molecular shuttles.

2.5 Experiments

2.5.1 General

Unless stated otherwise, all reagents and anhydrous solvents were purchased from Aldrich Chemicals and used without further purification. *P*-xylylene diamine was distilled under reduced pressure and isophthaloyl dichloride was recrystallised from *n*-hexane. Column chromatography was performed using Kiesegel C60 (Merck, Germany) as the stationary phase, and TLC was performed on precoated silica gel plates (0.25 mm thick, $60F_{254}$, Merck, Germany) and observed under UV light. All ^{1}H and ^{13}C NMR spectra were recorded on a Bruker AV 400 instrument, at a constant temperature of 25 °C. Chemical shifts are reported in parts per million from high to low field and referenced to TMS. Coupling constants (*J*) are reported in Hertz (Hz). Standard abbreviations indicating multiplicity are used as follows: m = multiplet, br = broad, d = doublet, q = quadruplet, t = triplet, s = singlet. All melting points were determined using Sanyo Gallenkamp apparatus and are reported uncorrected. FAB mass spectrometry was carried out by the services at the University of Edinburgh.

2.5.2 General Procedure for the Photoisomerisation Using the Multilamp Photo-Reactor

Rotaxanes (*E*/*Z*-**4**, *E*/*Z*-**6** and *E*/*Z*-**8**) or threads (*E*-**5**, *E*-**7** and *E*-**9**) were dissolved in CH_2Cl_2 ($\sim 10^{-4}$ M) in a quartz vessel. The solution was degassed by bubbling N_2 for 10 minutes, then directly irradiated at appropriate wavelength using a multilamp photo-reactor (Model MLU18, Model 3022 lamps, Photochemical Reactors Ltd., Reading, UK). The progress of the photoisomerisation was monitored by TLC or ^{1}H NMR. After the PSS was reached the reaction mixture was concentrated *in vacuo* to afford the crude product, purified by column chromatography or preparative TLC.

2.5.3 General Procedure for the Photoisomerisation of Rotaxanes *E*/*Z*-6 upon Laser Irradiation

One-photon irradiation of the *E* isomer (*E*-**6**) was performed using the xenon lamp and excitation monochromator of the SPEX fluorescence spectrometer at 365 nm. During irradiation, the sample (ca. 2.5 ml) was stirred with a small stirring bar

rotating at 1800 rpm. One-photon irradiation of the *Z* isomer (*Z*-**6**) was performed using a Zeiss mercury lamp and an Oriel monochromator set at 254 nm. Samples, stock solutions and neat rotaxanes were protected from ambient light. The solids were stored in the fridge in a tightly closed bottle together with blue silica.

The two-photon experiments were performed with the Infinity (Nd:YAG)-XPO setup delivering ~2 ns pulses at a repetitive rate of 10 Hz. A 35 mm lens was used for focusing light into the cuvet. The maximum pulse energy possible without damaging the 10 mm cuvet was used, in order to promote the simultaneous absorption of two photons.

The triplet-sensitised excitation experiments were performed with the xenon lamp of a SPEX Fluorolog 3 fluorescence spectrometer at 380 nm using an excitation slit width of 4 nm. 4,4'-bis(dimethylamino)benzophenone was used as the sensitiser, the concentrations of sensitiser and *Z* isomer (*Z*-**6**) were 1.0×10^{-2} M (1.008×10^{-2} M) and 1.0×10^{-5} M (9.64×10^{-6} M) respectively. CH_3CN was used as the solvent and the starting sample volume was 2.0 mL.

HPLC was taken as the method of choice for analysis, because it requires only small amounts of the rotaxanes (as opposed to ^1H NMR). Separation of the isomers was obtained using a 250 mm long C18 column. The Shimadzu HPLC system was equipped with a diode array absorption detector which facilitates peak identification. Samples were initially prepared in CH_2Cl_2, but in most experiments CH_3CN was used. For the two-photon experiments, the photostability of 2-propanol and 2,2,2-trifluoroethanol was also tested. Adequate separation was achieved by eluting the rotaxanes isocratically with a CH_3CN/H_2O (90:10) mixture. The sensitivities (area/concentration) appeared to be reproducible over several days. Therefore external calibration could be omitted, although it was used initially.

2,4-Di-*tert*-butyl-6-nitrophenol, S1

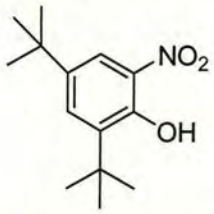

To a stirred suspension of 2,4-di-*tert*-butylphenol (20.0 g, 0.10 mol) in acetic acid (100 mL) cooled to 5-10 °C was added dropwise 70% nitric acid (6.1 mL, 0.10 mol). After 1.5 h, the reaction mixture was poured into the ice water and neutralized to pH ~7 with sat. $NaHCO_3$, then toluene (200 mL) was added and the resultant extract was dried over $MgSO_4$, concentrated *in vacuo* and the crude product purified by column chromatography (*n*-hexane) to yield **S1** as a yellow solid (13.5 g, yield = 55%). m.p. 58-60 °C; ^{1}H NMR (400 MHz, $CDCl_3$): δ = 1.33 (s, 9H, C(C*H*$_3$)$_3$), 1.46 (s, 9H, C(C*H*$_3$)$_3$), 7.67 (s, 1H, Ar*H*), 7.98 (s, 1H, Ar*H*), 11.48 (s, 1H, O*H*); ^{13}C NMR (100 MHz, $CDCl_3$): δ = 29.3, 31.1, 34.5, 35.7, 118.8, 132.6, 133.6, 139.8, 141.9, 153.0; HRMS calcd. for $C_{14}H_{22}NO_3$ $[M+H]^+$: 252.15997, Found (FAB, 3-NOBA matrix): 252.15993.

2-Amino-4,6-di-*tert*-butylphenol, S2

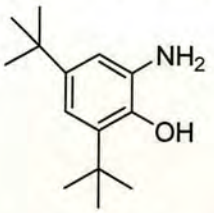

A stirred solution of **S1** (12.7 g, 0.05 mol), hydrazine hydrate (7.4 mL, 0.15 mol) and a catalytic amount of Pd-C (10% w/w) in ethanol (150 mL) was heated at reflux under an atmosphere of nitrogen. After 3 h the reaction mixture was filtered, concentrated *in vacuo* and the residue re-dissolved in chloroform, washed with brine (3 × 50 mL), dried over $MgSO_4$ and concentrated *in vacuo* to yield **S2** as a white solid (9.0 g, yield = 80%). m.p. 66-68 °C; ^{1}H NMR (400 MHz, $CDCl_3$): δ = 1.27 (s, 9H, C(C*H*$_3$)$_3$), 1.41 (s, 9H, C(C*H*$_3$)$_3$), 3.18 (br s, 2H, N*H*$_2$), 5.75 (br s, 1H, O*H*), 6.82 (s, 1H, Ar*H*), 6.91 (s, 1H, Ar*H*); ^{13}C NMR (100 MHz, $CDCl_3$): δ = 29.8, 31.6, 34.2,

34.7, 115.7, 117.0, 132.3, 135.7, 142.5, 144.0; HRMS calcd. for $C_{14}H_{24}NO$ $[M+H]^+$: 222.18579, Found (FAB, 3-NOBA matrix): 222.18570.

_N_-(2,2-Diphenylethyl)-fumaramide acid, S3

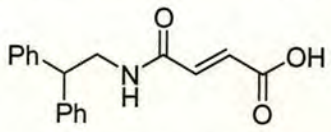

This compound was synthesized as described in Altieri, A.; Bottari, G.; Dehez, F.; Leigh, D. A.; Wong, J. K. Y.; Zerbetto, F. *Angew. Chem., Int. Ed.* **2003**, *42*, 2296-2300 and showed identical spectroscopic data to those reported therein.

N^1-(3,5-Di-*tert*-butyl-2-hydroxyphenyl)-N^4-(2,2-diphenylethyl)fumaramide, S4

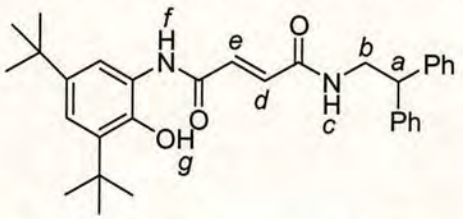

To a stirred solution of **S2** (0.50 g, 2.3 mmol), **S3** (0.67 g, 2.3 mmol) and 4-DMAP (0.28 g, 2.3 mmol) in dichloromethane/DMF (1:1, 40 mL) cooled on an ice bath was added EDCI•HCl (0.44 g, 2.3 mmol) and the reaction was allowed to stir for 70 h at room temperature under an atmosphere of nitrogen. The reaction mixture was concentrated *in vacuo* and the residue re-dissolved in chloroform, washed successively with 2M HCl (3 × 50 mL), sat. $NaHCO_3$ (3 × 50 mL) and brine (3 × 50 mL), dried over $MgSO_4$ and filtered. The resultant solid in the filter was washed with 5:1 $CHCl_3$:CH_3OH and the solution concentrated *in vacuo* to yield **S4** as a yellow solid (1.02 g, yield = 90%). m.p. 228-230 °C; ^{1}H NMR (400 MHz, DMSO-d_6): δ = 1.23 (s, 9H, C(CH_3)$_3$), 1.36 (s, 9H, C(CH_3)$_3$), 3.85 (dd, J = 5.7, 7.8 Hz, 2H, H_b), 4.25 (t, J = 7.8 Hz, 1H, H_a), 6.92 (d, J = 15.2 Hz, 1H, H_d or H_e), 7.08-7.33 (m, 13H, 12ArH+H_e or H_d), 8.63 (br t, J = 5.7 Hz, 1H, H_c), 9.12 (s, 1H, H_f), 10.59 (s, 1H, H_g); ^{13}C NMR (100 MHz, DMSO-d_6): δ = 29.6, 31.3, 33.9, 34.9, 43.4, 49.9, 118.9, 120.9, 126.4, 127.8, 128.4, 131.6, 134.2, 137.9, 140.9, 142.7, 146.1, 157.3, 163.3, 163.7;

HRMS calcd. for $C_{32}H_{39}N_2O_3$ $[M+H]^+$: 499.29607, Found (FAB, 3-NOBA matrix): 499.29603.

(*E*)-3-(5,7-Di-*tert*-butylbenzo[*d*]oxazol-2-yl)-*N*-(2,2-diphenylethyl)acrylamide, *E*-5

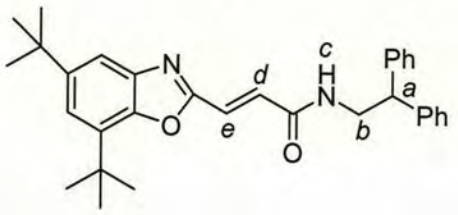

A stirred solution of **S4** (0.40 g, 0.80 mmol) and toluene-4-sulfonic acid monohydrate (0.76 g, 4.0 mmol) in toluene (20 mL) was heated at reflux. After 5 h, the reaction mixture was concentrated *in vacuo* and the residue re-dissolved in chloroform, washed with sat. $NaHCO_3$ (3 × 50 mL) and brine (3 × 50 mL), dried over $MgSO_4$, concentrated *in vacuo* and the crude product purified by column chromatography (99:1 $CHCl_3$:CH_3OH) to yield *E*-**5** as a brown solid (0.30 g, yield = 79%). m.p. 84-86 °C; ^{1}H NMR (400 MHz, $CDCl_3$/CD_3OD, 99:1): δ = 1.29 (s, 9H, $C(CH_3)_3$), 1.36 (s, 9H, $C(CH_3)_3$), 3.98 (dd, J = 5.7, 7.9 Hz, 2H, H_b), 4.22 (t, J = 7.9 Hz, 1H, H_a), 6.71 (br t, J = 5.7 Hz, 1H, H_c), 6.95 (d, J = 15.7 Hz, 1H, H_d or H_e), 7.07-7.20 (m, 11H, Ar*H*), 7.44 (d, J = 15.7 Hz, 1H, H_e or H_d), 7.48 (s, 1H, Ar*H*); ^{13}C NMR (100 MHz, $CDCl_3$): δ = 29.7, 31.6, 34.2, 34.9, 44.1, 50.3, 114.3, 120.6, 125.8, 126.6, 127.8, 128.5, 129.8, 133.7, 141.5, 141.9, 146.6, 147.9, 160.0, 164.1; HRMS calcd. for $C_{32}H_{37}N_2O_2$ $[M+H]^+$: 481.28550, Found (FAB, 3-NOBA matrix): 481.28579.

[2]-(1,7,14,20-Tetraaza-2,6,15,19-tetraoxo-3,5,9,12,16,18,22,25-tetrabenzocyclohexacosane)-(*E*)-3-(5,7-di-*tert*-butylbenzo[*d*]oxazol-2-yl)-*N*-(2,2-diphenylethyl)acrylamide-rotaxane, *E*-4

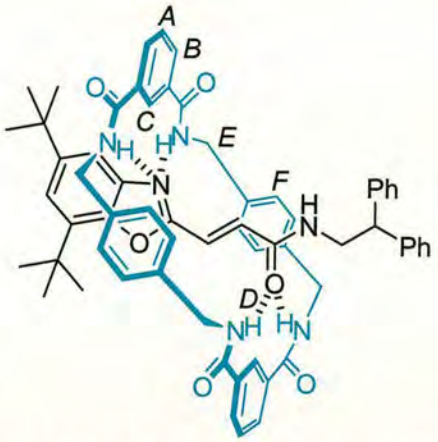

E-**5** (0.24 g, 0.50 mmol) and triethylamine (2.8 mL, 0.020 mol) were dissolved in chloroform (80 mL) and the mixture was stirred vigorously while solutions of *p*-xylylenediamine (1.36 g, 0.010 mol) in chloroform (40 mL) and isophthaloyl dichloride (2.03 g, 0.010 mol) in chloroform (40 mL) were simultaneously added over a period of 2 h using motor-driven syringe pumps at room temperature under nitrogen atmosphere. After a further 16 h the resulting suspension was filtered and concentrated *in vacuo*. The crude residue was purified by column chromatography (98.5:1.5 $CHCl_3$:CH_3OH) to yield *E*-**4** as a white solid (0.22 g, yield = 43%). Alternatively, *E*-**4** was also obtained when the solution of *Z*-**4** in dichloromethane was irradiated at 312 nm using a multilamp photo-reactor for 120 sec (yield = 73%, determined by ^{1}H NMR). m.p. 288-290 °C; ^{1}H NMR (400 MHz, $CDCl_3$/CD_3OD, 99:1): δ = 1.20 (s, 9H, C(CH_3)$_3$), 1.44 (s, 9H, C(CH_3)$_3$), 3.63 (dd, J = 5.7, 7.4 Hz, 2H, H_b), 4.16-4.24 (m, 5H, H_E+H_a), 4.43 (d, J = 14.1 Hz, 4H, H_E), 5.98 (d, J = 15.5 Hz, 1H, H_d or H_e), 6.25 (d, J = 15.5 Hz, 1H, H_e or H_d), 6.49 (s, 1H, Ar*H*), 6.76 (s, 8H, H_F), 7.09-7.34 (m, 11H, Ar*H*), 7.71 (t, J = 7.8 Hz, 2H, H_A), 7.91 (br t, J = 4.0 Hz, H_D, exchanged by CD_3OD), 8.23 (d, J = 7.8 Hz, 5H, H_B+H_c), 8.58 (s, 2H, H_C); ^{13}C NMR (100 MHz, $CDCl_3$/CD_3OD, 99:1): δ = 29.6, 31.3, 34.3, 34.9, 44.0, 44.8, 50.1, 112.3, 121.3, 122.0, 125.1, 126.9, 127.6, 128.0, 128.7 (× 2), 129.4, 131.3, 133.7, 134.5, 136.5, 139.8, 141.5, 146.6, 149.2, 160.3, 165.3, 167.2; HRMS calcd. for $C_{64}H_{65}N_6O_6$ $[M+H]^+$: 1013.49656, Found (FAB, 3-NOBA matrix): 1013.49492.

(*Z*)-3-(5,7-Di-*tert*-butylbenzo[*d*]oxazol-2-yl)-*N*-(2,2-diphenylethyl)acrylamide, *Z*-5

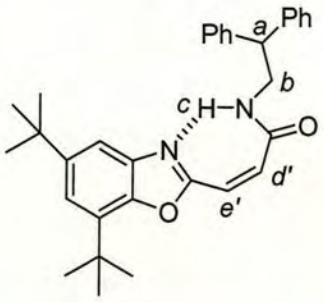

The solution of *E*-**5** in dichloromethane was irradiated at 350 nm using a multilamp photo-reactor for 20 min, and then concentrated *in vacuo*. The crude residue was purified by preparative TLC (1:1 EtOAc:*n*-hexane) to yield *Z*-**5** as a brown solid (yield = 78%, determined by ^{1}H NMR). m.p. 56-58 °C; ^{1}H NMR (400 MHz, $CDCl_3/CD_3OD$, 99:1): δ = 1.32 (s, 9H, $C(CH_3)_3$), 1.37 (s, 9H, $C(CH_3)_3$), 4.03 (dd, J = 5.2, 7.7 Hz, 2H, H_b), 4.33 (t, J = 7.7 Hz, 1H, H_a), 6.28 (d, J = 13.7 Hz, 1H, $H_{d'}$ or $H_{e'}$), 6.59 (d, J = 13.7 Hz, 1H, $H_{e'}$ or $H_{d'}$) 7.03-7.25 (m, 12H, Ar*H*), 10.72 (br t, J = 5.2 Hz, 1H, H_c); ^{13}C NMR (100 MHz, $CDCl_3$): δ = 29.8, 31.8, 34.4, 35.1, 44.6, 50.3, 114.2, 119.0, 121.1, 126.5, 128.1, 128.4, 134.0, 134.2, 140.5, 142.4, 145.9, 148.4, 159.1, 164.4; HRMS calcd. for $C_{32}H_{37}N_2O_2$ $[M+H]^+$: 481.28550, Found (FAB, 3-NOBA matrix): 481.28524.

[2]-(1,7,14,20-Tetraaza-2,6,15,19-tetraoxo-3,5,9,12,16,18,22,25-tetrabenzocyclohexacosane)-(*Z*)-3-(5,7-di-*tert*-butylbenzo[*d*]oxazol-2-yl)-*N*-(2,2-diphenylethyl)acrylamide-rotaxane, *Z*-4

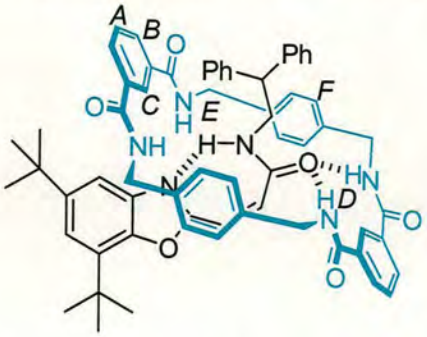

The solution of *E*-**4** in dichloromethane was irradiated at 350 nm using a multilamp photo-reactor for 120 sec, and then concentrated *in vacuo*. The crude residue was

purified by preparative TLC (98:2 $CHCl_3$:CH_3OH) to yield *Z*-**4** as a white solid (yield = 70%, determined by ^1H NMR). m.p. 150-152 °C; ^1H NMR (400 MHz, $CDCl_3/CD_3OD$, 99:1): δ = 1.14 (s, 9H, $C(CH_3)_3$), 1.37 (s, 9H, $C(CH_3)_3$), 3.12 (d, J = 7.6 Hz, 2H, H_b), 3.69 (t, J = 7.6 Hz, 1H, H_a), 4.07 (d, J = 14.4 Hz, 4H, $H_{E'}$), 4.44 (d, J = 14.4 Hz, 4H, H_E), 4.85 (d, J = 12.4 Hz, 1H, $H_{d'}$ or $H_{e'}$), 5.78 (d, J = 12.4 Hz, 1H, $H_{e'}$ or $H_{d'}$), 6.79 (s, 8H, H_F), 6.83-7.23 (m, 12H, Ar*H*), 7.56 (t, J = 7.8 Hz, 2H, H_A), 8.02 (br s, H_D, exchanged by CD_3OD), 8.12 (d, J = 7.8 Hz, 4H, H_B), 8.31 (s, 2H, H_C); ^{13}C NMR (100 MHz, $CDCl_3/CD_3OD$, 99:1): δ = 29.8, 31.5, 34.4, 34.9, 44.0, 44.1, 49.4, 113.6, 120.8, 122.7, 125.4, 126.5, 128.0, 128.4, 128.5, 129.2, 129.7, 131.0, 133.8, 133.9, 137.0, 140.9, 141.9, 146.0, 148.7, 157.8, 162.2, 166.8; HRMS calcd. for $C_{64}H_{65}N_6O_6$ $[M+H]^+$: 1013.49656, Found (FAB, 3-NOBA matrix): 1013.49644.

(*E*)-Ethyl 4-(3,5-di-*tert*-butyl-2-hydroxyphenylamino)-4-oxobut-2-enoate, S5

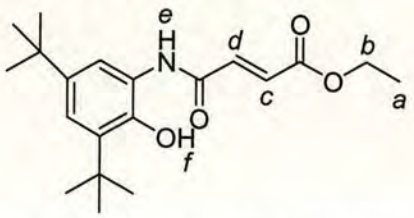

To a stirred solution of **S2** (3.21 g, 0.015 mol), fumaric acid monoethyl ester (2.09 g, 0.015 mol) and 4-DMAP (2.13 g, 0.017 mol) in dichloromethane(100 mL) cooled on an ice bath was added EDCI•HCl (3.34 g, 0.017 mol) and the reaction was allowed to stir for 17 h at room temperature under an atmosphere of nitrogen. The reaction mixture was washed successively with 1M HCl (3 × 50 mL), sat. $NaHCO_3$ (3 × 50 mL) and brine (3 × 50 mL), dried over $MgSO_4$ and concentrated *in vacuo*, the crude product purified by column chromatography (92:8 *n*-hexane:EtOAc) to yield **S5** as a yellow solid (2.18 g, yield = 43%). m.p. 172-174 °C; ^1H NMR (400 MHz, DMSO-d_6): δ = 1.25-1.29 (m, 12H, $C(CH_3)_3$+H_a), 1.38 (s, 9H, $C(CH_3)_3$), 4.23 (q, J = 7.1 Hz, 2H, H_b), 6.74 (d, J = 15.4 Hz, 1H, H_c or H_d), 7.13 (s, 2H, Ar*H*), 7.31 (d, J = 15.4 Hz, 1H, H_d or H_c), 8.93 (s, 1H, H_e), 10.51 (s, 1H, H_f); ^{13}C NMR (100 MHz, DMSO-d_6): δ = 14.0, 29.5, 31.3, 33.9, 34.9, 60.8, 119.0, 121.0, 125.7, 129.6, 136.7, 137.9, 141.0, 146.2, 162.7, 164.8; HRMS calcd. for $C_{20}H_{30}NO_4$ $[M+H]^+$: 348.21748, Found (FAB, 3-NOBA matrix): 348.21746.

(*E*)-3-(5,7-Di-*tert*-butylbenzo[*d*]oxazol-2-yl)acrylic acid, S6

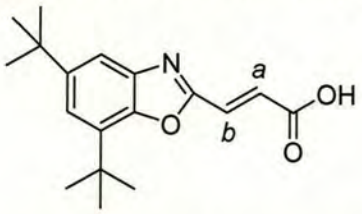

A stirred solution of **S5** (1.0 g, 2.9 mmol) and toluene-4-sulfonic acid monohydrate (2.7 g, 14.2 mmol) in toluene (100 mL) was heated to 90 °C under an atmosphere of nitrogen. After 3 h, the reaction mixture was concentrated *in vacuo* and the residue re-dissolved in EtOAc, washed with sat. $NaHCO_3$ (3 × 50 mL) and brine (3 × 50 mL), dried over $MgSO_4$ and concentrated *in vacuo* to afford a brown sticky oil. Without further purification, to a stirred solution of this brown sticky oil in THF (50 mL) was added dropwise a solution of 1M NaOH (15.3 mL). After 4 h, the THF was removed from the reaction mixture *in vacuo*, 1M HCl was added dropwise whereupon a yellow precipitate formed. It was filtered, washed with water and dried *in vacuo* to yield **S6** as a yellow solid (0.9 g, yield = 100% over 2 steps). m.p. 194-196 °C; ^{1}H NMR (400 MHz, DMSO-d_6): δ = 1.38 (s, 9H, C(CH_3)$_3$), 1.50 (s, 9H, C(CH_3)$_3$), 6.94 (d, J = 15.9 Hz, 1H, H_a or H_b), 7.40 (s, 1H, Ar*H*), 7.46 (d, J = 15.9 Hz, 1H, H_b or H_a), 7.67 (s, 1H, Ar*H*); ^{13}C NMR (100 MHz, DMSO-d_6): δ = 29.6, 31.4, 34.1, 34.8, 114.5, 120.8, 128.4, 128.6, 133.6, 141.8, 146.2, 147.9, 159.4, 166.0; HRMS calcd. for $C_{18}H_{24}NO_3$ $[M+H]^+$: 302.17562, Found (FAB, 3-NOBA matrix): 302.17560.

***N*-(12-*tert*-Butoxycarbonylaminododecyl)-succinamic acid 2,2-diphenylethyl ester, S7**

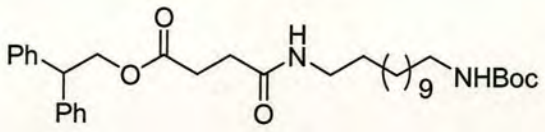

This compound was synthesized as described in Altieri, A.; Bottari, G.; Dehez, F.; Leigh, D. A.; Wong, J. K. Y.; Zerbetto, F. *Angew. Chem., Int. Ed.* **2003**, *42*, 2296-2300 and showed identical spectroscopic data to those reported therein.

(*E*)-2,2-Diphenylethyl 4-(12-(3-(5,7-di-*tert*-butylbenzo[*d*]oxazol-2-yl)acrylamido)dodecylamino)-4-oxobutanoate, *E*-7

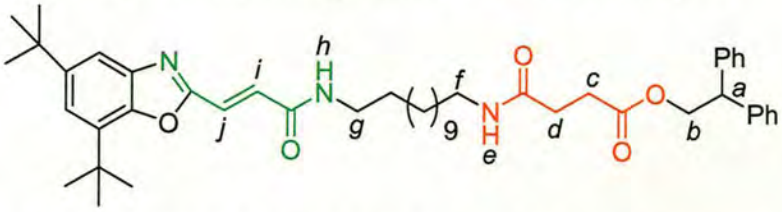

To a stirred solution of **S7** (0.74 g, 1.27 mmol) in anhydrous chloroform (40 mL) was added TFA (7.0 mL, 0.094 mol) and the solution allowed to stir at room temperature for 3 h. The solvent and the excess of TFA were removed *in vacuo*. The resulting oil was taken up in anhydrous dichloromethane (60 mL) and **S6** (0.46 g, 1.53 mmol), 4-DMAP (0.39 g, 3.19 mmol), EDCI•HCl (0.61 g, 3.18 mmol) added in order under nitrogen atmosphere at 0 °C whilst stirring. After 38 h, the reaction mixture was washed successively with 10% citric acid (3 × 50 mL), sat. $NaHCO_3$ (3 × 50 mL) and brine (3 × 50 mL), dried over $MgSO_4$ and concentrated *in vacuo*, the crude product purified by column chromatography (98:2 $CHCl_3$:CH_3OH) to yield *E*-**7** as a brown sticky oil (0.93 g, yield = 96% over 2 steps). ^{1}H NMR (400 MHz, $CDCl_3$): δ = 1.14-1.28 (m, 16H, -C*H*$_2$- (alkyl chain)), 1.30 (s, 9H, C(C*H*$_3$)$_3$), 1.33-1.41 (m, 11H, C(C*H*$_3$)$_3$ and -C*H*$_2$-CH$_f$), 1.45-1.55 (m, 2H, -C*H*$_2$-CH$_g$), 2.27 (t, *J* = 6.9 Hz, 2H, *H*$_d$), 2.51 (t, *J* = 6.9 Hz, 2H, *H*$_c$), 3.11 (m, 2H, *H*$_f$), 3.33 (m, 2H, *H*$_g$), 4.27 (t, *J* = 7.6 Hz, 1H, *H*$_a$), 4.55 (d, *J* = 7.6 Hz, 2H, *H*$_b$), 5.55 (br t, *J* = 5.3 Hz, 1H, *H*$_e$), 6.04 (br t, *J* = 5.7 Hz, 1H, *H*$_h$), 6.97 (d, *J* = 15.7 Hz, 1H, *H*$_i$ or *H*$_j$), 7.12-7.17 (m, 6H, Ar*H*), 7.20-7.25 (m, 4H, Ar*H*), 7.26 (s, 1H, Ar*H*), 7.48 (d, *J* = 15.7 Hz, 1H, *H*$_j$ or *H*$_i$), 7.53 (s, 1H, Ar*H*); ^{13}C NMR (100 MHz, $CDCl_3$): δ = 26.8, 26.9, 29.2 (× 2), 29.4 (× 2), 29.5 (× 2), 29.7, 29.9 (× 2), 31.0, 31.7 (× 2), 34.4, 35.1, 39.6, 40.0, 49.7, 66.8, 114.4, 120.9, 125.8, 126.8, 128.1, 128.5, 130.4, 133.9, 141.0, 141.7, 146.7, 148.3, 160.2, 164.0, 171.1, 172.8; HRMS calcd. for $C_{48}H_{66}N_3O_5$ $[M+H]^+$: 764.50025, Found (FAB, 3-NOBA matrix): 764.50022.

[2]-(1,7,14,20-Tetraaza-2,6,15,19-tetraoxo-3,5,9,12,16,18,22,25-tetrabenzocyclohexacosane)-(*E*)-2,2-diphenylethyl 4-(12-(3-(5,7-di-*tert*-butylbenzo[*d*]oxazol-2-yl)acrylamido)dodecylamino)-4-oxobutanoate-rotaxane, *E*-6

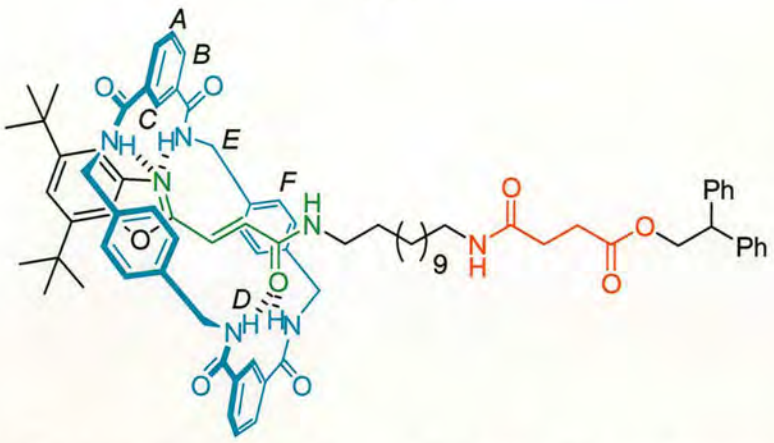

E-**7** (0.74 g, 0.97 mmol) and triethylamine (2.2 mL, 0.016 mol) were dissolved in chloroform (150 mL) and the mixture was stirred vigorously while solutions of *p*-xylylenediamine (1.06 g, 7.78 mmol) in chloroform (40 mL) and isophthaloyl dichloride (1.58 g, 7.78 mmol) in chloroform (40 mL) were simultaneously added over a period of 2 h using motor-driven syringe pumps at room temperature under nitrogen atmosphere. After a further 24 h the resulting suspension was filtered and concentrated *in vacuo*. The crude residue was purified by column chromatography (98.5:1.5 $CHCl_3$:CH_3OH) to yield *E*-**6** as a white solid (0.64 g, yield = 51%). Alternatively, *E*-**6** was also obtained when the solution of *Z*-**6** in dichloromethane was irradiated at 254 nm using a multilamp photo-reactor for 8 min (yield = 47%, determined by ^{1}H NMR). m.p. 120-122 °C; ^{1}H NMR (400 MHz, $CDCl_3$): δ = 1.17-1.31 (m, 25H, C(CH_3)$_3$ and -CH_2- (alkyl chain)), 1.40-1.56 (m, 13H, C(CH_3)$_3$, -CH_2-CH_f and -CH_2-CH_g), 2.04 (br s, 2H, H_d), 2.28 (br s, 2H, H_c), 3.12 (m, 4H, H_f and H_g), 4.31 (t, J = 7.6 Hz, 1H, H_a), 4.39 (d, J = 13.1 Hz, 4H, $H_{E'}$), 4.47-4.61 (m, 6H, H_E and H_b), 6.11 (br s, 1H, H_h), 6.39 (d, J = 15.0 Hz, 1H, H_i or H_j), 6.69 (d, J = 15.0 Hz, 1H, H_j or H_i), 6.79 (s, 1H, Ar*H*), 7.02 (s, 8H, H_F), 7.18-7.33 (m, 11H, Ar*H*), 7.50 (br s, 1H, H_e), 7.64 (t, J = 7.8 Hz, 2H, H_A), 7.74 (br s, 4H, H_D), 8.20 (d, J = 7.8 Hz, 4H, H_B), 8.45 (s, 2H, H_C); ^{13}C NMR (100 MHz, $CDCl_3$): δ = 26.7, 26.9, 29.1 (× 3), 29.3 (× 5), 29.8 (× 2), 31.6 (× 2), 34.5, 35.0, 39.7, 40.3, 44.3, 49.7, 67.1, 113.0, 121.3,

124.9, 126.9, 128.1, 128.3, 128.6, 128.9, 129.2, 129.5, 131.2, 133.9, 134.5, 137.1, 140.2, 140.8, 146.7, 149.0, 160.3, 164.8, 166.8, 171.6, 173.2; HRMS calcd. for $C_{80}H_{94}N_7O_9$ $[M+H]^+$: 1296.71130, Found (FAB, 3-NOBA matrix): 1296.71157.

(*Z*)-2,2-Diphenylethyl 4-(12-(3-(5,7-di-*tert*-butylbenzo[*d*]oxazol-2-yl)acrylamido)dodecylamino)-4-oxobutanoate, *Z*-7

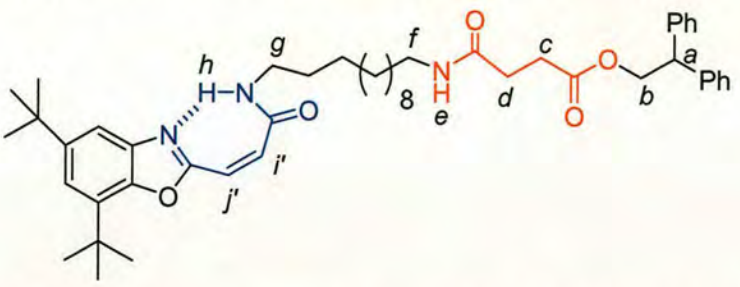

The solution of *E*-**7** in dichloromethane was irradiated at 350 nm using a multilamp photo-reactor for 10 min, and then concentrated *in vacuo*. The crude residue was purified by preparative TLC (2:1 EtOAc:*n*-hexane) to yield *Z*-**7** as a sticky oil (yield = 42%, determined by ^{1}H NMR). ^{1}H NMR (400 MHz, $CDCl_3$): δ = 1.13-1.27 (m, 16H, -C*H*$_2$- (alkyl chain)), 1.32 (s, 9H, C(C*H*$_3$)$_3$), 1.35-1.47 (m, 11H, C(C*H*$_3$)$_3$ and -C*H*$_2$-CH$_f$), 1.59-1.66 (m, 2H, -C*H*$_2$-CH$_g$), 2.26 (t, J = 6.9 Hz, 2H, H_d), 2.51 (t, J = 6.9 Hz, 2H, H_c), 3.10 (m, 2H, H_f), 3.39 (m, 2H, H_g), 4.28 (t, J = 7.6 Hz, 1H, H_a), 4.56 (d, J = 7.6 Hz, 2H, H_b), 5.50 (br t, J = 5.4 Hz, 1H, H_e), 6.33 (d, J = 13.9 Hz, 1H, $H_{i'}$ or $H_{j'}$), 6.67 (d, J = 13.9 Hz, 1H, $H_{j'}$ or $H_{i'}$), 7.12-7.24 (m, 10H, Ar*H*), 7.31 (s, 1H, Ar*H*), 7.46 (s, 1H, Ar*H*), 10.64 (br t, J = 4.5 Hz, 1H, H_h); ^{13}C NMR (100 MHz, $CDCl_3$): δ = 26.9, 27.3, 29.0, 29.3, 29.5 (× 3), 29.6, 29.7, 29.8 (× 2), 31.0, 31.7 (× 2), 34.5, 35.1, 39.6, 40.0, 49.7, 66.8, 113.9, 118.7, 121.3, 126.8, 128.1, 128.5, 134.4, 134.9, 140.7, 141.0, 146.1, 148.7, 159.5, 164.2, 171.1, 172.8; HRMS calcd. for $C_{48}H_{66}N_3O_5$ $[M+H]^+$: 764.50025, Found (FAB, 3-NOBA matrix): 764.50016.

[2]-(1,7,14,20-Tetraaza-2,6,15,19-tetraoxo-3,5,9,12,16,18,22,25-tetrabenzocyclohexacosane)-(*Z*)-2,2-diphenylethyl 4-(12-(3-(5,7-di-*tert*-butylbenzo[*d*]oxazol-2-yl)acrylamido)dodecylamino)-4-oxobutanoate-rotaxane, *Z*-6

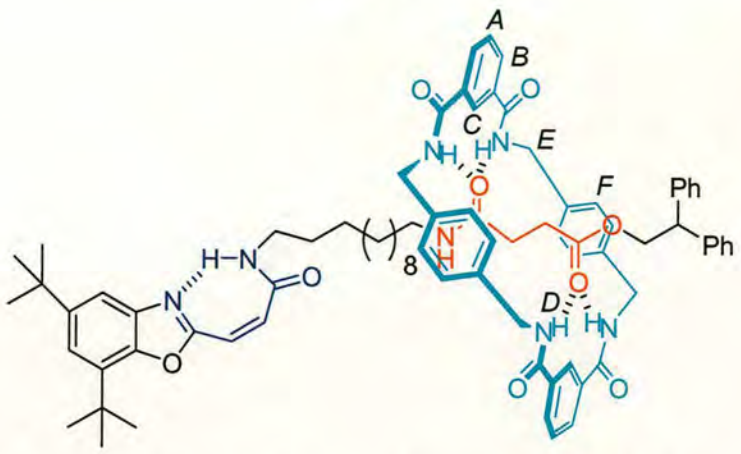

The solution of *E*-**6** in dichloromethane was irradiated at 350 nm using a multilamp photo-reactor for 2 min, and then concentrated *in vacuo*. The crude residue was purified by column chromatography (a gradient of EtOAc:$CHCl_3$:*n*-hexane 3:1:1 to EtOAc:$CHCl_3$:*n*-hexane:CH_3OH 3:1:1:0.1) to yield *Z*-**6** as a pale yellow solid (yield = 71%, determined by ^1H NMR). m.p. 102-104 °C; ^1H NMR (400 MHz, $CDCl_3$): δ = 1.04-1.09 (m, 2H, H_d), 1.16-1.43 (m, 27H, $C(CH_3)_3$, $-CH_2-$ (alkyl chain) and H_c), 1.46-1.53 (m, 11H, $C(CH_3)_3$ and $-CH_2-CH_f$), 1.66-1.73 (m, 2H, $-CH_2-CH_g$), 2.91 (m, 2H, H_f), 3.41 (m, 2H, H_g), 4.18 (t, J = 7.3 Hz, 1H, H_a), 4.38 (d, J = 7.3 Hz, 2H, H_b), 4.50 (m, 8H, H_E), 6.37 (d, J = 13.6 Hz, 1H, $H_{i'}$ or $H_{j'}$), 6.75 (d, J = 13.6 Hz, 1H, $H_{j'}$ or $H_{i'}$), 6.85 (br s, 1H, H_e), 7.03 (s, 8H, H_F), 7.12-7.14 (m, 4H, Ar*H*), 7.22-7.32 (m, 7H, Ar*H*), 7.42 (s, 1H, Ar*H*), 7.54-7.59 (m, 6H, H_D and H_A), 8.18 (d, J = 7.8 Hz, 4H, H_B), 8.29 (s, 2H, H_C), 10.85 (br s, 1H, H_h); ^{13}C NMR (100 MHz, $CDCl_3$): δ = 26.8, 27.0, 27.5, 28.5, 28.7, 28.9, 29.0 (× 2), 29.1 (× 2), 29.8 (× 2), 31.7 (× 2), 34.5, 35.2, 39.9, 40.2, 44.0, 49.5, 67.6, 113.7, 124.2, 127.1, 128.0, 128.1, 128.6, 128.7, 128.8, 128.9, 129.0, 129.1, 131.3, 133.8 (× 2), 134.0, 137.6, 140.6, 146.1, 159.3, 164.6, 166.6, 172.2, 174.1; HRMS calcd. for $C_{80}H_{94}N_7O_9$ $[M+H]^+$: 1296.71130, Found (FAB, 3-NOBA matrix): 1296.71101.

12-Aminododecylcarbamic acid *tert*-butyl ester, S8

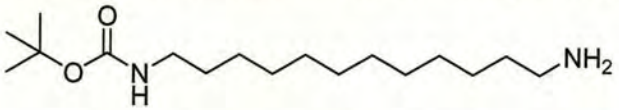

This compound was synthesized as described in Altieri, A.; Bottari, G.; Dehez, F.; Leigh, D. A.; Wong, J. K. Y.; Zerbetto, F. *Angew. Chem., Int. Ed.* **2003**, *42*, 2296-2300 and showed identical spectroscopic data to those reported therein.

(*E*)-*tert*-Butyl 12-(3-(5,7-di-*tert*-butylbenzo[*d*]oxazol-2-yl)acrylamido)dodecylcarbamate, S9

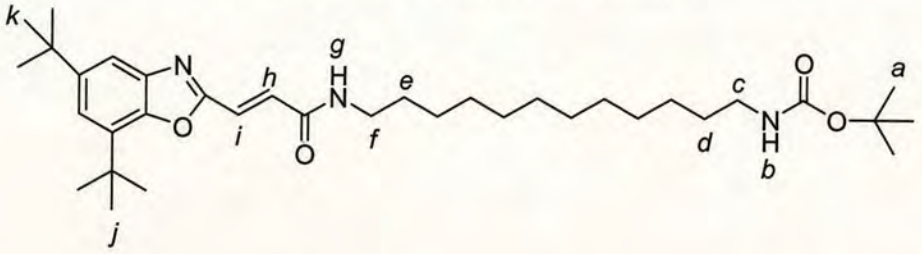

To a stirred solution of **S6** (0.50 g, 1.66 mmol), **S8** (0.50 g, 1.66 mmol) and 4-DMAP (0.26 g, 2.13 mmol) in dichloromethane(100 mL) cooled on an ice bath was added EDCI•HCl (0.41 g, 2.14 mmol) and the reaction was allowed to stir for 14 h at room temperature under an atmosphere of nitrogen. The reaction mixture was washed successively with 10% citric acid (3 × 50 mL), sat. $NaHCO_3$ (3 × 50 mL) and brine (3 × 50 mL), dried over $MgSO_4$ and concentrated *in vacuo* to yield **S9** as sticky oil (0.97 g, yield = 100%). ^{1}H NMR (400 MHz, $CDCl_3$): δ = 1.18-1.28 (m, 16H, -C*H*$_2$- (alkyl chain)), 1.30 (s, 9H, H_j or H_k), 1.37 (m, 11H, H_a and H_d), 1.41 (s, 9H, H_k or H_j), 1.48-1.55 (m, 2H, H_e), 3.02 (br t, J = 6.9 Hz, 2H, H_c), 3.34 (m, 2H, H_f), 4.46 (br s, 1H, H_b), 6.03 (t, J = 5.8 Hz, 1H, H_g), 6.96 (d, J = 15.7 Hz, 1H, H_h or H_i), 7.26 (s, 1H, Ar*H*), 7.48 (d, J = 15.7 Hz, 1H, H_i or H_h), 7.53 (s, 1H, Ar*H*); ^{13}C NMR (100 MHz, $CDCl_3$): δ = 26.7, 26.9, 28.4 (× 2), 29.2 (× 2), 29.4 (× 2), 29.5, 29.9 (× 2), 30.0, 31.4, 31.7, 34.4, 35.1, 40.0, 40.6, 114.5, 120.9, 126.0, 130.2, 133.9, 141.9, 146.7, 148.2, 156.0, 160.2, 164.0; HRMS calcd. for $C_{35}H_{58}N_3O_4$ $[M+H]^+$: 584.44273, Found (FAB, 3-NOBA matrix): 584.44245.

5-(2,2-Diphenylethylcarbamoyl)-pentanoic acid, S10

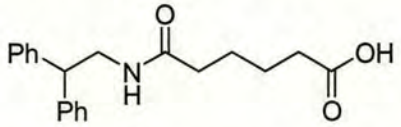

This compound was synthesized as described in Altieri, A.; Bottari, G.; Dehez, F.; Leigh, D. A.; Wong, J. K. Y.; Zerbetto, F. *Angew. Chem., Int. Ed.* **2003**, *42*, 2296-2300 and showed identical spectroscopic data to those reported therein.

(*E*)-N^1-(12-(3-(5,7-Di-*tert*-butylbenzo[*d*]oxazol-2-yl)acrylamido)dodecyl)-N^6-(2,2-diphenylethyl)adipamide, *E*-9

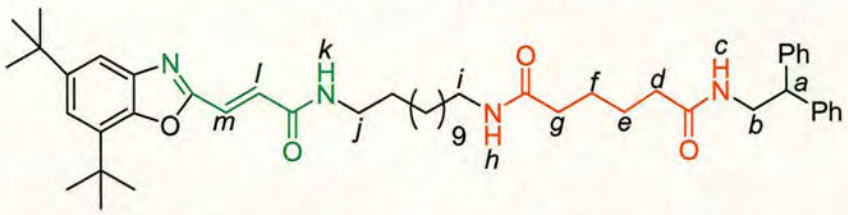

To a stirred solution of **S9** (0.97 g, 1.66 mmol) in anhydrous chloroform (60 mL) was added TFA (8.5 mL, 0.11 mol) and the solution allowed to stir at room temperature for 2 h. The solvent and the excess of TFA were removed *in vacuo*. The resulting oil was taken up in anhydrous dichloromethane (120 mL) and **S10** (0.57 g, 1.75 mmol), 4-DMAP (0.65 g, 5.32 mmol), EDCI•HCl (0.68 g, 3.55 mmol) added in order under nitrogen atmosphere at 0 °C whilst stirring. After 17 h, the reaction mixture was washed successively with 10% citric acid (3 × 50 mL), sat. $NaHCO_3$ (3 × 50 mL) and brine (3 × 50 mL), dried over $MgSO_4$ and concentrated *in vacuo*, the crude product purified by column chromatography (96:4 $CHCl_3$:CH_3OH) to yield *E*-**9** as a pale brown solid (1.13 g, yield = 86% over 2 steps). m.p. 78-80 °C; ^{1}H NMR (400 MHz, $CDCl_3$): δ = 1.18-1.27 (m, 16H, -C*H*$_2$- (alkyl chain)), 1.30 (s, 9H, C(C*H*$_3$)$_3$), 1.41 (m, 11H, C(C*H*$_3$)$_3$ and -C*H*$_2$-CH$_i$), 1.44-1.54 (m, 6H, H_f, H_e and -C*H*$_2$-CH$_j$), 2.04 (m, 4H, H_d and H_g), 3.15 (m, 2H, H_i), 3.32 (m, 2H, H_j), 3.82 (dd, J = 5.8, 8.1 Hz, 2H, H_b), 4.12 (t, J = 8.1 Hz, 1H, H_a), 5.76 (br t, J = 5.8 Hz, 1H, H_c), 5.85 (br s, 1H, H_h), 6.17 (t, J = 5.8 Hz, 1H, H_k), 6.94 (d, J = 15.5 Hz, 1H, H_l or H_m), 7.11-7.16 (m, 6H, Ar*H*), 7.19-7.24 (m, 4H, Ar*H*), 7.26 (s, 1H, Ar*H*), 7.47 (d, J = 15.5 Hz, 1H, H_m or H_l), 7.52 (s, 1H, Ar*H*); ^{13}C NMR (100 MHz, $CDCl_3$): δ = 24.7, 24.8, 26.8, 26.9, 29.1, 29.2, 29.3 (× 2), 29.4 (× 2), 29.9 (× 2), 31.7 (× 2), 34.4, 35.1, 35.8 (× 2), 39.6, 40.0, 43.8,

50.5, 114.5, 120.8, 126.0, 126.8, 128.0, 128.6, 130.1, 133.8, 141.8, 142.0, 146.8, 148.2, 160.2, 164.1, 172.9 (× 2); HRMS calcd. for $C_{50}H_{71}N_4O_4$ $[M+H]^+$: 791.54753, Found (FAB, THIOG matrix): 791.54830.

[2]-(1,7,14,20-Tetraaza-2,6,15,19-tetraoxo-3,5,9,12,16,18,22,25-tetrabenzocyclohexacosane)-(*E*)-N^1-(12-(3-(5,7-di-*tert*-butylbenzo[*d*]oxazol-2-yl)acrylamido)dodecyl)-N^6-(2,2-diphenylethyl)adipamide-rotaxane, *E*-8

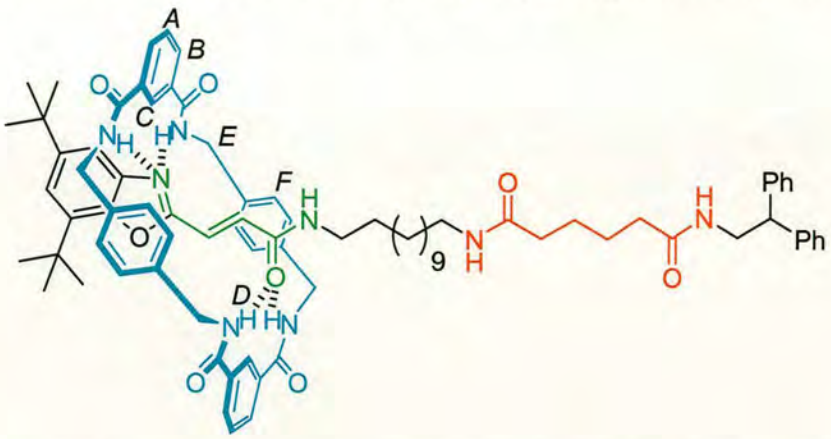

E-**9** (1.04 g, 1.31 mmol) and triethylamine (3.0 mL, 0.022 mol) were dissolved in chloroform (150 mL) and the mixture was stirred vigorously while solutions of *p*-xylylenediamine (1.44 g, 0.011 mol) in chloroform (45 mL) and isophthaloyl dichloride (2.15 g, 0.011 mol) in chloroform (45 mL) were simultaneously added over a period of 2 h using motor-driven syringe pumps at room temperature under nitrogen atmosphere. After a further 20 h the resulting suspension was filtered and concentrated *in vacuo*. The crude residue was purified by column chromatography (97.5:2.5 $CHCl_3$:CH_3OH) to yield *E*-**8** as a white solid (0.75 g, yield = 43%). Alternatively, *E*-**8** was also obtained when the solution of *Z*-**8** in dichloromethane was irradiated at 350 nm using a multilamp photo-reactor for 8 min (yield = 64%, determined by ^{1}H NMR). m.p. 198-200 °C; ^{1}H NMR (400 MHz, $CDCl_3$): δ = 1.10-1.21 (m, 25H, C(CH_3)$_3$ and -CH_2- (alkyl chain)), 1.23-1.31 (m, 4H, H_f and H_e), 1.32-1.44 (m, 13H, C(CH_3)$_3$, -CH_2-CH_i and -CH_2-CH_j), 1.85 (m, 4H, H_d and H_g), 2.94 (m, 2H, H_i), 3.08 (m, 2H, H_j), 3.76 (dd, J = 5.5, 7.9 Hz, 2H, H_b), 4.12 (t, J = 7.9 Hz, 1H, H_a), 4.35 (m, 8H, H_E), 6.14 (br t, J = 5.5 Hz, 1H, H_c), 6.22 (d, J = 15.3 Hz, 1H, H_l or H_m), 6.35 (br s, 1H, H_k), 6.46 (d, J = 15.3 Hz, 1H, H_m or H_l), 6.54 (s, 1H, Ar*H*), 6.92

(s, 8H, H_F), 7.09-7.23 (m, 11H, Ar*H*), 7.54 (t, J = 7.8 Hz, 2H, H_A), 7.62 (br s, 1H, H_h), 7.85 (br t, J = 4.7 Hz, 4H, H_D), 8.11 (d, J = 7.8 Hz, 4H, H_B), 8.46 (s, 2H, H_C); ^{13}C NMR (100 MHz, $CDCl_3$): δ = 24.6, 24.7, 26.6, 26.9, 28.8, 29.0 (× 2), 29.1 (× 3), 29.8 (× 2), 31.6 (× 2), 34.5, 35.0, 35.5, 35.6, 39.7, 40.3, 43.9, 44.2, 50.4, 112.9, 121.2, 122.8, 125.2, 126.8, 128.0, 128.7, 128.9, 129.1, 129.2, 131.3, 133.9, 134.5, 137.0, 140.4, 141.8, 146.8, 148.9, 160.3, 165.0, 166.9, 173.4, 173.6; HRMS calcd. for $C_{82}H_{99}N_8O_8$ $[M+H]^+$: 1323.75859, Found (FAB, 3-NOBA matrix): 1323.75935.

(*Z*)-N^1-(12-(3-(5,7-Di-*tert*-butylbenzo[*d*]oxazol-2-yl)acrylamido)dodecyl)-N^6-(2,2-diphenylethyl)adipamide, *Z*-9

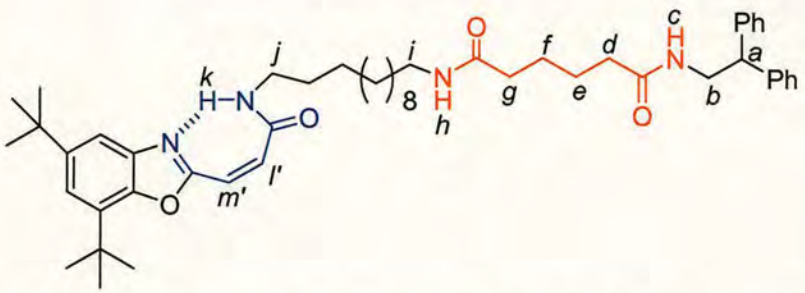

The solution of *E*-**9** in dichloromethane was irradiated at 350 nm using a multilamp photo-reactor for 12 min, and then concentrated *in vacuo*. The crude residue was purified by preparative TLC (EtOAc) to yield *Z*-**9** as a sticky oil (yield = 42%, determined by ^{1}H NMR). ^{1}H NMR (400 MHz, $CDCl_3$): δ = 1.10-1.27 (m, 16H, -CH_2-(alkyl chain)), 1.32 (s, 9H, C(CH_3)$_3$), 1.41-1.47 (m, 15H, C(CH_3)$_3$, H_f, H_e and -CH_2-CH$_i$), 1.58-1.67 (m, 2H, -CH_2-CH$_j$), 2.03 (m, 4H, H_d and H_g), 3.14 (m, 2H, H_i), 3.39 (m, 2H, H_j), 3.82 (m, 2H, H_b), 4.13 (t, J = 7.8 Hz, 1H, H_a), 5.66 (br s, 1H, H_c), 5.72 (br s, 1H, H_h), 6.35 (d, J = 13.4 Hz, 1H, $H_{l'}$ or $H_{m'}$), 6.68 (d, J = 13.4 Hz, 1H, $H_{m'}$ or $H_{l'}$), 7.12-7.24 (m, 10H, Ar*H*), 7.32 (s, 1H, Ar*H*), 7.47 (s, 1H, Ar*H*), 10.68 (br s, 1H, H_k); ^{13}C NMR (100 MHz, DMSO-d_6): δ = 24.9 (× 2), 26.4, 26.5 (× 2), 28.7 (× 2), 28.8, 29.0, 29.1, 29.5, 29.7, 31.5, 33.9, 34.7, 35.1, 35.2, 38.2, 38.3, 38.7, 43.0, 50.1, 113.9, 118.2, 119.6, 126.2, 127.8, 128.3, 133.4, 134.8, 141.3, 142.9, 146.0, 147.3, 159.7, 164.9, 171.6, 172.0; HRMS calcd. for $C_{50}H_{71}N_4O_4$ $[M+H]^+$: 791.54753, Found (FAB, THIOG matrix): 791.54515.

[2]-(1,7,14,20-Tetraaza-2,6,15,19-tetraoxo-3,5,9,12,16,18,22,25-tetrabenzocyclohexacosane)-(*Z*)-N^1-(12-(3-(5,7-di-*tert*-butylbenzo[*d*]oxazol-2-yl)acrylamido)dodecyl)-N^6-(2,2-diphenylethyl)adipamide-rotaxane, *Z*-8

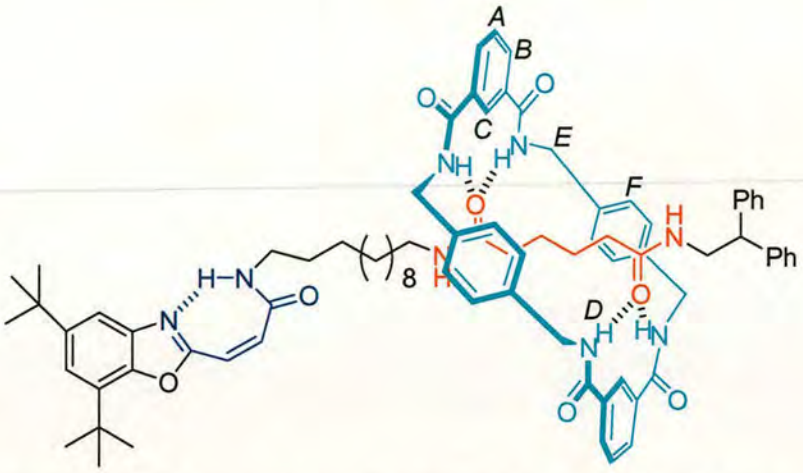

The solution of *E*-**8** in dichloromethane was irradiated at 312 nm using a multilamp photo-reactor for 2 min, and then concentrated *in vacuo*. The crude residue was purified by preparative TLC (96:4 $CHCl_3$:CH_3OH) to yield *Z*-**8** as a white solid (yield = 50%, determined by ^{1}H NMR). m.p. 102-104 °C; ^{1}H NMR (400 MHz, $CDCl_3$): δ = 0.49 (m, 4H, H_f and H_e), 0.96-1.21 (m, 20H, H_d, H_g, -CH_2-CH$_i$ and -CH_2- (alkyl chain)), 1.32 (s, 9H, C(CH_3)$_3$), 1.39-1.42 (m, 11H, C(CH_3)$_3$ and -CH_2- (alkyl chain)), 1.58-1.65 (m, 2H, -CH_2-CH$_j$), 2.71 (m, 2H, H_i), 3.38 (m, 2H, H_j), 3.53 (m, 2H, H_b), 4.03 (t, J = 7.9 Hz, 1H, H_a), 4.39-4.49 (m, 8H, H_E), 6.12 (br s, 1H, H_c), 6.30 (br, s, 1H, H_h), 6.43 (d, J = 13.6 Hz, 1H, $H_{l'}$ or $H_{m'}$), 6.71 (d, J = 13.6 Hz, 1H, $H_{m'}$ or $H_{l'}$), 7.01 (s, 8H, H_F), 7.11-7.24 (m, 10H, Ar*H*), 7.35 (s, 1H, Ar*H*), 7.43 (t, J = 7.8 Hz, 2H, H_A), 7.48 (s, 1H, Ar*H*), 7.80 (br s, 4H, H_D), 8.04 (d, J = 7.8 Hz, 4H, H_B), 8.22 (s, 2H, H_C), 10.78 (br s, 1H, H_k); ^{13}C NMR (100 MHz, $CDCl_3$): δ = 24.0, 24.1, 26.8, 27.0, 28.8, 28.9, 29.1 (× 2), 29.2, 29.7, 29.8 (× 2), 31.7 (× 2), 34.5, 34.9 (× 2), 35.2, 39.8, 40.4, 43.8, 44.2, 50.1, 113.6, 119.6, 121.9, 124.8, 126.8, 128.0, 128.7, 128.8, 129.1, 131.1, 131.3, 133.9, 134.1, 134.7, 137.8, 142.1, 146.2, 149.3, 157.6, 159.4, 164.7, 166.5, 173.6; HRMS calcd. for $C_{82}H_{99}N_8O_8$ $[M+H]^+$: 1323.75859, Found (FAB, 3-NOBA matrix): 1323.75961.

X-Ray Crystallographic Structure Determination

The structure determination for *E*-**4** proved problematic; we tried many data collections using different crystals from several different crystallisation experiments. The data were always poor, however, the structure is suitable for demonstrating the gross geometry and topology. X-ray crystal structural data for *E*-**4**•CH_3OH•$2H_2O$: $C_{65}H_{72}N_6O_9$, M_r = 1081.29, colourless plate, crystal size 0.200 × 0.080 × 0.010 mm^3, monoclinic *Cc*, a = 11.3772(15), b = 53.545(7), c = 10.9902(15) Å, β = 115.642(5)°, V = 6035.8(14) $Å^3$, Z = 4, ρ_{calcd} = 1.190 Mg/m^3; λ = 1.54178 Å, μ = 0.640 mm^{-1}, T = 173(2) K; 37458 reflections collected, 9748 independent reflections (R_{int} = 0.1959, 4.39 < θ < 67.47°) and 664 parameters. The structure was solved by direct methods and refined by full-matrix least-squares on F^2 to give $R1(F^2)$ = 0.2139 ($I > 2\sigma I$), $wR2(F^2)$ = 0.5048 (all data). Residual electron density extremes were 1.457 and -0.627 $eÅ^{-3}$. Rigaku MM007 Cu high brilliance rotating anode/confocal optic/Saturn92 detector.

X-Ray Crystal Structure Thermal Ellipsoids

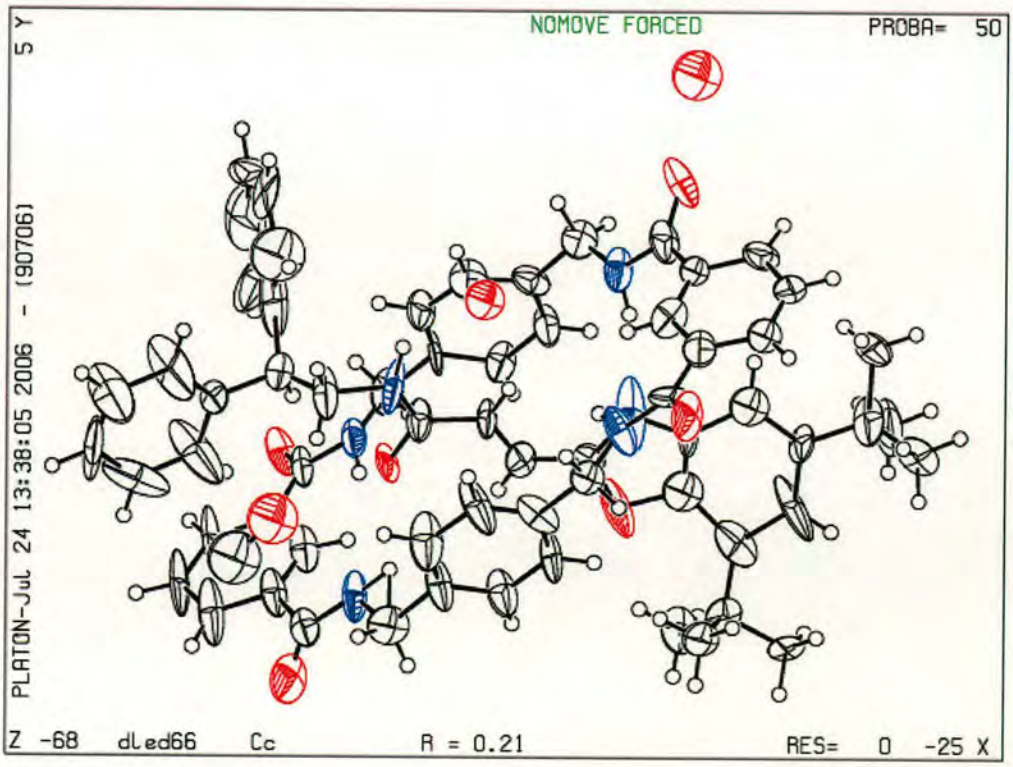

Photoisomerisation of *E*/*Z*-6 upon Laser Irradiation Determined by HPLC

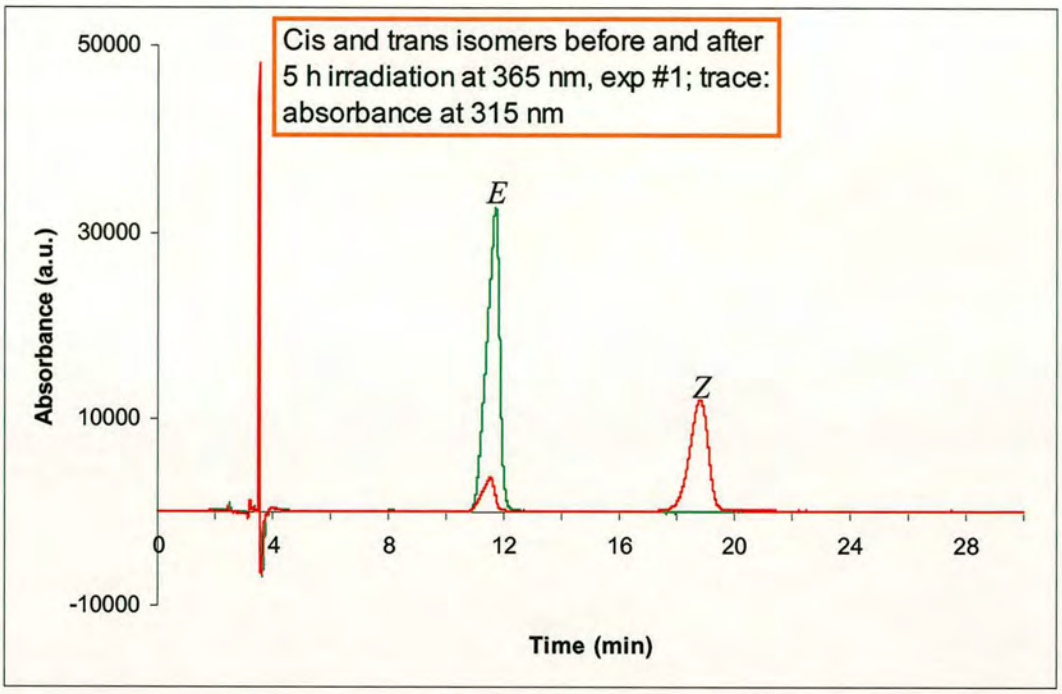

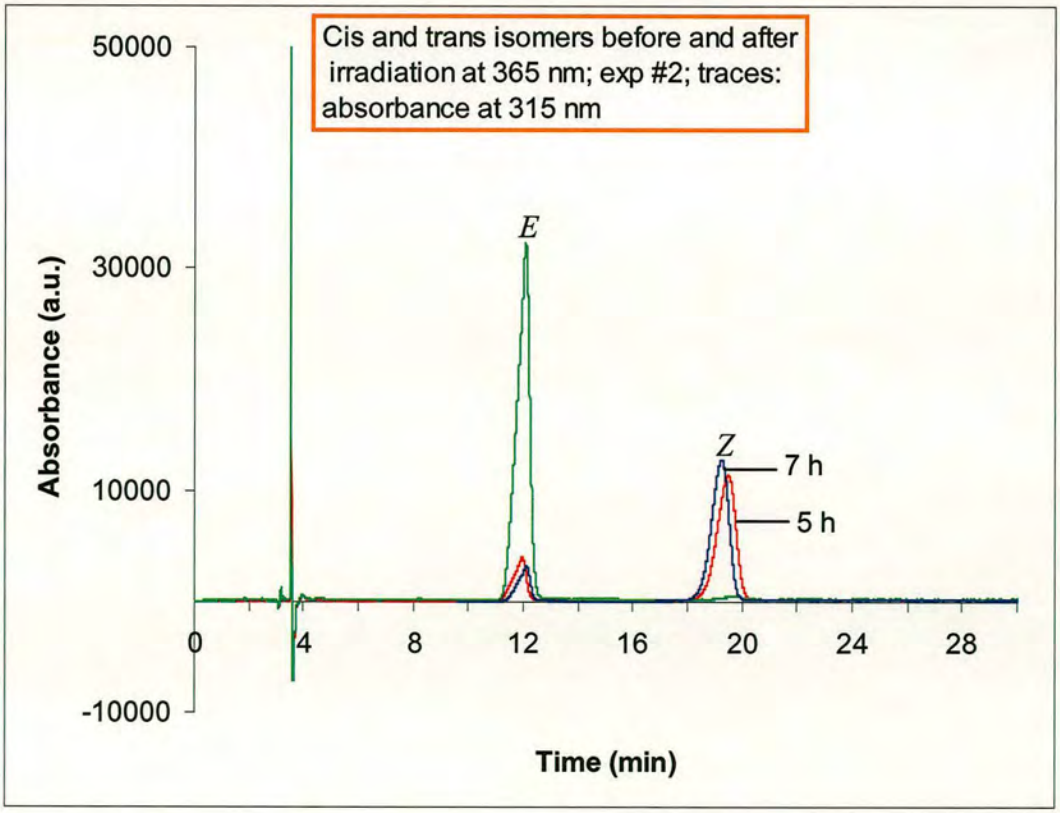

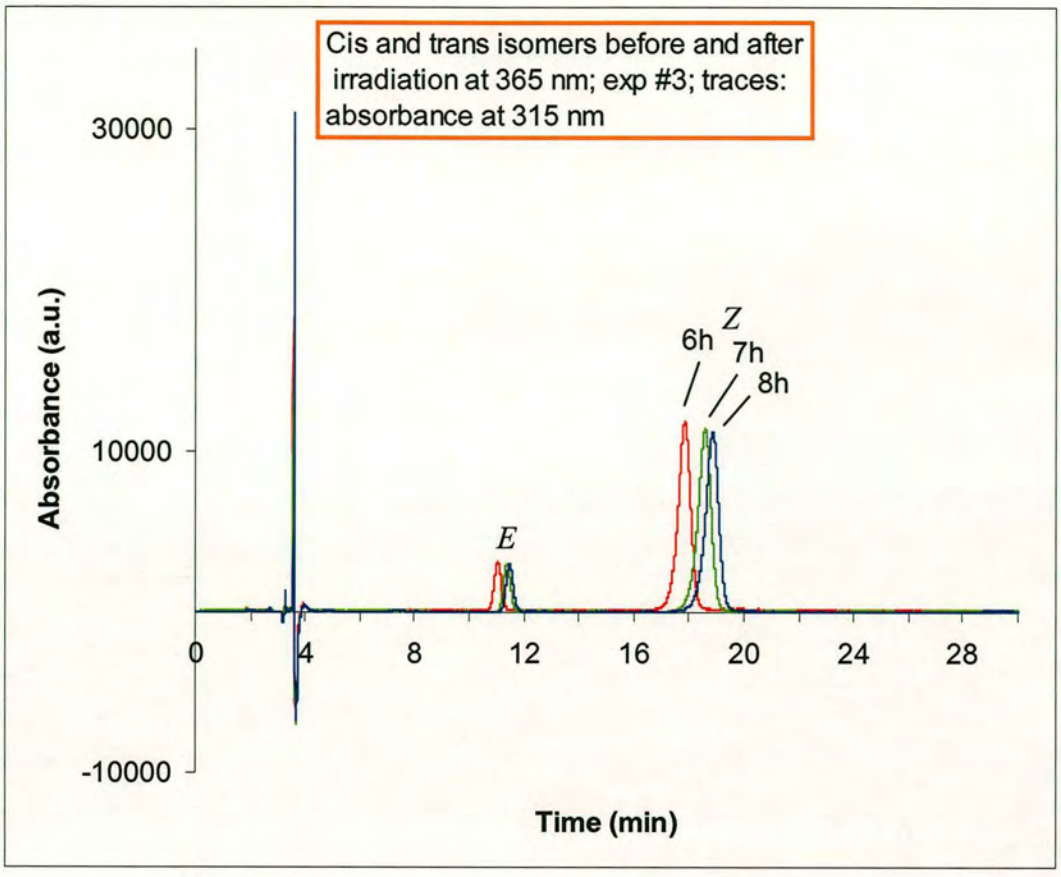

Figure A1 Chromatograms of *E*-**6** before and after irradiation with the xenon lamp of a SPEX fluorescence spectrometer at 365 nm.

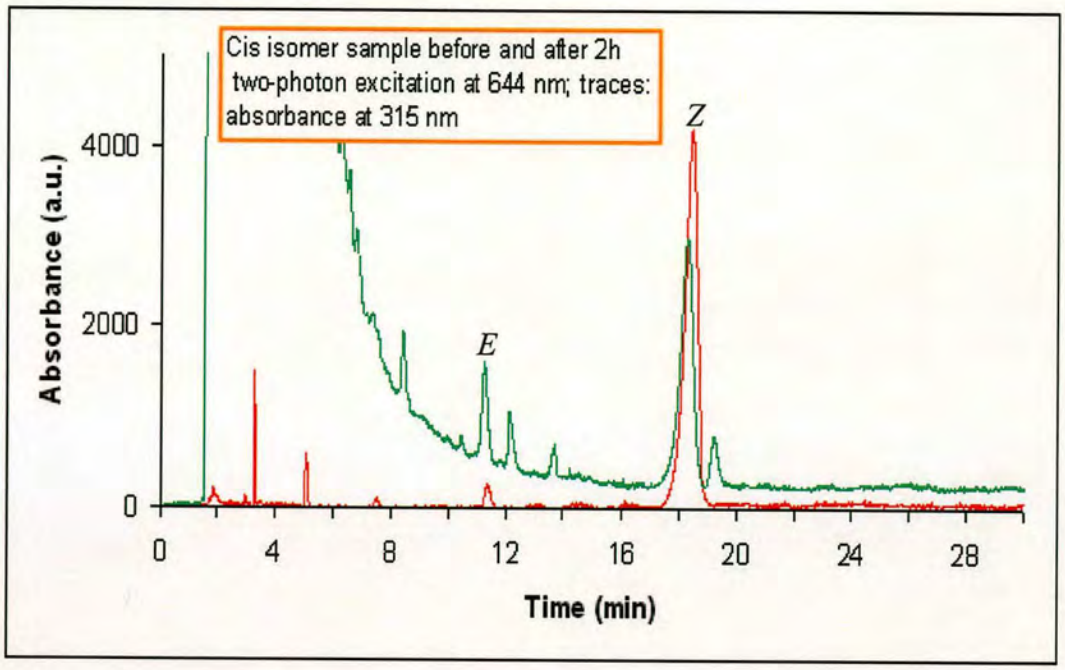

Figure A2 Chromatograms of *Z*-**6** before and after 2 h irradiation with Infinity-XPO at 644 nm (6.5 mJ per pulse; 10 Hz).

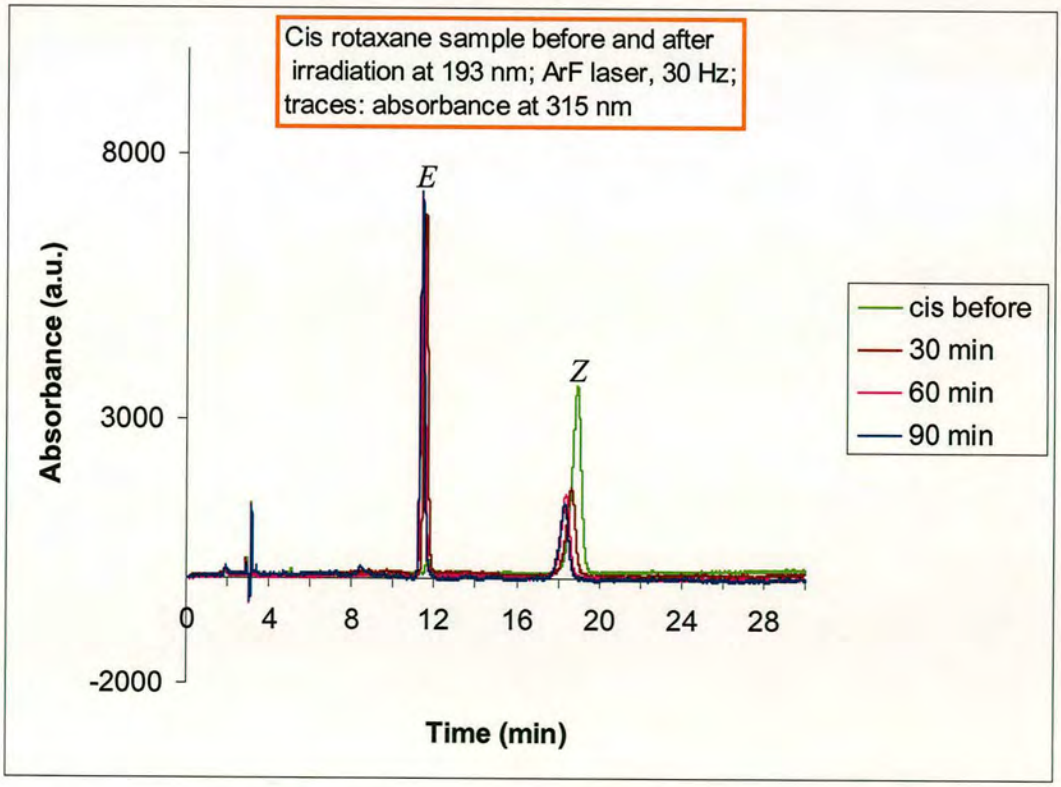

Figure A3 Chromatograms of *Z*-**6** before and after irradiation at 193 nm (ArF laser, 30Hz).

2.6 References and Notes

(1) Anelli, P. L.; Spencer, N.; Stoddart, J. F. *J. Am. Chem. Soc.* **1991**, *113*, 5131-5133.

(2) (a) Benniston, A. C.; Harriman, A. *Angew. Chem., Int. Ed. Engl.* **1993**, *32*, 1459-1461. (b) Benniston, A. C.; Harriman, A.; Lynch, V. M. *Tetrahedron Lett.* **1994**, *35*, 1473-1476. (c) Benniston, A. C.; Harriman, A.; Lynch, V. M. *J. Am. Chem. Soc.* **1995**, *117*, 5275-5291. (d) Murakami, H.; Kawabuchi, A.; Kotoo, K.; Kunitake, M.; Nakashima, N. *J. Am. Chem. Soc.* **1997**, *119*, 7605-7606. (e) Armaroli, N.; Balzani, V.; Collin, J.-P.; Gaviña, P.; Sauvage, J.-P.; Ventura, B. *J. Am. Chem. Soc.* **1999**, *121*, 4397-4408. (f) Ashton, P. R.; Ballardini, R.; Balzani, V.; Credi, A.; Dress, K. R.; Ishow, E.; Kleverlaan, C. J.; Kocian, O.; Preece, J. A.; Spencer, N.; Stoddart, J. F.; Venturi, M.; Wenger, S. *Chem. Eur. J.* **2000**, *6*, 3558-3574. (g) Wurpel, G. W. H.; Brouwer, A. M.; van Stokkum, I. H. M.; Farran, A.; Leigh, D. A. *J. Am. Chem. Soc.* **2001**, *123*, 11327-11328. (h) Brouwer, A. M.; Frochot, C.; Gatti, F. G.; Leigh, D. A.; Mottier, L.; Paolucci, F.; Roffia, S.; Wurpel, G. W. H. *Science* **2001**, *291*, 2124-2128. (i) Stanier, C. A.; Alderman, S. J.; Claridge, T. D. W.; Anderson, H. L. *Angew. Chem., Int. Ed.* **2002**, *41*, 1769-1772. (j) Altieri, A.; Bottari, G.; Dehez, F.; Leigh, D. A.; Wong, J. K. Y.; Zerbetto, F. *Angew. Chem., Int. Ed.* **2003**, *42*, 2296-2300. (k) Abraham, W.; Grubert, L.; Grummt, U. W.; Buck, K. *Chem. Eur. J.* **2004**, *10*, 3562-3568. (l) Murakami, H.; Kawabuchi, A.; Matsumoto, R.; Ido, T.; Nakashima, N. *J. Am. Chem. Soc.* **2005**, *127*, 15891-15899. (m) Schmidt-Schäffer, S.; Grubert, L.; Grummt, U. W.; Buck, K.; Abraham, W. *Eur. J. Org. Chem.* **2006**, 378-398. (n) Wang, Q.-C.; Ma, X.; Qu, D.-H.; Tian, H. *Chem. Eur. J.* **2006**, *12*, 1088-1096. (o) Balzani, V.; Clemente-León, M.; Credi, A.; Ferrer, B.; Venturi, M.; Flood, A. H.; Stoddart, J. F. *Proc. Natl. Acad. Sci. U.S.A.* **2006**, *103*, 1178-1183.

(3) (a) Lane, A. S.; Leigh, D. A.; Murphy, A. *J. Am. Chem. Soc.* **1997**, *119*, 11092-11093. (b) Gong, C.; Gibson, H. W. *Angew. Chem., Int. Ed. Engl.* **1997**, *36*, 2331-2333. (c) Gong, C. G.; Glass, T. E.; Gibson, H. W. *Macromolecules* **1998**, *31*, 308-313. (d) Jiménez, M. C.; Dietrich-Buchecker, C.; Sauvage, J.-P. *Angew. Chem., Int. Ed.* **2000**, *39*, 3284-3287. (e) Lee, J. W.; Kim, K.; Kim, K. *Chem. Commun.* **2001**, 1042-1043. (f) Jimenez-Molero, M. C.; Dietrich-Buchecker, C.;

Sauvage, J.-P. *Chem. Eur. J.* **2002**, *8*, 1456-1466. (g) Da Ros, T.; Guldi, D. M.; Farran Morales, A.; Leigh, D. A.; Prato, M.; Turco, R. *Org. Lett.* **2003**, *5*, 689-691. (h) Tseng, H.-R.; Vignon, S. A.; Stoddart, J. F. *Angew. Chem., Int. Ed.* **2003**, *42*, 1491-1495. (i) Laursen, B. W.; Nygaard, S.; Jeppesen, J. O.; Stoddart, J. F. *Org. Lett.* **2004**, *6*, 4167-4170. (j) Huang, T. J.; Tseng, H.-R.; Sha, L.; Lu, W. X.; Brough, B.; Flood, A. H.; Yu, B.-D.; Celestre, P. C.; Chang, J. P.; Stoddart, J. F.; Ho, C.-M. *Nano Lett.* **2004**, *4*, 2065-2071. (k) Leigh, D. A.; Pérez, E. M. *Chem. Commun.* **2004**, 2262-2263. (l)Tseng, H.-R.; Vignon, S. A.; Celestre, P. C.; Perkins, J.; Jeppesen, J. O.; Di Fabio, A.; Ballardini, R.; Gandolfi, M. T.; Venturi, M.; Balzani, V.; Stoddart, J. F. *Chem. Eur. J.* **2004**, *10*, 155-172. (m) Nørgaard, K.; Laursen, B. W.; Nygaard, S.; Kjaer, K.; Tseng, H.-R.; Flood, A. H.; Stoddart, J. F.; Bjørnholm, T. *Angew. Chem., Int. Ed.* **2005**, *44*, 7035-7039. (n) Jeppesen, J. O.; Nygaard, S.; Vignon, S. A.; Stoddart, J. F. *Eur. J. Org. Chem.* **2005**, 196-220.

(4) See 2e, 2o, 3l, 3n and (a) Bissell, R. A.; Córdova, E.; Kaifer, A. E.; Stoddart, J. F. *Nature* **1994**, *369*, 133-136. (b) Collin, J.-P.; Gaviña, P.; Sauvage, J.-P. *New J. Chem.* **1997**, 525-528. (c) Ballardini, R.; Balzani, V.; Dehaen, W.; Dell'Erba, A. E.; Raymo, F. M.; Stoddart, J. F.; Venturi, M. *Eur. J. Org. Chem.* **2000**, 591-602. (d) Ashton, P. R.; Ballardini, R.; Balzani, V.; Credi, A.; Dress, K. R.; Ishow, E.; Kleverlaan, C. J.; Kocian, O.; Preece, J. A.; Spencer, N.; Stoddart, J. F.; Venturi, M.; Wenger, S. *Chem. Eur. J.* **2000**, *6*, 3558-3574. (e) Altieri, A.; Gatti, F. G.; Kay, E. R.; Leigh, D. A.; Martel, D.; Paolucci, F.; Slawin, A. M. Z.; Wong, J. K. Y. *J. Am. Chem. Soc.* **2003**, *125*, 8644-8654. (f) Long, B.; Nikitin, K.; Fitzmaurice, D. *J. Am. Chem. Soc.* **2003**, *125*, 15490-15498. (g) Kihara, N.; Hashimoto, M.; Takata, T. *Org. Lett.* **2004**, *6*, 1693-1696. (h) Flood, A. H.; Peters, A. J.; Vignon, S. A.; Steuerman, D. W.; Tseng, H.-R.; Kang, S.; Heath, J. R.; Stoddart, J. F. *Chem. Eur. J.* **2004**, *10*, 6558-6564. (i) Tseng, H.-R.; Wu, D. M.; Fang, N. X. L.; Zhang, X.; Stoddart, J. F. *ChemPhysChem* **2004**, *5*, 111-116. (j) Steuerman, D. W.; Tseng, H.-R.; Peters, A. J.; Flood, A. H.; Jeppesen, J. O.; Nielsen, K. A.; Stoddart, J. F.; Heath, J. R. *Angew. Chem., Int. Ed.* **2004**, *43*, 6486-6491.

(5) See 4a and (a) Martínez-Díaz, M.-V.; Spencer, N.; Stoddart, J. F. *Angew. Chem., Int. Ed. Engl.* **1997**, *36*, 1904-1907. (b) Ashton, P. R.; Ballardini, R.; Balzani, V.;

Baxter, I.; Credi, A.; Fyfe, M. C. T.; Gandolfi, M. T.; Gómez-López, M.; Martínez-Díaz, M.-V.; Piersanti, A.; Spencer, N.; Stoddart, J. F.; Venturi, M.; White, A. J. P.; Williams, D. J. *J. Am. Chem. Soc.* **1998**, *120*, 11932-11942. (c) Elizarov, A. M.; Chiu, S.-H.; Stoddart, J. F. *J. Org. Chem.* **2002**, *67*, 9175-9181. (d) Badjić, J. D.; Balzani, V.; Credi, A.; Silvi, S.; Stoddart, J. F. *Science* **2004**, *303*, 1845-1849. (e) Keaveney, C. M.; Leigh, D. A. *Angew. Chem., Int. Ed.* **2004**, *43*, 1222-1224. (f) Garaudée, S.; Silvi, S.; Venturi, M.; Credi, A.; Flood, A. H.; Stoddart, J. F. *ChemPhysChem* **2005**, *6*, 2145-2152. (g) Badjić, J. D.; Ronconi, C. M.; Stoddart, J. F.; Balzani, V.; Silvi, S.; Credi, A. *J. Am. Chem. Soc.* **2006**, *128*, 1489-1499. (h) Tokunaga, Y.; Nakamura, T.; Yoshioka, M.; Shimomura Y. *Tetrahedron Lett.* **2006**, *47*, 5901-5904. (i) Cheng, K.-W.; Lai, C.-C.; Chiang, P.-T.; Chiu, S.-H. *Chem. Commun.* **2006**, 2854-2856.

(6) Bottari, G.; Dehez, F.; Leigh, D. A.; Nash, P. J.; Pérez, E. M.; Wong, J. K. Y.; Zerbetto, F. *Angew. Chem., Int. Ed.* **2003**, *42*, 5886-5889.

(7) (a) Vignon, S. A.; Jarrosson, T.; Iijima, T.; Tseng, H.-R.; Sanders, J. K. M.; Stoddart, J. F. *J. Am. Chem. Soc.* **2004**, *126*, 9884-9885. (b) Iijima, T.; Vignon, S. A.; Tseng, H.-R.; Jarrosson, T.; Sanders, J. K. M.; Marchioni, F.; Venturi, M.; Apostoli, E.; Balzani, V.; Stoddart, J. F. *Chem. Eur. J.* **2004**, *10*, 6375-6392. (c) Marlin, D. S.; González Carbrera, D.; Leigh, D. A.; Slawin, A. M. Z. *Angew. Chem., Int. Ed.* **2006**, *45*, 77-83. (d) Marlin, D. S.; González Carbrera, D.; Leigh, D. A.; Slawin, A. M. Z. *Angew. Chem., Int. Ed.* **2006**, *45*, 1385-1390.

(8) See 2h, 2o and (a) Koumura, N.; Zijlstra, R. W. J.; van Delden, R. A.; Harada, N.; Feringa, B. L. *Nature* **1999**, *401*, 152-155. (b) Hernández, J. V.; Kay, E. R.; Leigh, D. A. *Science* **2004**, *306*, 1532-1537. (c) Mobian, P.; Kern, J.-M.; Sauvage, J.-P. *Angew. Chem., Int. Ed.* **2004**, *43*, 2392-2395.

(9) Martínez, T.J. *Acc. Chem. Res.* **2006**, *39*, 119-126.

(10) (a) Gatti, F. G.; Leigh, D. A.; Nepogodiev, S. A.; Slawin, A. M. Z.; Teat, S. J.; Wong, J. K. Y. *J. Am. Chem. Soc.* **2001**, *123*, 5983-5989. (b) Gatti, F. G.; León, S.; Wong, J. K. Y.; Bottari, G.; Altieri, A.; Farran Morales, M. A.; Teat, S. J.; Frochot, C.; Leigh, D. A.; Brouwer, A. M.; Zerbetto, F. *Proc. Natl. Acad. Sci. U.S.A.* **2003**, *100*, 10-14.

(11) Ikegami, M.; Arai T. *J. Chem. Soc., Perkin Trans. 2* **2002**, 342-347.

(12) The rotaxanes *E*-**4**/*Z*-**4** are insufficiently soluble in pure $CDCl_3$ for ^1H NMR spectroscopic studies, so $CDCl_3/CD_3OD$ (99:1) is used.

(13) Brancato, G.; Coutrot, F.; Leigh, D. A.; Murphy, A.; Wong, J. K. Y.; Zerbetto, F. *Proc. Natl. Acad. Sci. U.S.A.* **2002**, *99*, 4967-4971.

(14) The prediction of the relative station-binding affinities from rotaxane yields is not completely accurate. In shuttles *Z*-**1** or *Z*-**2**, the macrocycle occupancy on succinic amide ester or succinamide station is greater than 95%, but in *Z*-**3**, the occupancy of the macrocycle on adipamide station is reduced to approximately 85%. The anomalously poor binding of the adipamide unit to the macrocycle in *Z*-**3** may indicate that the intramolecularly hydrogen-bonded nine-membered ring has differing stabilities in the one-binding-site model rotaxane (Figure 2.5c) and two-station shuttle *Z*-**3**. (See 2j and Gellman, S. H.; Dado, G. P.; Liang, G.-B.; Adams, B. R. *J. Am. Chem. Soc.* **1991**, *113*, 1164-1173.)

(15) Wolkenberg, S. E.; Wisnoski, D. D.; Leister, W. H.; Wang, Y.; Zhao, Z.; Lindsley, C. W. *Org. Lett.* **2004**, *6*, 1453-1456.

Synthesis and Photoisomerisation of a Benzimidazole-Containing [2]Rotaxane: Effects of Hydrogen Bonding and Mechanical Interlocking

Acknowledgements

The following people are gratefully acknowledged for their contribution to this chapter: Dr. C.-F. Lee and Dr. E. M. Pérez for many useful discussions; Prof. A. M. Z. Slawin of the University of St. Andrews solved the X-ray crystal structure of rotaxane *E*-**13**.

3.1 Summary

In chapter two *E/Z*-3-(benzoxazol-2-yl)-*N*-methylacrylamides were investigated as a novel type of photo-responsive station for rotaxane-based molecular shuttles. In this chapter, the potential application of *E*-3-(benzimidazol-2-yl)-*N*-methylacrylamide as a light-triggered station is explored. *E*-3-(benzimidazol-2-yl)-*N*-methylacrylamide can template the assembly of the benzylic amide macrocycle by a five component clipping reaction to form the corresponding [2]rotaxane in high yield (*E*-**14**→*E*-**13**, 76%). This structure has been confirmed by X-ray crystallography. Unfortunately the *E*→*Z* photoisomerisation of *E*-**13** at three different wavelengths (350, 312 and 254 nm) produced none of the corresponding *Z*-isomer. The heavily suppressed olefin photoisomerisation could be a result of strong hydrogen bonding.

3.2 Introduction

Establishing methods for controlling large amplitude molecular movements is a prerequisite for the development of artificial devices that function through motion at the molecular level. It has been previously demonstrated that the rate of rotation of the interlocked components of fumaramide-derived [2]rotaxanes can be accelerated by 6 orders of magnitude by photoisomerising them to the corresponding maleamide [2]rotaxanes (Scheme 3.1).[1] In chapter two excellent reversible photoisomerisations were described between *E/Z*-3-(benzoxazol-2-yl)-*N*-methylacrylamide templated rotaxanes. Based on this, two light-switchable molecular shuttles were assembled

successfully which achieve higher efficient photo conversions than fumaramide-derived rotaxanes. Here a benzimidazole system with a similar chemical structure to the benzoxazole motif is investigated. Particularly if the benzimidazole motif can be utilised as a new rotaxane formation template it could be useful for the future construction of synthetic molecular machines.

Scheme 3.1 Photo and Thermal Isomerisation of Fumaramide/Maleamide-Derived [2]Rotaxanes[1]

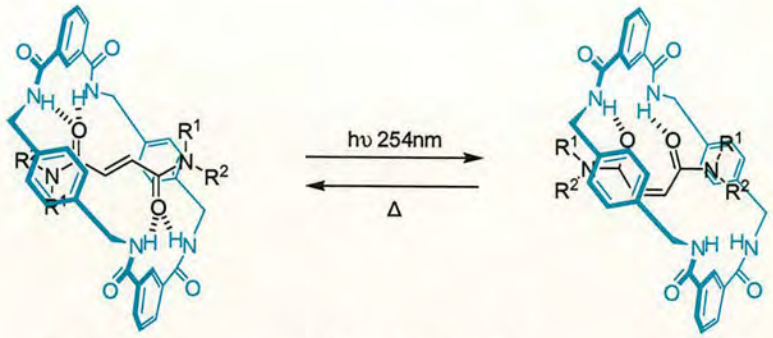

E-**10**
E-**11**
E-**12**

$R^1 = R^2 = CH_2CO_2CH_2Ph$
$R^1 = Me$, $R^2 = CH_2CHPh_2$
$R^1 = H$, $R^2 = CH_2CHPh_2$

Z-**10**
Z-**11**
Z-**12**

Benzimidazole ring structures have been used in a broad spectrum of applications, and this represents yet another motive for their study. They have been used in material applications as dyes[2] and polymers,[3] and their biological activity has led to their extensive use as fungicides and herbicides.[4] Therefore, if rotaxanes could be formed using benzimidazole systems a variety of valuable characteristics could be investigated, such as enhanced chemical stability, fluorescence efficiency and solubility.[5]

3.3 Results and Discussion

3.3.1 Synthesis of a Benzimidazole-Containing [2]Rotaxane

A model single-binding-site [2]rotaxane *E*-**13** was prepared in 76% yield using thread *E*-**14** in a five component clipping reaction (Scheme 3.2). In *E*-**14** one of the amide groups of the fumaramide template is substituted by a benzimidazole moiety, and the benzimidazole nitrogen atom behaves as a hydrogen-bonding acceptor, just like the benzoxazole-*N* described in chapter two. Rotaxane *E*-**13** was fully

characterised by ^{1}H and ^{13}C NMR spectroscopy and HRMS. Due to the shielding effect of the macrocycle, the olefin protons (H_d and H_e) of the rotaxane are significantly shifted upfield (0.9 ppm) compared with the thread; whereas the chemical shifts of the protons H_a and H_b are similar in both rotaxane and thread (Figure 3.1). This indicates that the macrocycle resides preferentially over the olefinic bond *via* intercomponent hydrogen bonding even in highly polar solvent DMSO, because normally hydrogen-bond is strongest in nonpolar solvents such as $CHCl_3$ or CH_2Cl_2, and will be disrupted by the competing polar solvent.[6]

Scheme 3.2 Synthesis of a Benzimidazole-Containing [2]Rotaxane *E*-**13** [a]

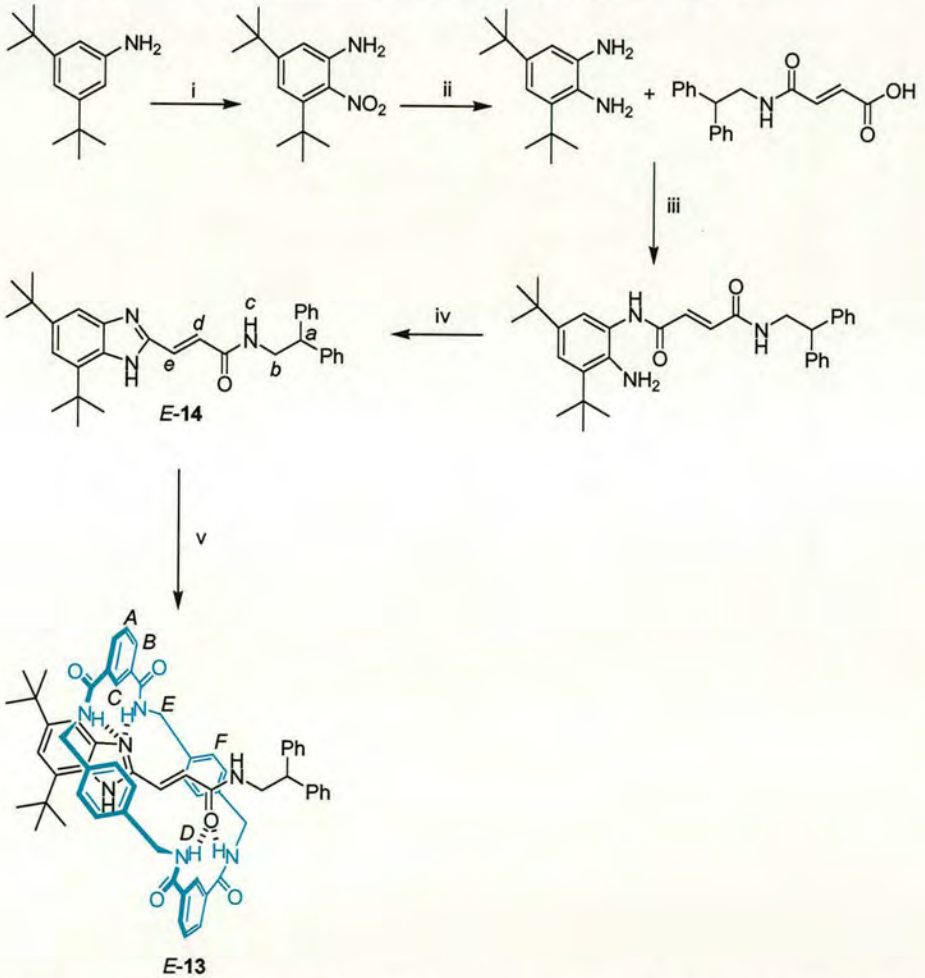

[a] Reagents and conditions: (i) HNO_3, acetic anhydride, 5-7 °C; then 37% HCl, EtOH, reflux; then 37% NH_3, 49% over 3 steps; (ii) $NH_2NH_2{\cdot}H_2O$, Pd-C, EtOH, reflux, N_2, 95%; (iii) *N*-(2,2-diphenylethyl)-fumaramide acid, 4-dimethylaminopyridine (DMAP), 1-(3-dimethylaminopropyl)-3-ethyl-carbodiimide hydrochloride (EDCI·HCl), CH_2Cl_2/DMF, 0 °C to rt, N_2, 37%; (iv) toluene-4-sulfonic acid monohydrate, toluene, rt, N_2, 75%; (v) *p*-xylylenediamine, isophthaloyl dichloride, Et_3N, $CHCl_3$, N_2, rt, 76%.

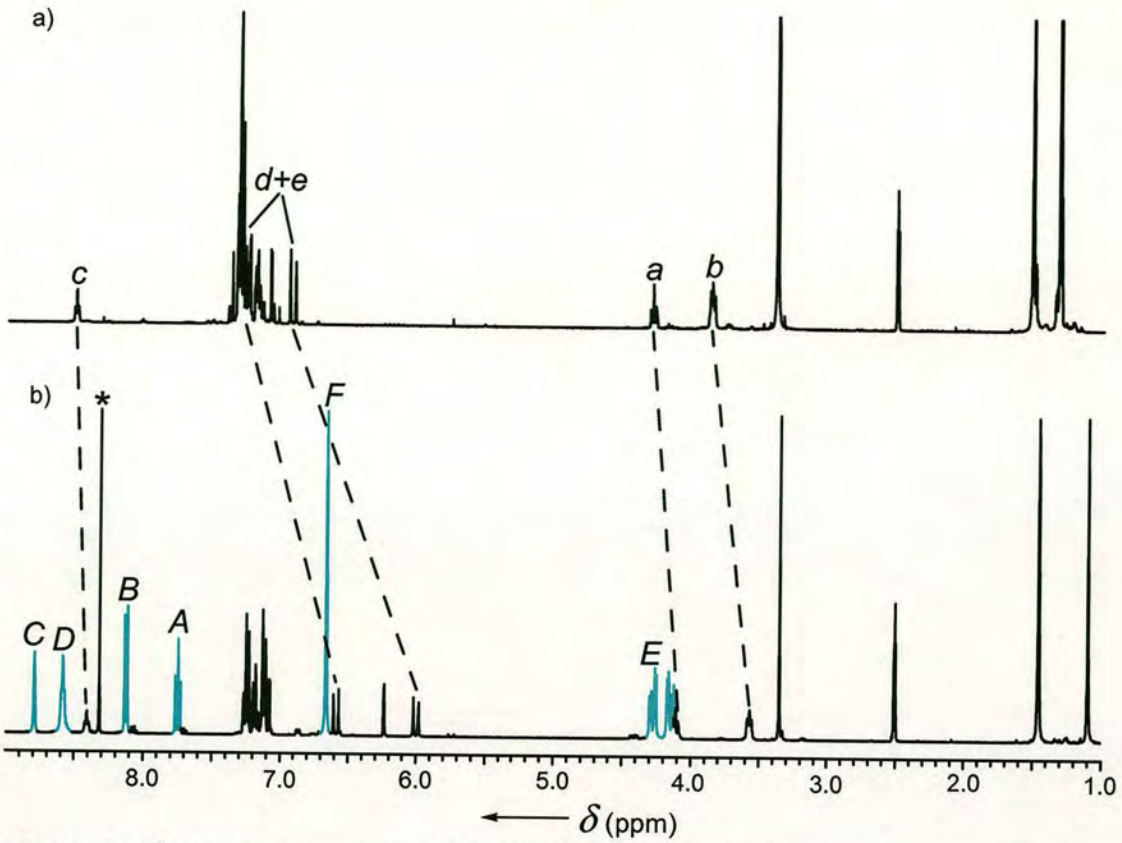

Figure 3.1 ^{1}H NMR spectra (400 MHz, 298 K) of a) thread *E*-**14** and b) rotaxane *E*-**13** in DMSO-d_6. The letters correspond to the assignments shown in Scheme 3.2. The peak highlighted with star corresponds to residual chloroform.

Single crystals of rotaxane *E*-**13** suitable for investigation by X-ray crystallography were grown directly from slow evaporation of a saturated solution of *E*-**13** in $CH_3OH/CHCl_3$. The crystal structure (Figure 3.2) again unambiguously confirms the interlocked nature of the rotaxane in the solid state and shows two sets of bifurcated unsymmetrical intercomponent hydrogen bonds. The benzimidazole nitrogen atom is H-bonded to the two macrocycle amides and the carbonyl group of the thread H-bonded to another two amides of the ring.

Figure 3.2 X-ray crystal structure of rotaxane *E*-**13** (for clarity carbon atoms of the macrocycle are shown in blue and the carbon atoms of the thread in yellow; oxygen atoms are depicted in red, nitrogen atoms in dark blue, and selected hydrogen atoms for the amide, imidazole and olefin protons in white). Intramolecular hydrogen bond distances (Å) are the following: N20H-N51 2.155, N29H-N51 2.082, N2H-O40 1.939, N11H-O40 2.207.

3.3.2 Photoisomerisation of [2]Rotaxane *E*-13 and Thread *E*-14

The $E \rightarrow Z$ photoisomerisation of rotaxane *E*-**13** was investigated in CH_2Cl_2/CH_3OH (90:10) at room temperature using a multilamp photo-reactor. The solution was directly irradiated at 350, 312 and 254 nm and the progress of photoisomerisation was monitored by TLC and ^1H NMR. Unfortunately, over a range of reaction times from minutes to hours, none of the corresponding *Z*-isomer *Z*-**13** was formed (Scheme 3.3).

Scheme 3.3 Photoisomerisation of [2]Rotaxane *E*-**13**

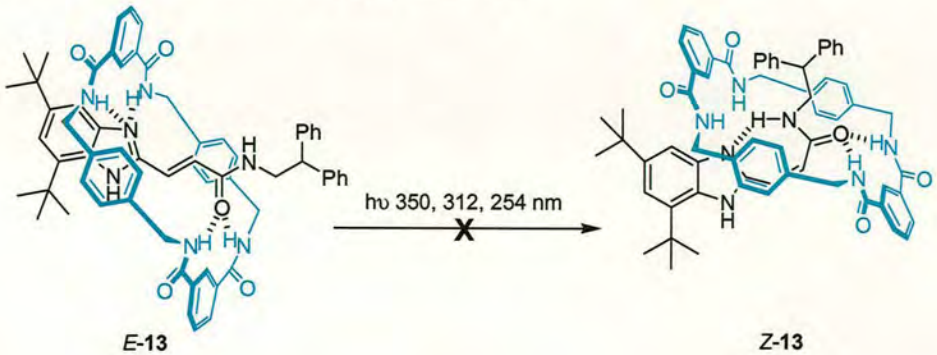

The failure of the olefin photoisomerisation could be a result of effects of hydrogen bonding and/or the mechanically interlocked structure,[7, 8] which reflects the fact that rotaxane *E*-**13** is tightly constrained. To prove this, irradiation of naked thread *E*-**14** in CH_2Cl_2/CH_3OH (90:10) was performed at 254 nm, after 1 h, clear changes of ^1H NMR (DMSO-d_6) resonance signals were detected and the reaction mixture consisted of 44% *Z*-isomer with a little decomposition.

Two mechanisms for photo-induced shuttling in a photoisomerisable rotaxane are shown in Figure 3.3.[8] In this model, the macrocycle prefers to sit on the photoactive unit in the *E* isomer (A is lower in energy than C), but it prefers to sit near one end in the *Z* isomer (D is lower in energy than B). In route A→B→D, photoisomerisation occurs while the macrocycle is over the photoactive unit; this forces it to relocate. In route A→C→D, the photoactive unit waits until random thermal motion has relocated the macrocycle, then photoisomerises to block its return. Both mechanisms may apply, but its failure of photoisomerisation indicates that rotaxane *E*-**13** operates by route A→C→D rather than A→B→D. The macrocycle completely prevents *E*→*Z* photoisomerisation because it does not allow the olefinic bond to move partly out of the cavity prior to photoisomerisation due to the effects of strong hydrogen bonding.

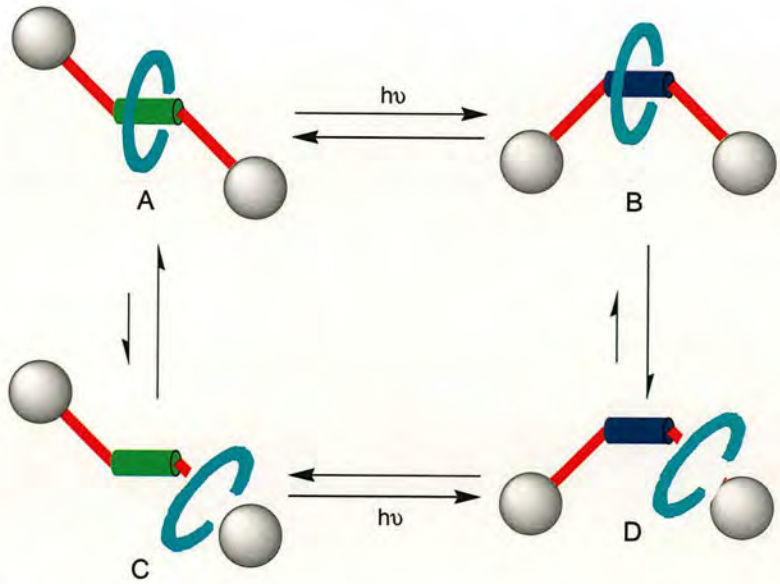

Figure 3.3 Two mechanisms for rotaxane photoisomerisation.

3.4 Conclusions

A hydrogen-bonded benzimidazole-containing [2]rotaxane *E*-**13** was synthesised in 76% yield from corresponding thread *E*-**14**. This demonstrates that having cooperative binding sites in an ideal spatial arrangement on a rigid backbone is a powerful method for facilitating the hydrogen bond-directed synthesis of rotaxanes. Unfortunately the strong intercomponent interactions between the thread and the macrocycle provide no freedom for translation motion, thus the photoisomerisation of *E*-**13** is heavily suppressed and produces none of the corresponding *Z*-isomer upon UV irradiation.

3.5 Experiments

3.5.1 General

Unless stated otherwise, all reagents and anhydrous solvents were purchased from Aldrich Chemicals and used without further purification. *P*-xylylene diamine was distilled under reduced pressure and isophthaloyl dichloride was recrystallised from *n*-hexane. Column chromatography was performed using Kiesegel C60 (Merck, Germany) as the stationary phase, and TLC was performed on precoated silica gel plates (0.25 mm thick, $60F_{254}$, Merck, Germany) and observed under UV light. All ^{1}H and ^{13}C NMR spectra were recorded on a Bruker AV 400 instrument, at a constant temperature of 25 °C. Chemical shifts are reported in parts per million from high to low field and referenced to TMS. Coupling constants (*J*) are reported in Hertz (Hz). Standard abbreviations indicating multiplicity are used as follows: m = multiplet, br = broad, d = doublet, q = quadruplet, t = triplet, s = singlet. All melting points were determined using Sanyo Gallenkamp apparatus and are reported uncorrected. FAB mass spectrometry was carried out by the services at the University of Edinburgh.

3.5.2 General Procedure for the Photoisomerisation Using the Multilamp Photo-Reactor

Rotaxane *E*-**13** was dissolved in 90:10 CH_2Cl_2:CH_3OH ($\sim 10^{-4}$ M) in a quartz vessel. The solution was degassed by bubbling N_2 for 10 minutes, then directly irradiated at appropriate wavelengths (350, 312, 254 nm respectively) using a multilamp photo-

reactor (Model MLU18, Model 3022 lamps, Photochemical Reactors Ltd., Reading, UK). The progress of the photoisomerisation was monitored by TLC and ^{1}H NMR.

Thread *E*-**14** was also dissolved in 90:10 CH_2Cl_2:CH_3OH (~10^{-4} M) in a quartz vessel and directly irradiated for 1 h at 254 nm after 10 minutes N_2 bubbling, then concentrated *in vacuo* and ^{1}H NMR (DMSO-d_6) spectra of crude residue were recorded without purification.

3,5-Di-*tert*-butyl-2-nitroaniline, S11

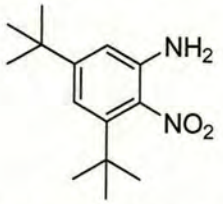

A suspension of 3,5-di-*tert*-butylaniline (0.80 g, 3.9 mmol) in acetic anhydride (30 mL) was cooled to 5-7 °C and stirred for 3 h. To this suspension was added dropwise fuming nitric acid (0.40 mL, 8.6 mmol) and stirred over ice for 2 h. Then the reaction mixture was poured into the ice water and the solid was collected by suction. To the solution of resulting solid in ethanol (50 mL) was added 37% hydrochloric acid (4 mL) and was heated at reflux for 3 h. Cooled to room temperature, concentrated *in vacuo* and 37% ammonia solution (4 mL) was added. Then the mixture was dissolved in chloroform and washed with brine (3 × 50 mL), dried over $MgSO_4$, concentrated *in vacuo* and the crude product purified by column chromatography ($CHCl_3$) to yield **S11** as a yellow solid (0.48 g, yield = 49%). m.p. 90-92 °C; ^{1}H NMR (400 MHz, $CDCl_3$): δ = 1.28 (s, 9H, C(CH_3)$_3$), 1.38 (s, 9H, C(CH_3)$_3$), 3.98 (br s, 2H, NH_2), 6.69 (s, 1H, Ar*H*), 6.93 (s, 1H, Ar*H*); ^{13}C NMR (100 MHz, $CDCl_3$): δ = 31.0 (× 2), 34.9, 36.0, 112.6, 115.3, 137.7, 138.6, 142.1, 153.6; HRMS calcd. for $C_{14}H_{22}N_2O_2$ $[M]^+$: 250.16813, Found (FAB, 3-NOBA matrix): 250.16777.

3,5-Di-*tert*-butyl-2-aminoaniline, S12

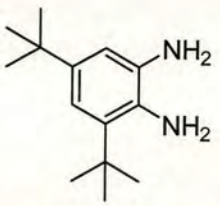

A stirred solution of **S11** (0.22 g, 0.88 mmol), hydrazine hydrate (0.5 mL, 0.01 mol) and a catalytic amount of Pd-C (10% w/w) in ethanol (25 mL) was heated at reflux under an atmosphere of nitrogen. After 3 h the reaction mixture was filtered, concentrated *in vacuo* and the residue re-dissolved in chloroform, washed with brine (3 × 50 mL), dried over $MgSO_4$ and concentrated *in vacuo* to yield **S12** as a green solid (0.18 g, yield = 95%). m.p. 74-76 °C; ^{1}H NMR (400 MHz, $CDCl_3$): δ = 1.37 (s,

9H, C(CH_3)$_3$), 1.52 (s, 9H, C(CH_3)$_3$), 3.53 (br s, 4H, 2NH_2), 6.77 (s, 1H, Ar*H*), 6.96 (s, 1H, Ar*H*); ^{13}C NMR (100 MHz, $CDCl_3$): δ = 30.0, 31.5, 34.1, 34.4, 112.6, 115.1, 131.0, 134.2, 134.5, 141.4; HRMS calcd. for $C_{14}H_{24}N_2$ $[M]^+$: 220.19395, Found (FAB, 3-NOBA matrix): 220.19392.

N^1-(2-Amino-3,5-di-*tert*-butylphenyl)-N^4-(2,2-diphenylethyl)fumaramide, S13

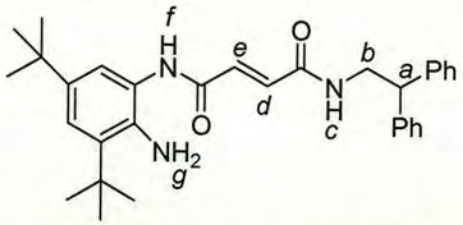

To a stirred solution of **S12** (0.26 g, 1.2 mmol), **S3** (0.35 g, 1.2 mmol) and 4-DMAP (0.17 g, 1.4 mmol) in dichloromethane/DMF (1:1, 20 mL) cooled on an ice bath was added EDCI•HCl (0.25 g, 1.3 mmol) and the reaction was allowed to stir for 14 h at room temperature under an atmosphere of nitrogen. The reaction mixture was concentrated *in vacuo* and the residue re-dissolved in dichloromethane, washed successively with 10% citric acid (3 × 50 mL), sat. $NaHCO_3$ (3 × 50 mL) and brine (3 × 50 mL), dried over $MgSO_4$, concentrated *in vacuo* and the crude product purified by column chromatography (98:2 $CHCl_3$:CH_3OH) to yield **S13** as a pale yellow solid (0.22 g, yield = 37%). m.p. 216-218 °C; ^{1}H NMR (400 MHz, DMSO-d_6): δ = 1.20 (s, 9H, C(CH_3)$_3$), 1.35 (s, 9H, C(CH_3)$_3$), 3.84 (dd, J = 5.8, 7.7 Hz, 2H, H_b), 4.24 (t, J = 7.7 Hz, 1H, H_a), 4.42 (br s, 2H, H_g), 6.84 (d, J = 15.2 Hz, 1H, H_d or H_e), 7.05-7.32 (m, 13H, 12Ar*H*+H_e or H_d), 8.54 (br t, J = 5.8 Hz, 1H, H_c), 9.56 (s, 1H, H_f); ^{13}C NMR (100 MHz, DMSO-d_6): δ = 29.4, 31.4, 33.6, 34.3, 43.3, 50.0, 120.6, 121.0, 123.4, 126.3, 127.8, 128.4, 132.9, 133.0 (× 2), 137.4, 137.5, 142.7, 162.7, 163.7; HRMS calcd. for $C_{32}H_{40}N_3O_2$ $[M+H]^+$: 498.31205, Found (FAB, 3-NOBA matrix): 498.31358.

(*E*)-3-(5,7-Di-*tert*-butyl-1*H*-benzo[*d*]imidazol-2-yl)-*N*-(2,2-diphenylethyl)acrylamide, *E*-14

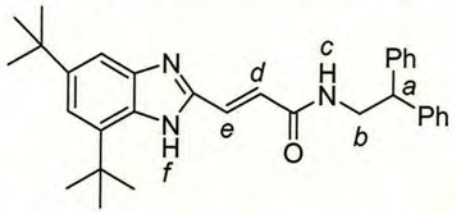

A stirred solution of **S13** (0.21 g, 0.42 mmol) and toluene-4-sulfonic acid monohydrate (0.08 g, 0.42 mmol) in toluene (40 mL) was stored at room temperature under an atmosphere of nitrogen. After 26 h, the reaction mixture was concentrated *in vacuo* and the residue re-dissolved in chloroform, washed with sat. $NaHCO_3$ (3 × 50 mL) and brine (3 × 50 mL), dried over $MgSO_4$, concentrated *in vacuo* and the crude product purified by column chromatography (98:2 $CHCl_3$:CH_3OH) to yield ***E*-14** as a yellow solid (0.15 g, yield = 75%). m.p. 234-236 °C; ^{1}H NMR (400 MHz, DMSO-d_6): δ = 1.32 (s, 9H, C(CH_3)$_3$), 1.51 (s, 9H, C(CH_3)$_3$), 3.86 (dd, J = 5.7, 7.8 Hz, 2H, H_b), 4.29 (t, J = 7.8 Hz, 1H, H_a), 6.93 (d, J = 15.7 Hz, 1H, H_d or H_e), 7.09-7.40 (m, 13H, 12ArH + H_e or H_d), 8.50 (t, J = 5.7 Hz, 1H, H_c), 12.55 (s, 1H, H_f); ^{13}C NMR (100 MHz, DMSO-d_6): δ = 30.2, 31.5, 34.7, 35.2, 43.4, 50.0, 105.3, 115.6, 126.2, 126.3, 127.8, 128.3, 128.4, 134.9, 140.0, 140.4, 142.8, 145.5, 146.4, 164.4; HRMS calcd. for $C_{32}H_{38}N_3O$ $[M+H]^+$: 480.30149, Found (FAB, 3-NOBA matrix): 480.30232.

[2]-(1,7,14,20-tetraaza-2,6,15,19-tetraoxo-3,5,9,12,16,18,22,25-tetrabenzocyclohexacosane)-(*E*)-3-(5,7-Di-*tert*-butyl-1*H*-benzo[*d*]imidazol-2-yl)-*N*-(2,2-diphenylethyl)acrylamide-rotaxane, *E*-13

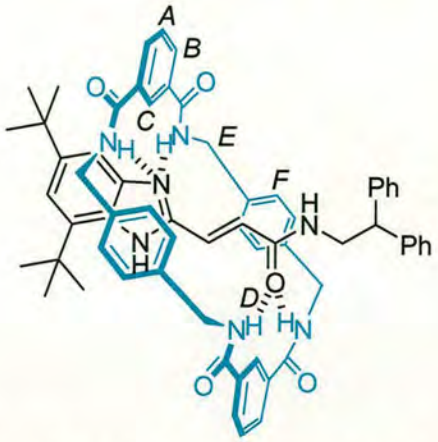

E-**14** (0.08 g, 0.17 mmol) and triethylamine (0.9 mL, 6.5 mmol) were dissolved in chloroform (100 mL) and the mixtures were stirred vigorously while solutions of *p*-xylylenediamine (0.45 g, 3.3 mmol) in chloroform (20 mL) and isophthaloyl dichloride (0.68 g, 3.3 mmol) in chloroform (20 mL) were simultaneously added over a period of 2 h using motor-driven syringe pumps at room temperature under nitrogen atmosphere. After a further 20 h the resulting suspension was filtered and concentrated *in vacuo*. The crude residue was purified by column chromatography (98:2 $CHCl_3$:CH_3OH) to yield *E*-**13** as a white solid (0.13 g, yield = 76%). m.p. 352-354 °C; ^{1}H NMR (400 MHz, DMSO-d_6): δ = 1.09 (s, 9H, C(CH_3)$_3$), 1.45 (s, 9H, C(CH_3)$_3$), 3.56 (t, J = 6.6 Hz, 2H, H_b), 4.09-4.17 (m, 5H, H_E,+H_a), 4.27 (dd, J = 4.4, 14.0 Hz, 4H, H_E), 6.00 (d, J = 15.4 Hz, 1H, H_d or H_e), 6.23 (s, 1H, Ar*H*), 6.59 (d, J = 15.4 Hz, 1H, H_e or H_d), 6.66 (s, 8H, H_F), 7.08-7.27 (m, 11H, Ar*H*), 7.75 (t, J = 7.8 Hz, 2H, H_A), 8.12 (d, J = 7.8 Hz, 4H, H_B), 8.41 (t, J = 5.4 Hz, 1H, H_c), 8.59 (t, J = 4.4 Hz, 4H, H_D), 8.79 (s, 2H, H_C), 11.96 (s, 1H, H_f); ^{13}C NMR (100 MHz, DMSO-d_6): δ = 29.6, 31.4, 34.2 (× 2), 43.6, 43.8, 50.1, 111.2, 117.2, 124.5, 124.7, 126.2, 126.5, 127.6, 128.4, 128.5, 129.0, 129.1, 130.8, 134.0, 134.2, 136.1, 142.5, 143.1, 144.7, 148.4, 166.1 (× 2); HRMS calcd. for $C_{64}H_{66}N_7O_5$ $[M+H]^+$: 1012.51254, Found (FAB, 3-NOBA matrix): 1012.51225.

X-Ray Crystallographic Structure Determination

X-ray crystal structural data for *E*-**13**•2H_2O: $C_{64}H_{69}N_7O_7$, M_r = 1048.26, colourless platelet, crystal size 0.1000 × 0.1000 × 0.0300 mm^3, monoclinic P2(1)/n, a = 20.062(13), b = 10.644(8), c = 26.399(16) Å, β = 102.65(3)°, V = 5500(6) $Å^3$, Z = 4, ρ_{calcd} = 1.266 Mg/m^3; λ = 0.71073 Å, $\mu(Mo_{K\alpha})$ = 0.083 mm^{-1}, T = 93(2) K; 20983 reflections collected, 8124 independent reflections (R_{int} = 0.2144, 2.18 < θ < 25.35°) and 727 parameters. The structure was solved by direct methods and refined by full-matrix least-squares on F^2 to give $R1(F^2)$ = 0.1549 ($I > 2\sigma I$), $wR2(F^2)$ = 0.4680 (all data). Residual electron density extremes were 0.325 and -0.338 $eÅ^{-3}$.

X-Ray Crystal Structure Thermal Ellipsoids

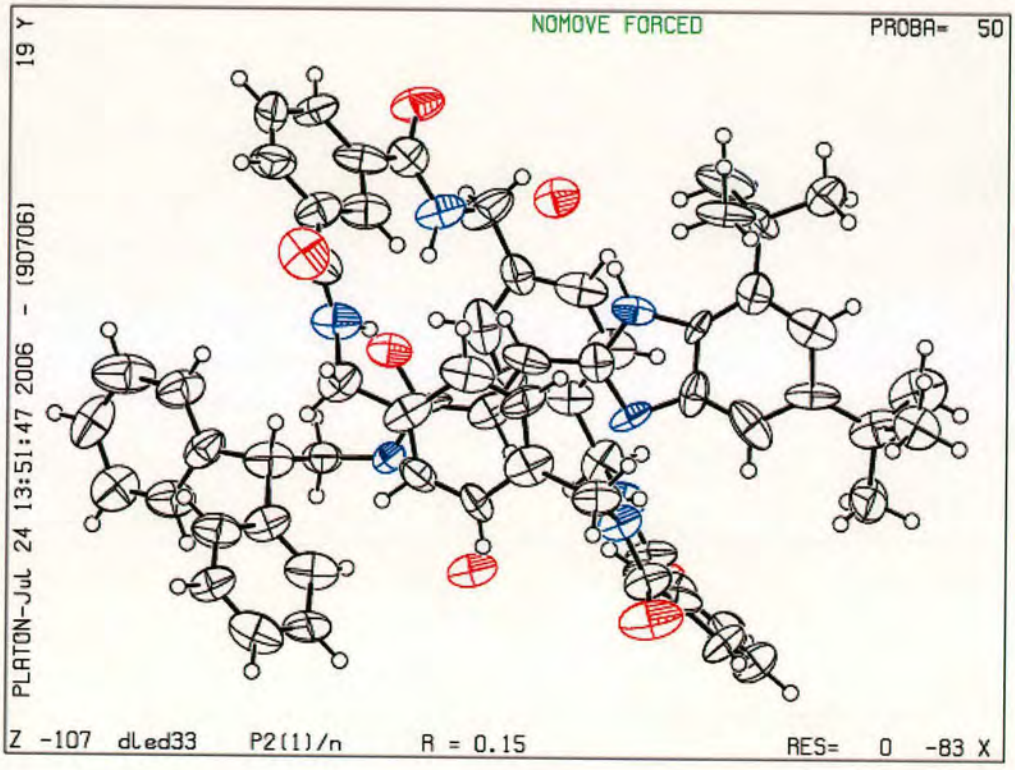

3.6 References and Notes

(1) Gatti, F. G.; León, S.; Wong, J. K. Y.; Bottari, G.; Altieri, A.; Farran Morales, M. A.; Teat, S. J.; Frochot, C.; Leigh, D. A.; Brouwer, A. M.; Zerbetto, F. *Proc. Natl. Acad. Sci. U.S.A.* **2003**, *100*, 10-14.

(2) Schwartz, G.; Fehse, K.; Pfeiffer, M.; Walzer, K.; Leo, K. *Appl. Phys. Lett.* **2006**, *89*, 083509.

(3) Asensio, J. A.; Gomez-Romero, P. *Fuel Cells* **2005**, *5*, 336-343.

(4) (a) Zou, B.; Yuan, Q.; Ma, D. *Angew. Chem., Int. Ed.* **2007**, *46*, 2598-2601. (b) Zheng, N.; Anderson, K. W.; Huang, X.; Nguyen, H. N.; Buchwald, S. L. *Angew. Chem., Int. Ed.* **2007**, *46*, DOI: 10.1002/anie.200702542, and references there in.

(5) (a) Arunkumar, E.; Forbes, C. C.; Noll, B. C.; Smith, B. D. *J. Am. Chem. Soc.* **2005**, *127*, 3288-3289. (b) Arunkumar, E.; Forbes, C. C.; Smith, B. D. *Eur. J. Org. Chem.* **2005**, 4051-4059. (c) Cheetham, A. G.; Hutchings, M. G.; Claridge, T. D. W.; Anderson, H. L. *Angew. Chem., Int. Ed.* **2006**, *45*, 1596-1599. (d) Arunkumar, E.; Fu, N.; Smith, B. D. *Chem. Eur. J.* **2006**, *12*, 4684-4690. (e) Stone, M. T.; Anderson, H. L. *Chem. Commun.* **2007**, 2387-2389.

(6) (a) Lane, A. S.; Leigh, D. A.; Murphy, A. *J. Am. Chem. Soc.* **1997**, *119*, 11092-11093. (b) Brouwer, A. M.; Frochot, C.; Gatti, F. G.; Leigh, D. A.; Mottier, L.; Paolucci, F.; Roffia, S.; Wurpel, G. W. H. *Science* **2001**, *291*, 2124-2128. (c) Altieri, A.; Gatti, F. G.; Kay, E. R.; Leigh, D. A.; Martel, D.; Paolucci, F.; Slawin, A. M. Z.; Wong, J. K. Y. *J. Am. Chem. Soc.* **2003**, *125*, 8644-8654. (d) Altieri, A.; Bottari, G.; Dehez, F.; Leigh, D. A.; Wong, J. K. Y.; Zerbetto, F. *Angew. Chem., Int. Ed.* **2003**, *42*, 2296-2300. (e) Da Ros, T.; Guldi, D. M.; Farran Morales, A.; Leigh, D. A.; Prato, M.; Turco, R. *Org. Lett.* **2003**, *5*, 689-691. (f) Keaveney, C. M.; Leigh, D. A. *Angew. Chem., Int. Ed.* **2004**, *43*, 1222-1224. (g) Hunter, C. A. *Angew. Chem., Int. Ed.* **2004**, *43*, 5310-5324. (h) Leigh, D. A.; Morales, M. A. F.; Perez, E. M.; Wong, J. K. Y.; Saiz, C. G.; Slawin, A. M. Z.; Carmichael, A. J.; Haddleton, D. M.; Brouwer, A. M.; Buma, W. J.; Wurpel, G. W. H.; Leon, S.; Zerbetto, F. *Angew. Chem., Int. Ed.* **2005**, *44*, 3062-3067. (i) Mateo-Alonso, A.; Fioravanti, G.; Marcaccio, M.; Paolucci, F.; Rahman, G. M. A.; Ehli, C.; Guldi, D. M.; Prato, M. *Chem. Commun.* **2007**, 1945-1947.

(7) (a) Berná, J; Brouwer, A. M.; Fazio, S. M.; Haraszkiewicz, N.; Leigh, D. A.; Lennon, C. M. *Chem. Commun.* **2007**, 1910-1912 (b) Brouwer, A. M.; Fazio, S. M.; Haraszkiewicz, N.; Leigh, D. A.; Lennon, C. M. *Photochem. Photobiol. Sci.* **2007**, *6*, 480-486.

(8) Stanier, C. A.; Alderman, S. J.; Claridge, T. D. W.; Anderson, H. L. *Angew. Chem., Int. Ed.* **2002**, *41*, 1769-1772.

Shuttling through Acid-Base or Zinc(II)-EDTA Control

Acknowledgements

Dr. C.-F. Lee is gratefully acknowledged for many useful discussions.

4.1 Summary

A chemically addressable, bistable [2]rotaxane *E*-**6** which incorporates a thread containing *E*-3-(benzoxazol-2-yl)-*N*-methylacrylamide and succinic amide ester stations and a benzylic amide macrocycle has been assembled. ^{1}H NMR spectroscopy has demonstrated that reversible protonation/deprotonation or Zn^{2+}-complexation/EDTA-decomplexation can induce translocation of the macrocycle between these two stations along the linear thread. Model rotaxanes show the *E*-3-(benzoxazol-2-yl)-*N*-methylacrylamide site to be a better H-bond acceptor for the benzylic amide macrocycle than the succinic amide ester, so in the neutral or free form of *E*-**6**, intercomponent hydrogen bonding between the benzoxazole moiety and the macrocycle dominates. However, when the thread is protonated or coordinated with Zn^{2+} the binding affinity of the resulting [*E*-3-(benzoxazol-2-yl)-*N*-methylacrylamide•H]$^+$ or [*E*-3-(benzoxazol-2-yl)-*N*-methylacrylamide•Zn]$^{2+}$ for macrocycle decreases significantly. This results in the macrocycle shuttling to the second station through biased Brownian motion, as the succinic amide ester is now the preferred binding site. The shuttling process can be reversed by addition of a base or EDTA, and the initial state is restored. This macrocycle translocation behaviour has excellent positional integrity using the external input of protons or Zn^{2+}; and it may be applied in the future design of potential probes for detection and imaging of protons and zinc ions.

4.2 Introduction

Molecular and supramolecular systems that can be switched between two or more stable states have attracted considerable attention.[1] [2]Rotaxanes that possess two (or more) recognition sites are thus prototypes for the design and construction of controllable molecular switches.[2] Various stimuli have been employed to induce such

switching,[3] including solvent,[4] metal binding,[5] configurational changes,[6] and alteration of the oxidation state[7] or protonation level[8] of the molecule. Here the use of external inputs of acid-base and Zn^{2+}-EDTA to induce fully reversible translocation of a macrocycle is described.

4.3 Results and Discussion

4.3.1 Neutral or Free State of [2]Rotaxane *E*-6

[2]Rotaxane *E*-**6** (Figure 4.1) is made of a benzylic amide macrocycle, and a thread containing both *E*-3-(benzoxazol-2-yl)-*N*-methylacrylamide (shown in green) and succinic amide ester (orange) stations. The occupation ratio by the macrocycle between the two stations can be attributed to their differences in the free energies ($\Delta\Delta G$) of binding the macrocycle. Both stations can template the formation of benzylic amide macrocycles about them to give rotaxanes in five component clipping reactions; however, investigations of model rotaxanes show the *E*-3-(benzoxazol-2-yl)-*N*-methylacrylamide site to be a better H-bond acceptor than the succinic amide ester. In the neutral or free state of rotaxane *E*-**6**, the hydrogen-bonding interactions between *E*-3-(benzoxazol-2-yl)-*N*-methylacrylamide and macrocycle are stronger and the most stable 'co-conformation'[9] has the ring component on the benzoxazole unit. This is apparent from comparison of the ^{1}H NMR spectra of the rotaxane and thread (Figure 4.2). The occupied benzoxazole site protons (H_i and H_j) are shielded by the xylylene rings of the macrocycle and experience significant shifts. Protons on succinic amide ester station (H_c and H_d) experience little shielding compared to the analogous protons on the thread, indicating that the macrocycle spends no appreciable time on this station.

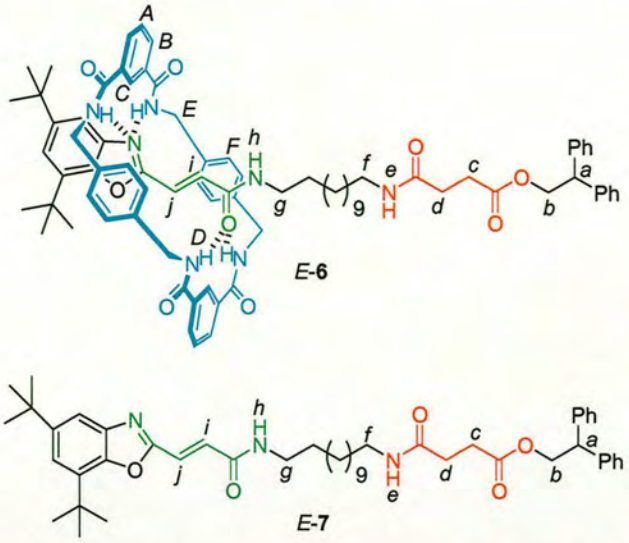

Figure 4.1 Chemical structures of the investigated [2]rotaxane *E*-**6** and its thread *E*-**7**.

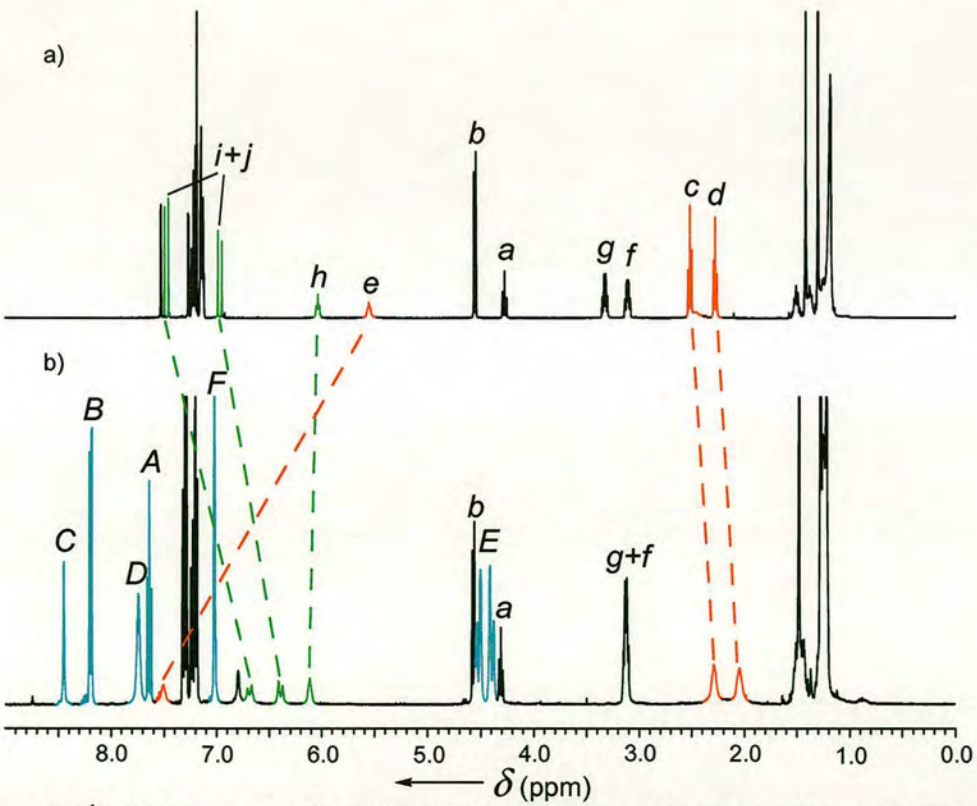

Figure 4.2 ^{1}H NMR spectra (400 MHz, 298 K) of a) thread *E*-**7** and b) rotaxane *E*-**6** in $CDCl_3$. The letters correspond to the assignments shown in Figure 4.1.

4.3.2 Acid-Base Switching

Stimuli-responsive molecular shuttles all operate through the same basic principle.[6c] The external stimulus does not intrinsically induce directional motion of

the macrocycle. Rather, it alters the equilibrium between different translational co-conformers by increasing the binding strength of the less populated station and/or destabilising the initially preferred binding site. The motion of the components arises from the thermal energy, the net result being a change in the position of the ring component through biased Brownian motion.

Given this mode of action, it might be possible to decrease the binding affinity of *E*-3-(benzoxazol-2-yl)-*N*-methylacrylamide site by protonation of the benzoxazole nitrogen atom in shuttle *E*-**6**. The benzoxazole nitrogen atom behaves as hydrogen-bonding acceptor in the neutral form, thus protonating it should induce translocation of the macrocycle (Scheme 4.1). The process should be reversed by deprotonation and the initial state will be restored.

Scheme 4.1 Presumed Reversible Translational Motion of *E*-**6** between Its Neutral and Protonated Forms

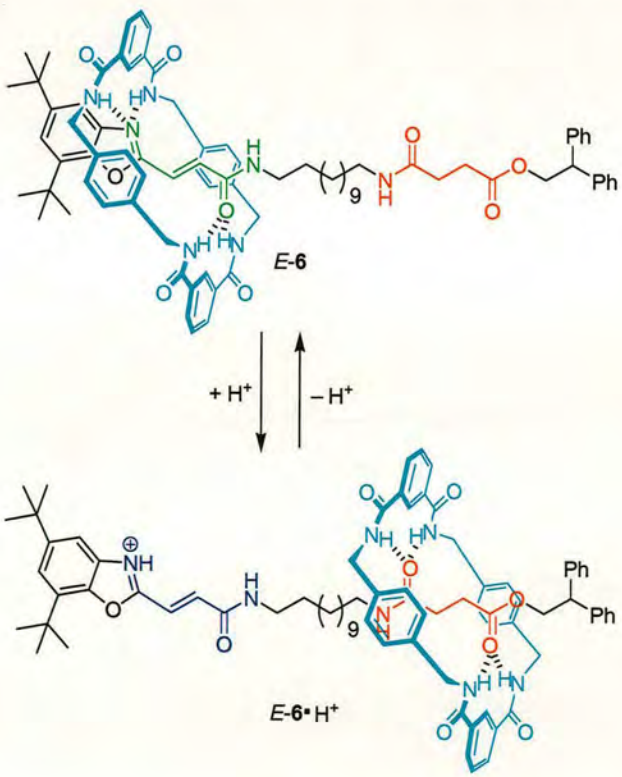

The first step involved investigating the protonation of the thread *E*-**7**. The reported pK_a data for aromatic benzoxazole derivatives indicates that the benzoxazole nitrogen atom is considerably less basic than the other *N*-heterocycles (pK_a,

$_{benzimidazole}$= 5.56; p$K_{a,\ benzothiazole}$= 1.2; p$K_{a,\ benzoxazole}$= -0.13),[10] thus it requires relatively strong acidic conditions and significantly high acid concentrations for protonation.[11] Accordingly, when the thread *E*-**7** in $CDCl_3$ solution was treated with 5 molar equiv of TFA (pK_a= 0.3), the ^{1}H NMR spectrum reveals the expected chemical shift differences relative to its neutral form; most notably in the signals assigned to the olefin protons H_i and H_j (Figure 4.3a and 4.2a). Their downfield shifts of 0.5 and 0.2 ppm respectively point to this compound being *E*-**7**•H^+ in which the benzoxazole nitrogen atom has been protonated. Deprotonation by addition of excess of K_2CO_3 regenerates the initial neutral state.

The addition of 5 molar equiv of TFA to the $CDCl_3$ solution of *E*-**6** results in its complete conversion to a new compound; where the benzoxazole nitrogen atom has been protonated and the benzylic amide macrocycle has migrated to the succinic amide ester station. The structure is confirmed unambiguously by the chemical shift differences of the protons when compared with its corresponding protonated thread *E*-**7**•H^+ (Figure 4.3). The succinic amide ester protons H_c and H_d are shielded by 1.0 ppm in the protonated rotaxane relative to the protonated thread, while the chemical shifts of the olefin protons H_i and H_j are only shielded by 0.3 and 0.2 ppm, respectively. This shuttling process is fully reversible: deprotonation of the benzoxazole moiety upon addition of K_2CO_3 leads to the complete displacement of the ring component to the *E*-3-(benzoxazol-2-yl)-*N*-methylacrylamide site again and the initial state is regained confirmed by ^{1}H NMR spectroscopy. As expected, addition of less acidic acetic acid-d_4 (pK_a= 4.76) did not translocate the macrocycle in *E*-**6**, as it was unable to protonate the benzoxazole nitrogen atom.

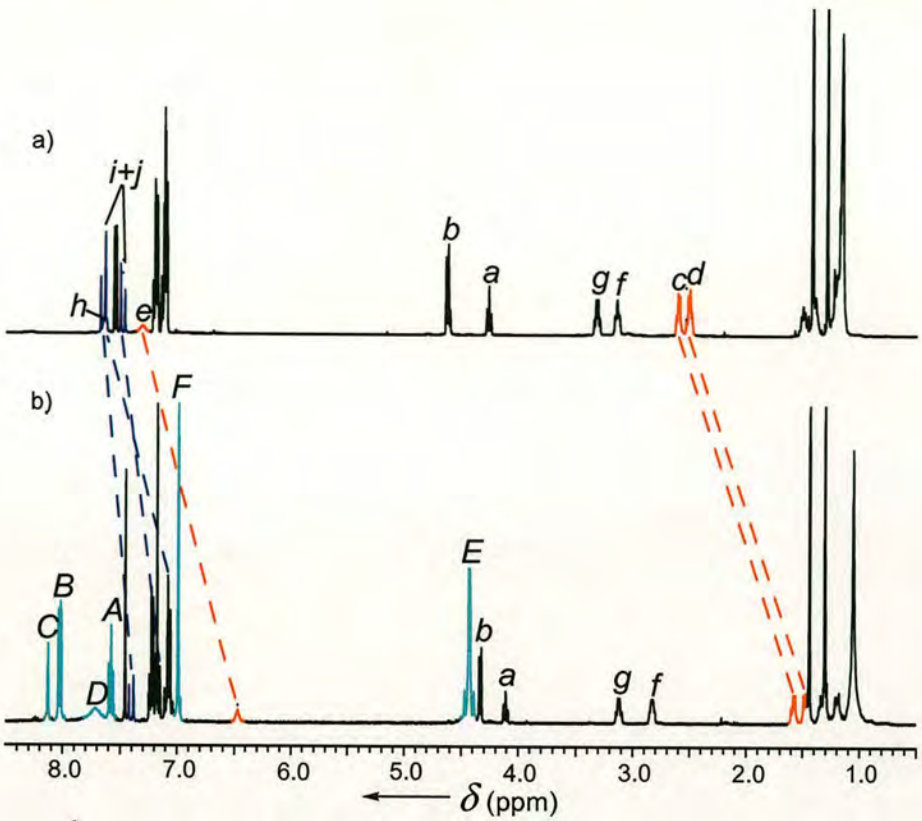

Figure 4.3 ^{1}H NMR spectra (400 MHz, 298 K) of a) protonated thread *E*-**7**•H^+ and b) protonated rotaxane *E*-**6**•H^+ in $CDCl_3$. The letters correspond to the assignments shown in Figure 4.1.

4.3.3 Zinc(II)-EDTA Switching

Zinc is the second-most-abundant transition-metal ion in the human body, and it has multiple roles in both intra- and extracellular functions.[12] Besides growth, numerous body functions are affected by zinc ions, including the immune, endocrine and gastroenterological systems.[13] Owing to the role this cation plays in the physiological functions, the detection and imaging of Zn^{2+} in biological samples are of paramount interest. Imaging is possible only with molecular probes that specifically bind to Zn^{2+} and result in properties changes. Taking account of the binding property of benzoxazole-*N* towards Zn^{2+},[14] coordination of *E*-**6** with Zn^{2+} might decrease the binding affinity of the benzoxazole moiety for the macrocycle. Shuttling would be induced as the hydrogen-bonding-acceptor nitrogen of the benzoxazole is now occupied by Zn^{2+} (Scheme 4.2). If elaborately designed, this Zn^{2+} controlled large amplitude motion can be applied to image and detect zinc ions.

Scheme 4.2 Presumed Reversible Translational Motion of *E*-**6** between Its Free and Zn^{2+}-Coordinated Forms

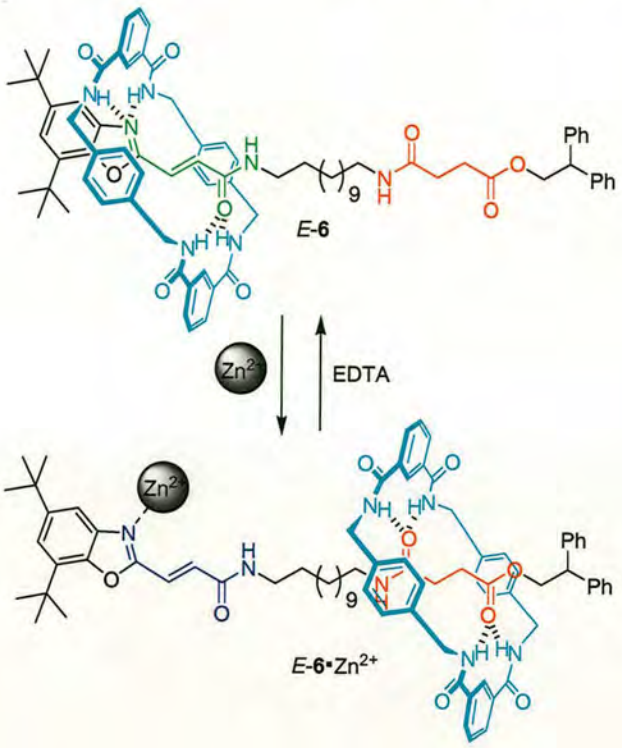

The treatment of a $CHCl_3$ solution of shuttle *E*-**6** with 5 molar equiv of $ZnCl_2$, followed by stirring the solution at rt for 1 h, resulted in the formation of *E*-**6**•Zn^{2+}. The same process was applied to the thread *E*-**7**, resulting in *E*-**7**•Zn^{2+}. The *E*-**6**•Zn^{2+} complex was insufficiently soluble in pure $CDCl_3$ or CD_2Cl_2 thus $CDCl_3/CD_3OD$ (97:3) was used for ^1H NMR spectroscopic studies. The olefin protons H_i and H_j of coordinated thread *E*-**7**•Zn^{2+} experience notable downfield shifts (0.4 and 0.4 ppm respectively, Figure 4.4a) compared to the free thread *E*-**7** (Figure 4.2a). Furthermore, the FAB mass spectrum revealed signal at m/z 862 which corresponds to [*E*-**7**•ZnCl]$^+$. This suggests Zn^{2+} coordination of the benzoxazole nitrogen atom, but no further overall structural information can be obtained without a single crystal X-ray diffraction study of this complex. Zinc halide complexes containing *N*-donor atom ligands can possess coordination numbers of four, five or six and are known to adopt a wide variety of structural motifs, including pseudo-tetrahedral, square pyramidal, trigonal bipyramidal and distorted octahedral.[14b]

The binding mode of the Zn^{2+} coordinated thread and shuttle is not clear. However, H_c and H_d protons of the succinic amide ester site are shielded in the shuttle complex

E-**6**•Zn^{2+}, compared to the thread complex *E*-**7**•Zn^{2+}, by δ = 0.92 and 0.93 ppm, respectively. The change in chemical shifts of H_i and H_j protons of the benzoxazole site are only 0.39 and 0.35 ppm, respectively (Figure 4.4). This indicates that the macrocycle is now located overwhelmingly over the succinic amide ester station. The FAB mass spectrum revealed signal at m/z 1395 which corresponds to [*E*-**6**•ZnCl]$^+$.

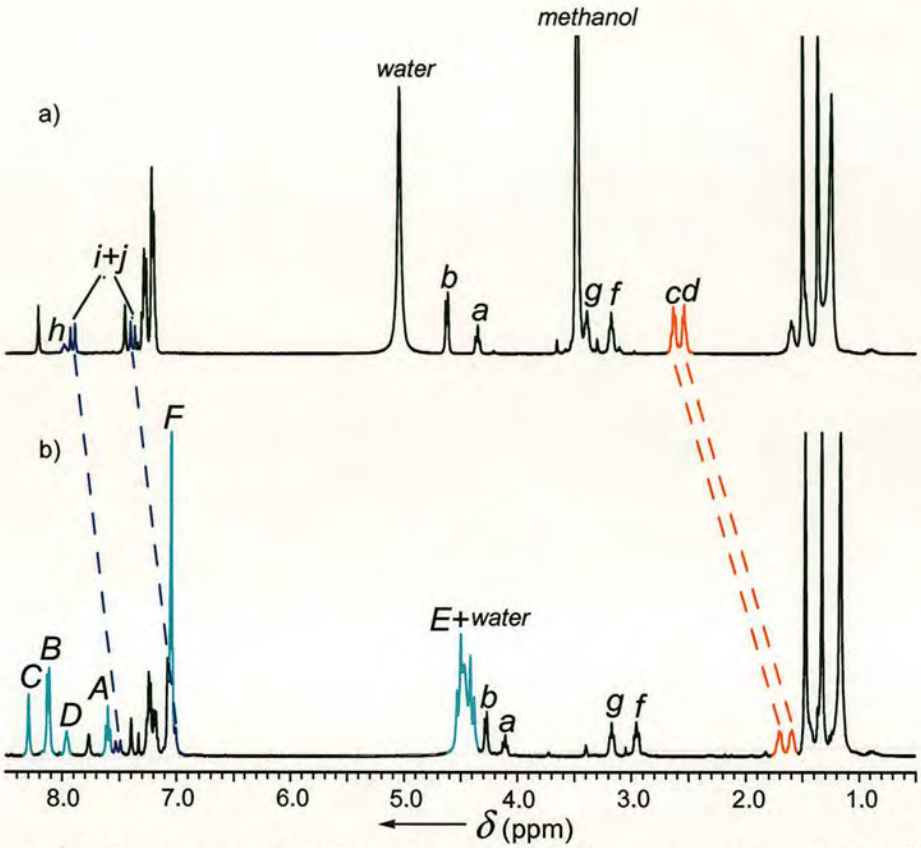

Figure 4.4 ^{1}H NMR spectra (400 MHz, 298 K) of a) Zn^{2+}-coordinated thread *E*-**7**•Zn^{2+} and b) Zn^{2+}-coordinated rotaxane *E*-**6**•Zn^{2+} in $CDCl_3/CD_3OD$, 97:3. The letters correspond to the assignments shown in Figure 4.1.

Noting the addition of 3% highly polar solvent CD_3OD, as a control, ^{1}H NMR spectroscopic study of free rotaxane *E*-**6** in 97:3 $CDCl_3/CD_3OD$ was investigated. It shows the hydrogen bonds between the macrocycle and the binding sites are disrupted by the CD_3OD competition (H_i and H_j protons of rotaxane *E*-**6** experience 0.7 and 0.6 ppm upfield chemical shifts relative to thread *E*-**7**, whereas H_c and H_d protons are also shielded by 0.5 and 0.5 ppm). However the macrocycle binding affinity with these two stations can not be reversed by only changing the solvents.

Furthermore, the shuttling is reversible and addition of EDTA extracts the Zn^{2+} from the benzoxazole nitrogen atom; this returns the macrocycle to the original benzoxazole site (Scheme 4.2) and has been confirmed by ^1H NMR spectroscopy.

4.4 Conclusions

There are many reasons for the development and construction of molecular machinery, one is certainly the desire to be able to turn chemical into mechanical energy at a molecular level and utilise synthetic molecular structures to perform tasks using mechanical motion. Herein a chemically driven molecular machine has been designed, based on a switchable [2]rotaxane which is pH or Zn^{2+} controllable. With reactions which are easily accomplished (acid/base or $ZnCl_2$/EDTA), this molecular shuttle *E*-**6**/*E*-**6**•H^+ or *E*-**6**/*E*-**6**•Zn^{2+} can quickly switch the macrocycle between two distinct translational forms with high positional integrity. The study of such a simple process is useful for the future design of molecular devices as a logical step toward mimicking the actions of extremely complex biomolecular machines. Furthermore, the proton- or Zn^{2+}-induced large amplitude motion in *E*-**6** implies that it can act as a potential probe to detect protons and zinc ions.

4.5 Experiments

4.5.1 General

Unless stated otherwise, all reagents and anhydrous solvents were purchased from Aldrich Chemicals and used without further purification. *P*-xylylene diamine was distilled under reduced pressure and isophthaloyl dichloride was recrystallised from *n*-hexane. Column chromatography was performed using Kiesegel C60 (Merck, Germany) as the stationary phase, and TLC was performed on precoated silica gel plates (0.25 mm thick, $60F_{254}$, Merck, Germany) and observed under UV light. All ^1H and ^{13}C NMR spectra were recorded on a Bruker AV 400 instrument, at a constant temperature of 25 °C. Chemical shifts are reported in parts per million from high to low field and referenced to TMS. Coupling constants (*J*) are reported in Hertz (Hz). Standard abbreviations indicating multiplicity are used as follows: m = multiplet, br = broad, d = doublet, q = quadruplet, t = triplet, s = singlet. FAB mass spectrometry was carried out by the services at the University of Edinburgh.

4.5.2 General Procedure for Protonation/Deprotonation of Thread *E*-7 or Rotaxane *E*-6

TFA (5 molar equiv) was added to a solution of thread *E*-**7** or rotaxane *E*-**6** in $CDCl_3$ in an NMR tube by using a microsyringe. The deprotonation was accomplished by the addition of excess of K_2CO_3. Both protonation and deprotonation were confirmed by ^1H NMR.

Protonation/Deprotonation of Thread *E*-**7**:

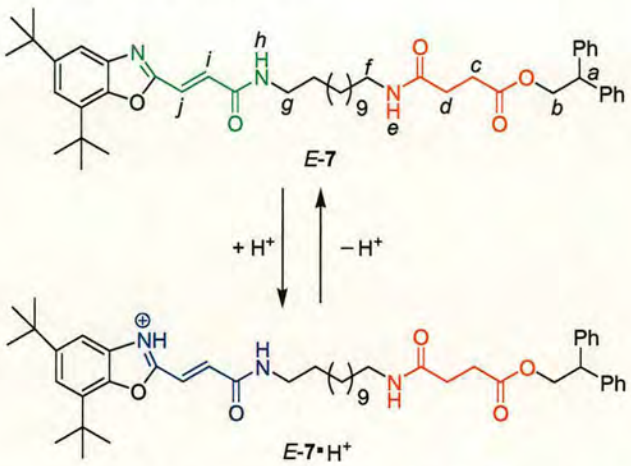

E-**7**: This compound was synthesised as described in chapter two. ^1H NMR (400 MHz, $CDCl_3$): δ = 1.14-1.28 (m, 16H, -C*H*$_2$- (alkyl chain)), 1.30 (s, 9H, C(C*H*$_3$)$_3$), 1.33-1.41 (m, 11H, C(C*H*$_3$)$_3$ and -C*H*$_2$-CH$_f$), 1.45-1.55 (m, 2H, -C*H*$_2$-CH$_g$), 2.27 (t, *J* = 6.9 Hz, 2H, *H*$_d$), 2.51 (t, *J* = 6.9 Hz, 2H, *H*$_c$), 3.11 (m, 2H, *H*$_f$), 3.33 (m, 2H, *H*$_g$), 4.27 (t, *J* = 7.6 Hz, 1H, *H*$_a$), 4.55 (d, *J* = 7.6 Hz, 2H, *H*$_b$), 5.55 (br t, *J* = 5.3 Hz, 1H, *H*$_e$), 6.04 (br t, *J* = 5.7 Hz, 1H, *H*$_h$), 6.97 (d, *J* = 15.7 Hz, 1H, *H*$_i$ or *H*$_j$), 7.12-7.17 (m, 6H, Ar*H*), 7.20-7.25 (m, 4H, Ar*H*), 7.26 (s, 1H, Ar*H*), 7.48 (d, *J* = 15.7 Hz, 1H, *H*$_j$ or *H*$_i$), 7.53 (s, 1H, Ar*H*).

E-**7**•H$^+$: ^1H NMR (400 MHz, $CDCl_3$): δ = 1.16-1.21 (m, 16H, -C*H*$_2$- (alkyl chain)), 1.29 (s, 9H, C(C*H*$_3$)$_3$), 1.39-1.42 (m, 11H, C(C*H*$_3$)$_3$ and -C*H*$_2$-CH$_f$), 1.47-1.54 (m, 2H, -C*H*$_2$-CH$_g$), 2.50 (t, *J* = 6.1 Hz, 2H, *H*$_d$), 2.61 (t, *J* = 6.1 Hz, 2H, *H*$_c$), 3.15 (m, 2H, *H*$_f$), 3.32 (m, 2H, *H*$_g$), 4.27 (t, *J* = 7.8 Hz, 1H, *H*$_a$), 4.63 (d, *J* = 7.8 Hz, 2H, *H*$_b$), 7.10-7.22 (m, 10H, Ar*H*), 7.32 (br, 1H, *H*$_e$), 7.49 (d, *J* = 16.2 Hz, 1H, *H*$_i$ or *H*$_j$), 7.55 (s, 1H, Ar*H*), 7.57 (s, 1H, Ar*H*), 7.63-7.68 (m, 2H, *H*$_j$ or *H*$_i$ and *H*$_h$).

Protonation/Deprotonation of Rotaxane *E*-**6**:

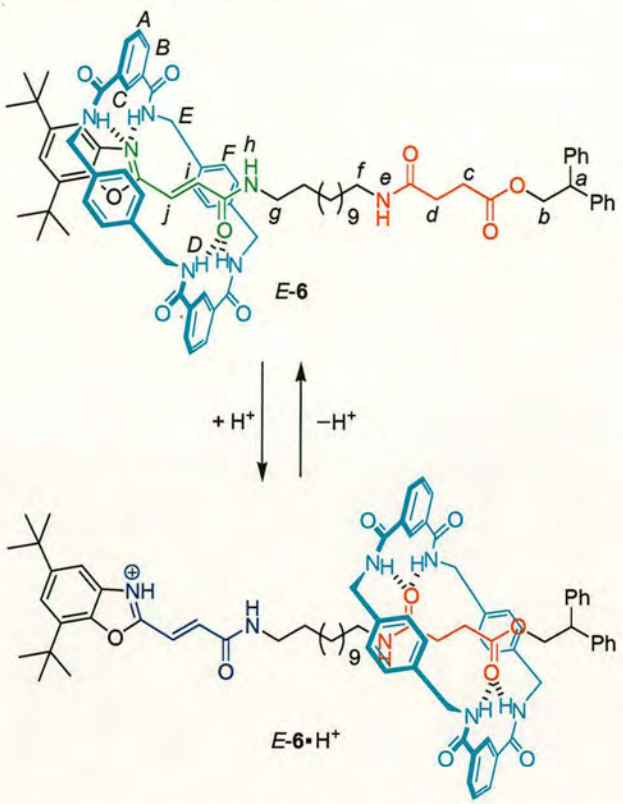

E-**6**: This compound was synthesised as described in chapter two. ^{1}H NMR (400 MHz, $CDCl_3$): δ = 1.17-1.31 (m, 25H, C(CH_3)$_3$ and -CH_2- (alkyl chain)), 1.40-1.56 (m, 13H, C(CH_3)$_3$, -CH_2-CH_f and -CH_2-CH_g), 2.04 (br s, 2H, H_d), 2.28 (br s, 2H, H_c), 3.12 (m, 4H, H_f and H_g), 4.31 (t, J = 7.6 Hz, 1H, H_a), 4.39 (d, J = 13.1 Hz, 4H, $H_{E'}$), 4.47-4.61 (m, 6H, H_E and H_b), 6.11 (br s, 1H, H_h), 6.39 (d, J = 15.0 Hz, 1H, H_i or H_j), 6.69 (d, J = 15.0 Hz, 1H, H_j or H_i), 6.79 (s, 1H, Ar*H*), 7.02 (s, 8H, H_F), 7.18-7.33 (m, 11H, Ar*H*), 7.50 (br s, 1H, H_e), 7.64 (t, J = 7.8 Hz, 2H, H_A), 7.74 (br s, 4H, H_D), 8.20 (d, J = 7.8 Hz, 4H, H_B), 8.45 (s, 2H, H_C).

E-**6**•H$^+$: ^{1}H NMR (400 MHz, $CDCl_3$): δ = 1.05 (m, 16H, -CH_2- (alkyl chain)), 1.18-1.21 (m, 2H, -CH_2-CH_f), 1.30-1.35 (m, 11H, C(CH_3)$_3$ and -CH_2-CH_g), 1.44-1.49 (m, 11H, C(CH_3)$_3$ and H_d), 1.58 (t, J = 6.9 Hz, 2H, H_c), 2.82 (m, 2H, H_f), 3.12 (m, 2H, H_g), 4.11 (t, J = 7.6 Hz, 1H, H_a), 4.33 (d, J = 7.6 Hz, 2H, H_b), 4.43 (m, 8H, H_E), 6.47 (br t, 1H, H_e), 7.00 (s, 8H, H_F), 7.07-7.23 (m, 12H, 10Ar*H*, H_i or H_j and H_h), 7.41 (d, J = 15.9 Hz, 1H, H_j or H_i), 7.46 (s, 2H, Ar*H*), 7.58 (t, J = 7.8 Hz, 2H, H_A), 7.73 (br s, 4H, H_D), 8.03 (d, J = 7.8 Hz, 4H, H_B), 8.13 (s, 2H, H_C).

4.5.3 General Procedure for Zn^{2+} Complexation/EDTA Decomplexation of Thread *E*-7 or Rotaxane *E*-6

The treatment of a $CHCl_3$ solution of thread *E*-**7** or shuttle *E*-**6** with 5 molar equiv of a 1 M Et_2O solution of $ZnCl_2$ and stirring the resulting solution at rt for 1 h, followed by evaporation of the solvent and washing with Et_2O, yielded a pale yellow solid. The decomplexation was accomplished by the addition of excess of EDTA/K_2CO_3. Complexation was confirmed by ^1H NMR, ^{13}C NMR and FAB-MS. Decomplexation was confirmed by ^1H NMR.

Zn^{2+} Complexation/EDTA Decomplexation of Thread *E*-**7**:

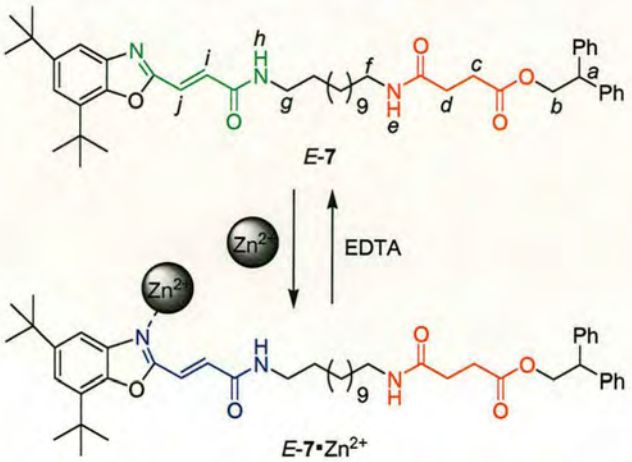

E-**7**•Zn^{2+}: ^1H NMR (400 MHz, 97:3 $CDCl_3/CD_3OD$): δ = 1.11-1.24 (m, 16H, -CH_2-(alkyl chain)), 1.29 (s, 9H, $C(CH_3)_3$), 1.40-1.43 (m, 11H, $C(CH_3)_3$ and -CH_2-CH_f), 1.47-1.57 (m, 2H, -CH_2-CH_g), 2.46 (t, J = 6.3 Hz, 2H, H_d), 2.56 (t, J = 6.3 Hz, 2H, H_c), 3.11 (m, 2H, H_f), 3.32 (m, 2H, H_g), 4.28 (t, J = 7.5 Hz, 1H, H_a), 4.55 (d, J = 7.5 Hz, 2H, H_b), 7.13-7.24 (m, 10H, Ar*H*), 7.32 (d, J = 15.5 Hz, 1H, H_i or H_j), 7.38 (s, 1H, Ar*H*), 7.84 (d, J = 15.5 Hz, 1H, H_j or H_i), 7.92 (br t, H_h, exchanged by CD_3OD), 8.14 (s, 1H, Ar*H*); ^{13}C NMR (100 MHz, 97:3 $CDCl_3/CD_3OD$): δ = 26.4, 26.6, 28.5, 28.6, 28.8 (× 2), 29.1 (× 2), 29.6, 29.7, 30.7, 31.2, 34.2, 35.1, 40.0, 40.1, 40.3, 40.4, 49.3, 67.0, 113.9, 122.5, 122.8, 126.6, 127.8, 128.3, 133.8, 134.4, 137.8, 140.6, 145.7, 150.1, 161.3, 164.6, 172.9, 174.0; MS (FAB): m/z = 862 [*E*-**7**•ZnCl]$^+$.

Zn^{2+} Complexation/EDTA Decomplexation of Rotaxane *E*-**6**:

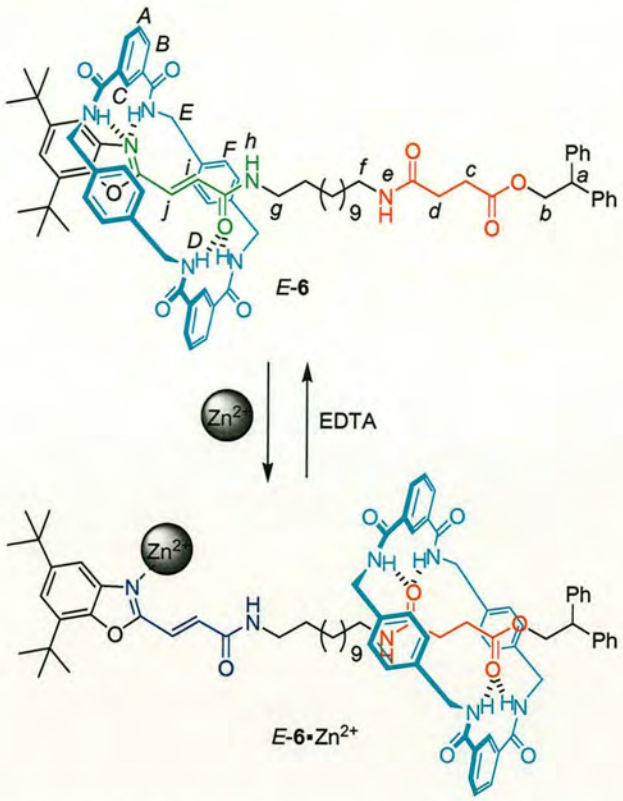

E-**6**•Zn^{2+}: ^{1}H NMR (400 MHz, 97:3 $CDCl_3/CD_3OD$): δ = 1.10 (m, 16H, -C*H*$_2$- (alkyl chain)), 1.27 (m, 11H, C(C*H*$_3$)$_3$ and -C*H*$_2$-CH$_f$), 1.41 (m, 11H, C(C*H*$_3$)$_3$ and -C*H*$_2$-CH$_g$), 1.53 (br t, *J* = 6.6 Hz, 2H, *H*$_d$), 1.64 (br t, *J* = 6.6 Hz, 2H, *H*$_c$), 2.89 (t, *J* = 7.2 Hz, 2H, *H*$_f$), 3.11 (t, *J* = 6.9 Hz, 2H, *H*$_g$), 4.04 (t, *J* = 7.5 Hz, 1H, *H*$_a$), 4.22 (d, *J* = 7.5 Hz, 2H, *H*$_b$), 4.32-4.47 (m, 8H, *H*$_E$), 6.95-7.02 (m, 14H, *H*$_F$, 5Ar*H* and *H*$_i$ or *H*$_j$), 7.11-7.20 (m, 5H, Ar*H*), 7.34 (s, 1H, Ar*H*), 7.45 (d, *J* = 16.4 Hz, 1H, *H*$_j$ or *H*$_i$), 7.54 (t, *J* = 7.6 Hz, 2H, *H*$_A$), 7.71 (s, 1H, Ar*H*), 7.91 (br t, *H*$_D$, exchanged by CD_3OD), 8.07 (d, *J* = 7.6 Hz, 4H, *H*$_B$), 8.24 (s, 2H, *H*$_C$); ^{13}C NMR (100 MHz, 97:3 $CDCl_3/CD_3OD$): δ = 26.5, 26.6, 28.6, 28.7 (× 2), 28.8, 29.0, 29.1 (× 2), 29.4, 29.5, 29.6, 31.3, 34.2, 35.0, 39.7, 40.0, 43.9, 44.0, 49.3, 67.0, 113.7, 122.1, 122.6, 124.9, 126.7, 127.7, 128.4, 128.9, 129.2, 131.2, 132.5, 133.4, 134.3, 136.8, 138.6, 140.5, 145.9, 149.7, 161.0, 164.6, 167.4, 172.8, 173.4; MS (FAB): m/z = 1395 [*E*-**6**•ZnCl]$^+$.

4.6 References and Notes

(1) Garaudée, S.; Silvi, S.; Venturi, M.; Credi, A.; Flood, A. H.; Stoddart, J. F. *ChemPhysChem* **2005**, *6*, 2145-2152.

(2) Anelli, P. L.; Spencer, N.; Stoddart, J. F. *J. Am. Chem. Soc.* **1991**, *113*, 5131-5133.

(3) For recent reviews, see (a) Flood, A. H.; Ramirez, R. J. A.; Deng, W.-Q.; Muller, R. P.; Goddard III, W. A.; Stoddart, J. F. *Aust. J. Chem.* **2004**, *57*, 301-322. (b) Tian, H.; Wang Q.-C. *Chem. Soc. Rev.* **2006**, *35*, 361-374. (c) Balzani, V.; Credi, A.; Silvi, S.; Venturi, M. *Chem. Soc. Rev.* **2006**, *35*, 1135-1149. (d) Browne, W. R.; Feringa, B. L. *Nature Nanotechnology* **2006**, *1*, 25-35. (e) Kay, E. R.; Leigh, D. A.; Zerbetto, F. *Angew. Chem., Int. Ed.* **2007**, *46*, 72-191. (f) Saha, S.; Stoddart, J. F. *Chem. Soc. Rev.* **2007**, *36*, 77-92. (g) Loeb, S. J. *Chem. Soc. Rev.* **2007**, *36*, 226-235. (h) Champin, B.; Mobian, P.; Sauvage, J.-P. *Chem. Soc. Rev.* **2007**, *36*, 358-366.

(4) (a) Lane, A. S.; Leigh, D. A.; Murphy, A. *J. Am. Chem. Soc.* **1997**, *119*, 11092-11093. (b) Asakawa, M.; Brancato, G.; Fanti, M.; Leigh, D. A.; Shimizu, T.; Slawin, A. M. Z.; Wong, J. K. Y.; Zerbetto, F.; Zhang, S. *J. Am. Chem. Soc.* **2002**, *124*, 2939-2950. (c) Bottari, G.; Dehez, F.; Leigh, D. A.; Nash, P. J.; Pérez, E. M.; Wong, J. K. Y.; Zerbetto, F. *Angew. Chem., Int. Ed.* **2003**, *42*, 5886-5889. (d) Bottari, G.; Leigh, D. A.; Pérez, E. M. *J. Am. Chem. Soc.* **2003**, *125*, 13360-13361.

(5) (a) Armaroli, N.; Balzani, V.; Collin, J.-P.; Gaviña, P.; Sauvage, J.-P.; Ventura, B. *J. Am. Chem. Soc.* **1999**, *121*, 4397-4408. (b) Vignon, S. A.; Jarrosson, T.; Iijima, T.; Tseng, H.-R.; Sanders, J. K. M.; Stoddart, J. F. *J. Am. Chem. Soc.* **2004**, *126*, 9884-9885. (c) Iijima, T.; Vignon, S. A.; Tseng, H.-R.; Jarrosson, T.; Sanders, J. K. M.; Marchioni, F.; Venturi, M.; Apostoli, E.; Balzani, V.; Stoddart, J. F. *Chem. Eur. J.* **2004**, *10*, 6375-6392. (d) Marlin, D. S.; González Cabrera, D.; Leigh, D. A.; Slawin, A. M. Z. *Angew. Chem., Int. Ed.* **2006**, *45*, 77-83. (e) Marlin, D. S.; González Cabrera, D.; Leigh, D. A.; Slawin, A. M. Z. *Angew. Chem., Int. Ed.* **2006**, *45*, 1385-1390. (f) Tokunaga, Y.; Nakamura, T.; Yoshioka, M.; Shimomura, Y. *Tetrahedron Lett.* **2006**, *47*, 5901-5904.

(6) (a) Murakami, H.; Kawabuchi, A.; Kotoo, K.; Kunitake, M.; Nakashima, N. *J. Am. Chem. Soc.* **1997**, *119*, 7605-7606. (b) Stanier, C. A.; Alderman, S. J.; Claridge, T. D. W.; Anderson, H. L. *Angew. Chem., Int. Ed.* **2002**, *41*, 1769-1772. (c) Altieri, A.; Bottari, G.; Dehez, F.; Leigh, D. A.; Wong, J. K. Y.; Zerbetto, F. *Angew. Chem., Int. Ed.* **2003**, *42*, 2296-2300. (d) Wang, Q.-C.; Qu, D.-H.; Ren, J.; Chen, K.; Tian, H. *Angew. Chem., Int. Ed.* **2004**, *43*, 2661-2665. (e) Qu, D.-H.; Wang, Q.-C.; Tian, H. *Angew. Chem., Int. Ed.* **2005**, *44*, 5296-5299. (f) Murakami, H.; Kawabuchi, A.; Matsumoto, R.; Ido, T.; Nakashima, N. *J. Am. Chem. Soc.* **2005**, *127*, 15891-15899.

(7) (a) Bissell, R. A.; Córdova, E.; Kaifer, A. E.; Stoddart, J. F. *Nature* **1994**, *369*, 133-136. (b) Collin, J.-P.; Gaviña, P.; Sauvage, J.-P. *New J. Chem.* **1997**, 525-528. (c) Ashton, P. R.; Ballardini, R.; Balzani, V.; Credi, A.; Dress, K. R.; Ishow, E.; Kleverlaan, C. J.; Kocian, O.; Preece, J. A.; Spencer, N.; Stoddart, J. F.; Venturi, M.; Wenger, S. *Chem. Eur. J.* **2000**, *6*, 3558-3574. (d) Brouwer, A. M.; Frochot, C.; Gatti, F. G.; Leigh, D. A.; Mottier, L.; Paolucci, F.; Roffia, S.; Wurpel, G. W. H. *Science* **2001**, *291*, 2124-2128. (e) Altieri, A.; Gatti, F. G.; Kay, E. R.; Leigh, D. A.; Martel, D.; Paolucci, F.; Slawin, A. M. Z.; Wong, J. K. Y. *J. Am. Chem. Soc.* **2003**, *125*, 8644-8654. (f) Tseng, H.-R.; Vignon, S. A.; Stoddart, J. F. *Angew. Chem., Int. Ed.* **2003**, *42*, 1491-1495. (g) Long, B.; Nikitin, K.; Fitzmaurice, D. *J. Am. Chem. Soc.* **2003**, *125*, 15490-15498. (h) Kihara, N.; Hashimoto, M.; Takata, T. *Org. Lett.* **2004**, *6*, 1693-1696. (i) Steuerman, D. W.; Tseng, H.-R.; Peters, A. J.; Flood, A. H.; Jeppesen, J. O.; Nielsen, K. A.; Stoddart, J. F.; Heath, J. R. *Angew. Chem., Int. Ed.* **2004**, *43*, 6486-6491. (j) Jeppesen, J. O.; Nygaard, S.; Vignon, S. A.; Stoddart, J. F. *Eur. J. Org. Chem.* **2005**, 196-220. (k) Cooke, G.; Garety, J. F.; Mabruk, S.; Rabani, G.; Rotello, V. M.; Surpateanu, G.; Woisel, P. *Tetrahedron Lett.* **2006**, *47*, 783-786.

(8) See 5f, 7a and (a) Martínez-Díaz, M. V.; Spencer, N.; Stoddart, J. F. *Angew. Chem., Int. Ed. Engl.* **1997**, *36*, 1904-1907. (b) Badjić, J. D.; Balzani, V.; Credi, A.; Silvi, S.; Stoddart, J. F. *Science* **2004**, *303*, 1845-1849. (c) Keaveney, C. M.; Leigh, D. A. *Angew. Chem., Int. Ed.* **2004**, *43*, 1222-1224. (d) Badjić, J. D.; Ronconi, C. M.; Stoddart, J. F.; Balzani, V.; Silvi, S.; Credi, A. *J. Am. Chem. Soc.* **2006**, *128*, 1489-1499. (e) Clemente-León, M.; Credi, A.; Martínez-Díaz, M.

V.; Mingotaud, C.; Stoddart, J. F. *Adv. Mater.* **2006**, *18*, 1291-1296. (f) Leigh, D. A.; Thomson, A. R. *Org. Lett.* **2006**, *8*, 5377-5379.

(9) 'Co-conformation' refers to the relative positions of the mechanically interlocked components with respect to each other, see: Fyfe, M. C. T.; Glink, P. T.; Menzer, S.; Stoddart, J. F.; White, A. J. P.; Williams, D. J. *Angew. Chem., Int. Ed. Engl.* **1997**, *36*, 2068-2070.

(10) (a) Notario, R.; Herreros, M.; Ballesteros, E.; Essefar, M.; Abboud, J.-L. M.; Sadekov, I. D.; Minkin, V. I.; Elguero, J. *J. Chem. Soc., Perkin Trans. 2* **1994**, 2341-2344. (b) Matthews, C. J.; Clegg, W.; Elsegood, M. R. J.; Leese, T. A.; Thorp, D.; Thornton, P.; Lockhart, J. C. *J. Chem. Soc., Dalton Trans.* **1996**, 1531-1538.

(11) (a) Henary, M. M.; Fahrni, C. J. *J. Phys. Chem. A* **2002**, *106*, 5210-5220. (b) Ihmels, H.; Meiswinkel, A.; Mohrschladt, C. J.; Otto, D.; Waidelich, M.; Towler, M.; White, R.; Albrecht, M.; Schnurpfeil, A. *J. Org. Chem.* **2005**, *70*, 3929-3938.

(12) (a) Berg, J. M.; Shi, Y. *Science* **1996**, *271*, 1081-1085. (b) Jiang, P.; Guo, Z. *Coord. Chem. Rev.* **2004**, *248*, 205-229. (c) Lim, N. C.; Freake, H. C.; Bruckner, C. *Chem. Eur. J.* **2005**, *11*, 38-49.

(13) Carol, P.; Sreejith, S.; Ajayaghosh, A. *Chem. Asian J.* **2007**, *2*, 338-348.

(14) See 11a and (a) Taki, M.; Wolford, J. L.; O'Halloran, T. V. *J. Am. Chem. Soc.* **2004**, *126*, 712-713. (b) Decken, A.; Gossage, R. A. *J. Inorg. Biochem.* **2005**, *99*, 664-667. (c) Yang, C.-C.; Tian, Y.; Chen, C.-Y.; Jen, A. K.-Y.; Chen, W.-C. *Macromol. Rapid Commun.* **2007**, *28*, 894-899.

First Synthesis and Characterisation of a [2]Rotaxane Containing an Octanuclear Heterometallic {Cr_7Ni} Wheel

Acknowledgements

The following people are gratefully acknowledged for their contribution to this chapter: Dr. C.-F. Lee synthesised the thread **S17** for the first time; Prof. R. E. P. Winpenny and Dr. G. A. Timco of the University of Manchester synthesised the [2]rotaxane **R1** and solved its X-ray crystal structure.

5.1 Summary

A wide variety of templating motifs for the self-assembly of interpenetrated and mechanically interlocked structures have been reported, ranging from cationic[1] and neutral[2] to anionic.[3] One of the simplest recognition motifs is the binding of secondary dialkylammonium ions with suitably large polyether macrocycles, for example, dibenzo-24-crown-8 (DB24C8) or bis-*p*-phenylene-34-crown-10 (BPP34C10).[1b] Rotaxanes based on secondary alkylammonium threads and crown ether rings have been developed by the 'threading-followed-by-stoppering',[4] 'clipping'[5] and 'slippage'[6] approaches. In this chapter, the assembly of an octanuclear wheel $[Cr_7NiF_8(O_2CCMe_3)_{16}]^-$ about a pre-stoppered secondary ammonium cation $[\{(Me_3C)_2C_6H_3CO_2(CH_2)_6\}_2NH_2]^+$ to form the first heterometallic-ring-containing [2]rotaxane is described. The interlocked structure was undoubtedly confirmed by mass spectroscopy, elemental analysis and X-ray crystallographic determination. As {Cr_7Ni} is an antiferromagnetically coupled wheel with a nondiamagnetic ground state ($S = 1/2$),[7] this methodology will make it possible to examine such fascinating magnetic properties within interlocked structures for the first time.

5.2 Introduction

The discovery of beautiful cyclic metal complex structures has recently inspired a great deal of research, for example the 'ferric wheel' $[Fe(OMe)_2(O_2CCH_2Cl)]_{10}$, first

reported by Taft and Lippard,[8] the giant wheels from Müller and co-workers,[9] and another ring with the formula $[CrF(O_2CCMe_3)_2]_8$ (Figure 5.1).[7b]

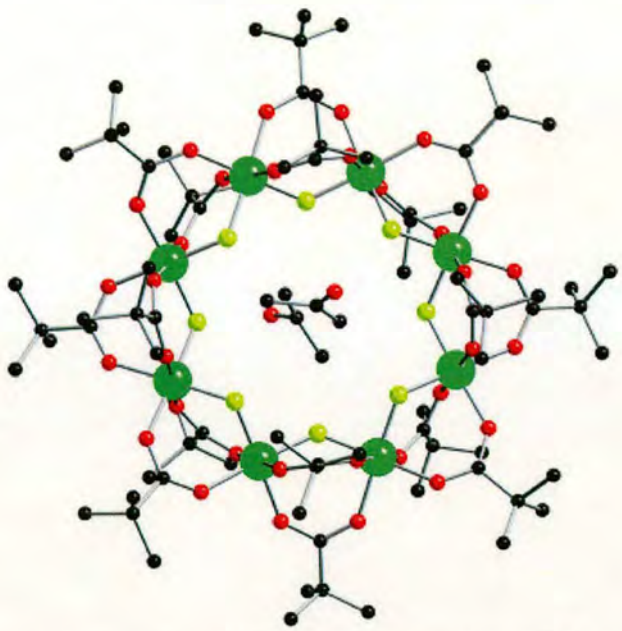

Figure 5.1 X-ray crystal structure of $[CrF(O_2CCMe_3)_2]_8 \cdot 2Me_2CO$.[7b] Colours: Cr, green; F, yellow; O, red; C, black. H-atoms omitted for clarity.

Besides these homometallic rings, the first heterometallic rings of the type $[NH_2R_2][Cr_7MF_8(O_2CCMe_3)_{16}]$ (R = alkyl sidechain; M = Ni^{2+}, Co^{2+}, Fe^{2+}, Mn^{2+}, or Cd^{2+}) were made by the Winpenny group,[7] with the motivation to test the theory of 'quantum tunneling'[10] proposed by Meier and Loss.[11] A single chromium (III) center in the neutral homometallic ring $[CrF(O_2CCMe_3)_2]_8$ was replaced by a dication (M) (Scheme 5.1):[7]

Scheme 5.1 Overall Reaction for Synthesis of $[NH_2R_2][Cr_7MF_8(O_2CCMe_3)_{16}]$[7]

$$7CrF_3 \cdot 4H_2O + MX_2 + HNR_2 + HO_2CCMe_3 \longrightarrow [H_2NR_2][Cr_7MF_8(O_2CCMe_3)_{16}]$$

The use of a divalent metal (M) produced the monoanionic species $[Cr_7MF_8(O_2CCMe_3)_{16}]^-$ in the presence of a suitable secondary ammonium cation, following separation from the neutral homometallic ring $[CrF(O_2CCMe_3)_2]_8$, which may also be present. The stability of all the octanuclear rings was found to be very high. The $\{Cr_7Ni\}$ structures such as $[NH_2{}^nPr_2][Cr_7NiF_8(O_2CCMe_3)_{16}]$ (Figure 5.2)[7b]

have received most interest due to their interesting physics. Because the ammonium cation added to the reaction is found at the center of the ring, H-bonded to the bridging fluorides (Figure 5.2), one question was whether pre-stoppered ammonium ions can template the assembly of such heterometallic rings to form the corresponding rotaxanes? Herein, the first synthesis and characterisation of a [2]rotaxane containing an octanuclear heterometallic {Cr_7Ni} wheel is described. As it has been possible to change both the divalent and chromium metals in the non-interlocked wheels,[12] this methodology can be used to prepare a series of interlocked molecules with varying and fascinating magnetic behaviour.

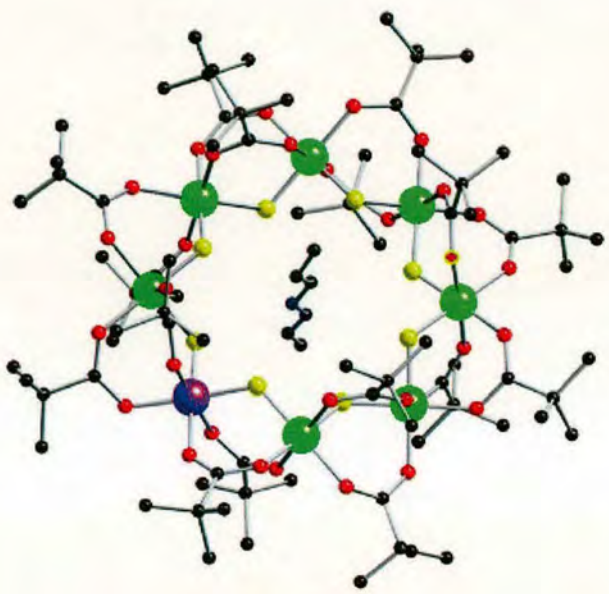

Figure 5.2 X-ray crystal structure of $[NH_2{}^nPr_2][Cr_7NiF_8(O_2CCMe_3)_{16}]$.[7b] The heterometal site is disordered, the purple metal colour is present for aesthetic reasons. Colours: Cr, green; F, yellow; O, red; C, black; Ni, purple. H-atoms omitted for clarity.

5.3 Results and Discussion

The [2]rotaxane **R1** was prepared from the thread **S17**, which has a carbon chain of sufficient length so that an octanuclear {Cr_7Ni} wheel can be templated about the central protonated amine cation (Scheme 5.2). In initial experiments it was found that a secondary ammonium cation with a short chain length cannot be encapsulated and the heterometallic anionic ring did not form (Scheme 5.3).

Scheme 5.2 Synthesis of the Heterometallic-Wheel-Containing [2]Rotaxane **R1**: $[\{(Me_3C)_2C_6H_3CO_2(CH_2)_6\}_2NH_2][Cr_7NiF_8(O_2CCMe_3)_{16}]$ [a]

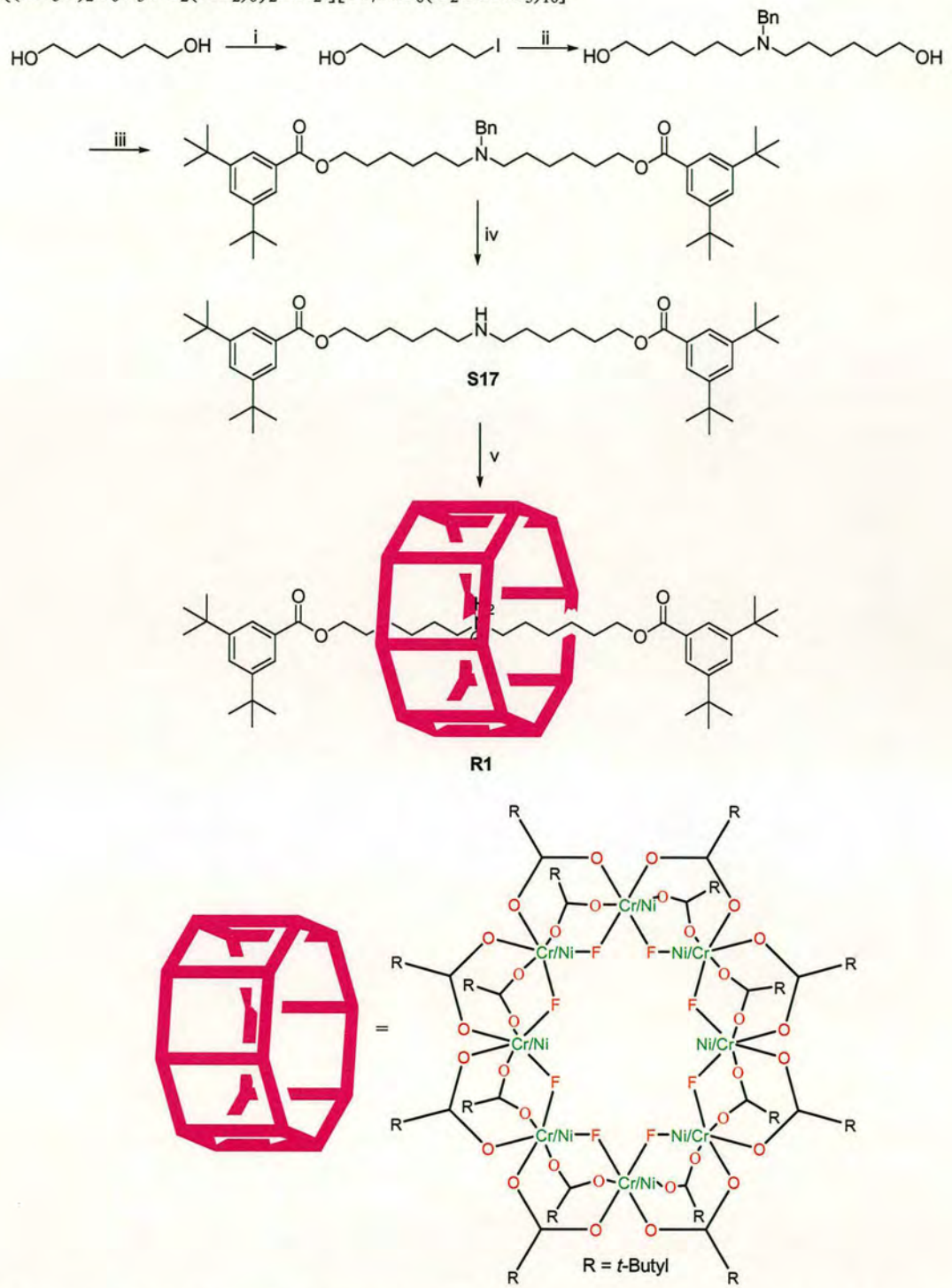

[a] Reagents and conditions: (i) PPh_3, imidazole, I_2, THF, 0 °C, 58%; (ii) benzylamine, K_2CO_3, EtOH, reflux, 45%; (iii) 3,5-di-*tert*-butylbenzoic acid, 4-dimethylaminopyridine (DMAP), 1-(3-dimethylaminopropyl)-3-ethyl-carbodiimide hydrochloride (EDCI·HCl), CH_2Cl_2, 0 °C to rt, N_2, 64%; (iv) $Pd(OH)_2$, H_2, EtOH/EtOAc (1:1), rt, 90%; (v) $CrF_3 \cdot 4H_2O$, $[2NiCO_3 \cdot 3Ni(OH)_2 \cdot 4H_2O]$, pivalic acid, 140 °C, 10% (calculated from $CrF_3 \cdot 4H_2O$ used).

Scheme 5.3 Short Ammonium Cation Fails to Template the Assembly of the Octanuclear Heterometallic Wheel $[Cr_7NiF_8(O_2CCMe_3)_{16}]$ about it [a]

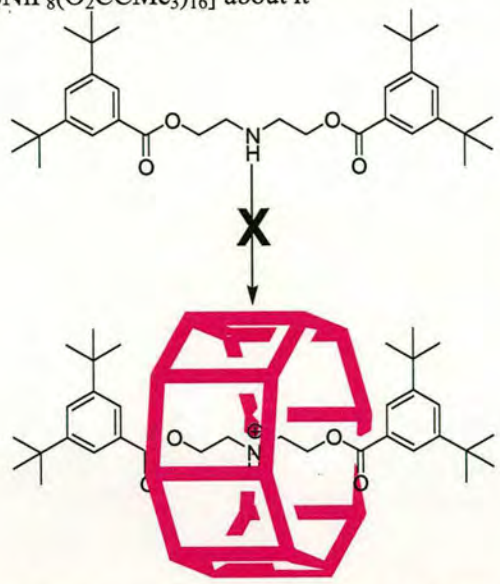

[a] Reagents and conditions: $CrF_3 \cdot 4H_2O$, $[2NiCO_3 \cdot 3Ni(OH)_2 \cdot 4H_2O]$, pivalic acid, 140 °C.

Support for the interlocked structure **R1** firstly comes from mass spectroscopy. In the positive-ion spectra the peaks at +2842 and +2865 reveal the molecular ion $[M]^+$ and the Na^+ incorporated cation $[M+Na]^+$, respectively. Further evidence is provided by elemental analysis. Both present metals, C, H and N were analysed and the stoichiometry found to fit the molecular formula $[\{(Me_3C)_2C_6H_3CO_2(CH_2)_6\}_2NH_2][Cr_7NiF_8(O_2CCMe_3)_{16}]$. Finally, X-ray quality crystals were formed from the crystallisation of **R1** from Et_2O/CH_3CN. The crystal structure (Figure 5.3) again unambiguously confirms the interlocked nature of the rotaxane in the solid state. In **R1** the structure of the interlocked wheel is similar to that of the free one,[7a] with each M•••M vector bridged by a μ-fluoride and two 1,3-bridging pivalates and the M site is disordered over all possible metal sites. The ammonium cation is found in the cavity centre of the macrocycle, forming three N^+-H•••F hydrogen bonds.

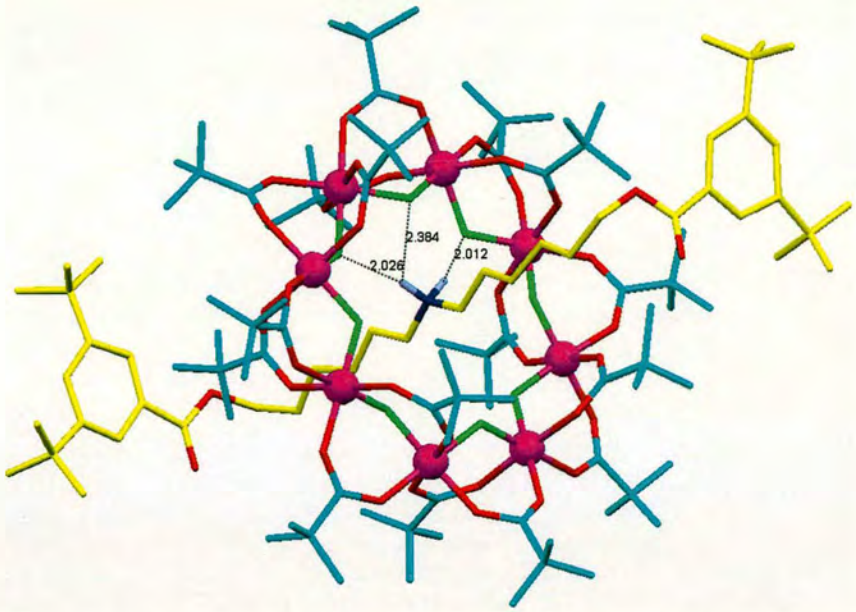

Figure 5.3 X-ray crystal structure of [2]rotaxane **R1**. The heterometal site is disordered. Colours: M, pink; F, green; O, red; C of the thread, yellow; C of the wheel, blue; N, dark blue; selected H for ammonium, grey. Intramolecular hydrogen bond distances (Å) are the following: N1H-F1 2.026, N1H-F8 2.384, N1H-F7 2.012.

With the first success of this methodology, thread **S21** was prepared in order to make a two-identical-station molecular shuttle (Scheme 5.4). The rotaxanation of **S21** is still in progress now in our lab.

Scheme 5.4 Synthesis of the Two-Identical-Station Thread **S21**[a]

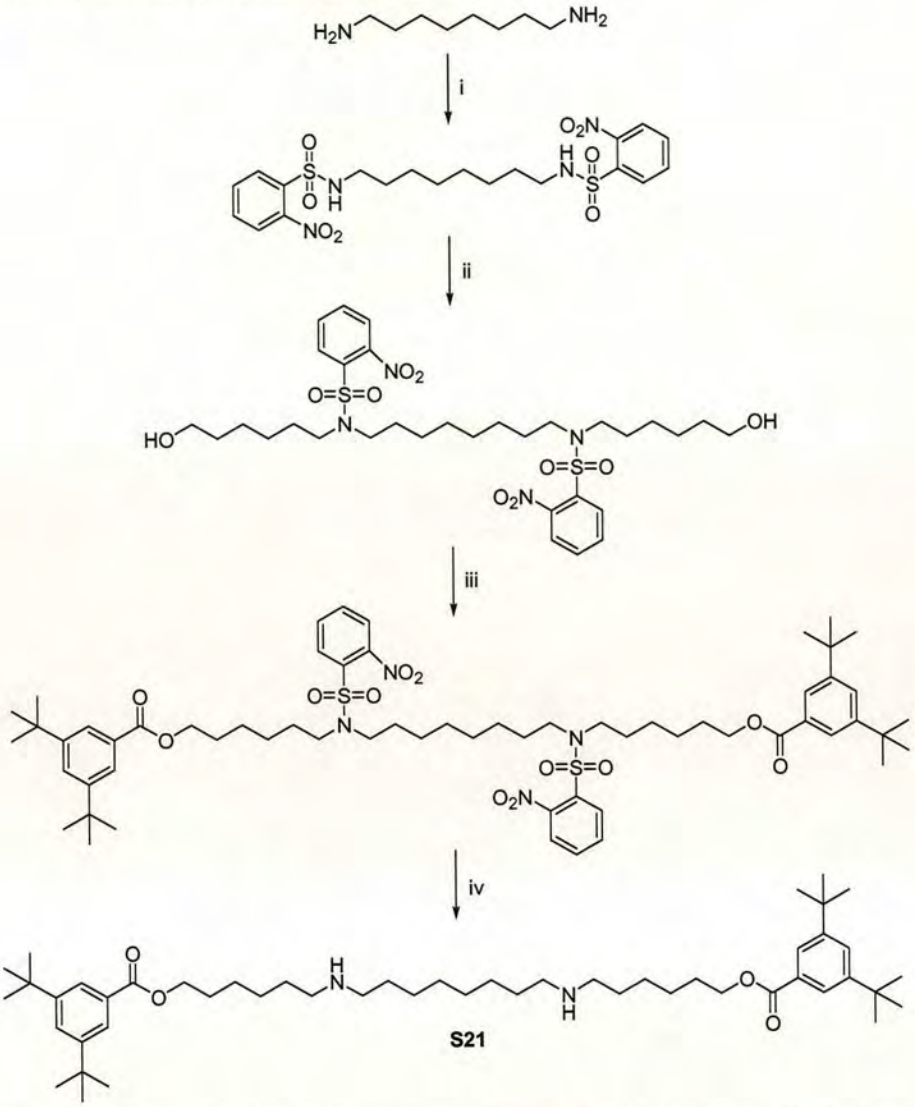

[a] Reagents and conditions: (i) 2-nitrobenzenesulfonyl chloride, Et_3N, CH_2Cl_2, 0 °C to rt, 91%; (ii) 6-bromo-1-hexanol, K_2CO_3, KI, DMF, 80 °C, 91%; (iii) 3,5-di-*tert*-butylbenzoic acid, 4-DMAP, EDCI·HCl, CH_2Cl_2, 0 °C to rt, N_2, 81%; (iv) mercaptoacetic acid, LiOH, DMF, rt, N_2, 56%.

5.4 Conclusions

The pre-stoppered secondary ammonium cation $[\{(Me_3C)_2C_6H_3CO_2(CH_2)_6\}_2NH_2]^+$ templated the assembly of an octanuclear heterometallic wheel $[Cr_7NiF_8(O_2CCMe_3)_{16}]^-$ about it to form the [2]rotaxane $[\{(Me_3C)_2C_6H_3CO_2(CH_2)_6\}_2NH_2][Cr_7NiF_8(O_2CCMe_3)_{16}]$. This represents the first heterometallic-ring-containing interlocked structure. Because it has already been possible to provide different heterometallic rings by changing both the divalent and chromium metals, this method should be applicable to a series of such novel

interlocked molecules and will allow for a detailed analysis of their fascinating magnetic properties.

5.5 Experiments

5.5.1 General

Unless stated otherwise, all reagents and anhydrous solvents were purchased from Aldrich Chemicals and used without further purification. Column chromatography was performed using Kiesegel C60 (Merck, Germany) as the stationary phase, and TLC was performed on precoated silica gel plates (0.25 mm thick, $60F_{254}$, Merck, Germany) and observed under UV light. All ^{1}H and ^{13}C NMR spectra were recorded on a Bruker AV 400 instrument, at a constant temperature of 25 °C. Chemical shifts are reported in parts per million from high to low field and referenced to TMS. Coupling constants (*J*) are reported in Hertz (Hz). Standard abbreviations indicating multiplicity are used as follows: m = multiplet, br = broad, d = doublet, q = quadruplet, t = triplet, s = singlet. LRFAB mass spectrometry for **S14-S17** was carried out by the services at the University of Edinburgh; HRES mass spectrometry for **S15-S17** was carried out by the EPSRC National Mass Spectrometry Service Centre at the University of Wales Swansea; ES mass spectrometry and elemental analysis for **R1** was carried out by the services at the University of Manchester; FAB mass spectrometry for **S18-S21** was carried out by the services at the University of Edinburgh.

S14[13]

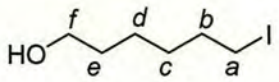

To a stirred solution of 1,6-hexanediol (10.75 g, 0.091 mol), triphenylphosphine (9.52 g, 0.036 mol) and imidazole (4.94 g, 0.073 mol) in THF (300 mL) cooled to 0 °C was added dropwise a solution of iodine (9.22 g, 0.036 mol) in THF (20 mL) and the reaction was allowed to stir for 5 h. The reaction mixture was concentrated *in vacuo*. The crude residue was purified by column chromatography (a gradient of 90:10 *n*-hexane:EtOAc to 80:20 *n*-hexane:EtOAc) to yield **S14** as a pale yellow liquid (4.81 g, yield = 58%). ^{1}H NMR (400 MHz, $CDCl_3$): δ = 1.20-1.48 (m, 5H, H_c, H_d and O*H*), 1.52-1.62 (m, 2H, H_e), 1.80-1.87 (m, 2H, H_b), 3.19 (t, J = 7.0 Hz, 2H, H_a), 3.64 (t, J = 6.6 Hz, 2H, H_f); ^{13}C NMR (100 MHz, $CDCl_3$): δ = 7.1, 24.6, 30.2, 32.3, 33.3, 62.5; LRFAB-MS: m/z = 229 $[M+H]^+$.

S15

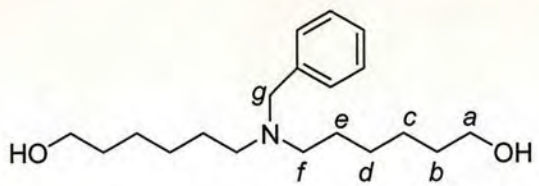

A stirred solution of **S14** (8.69 g, 0.038 mol), benzylamine (2.1 mL, 0.019 mol) and excess of potassium carbonate (26.34 g, 0.19 mol) in ethanol (200 mL) was heated at reflux overnight. The reaction mixture was filtered, concentrated *in vacuo*. The crude residue was purified by column chromatography (85:15 CH_2Cl_2:CH_3OH) to yield **S15** as a pale yellow liquid (2.63 g, yield = 45%).^{1}H NMR (400 MHz, $CDCl_3$): δ = 1.22-1.38 (m, 8H, H_c and H_d), 1.40-1.60 (m, 10H, H_b, H_e and O*H*), 2.40 (t, J = 6.0 Hz, 4H, H_f), 3.54 (s, 2H, H_g), 3.61 (t, J = 6.0 Hz, 4H, H_a), 7.18-7.34 (m, 5H, Ar*H*); ^{13}C NMR (100 MHz, $CDCl_3$): δ = 25.5, 26.8, 27.1, 32.7, 53.5, 58.6, 62.8, 126.7, 128.0, 128.9, 139.8; LRFAB-MS: m/z = 308 $[M+H]^+$; HRMS calcd. for $C_{19}H_{34}NO_2$ $[M+H]^+$: 308.2590, Found (ES): 308.2588.

S16

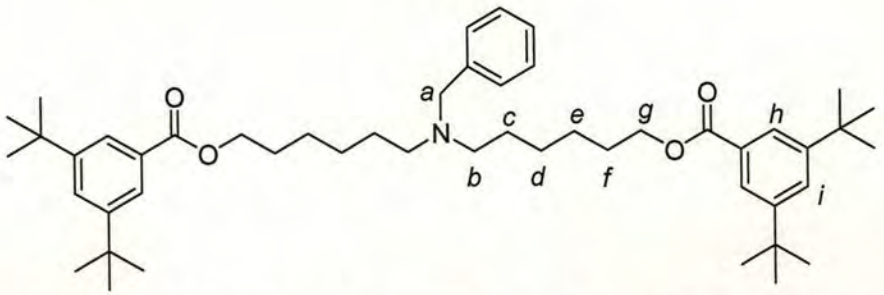

To a stirred solution of **S15** (0.95 g, 3.1 mmol), 3,5-di-*tert*-butylbenzoic acid (1.60 g, 6.8 mmol) and 4-DMAP (0.91 g, 7.4 mmol) in dichloromethane (150 mL) cooled on an ice bath was added EDCI•HCl (1.43 g, 7.4 mmol) and the reaction was allowed to stir overnight at room temperature under an atmosphere of nitrogen. The reaction mixture was concentrated *in vacuo* and the residue re-dissolved in dichloromethane, washed successively with 10% citric acid (3 × 50 mL), sat. $NaHCO_3$ (3 × 50 mL) and brine (3 × 50 mL), dried over $MgSO_4$, concentrated *in vacuo* and the crude product purified by column chromatography (80:20 *n*-hexane:EtOAc) to yield **S16** as a colourless sticky oil (1.47 g, yield = 64%). ^{1}H NMR (400 MHz, $CDCl_3$): δ = 1.28-1.52 (m, 44H, H_d, H_e and $C(CH_3)_3$), 1.70-1.82 (m, 4H, H_f), 1.82-2.00 (m, 4H, H_c), 2.75-3.10 (m, 4H, H_b), 4.16 (br s, 2H, H_a), 4.29 (t, J = 7.4 Hz, 4H, H_g), 7.42 (br s, 3H, Ar*H*), 7.56-7.66 (m, 4H, H_i and Ar*H*), 7.87 (d, J = 2.0 Hz, 4H, H_h); ^{13}C NMR (100 MHz, $CDCl_3$): δ = 25.6, 26.6, 28.6 (× 2), 31.4, 34.9 (× 2), 39.1, 64.5, 123.7 (× 2), 127.1 (× 2), 129.2, 129.7, 151.0 (× 2), 167.3; LRFAB-MS: *m/z* = 741 $[M+H]^+$; HRMS calcd. for $C_{49}H_{74}NO_4$ $[M+H]^+$: 740.5618, Found (ES): 740.5619.

S17

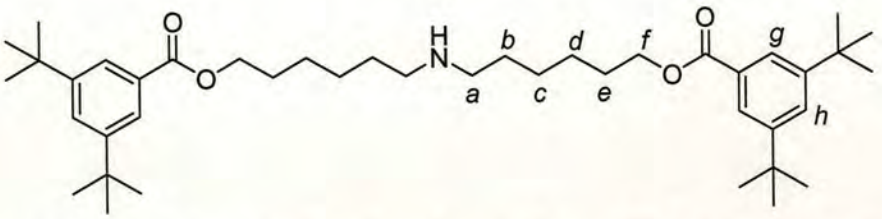

A solution of **S16** (1.15 g, 1.55 mmol) and a catalytic palladium hydroxide on carbon (20% w/w) in ethanol/EtOAc (1:1, 80 mL) was stirred at room temperature under an atmosphere of hydrogen. After 1.5 h, the reaction mixture was filtered, concentrated *in vacuo* to yield **S17** as a colourless sticky oil (0.91 g, yield = 90%). ^{1}H NMR (400

MHz, $CDCl_3$): δ = 1.34 (s, 36H, $C(CH_3)_3$), 1.40-1.50 (m, 8H, H_c and H_d), 1.72-1.82 (m, 4H, H_e), 1.84-1.98 (m, 4H, H_b), 2.92 (t, J = 8.0 Hz, 4H, H_a), 4.29 (t, J = 6.6 Hz, 4H, H_f), 7.61 (t, J = 1.9 Hz, 2H, H_h), 7.87 (d, J = 1.9 Hz, 4H, H_g); ^{13}C NMR (100 MHz, $CDCl_3$): δ = 25.5, 25.7, 26.5, 28.6, 31.4, 34.9, 47.3, 64.5, 123.7, 127.1, 129.7, 151.0, 167.3; LRFAB-MS: m/z = 651 $[M+H]^+$; HRMS calcd. for $C_{42}H_{68}NO_4$ $[M+H]^+$: 650.5148, Found (ES): 650.5141.

R1

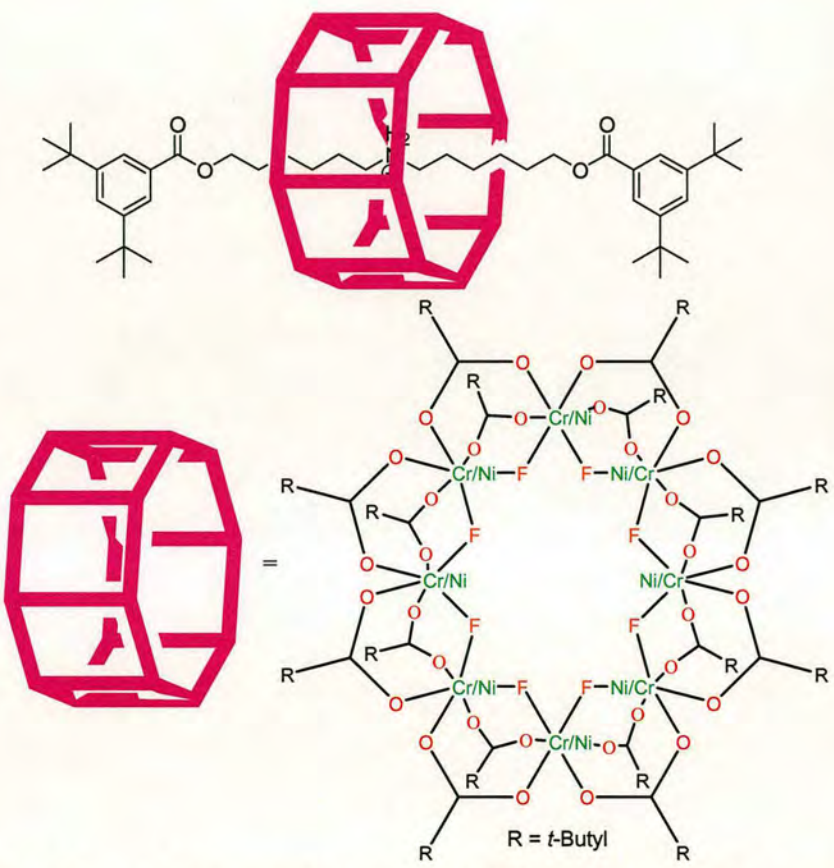

$CrF_3 \cdot 4H_2O$ (0.70 g, 3.87 mmol), $[2NiCO_3 \cdot 3Ni(OH)_2 \cdot 4H_2O]$ (0.080 g, 0.14 mmol), pivalic acid (7.0 g, 0.068 mol) and **S17** (0.38 g, 0.58 mmol) were heated at 140 ^{0}C for 10 h with stirring in a Teflon flask. Then the flask was cooled to room temperature and CH_3CN (20 mL) was added while stirring. The product was filtered, washed with CH_3CN, dried in air, then extracted with Et_2O (20 mL), concentrated *in vacuo* and the green residue (0.28 g) was purified by column chromatography on silica gel using toluene as eluent. The trace of less polar impurity $[Cr_8F_8(O_2CCMe_3)_{16}]$ eluted first, then using a gradient of toluene/EtOAc (1:1) to toluene/CH_3OH (1:1), another

two fractions were collected. According to the ES-MS investigation only second toluene fraction contained pure **R1**. The fraction containing **R1** was then evaporated under reduced pressure to give a green microcrystalline product, which was additionally dried *in vacuo*. (0.16 g, yield = 10 %, calculated from $CrF_3 \cdot 4H_2O$ used). Elemental analysis calcd. (%) for $C_{122}H_{212}Cr_7F_8N_1Ni_1O_{36}$: Cr 12.80, Ni 2.06, C 51.53, H 7.51, N 0.49; Found: Cr 12.64, Ni 2.07, C 51.39, H 7.68, N 0.50; ES-MS (sample dissolved in THF, run in CH_3OH): +2901 $[M+Na+2H_2O]^+$ (100%); +2865 $[M+Na]^+$; +2842 $[M]^+$.

S18

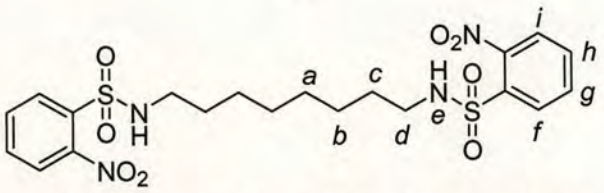

To a stirred solution of 1,8-diaminooctane (8.0 g, 55 mmol) and triethylamine (31.0 mL, 222 mmol) in dry CH_2Cl_2 (150 mL) cooled to 0 °C was added dropwise a solution of 2-nitrobenzenesulfonyl chloride (24.6 g, 111 mmol) in dry CH_2Cl_2 (50 mL) using a syringe pump and the reaction was allowed to stir at room temperature for 22 h. The reaction mixture was filtered and the resulting white solid washed successively with CH_2Cl_2, water and *n*-hexane, which was additionally dried *in vacuo* to yield **S18** as a white solid. (25.8 g, yield = 91%). m.p. 150-152 °C; ^{1}H NMR (400 MHz, DMSO-d_6): δ = 1.00-1.35 (m, 8H, H_a+H_b), 1.35-1.45 (m, 4H, H_c), 2.86 (t, J = 7.0 Hz, 4H, H_d), 7.81-8.00 (m, 8H, H_f+H_g+H_h+H_i), 8.04 (s, 2H, H_e); ^{13}C NMR (100 MHz, DMSO-d_6): δ = 25.7, 28.3, 29.0, 42.6, 124.3, 129.4, 132.5, 132.8, 133.9, 147.7; LRFAB-MS: *m/z* = 515 $[M+H]^+$; HRFAB-MS calcd. for $C_{20}H_{27}N_4O_8S_2$ $[M+H]^+$: 515.1270, Found: 515.1282.

S19

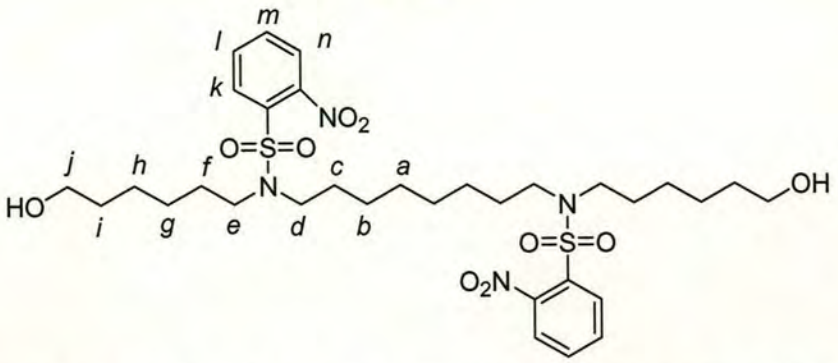

A stirred solution of **S18** (5.0 g, 9.7 mmol), 6-bromo-1-hexanol (2.5 mL, 19.1 mmol), excess of potassium carbonate (6.7 g, 48.5 mmol) and a catalytic potassium iodide (0.3 g, 1.8 mmol) in dry DMF (60 mL) was heated at 80 °C for 40 h. The reaction mixture was filtered and the resulting solution diluted with EtOAc, then washed with brine (3 × 50 mL), dried over $MgSO_4$, concentrated *in vacuo*. The crude residue was purified by column chromatography using a gradient of $CHCl_3$/EtOAc (1:1) to $CH_3OH/CHCl_3$ (4:96) to yield **S19** as a pale yellow liquid (6.2 g, yield = 91%).^{1}H NMR (400 MHz, $CDCl_3$): δ = 1.16-1.54 (m, 28H, H_a+H_b+H_c+H_f+H_g+H_h+H_i), 1.91 (s, 2H, O*H*), 3.20-3.26 (m, 8H, H_d+H_e), 3.56 (t, J = 6.5 Hz, 4H, H_j), 7.57-7.96 (m, 8H, H_k+H_l+H_m+H_n); ^{13}C NMR (100 MHz, $CDCl_3$): δ = 25.3, 26.3 (×2), 28.0, 28.1, 28.9, 32.3, 47.2 (×2), 62.5, 124.1, 130.5, 131.7, 133.5 (×2), 147.9; LRFAB-MS: m/z = 715 $[M+H]^+$; HRFAB-MS calcd. for $C_{32}H_{51}N_4O_{10}S_2$ $[M+H]^+$: 715.3047, Found: 715.2903.

S20

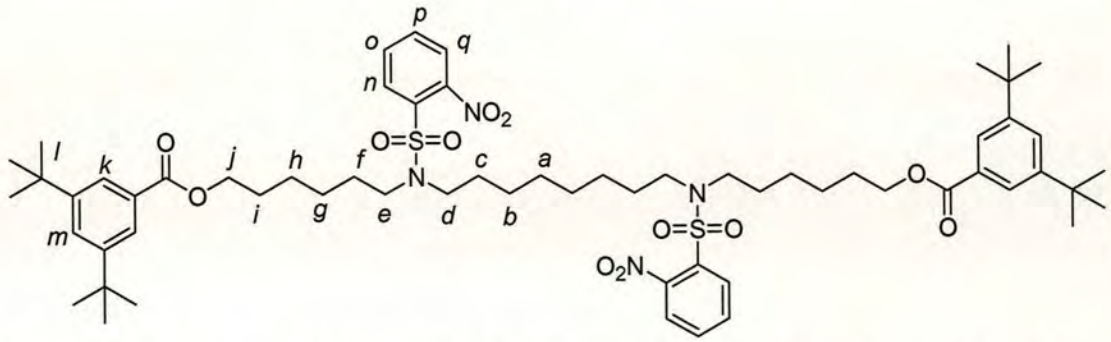

To a stirred solution of **S19** (6.2 g, 8.7 mmol), 3,5-di-*tert*-butylbenzoic acid (4.5 g, 19.2 mmol) and 4-DMAP (3.2 g, 26.2 mmol) in CH_2Cl_2 (200 mL) cooled on an ice

bath was added EDCI•HCl (5.0 g, 26.1 mmol) and the reaction was allowed to stir overnight at room temperature under an atmosphere of nitrogen. The reaction mixture was concentrated *in vacuo* and the residue re-dissolved in CH_2Cl_2, washed successively with 10% citric acid (3 × 50 mL), sat. $NaHCO_3$ (3 × 50 mL) and brine (3 × 50 mL), dried over $MgSO_4$, concentrated *in vacuo* and the crude product purified by column chromatography (5:2 *n*-hexane:EtOAc) to yield **S20** as a sticky oil (8.1 g, yield = 81%). ^{1}H NMR (400 MHz, $CDCl_3$): δ = 1.15-1.60 (m, 24H, H_h+H_g+H_f+H_c+H_b+H_a), 1.35 (s, 36H, H_l), 1.65-1.80 (m, 4H, H_i), 3.20-3.40 (m, 8H, H_e+H_d), 4.28 (t, J = 6.0 Hz, 4H, H_j), 7.59-8.01 (m, 14H, H_k+H_m+H_n+H_o+H_p+H_q); ^{13}C NMR (100 MHz, $CDCl_3$): δ = 25.7, 26.3, 26.4, 28.0 (×2), 28.7, 29.0, 31.4, 35.0, 47.0, 47.1, 64.7, 123.7, 124.1, 127.1, 129.8, 130.7, 131.6, 133.4, 133.7, 148.0, 151.0, 167.3; LRFAB-MS: *m/z* = 1147 $[M]^+$; HRFAB-MS calcd. for $C_{62}H_{91}N_4O_{12}S_2$ $[M+H]^+$: 1147.6075, Found: 1147.6062.

S21

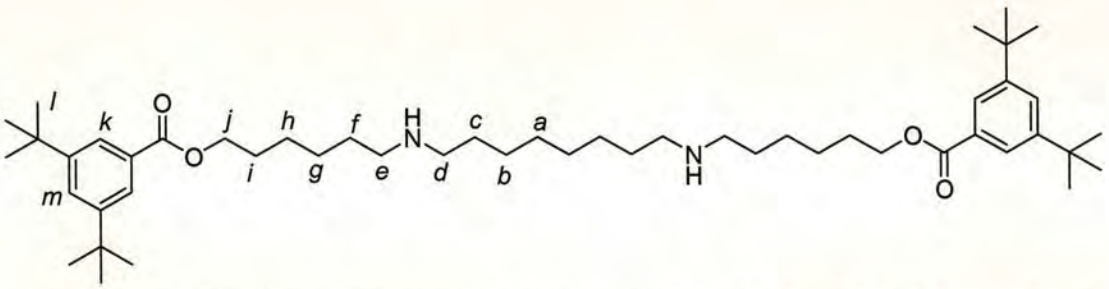

A mixture of **S20** (8.1 g, 7.1 mmol), mercaptoacetic acid (6.4 mL, 92.1 mmol) and lithium hydroxide (7.7 g, 0.3 mol) in dry DMF (100 mL) was stirred at room temperature under an atmosphere of nitrogen. After 3 h, the reaction mixture was diluted with water, extracted with $CHCl_3$, then the combined $CHCl_3$ phases were washed successively with $NaHCO_3$ (3 × 50 mL) and brine (3 × 50 mL), dried over $MgSO_4$, concentrated *in vacuo*. The crude residue was purified by column chromatography using a gradient of $CH_3OH/CHCl_3/NH_3•H_2O$ (10:90:1) to $CH_3OH/CHCl_3/NH_3•H_2O$ (20:80:1) to yield **S21** as a white solid (3.1 g, yield = 56%). m.p. 65-67 °C ; ^{1}H NMR (400 MHz, $CDCl_3$): δ = 1.30-1.57 (m, 60H, H_a+H_b+H_c+H_f+H_g+H_h+H_l), 1.74-1.81 (m, 4H, H_i), 2.57-2.63 (m, 8H, H_d+H_e), 4.31 (t, J = 6.7 Hz, 4H, H_j), 7.62 (t, J = 1.9 Hz, 2H, H_m), 7.88 (d, J = 1.9 Hz, 4H, H_k); ^{13}C

NMR (100 MHz, $CDCl_3$): δ = 26.0, 27.1, 27.3, 28.7, 29.4, 30.0 (×2), 31.4, 34.9, 50.0, 50.1, 64.8, 123.7, 127.0, 129.8, 151.0, 167.4; LRFAB-MS: m/z = 777 $[M]^+$; HRFAB-MS calcd. for $C_{50}H_{85}N_2O_4$ $[M+H]^+$: 777.6509, Found: 777.6542.

X-Ray Crystallographic Structure Determination

X-ray crystal structural data for **R1**: $C_{122}H_{212}Cr_7F_8NNiO_{36}$, M_r = 2843.63, green prism, crystal size 0.25 × 0.14 × 0.08 mm^3, monoclinic P 1 21/n 1, a = 16.8712(3), b = 27.5463(4), c = 36.4760(7) Å, β = 102.254(1)°, V = 16565.6(5) $Å^3$, Z = 4, ρ_{calcd} = 1.138 Mg/m^3; λ = 0.71073 Å, $\mu(Mo_{K\alpha})$ = 0.574 mm^{-1}, T = 150(2) K; 19488 reflections collected, 19488 independent reflections (R_{int} = 0.145, 2.92 < θ < 22°) and 1576 parameters. The structure was solved by direct methods and refined by full-matrix least-squares on F^2 to give $R1(F^2)$ = 0.1074 ($I > 2\sigma I$), $wR2(F^2)$ = 0.265 (all data).

X-Ray Crystal Structure Thermal Ellipsoids

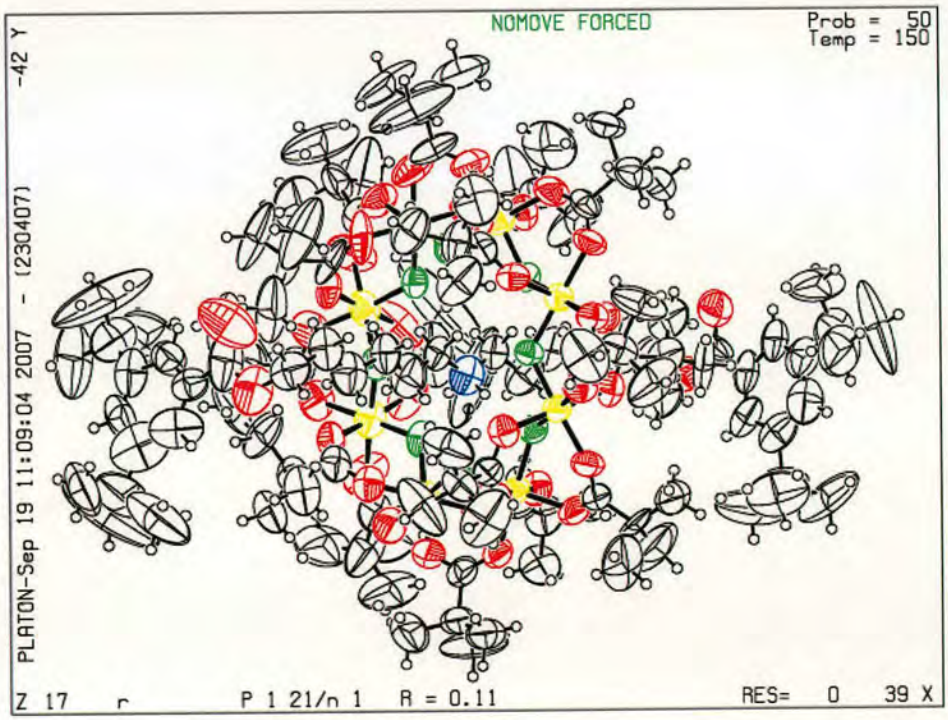

5.6 References and Notes

(1) (a) Allwood, B. L.; Spencer, N.; Shahriari-Zavareh, H.; Stoddart J. F.; Williams, D. J. *J. Chem. Soc., Chem. Commun.* **1987**, 1064-1066. (b) Glink, P. T.; Schiavo, C.; Stoddart, J. F.; Williams, D. J. *Chem. Commun.* **1996**, 1483-1490. (c) Kaiser, G.; Jarrosson, T.; Otto, S.; Ng, Y.-F.; Bond, A. D.; Sanders, J. K. M. *Angew. Chem., Int. Ed.* **2004**, *43*, 1959-1962.

(2) See for example: (a) Ogino, H. *J. Am. Chem. Soc.* **1981**, *103*, 1303-1304. (b) Hunter, C. A. *J. Am. Chem. Soc.* **1992**, *114*, 5303-5311. (c) Leigh, D. A.; Murphy, A.; Smart, J. P.; Slawin, A. M. Z. *Angew. Chem., Int. Ed. Engl.* **1997**, *36*, 728-732. (d) Jäger, R.; Vögtle, F. *Angew. Chem., Int. Ed. Engl.* **1997**, *36*, 930-944.

(3) See for example: (a) Wisner, J. A.; Beer, P. D.; Drew, M. G. B.; Sambrook, M. R. *J. Am. Chem. Soc.* **2002**, *124*, 12469-12476. (b) Beer, P. D.; Sambrook, M. R.; Curiel, D. *Chem. Commun.* **2006**, 2105-2117.

(4) Ashton, P. R.; Glink, P. T.; Stoddart, J. F.; Tasker, P. A.; White, A. J. P.; Williams, D. J. *Chem. Eur. J.* **1996**, *2*, 729-736.

(5) Glink, P. T.; Oliva, A. I.; Stoddart, J. F.; White, A. J. P.; Williams, D. J. *Angew. Chem., Int. Ed.* **2001**, *40*, 1870-1875.

(6) Ashton, P. R.; Baxter, I.; Fyfe, M. C. T.; Raymo, F. M.; Spencer, N.; Stoddart, J. F.; White, A. J. P.; Williams, D. J. *J. Am. Chem. Soc.* **1998**, *120*, 2297-2307.

(7) (a) Larsen, F. K.; McInnes, E. J. L.; Mkami, H. E.; Overgaard, J.; Piligkos, S.; Rajaraman, G.; Rentschler, E.; Smith, A. A.; Smith, G. M.; Boote, V.; Jennings, M.; Timco, G. A.; Winpenny, R. E. P. *Angew. Chem., Int. Ed.* **2003**, *42*, 101-105. (b) Affronte, M.; Carretta, S.; Timco, G. A.; Winpenny, R. E. P. *Chem. Commun.* **2007**, 1789-1797.

(8) (a) Taft, K. L.; Lippard, S. J. *J. Am. Chem. Soc.* **1990**, *112*, 9629-9630. (b) Taft, K. L.; Delfs, C. D.; Papaefthymiou, G. C.; Foner, S.; Gatteschi, D.; Lippard, S. J. *J. Am. Chem. Soc.* **1994**, *116*, 823-832.

(9) Müller, A.; Krickemeyer, E.; Meyer, J.; Bögge, H.; Peters, F.; Plass, W.; Diemann, E.; Dillinger, S.; Nonnenbruch, F.; Randerath, M.; Menke, C. *Angew. Chem., Int. Ed. Engl.* **1995**, *34*, 2122-2124.

(10) Gatteschi, D.; Sessoli, R. *Angew. Chem., Int. Ed.* **2003**, *42*, 268-297.

(11) Meier, F.; Loss, D. *Phys. Rev. B* **2001**, *64*, 224411/1-14.

(12) (a) Laye, R. H.; Larsen, F. K.; Overgaard, J.; Muryn, C. A.; McInnes, E. J. L.; Rentschler, E.; Sanchez, V.; Teat, S. J.; Güdel, H. U.; Waldmann, O.; Timco, G. A.; Winpenny, R. E. P. *Chem. Commun.* **2005**, 1125-1127. (b) Sañudo, E. C.; Muryn, C. A.; Helliwell, M. A.; Timco, G. A.; Wernsdorfer, W.; Winpenny, R. E. P. *Chem. Commun.* **2007**, 801-803.

(13) McGeary, R. P. *Tetrahedron Lett.* **1998**, *39*, 3319-3322.